SIMPLE, BIOCOMPATIBLE AND ROBUST MODIFICATION OF CELLULOSE MEMBRANES FOR THE ECO^2-FRIENDLY PREPARATION OF IMMUNOASSAY DEVICES

Julie Credou

Thèse de doctorat de l'École Polytechnique

Spécialité : Science des matériaux

Présentée par

Julie CREDOU

SIMPLE, BIOCOMPATIBLE AND ROBUST MODIFICATION OF CELLULOSE MEMBRANES FOR THE ECO^2-FRIENDLY PREPARATION OF IMMUNOASSAY DEVICES

MODIFICATION SIMPLE, BIOCOMPATIBLE ET ROBUSTE DE MEMBRANES DE CELLULOSE POUR LA PREPARATION ECOLOGIQUE ET ECONOMIQUE DE DISPOSITIFS D'IMMUNOANALYSE

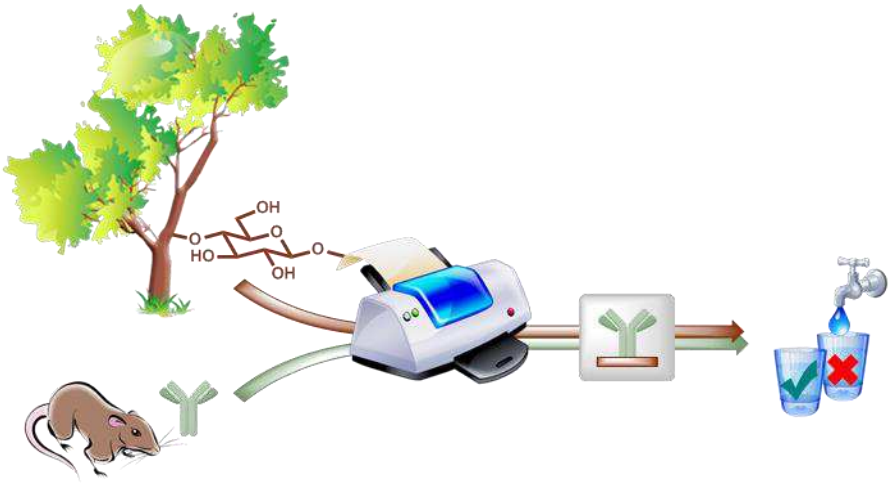

Soutenance prévue le 18 Septembre 2014 devant le jury composé de :

Dr. Vincent HUC	*Université Paris-Sud*	Rapporteur
Pr. Nicole JAFFREZIC	*Université Claude Bernard Lyon 1*	Rapporteur
Pr. Vincent SOL	*Université de Limoges*	Examinateur
Pr. Laura FIONI	*Ecole Polytechnique*	Examinateur
Dr. Thomas BERTHELOT	*CEA Saclay*	Directeur de Thèse

Acknowledgements

Ces travaux de thèse ont été réalisés au CEA de Saclay, dans le Laboratoire d'Innovation en Chimie des Surfaces et Nanosciences (CEA / DSM / IRAMIS / NIMBE / LICSEN) et le Laboratoire d'Études et de Recherches en Immunoanalyse (CEA / DSV / iBiTec-S / SPI / LERI).

Je tiens tout d'abord à remercier Serge Palacin et Hervé Volland de m'avoir accueillie dans leurs laboratoires respectifs (LCSI, ancêtre du LICSEN, et LERI). Merci d'avoir cru en ma capacité à mener à bien ce projet.

Je souhaite ensuite remercier tout particulièrement Thomas Berthelot, d'abord encadrant puis directeur de cette thèse, pour m'avoir guidée tout au long de ces trois années. S'il est facile pour un superviseur de pointer du doigt les choses qui ne conviennent pas, il paraît beaucoup moins naturel de féliciter un travail satisfaisant. Pourtant, Thomas a toujours su honorer cet aspect du travail d'encadrant et n'a jamais caché sa satisfaction devant les travaux accomplis, qu'il s'agisse de la rédaction d'articles ou de résultats d'expérimentations. Ce fut un aspect très appréciable de son encadrement. Il est très motivant de savoir que son travail est apprécié et estimé, que l'on vous fait confiance. Merci donc Thomas pour la confiance que tu m'as accordée au long de ces trois années.

J'aimerais ensuite remercier tous ceux qui m'ont consacré un peu (voire beaucoup) de leur temps et m'ont aidée au laboratoire. Tout d'abord, merci à Julie Dano pour m'avoir initiée aux manipulations de Biologie et transmis son savoir-faire dans l'élaboration de bandelettes de diagnostic. Un grand merci également à Elyse Yang pour m'avoir initiée à la bactériologie, avoir pris le temps de me coacher dans les manipulations et avoir répondu à toutes mes questions du mieux qu'elle pouvait. Merci à Xavier Lefevre pour avoir accompagné mes premiers pas dans le laboratoire de Chimie. Merci à Cédric Zobrist et son sbire Thibault Percerou, les magiciens du laboratoire, qui faisaient sortir les produits finis de leur chapeau…ou plutôt du frigo. Merci à Laure Fillaud pour m'avoir, le temps d'une journée, fais rencontrer les petits canards de l'électrochimie. Merci à Pascale Jegou et Jocelyne Leroy, les reines de l'XPS.

Je tiens également à remercier mes compagnons de galère, les autres doctorants - Jérôme Laporte, Ingrid Kikkas, Tiphaine Bourgeteau, Romain Brisse, Claire Soum - pour leur écoute et leur soutien tout au long de ces trois ans. Romain, je te laisse les clés du bureau. Tu es le nouveau concierge. J'espère que tu ne te sentiras pas trop seul pour les nocturnes. Claire, bon courage pour la fin. Tu es la prochaine sur la liste.

Je remercie également mes compagnons de nocturne au bâtiment de Biologie : Hervé Bernard et Alexandre Charcosset. Merci également aux compagnons de jour, notamment Karine Moreau pour sa bonne humeur communicative. Côté Chimie, merci aux sportifs : Bruno Jousselme, le roi du catch en mousse, et Guy Deniau, le spécialiste Rugby. Merci à la « Team Berthel' », en particulier à sa doyenne, Cécile Baudin, et à l'Anglais de l'équipe, Alexandre Causier. Merci aux LEMuriens avec qui nous avons fusionné : Vincent Derycke, notre nouveau chef, et Stéphane Campidelli, mon compatriote Ciel & Blanc (Vive le Racing !). Merci à tous les membres du LICSEN, aux stagiaires de passage que j'ai plus ou moins connus. Merci à « la maman » du labo, ou plutôt la marraine la bonne fée, Catherine Julien, pour son écoute, son soutien et son incroyable capacité à rendre les méandres de l'administratif moins tortueux.

Ensuite, je voudrais remercier chaleureusement ceux sans qui cette thèse n'aurait jamais commencé, Pascal Viel et Vincent Huc, et celle sans qui elle n'aurait pas fini aussi bien, Rita Faddoul. Docteur Faddoul ! Je ne saurais dire à quel point j'ai apprécié faire équipe avec toi pour cette dernière ligne droite. Merci pour tous ces moments passés ensemble au laboratoire, les discussions devant le MEB ou l'imprimante, les pauses (café ou non), et tes nombreux conseils. Et Vincent, merci d'avoir toujours été là quand j'en ai eu besoin, d'avoir été à l'écoute. Et un grand merci d'avoir accepté d'être rapporteur de cette thèse. Et merci de m'avoir présenté Pascal.

Je voudrais particulièrement adresser un énorme merci à Pascal Viel et Ekaterina Shilova pour leur soutien inconditionnel, au labo comme en dehors. Et pour ce qui est d'en dehors, je voudrais également remercier mes consultants en mécanique des matériaux et amis : Aurélien Souto Lebel, Benoît Beaubier, Pierre Gaborit et tous les membres du LMT-Cachan. Merci pour votre soutien moral tout au long de ces trois ans.

Pour finir, je voudrais remercier mes amis et ma famille de m'avoir épaulée et d'avoir supporté sans broncher mon mode de vie « aléatoire » pendant les phases de rédaction. Merci Maman pour les croq' de 6h du matin, et Stall pour les montagnes de vaisselle.

Ma dernière pensée ira à Christophe Agius qui, sans le savoir, m'a tenu compagnie pendant de longues nuits de rédaction.

Keywords

Point-of-care diagnostics; Bioactive Paper; Immunoassay; Biosensor; Cellulose; Surface Chemistry

Abstract

Since the *papyri*, cellulose has played a significant role in human culture, especially as paper. Nowadays, this ancient product has found new applications in the expanding sector of bioactive paper. Simple paper-based detection devices such as lateral flow immunoassays (LFIAs) are inexpensive, rapid, user-friendly and therefore highly promising for providing resource-limited settings with point-of-care diagnostics. Recently, paper-based biosensing technology has trended towards three-dimensional microfluidic devices and multiplexed assay platforms. Yet, many multiplexed paper-based biosensors implement methods incompatible with the conventional LFIA carrier material: nitrocellulose. It thus tends to be replaced by pure cellulose. This major material change implies to undertake a covalent immobilization of biomolecules on cellulose which preserves their biological activity.

Furthermore, the current global issues have stimulated the search for both ecologically and economically friendly (eco²-friendly) materials and processes. As a sustainable and affordable biopolymer, cellulose is an ideal material for developing diagnostic devices. However, the frame material is not the only aspect to consider. The whole device design and production, as well as the biosensing material immobilization or the non-sensing membranes treatment, should be as eco²-friendly as possible. Hence, the spatially controlled modification of cellulose surface seems crucial in the development of such devices since it enables to save expensive matter and to pattern surface properties. In any case, modification procedures should abide by the economic and ecological objectives aforementioned.

In this perspective, three processes allowing easy, robust and sustainable modification of cellulose sheets were developed. All are environmentally friendly, simple, time and cost-saving, and versatile.

The first procedure is a functionalization of cellulose membranes for covalent antibody immobilization. While cellulose chemical modification is usually operated under harsh conditions in organic solvents, the diazonium-based procedure developed was performed in water, at room temperature, in a single step. Paper sheets have thus been modified and bear different chemical functions which enable to graft biomolecules by common bioconjugate techniques and to perform LFIAs.

The second is a chemical-free photoimmobilization procedure which allowed antibodies to be immobilized on cellulose without any photocoupling intermediate nor any biomolecule or substrate pretreatment. This immobilization technique was further combined to inkjet printing to localize the antibodies according to any desired pattern. Native antibodies have thus been printed and immobilized on paper sheets which therefore enable to perform LFIAs. Membranes' performances were evaluated in terms of visual detection limit and challenged nitrocellulose performances.

The third is a modification of cellulose membranes by polymer grafting. Unlike the two previous processes, this technique was developed in order to increase the functionality of the non-sensing cellulose parts of paper-based devices. Yet, it may be employed as another functionalization method for covalent antibody immobilization on cellulose. While cellulose graft copolymerization is usually performed through complex and expensive procedures, the diazonium-based approach employed was performed in water, at room temperature, in a short single step. Cellulose sheets have thus been grafted with several acrylic polymers, first globally through a dipping procedure and then locally by inkjet printing.

All the strategies developed herein would be helpful to immobilize sensitive proteins on selected specific areas of cellulose sheets. More generally, these are powerful tools for easy and rapid modulation of cellulose surface properties according to complex designs, under soft and biocompatible conditions.

Contents

INTRODUCTION 11

CHAPTER 1 CELLULOSE: FROM BIOCOMPATIBLE TO BIOACTIVE MATERIAL 15

1. INTRODUCTION 17

2. CELLULOSE: A BIOCOMPATIBLE MATERIAL 18

2.1. FEATURES 18

2.1.1. Structure 18

2.1.1.1. Molecular structure 18

2.1.1.2. Supramolecular structure 19

2.1.1.3. Morphological structure 19

2.1.2. Bioavailability and fiber components 20

2.1.3. Biodegradability 22

2.2. PHYSICOCHEMICAL PROPERTIES 22

2.2.1. Mechanical properties: "the branch bends but does not break" 22

2.2.2. Chemical reactivity: functional cellulose derivatives 23

2.2.2.1. Oxidation 23

2.2.2.2. Amination 24

2.2.2.3. Esterification and etherification 24

2.2.2.4. Radical Copolymerization 24

2.3. FROM PAPYRUS TO NANOMATERIAL 25

2.3.1. Paper 26

2.3.2. Bioactive paper 26

3. BIOMOLECULE-BEARING CELLULOSE: A BIOACTIVE MATERIAL 27

3.1. PHYSICAL METHODS 27

3.1.1. Direct adsorption 28

3.1.2. Adsorption of carrier particles: bioactive inks 28

3.1.3. Confinement 29

3.2. BIOLOGICAL METHODS: BIOAFFINITY ATTACHMENT 29

3.2.1. Cellulose-binding domain (CBD) / Cellulose 29

3.2.2. Protein / Ligand 30

3.2.3. Protein A, G or L / Antibody 30

3.2.4. Metal ion / Chelator 30

3.3. CHEMICAL METHODS 31

3.3.1. Crosslinking 31

3.3.2. Direct covalent bonding 31

3.3.3. Bonding to a polymeric primer 33

4. SUMMARY AND OUTLOOK 33

REFERENCES 35

CHAPTER 2 A ONE-STEP AND BIOCOMPATIBLE CELLULOSE FUNCTIONALIZATION FOR COVALENT ANTIBODY IMMOBILIZATION ON IMMUNOASSAY MEMBRANES 41

1 INTRODUCTION 43

2 EXPERIMENTAL 44

2.1 REAGENTS AND MATERIALS 44

2.2 SPECTROSCOPIES 44

2.3 CELLULOSE MODIFICATION 45
2.4 GRAFTING OF ANTIBODIES 45
2.4.1 Paper activation: EDC/NHS activation of carboxyl groups 45
2.4.2 Paper activation: SATA derivatization of primary amine groups 45
2.4.3 Antibody activation: Preparation of maleimido-antibodies 45
2.5 IMMUNOASSAYS 45
2.5.1 Preparation of colloidal-gold-labeled antibodies 45
2.5.2 Detection of the grafted antibodies (incubation assay) 46
2.5.3 Detection of antigen by sandwich immunoassay (incubation assay) 46
2.5.4 Immunochromatographic strips (LFIA) 46

3 RESULTS AND DISCUSSION 46

3.1 ONE-STEP CELLULOSE SHEET FUNCTIONALIZATION UNDER SOFT CONDITIONS 46
3.2 COVALENT BINDING OF ANTIBODIES TO CELLULOSE PAPER SHEETS 48
3.3 CONSERVATION OF THE BIOLOGICAL ACTIVITY 49
3.4 USE IN LATERAL FLOW IMMUNOASSAY 50

4 CONCLUSIONS 51

REFERENCES 51

SUPPLEMENTARY MATERIAL 53

CHAPTER 3 CHEMICAL-FREE PHOTOIMMOBILIZATION OF ANTIBODIES ONTO CELLULOSE FOR THE PREPARATION OF IMMUNOASSAY MEMBRANES 55

1. INTRODUCTION 57

2. EXPERIMENTAL 58

2.1. REAGENTS AND MATERIALS 58
2.2. PHOTOIMMOBILIZATION OF ANTIBODIES 58
2.2.1. General procedure 58
2.2.2. Variable parameters 59
2.3. IMMUNOCHROMATOGRAPHIC ASSAYS (LFIA) 59
2.3.1. Preparation of colloidal-gold-labeled antibodies 59
2.3.2. Preparation of immunochromatographic strips 59
2.3.3. Evaluation of the immobilization rate 60
2.3.4. Evaluation of the activity rate 60
2.4. PHOTOIMMOBILIZATION OF PROBE ANTIBODIES 60

3. RESULTS AND DISCUSSION 60

3.1. OPTIMIZATION OF IMMOBILIZATION PARAMETERS 60
3.1.1. Photoenergy 60
3.1.2. Pre-irradiation drying step 61
3.1.3. Post-irradiation washing step 62
3.1.4. Wavelength 62
3.1.5. Optimal procedure 62
3.2. USE OF VARIOUS PAPER SUBSTRATES 63
3.3. AGEING OF THE MEMBRANES 63
3.4. STRENGTH OF THE IMMOBILIZATION 64
3.5. PROPOSED MECHANISM 64

4. CONCLUSION 64

REFERENCES 65

CHAPTER 4 INKJET PRINTING OF ANTIBODIES ONTO CELLULOSE FOR THE ECO²-FRIENDLY PREPARATION OF IMMUNOASSAY MEMBRANES 69

1. INTRODUCTION 71

2. EXPERIMENTAL 72

2.1. REAGENTS AND REACTION MATERIALS 72
2.2. CHARACTERIZATION MATERIALS 73
2.3. SUBSTRATES PRETREATMENT 73
2.4. IMMOBILIZATION PROCEDURE 73
2.4.1. Printing 73
2.4.2. Immobilization 74
2.5. IMMUNOCHROMATOGRAPHIC ASSAYS (LFIA) 74
2.5.1. Preparation of colloidal-gold-labeled antibodies 74
2.5.2. Preparation of immunochromatographic strips 74
2.5.3. Assessment of the immobilization 74
2.5.4. Assessment of the biological activity and determination of the visual detection limit 74
2.6. PATTERNED PHOTOIMMOBILIZATION OF PROBE ANTIBODIES 75

3. RESULTS AND DISCUSSION 75

3.1. LOCALIZED IMMOBILIZATION OF PROBE ANTIBODIES 75
3.2. FROM CLASSICAL AUTOMATIC DISPENSING TO INKJET PRINTING OF ANTIBODIES 75
3.3. INKJET PRINTING OF ANTIBODIES ONTO VARIOUS SUBSTRATES 76
3.3.1. Inks 77
3.3.1.1. Composition 77
3.3.1.2. Rheology 77
3.3.2. Initial substrates 77
3.3.2.1. Molecular structure 77
3.3.2.2. Surface chemical analysis 78
3.3.2.3. Surface morphological structure 78
3.3.3. Printed substrates 79
3.3.3.1. Surface chemical analysis 79
3.3.3.2. Surface morphological structure 80
3.3.4. Lateral Flow Immunoassays (LFIAs) 80
3.4. INKJET PRINTING OF COMPLEX DESIGNS 81

4. CONCLUSION 82

REFERENCES 82

CHAPTER 5 ONE-STEP AND ECO-FRIENDLY MODIFICATION OF CELLULOSE MEMBRANES BY POLYMER GRAFTING 87

1. INTRODUCTION 89

2. EXPERIMENTAL 90

2.1. REAGENTS AND REACTION MATERIALS 90
2.2. CHARACTERIZATION MATERIALS 90
2.3. CELLULOSE GRAFT COPOLYMERIZATION 90
2.3.1. Dipping procedure 90
2.3.2. Printing procedure 91
2.3.2.1. Ink formulation 91
2.3.2.2. Inkjet printing and graft copolymerization 91

3. RESULTS AND DISCUSSION 91

3.1. ONE-STEP CELLULOSE GRAFT COPOLYMERIZATION 91
3.1.1. Molecular level 91
3.1.2. Surface chemical analysis 92
3.1.3. Surface morphological structure 92
3.2. SPATIALLY CONTROLLED CELLULOSE GRAFT COPOLYMERIZATION 94
3.2.1. Ink behavior 95
3.2.2. Surface chemical analysis 95
3.2.3. Surface morphological structure 95
3.3. INKJET PRINTING OF COMPLEX PATTERNS 95
4. CONCLUSION 97
REFERENCES 97
CONCLUSION 101
REFERENCES 105

Introduction

Socio-economic context

In various domains such as clinical diagnosis [1–5], drug screening [6–9], food quality control [10–12], and environmental monitoring [13–16], there is a need for easy and rapid detection of target molecules. Several methods have been developed for manufacturing biosensors, biochips, microarray and other immunoassay devices [7,17–22]. According to the World Health Organization (WHO), diagnostic devices for developing countries should be **ASSURED**: **A**ffordable, **S**ensitive, **S**pecific, **U**ser-friendly, **R**apid and robust, **E**quipment free and **D**eliverable to end-users [1,23,24]. Furthermore, the current ecological and economic global issues have resulted in an increasing will for sustainable technologic development. Hence, the search for renewable-resources-based procedures and environmentally friendly materials and processes, as well as cost-saving approaches, has been stimulated widely [25].

Scientific context

As the main component of plant skeleton, cellulose is an almost inexhaustible raw material [26,27] and the most abundant form of worldwide biomass (about 1.5×10^{12} tons per year) [28]. It is therefore an affordable biopolymer with lots of appealing properties such as large bioavailability, good biodegradability and biocompatibility [26,27,29,30]. Moreover, cellulose is insoluble in most usual organic solvents. It swells but does not dissolve in water, hence enabling aqueous fluids and their contained components to penetrate within the fibers matrix and to wick by capillarity with no need for any external power source. With special regard to cellulose paper, porosity combined to biocompatibility allows biological compounds to be stored in the paper device [31]. Besides, cellulose sheets are available in a broad range of thicknesses and well-defined pore sizes, easy to store and handle, and lastly safely disposable [1,32,33]. All of its features make cellulose an ideal material for creating novel diagnostic devices and improving point-of-care (POC) testing [29]. Paper-based assays such as dipstick tests or lateral flow assays have already been marketed and extensively employed for point-of-care (POC) diagnostics and pathogen detection since the 80s (diabetes and pregnancy tests being the most famous) [24,34–40]. Yet, the recent impetus given to paper-based microfluidics by American, Canadian and Finnish research teams [41–43] has resulted in the development of new paper-based bioanalytical devices with complex designs allowing multiplex diagnosis [2,14,21,44–48].

The preparation of efficient immunoassay devices requires the robust immobilization of a large number of biosensing molecules on a support [49]. Because of its ability to immobilize all kind of proteins by a combination of electrostatic, hydrogen, and hydrophobic interactions involving the nitro functions displayed on its surface [37], nitrocellulose constitutes the most commonly used support material for preparing immunochromatographic devices [35–37,50]. However, nitrocellulose is an expensive, fragile and inflammable material [51,52], which was shown to be incompatible with most procedures implemented in the development of new multiplex biosensors such as lab-on-paper devices, microfluidic paper analytical devices (µPADs), or other paper-based analytical devices [7,21,33]. In addition, some agents such as spores and some *bacteria* may have difficulty in migrating along nitrocellulose. For these reasons, nitrocellulose tends to be replaced by cellulose [25,33].

Objectives

Several methods for immobilizing biomolecules onto cellulose are known. They may be classified into three major families which are presented in Chapter 1. Each of these methods displays specific advantages and drawbacks which are also discussed in this chapter. However, cellulose does not immobilize proteins by adsorption as well as nitrocellulose. Recent findings revealed that about 40% of antibody molecules adsorbed onto cellulose paper can actually desorb from the fibers [53]. Direct adsorption of antibodies onto cellulose is therefore too weak to allow the permanent immobilization required in the development of effective immunoassay [49]. Biomolecules should therefore be covalently bound to the paper [32,49] and thus cellulose needs to be functionalized or activated [32,54,55]. Ideally, chemical covalent bonding should be conducted in mild conditions, with few side reactions, in few steps, with a minimum denaturation of the immobilized biomolecule which needs to keep its original functionality [32,49]. There is therefore an ongoing need for time and cost-saving methods allowing immunoassay devices to be prepared by robust and sustainable binding of biomolecules to cellulose.

Furthermore, the frame material and the resulting method for immobilizing biomolecules onto it are not the only aspects to consider. The whole device design and production, as well as the biosensing material dispensing or the non-sensing

membranes treatment, should be as ecologically and economically friendly (eco²-friendly) as possible. There is therefore a growing need for proteins immobilization methods and cellulose modification techniques allowing to save significant amounts of reagents, solvents and adjuvants. Hence, the spatially controlled modification of cellulose surface seems crucial in the development of such devices since it enables to save expensive matter and to pattern surface properties [56]. In any case, modification procedures should abide by the economic and ecological objectives aforementioned.

Achievements

In this perspective, three processes allowing easy, robust and sustainable modification of cellulose sheets were developed. All are environmentally friendly, simple, time and cost-saving, and versatile. The first procedure (Chapter 2) is a functionalization of cellulose membranes for covalent antibody immobilization. While cellulose chemical modification is usually operated under harsh conditions in organic solvents, the diazonium-based procedure developed was performed in water, at room temperature, in a single step. Paper sheets have thus been modified and bear different chemical functions which enable to graft biomolecules by common bioconjugate techniques and to perform LFIAs. The second (Chapter 3) is a chemical-free photoimmobilization procedure which allowed antibodies to be immobilized onto cellulose without any photocoupling intermediate nor any biomolecule or substrate pretreatment. This immobilization technique was further combined to inkjet printing to localize the antibodies according to any pattern desired (Chapter 4). Native antibodies have thus been printed and immobilized onto paper sheets which therefore enable to perform LFIAs. Membranes' performances were evaluated in terms of visual detection limit and challenged nitrocellulose performances. The third is a modification of cellulose membranes by polymer grafting (Chapter 5). Unlike the two previous processes, this technique was developed in order to increase the functionality of the non-sensing cellulose parts of paper-based devices. Yet, it may be employed as another functionalization method for covalent antibody immobilization onto cellulose. While cellulose graft copolymerization is usually performed through complex and expensive procedures, the employed diazonium-based approach was performed in water, at room temperature, in a short single step. Cellulose sheets have thus been grafted with several acrylic polymers: first globally through a dipping procedure and then locally by inkjet printing. All the strategies developed herein would be helpful to immobilize sensitive proteins on selected specific areas of cellulose sheets. More generally, these are powerful tools for easy and rapid modulation of cellulose surface properties according to complex designs, under soft and biocompatible conditions.

Outline

To sum up, this work focuses on the eco²-friendly preparation of paper-based immunoassay devices by means of simple and sustainable modification of cellulose membranes. To this end, Chapter 1 first provides an overview of cellulose structural features and physicochemical properties and then reviews current techniques for the immobilization of biomolecules onto cellulose membranes. Then, two aspects of paper-based immunoassay devices were considered: on one hand, the biosensing material immobilization and resulting membranes' performances (Chapter 2 to Chapter 4); and on the other hand, the modification of the non-sensing membranes' properties (Chapter 5) (see Figure 1). Hence, the two methods developed for immobilizing proteins are described in Chapter 2 and Chapter 3. Chapter 4 emphasizes the advantages of using inkjet printing as biomolecule dispensing technique and displays the results of its combination to the immobilization method described in Chapter 3. Finally, Chapter 5 presents the polymer grafting method elaborated to increase cellulose functionality.

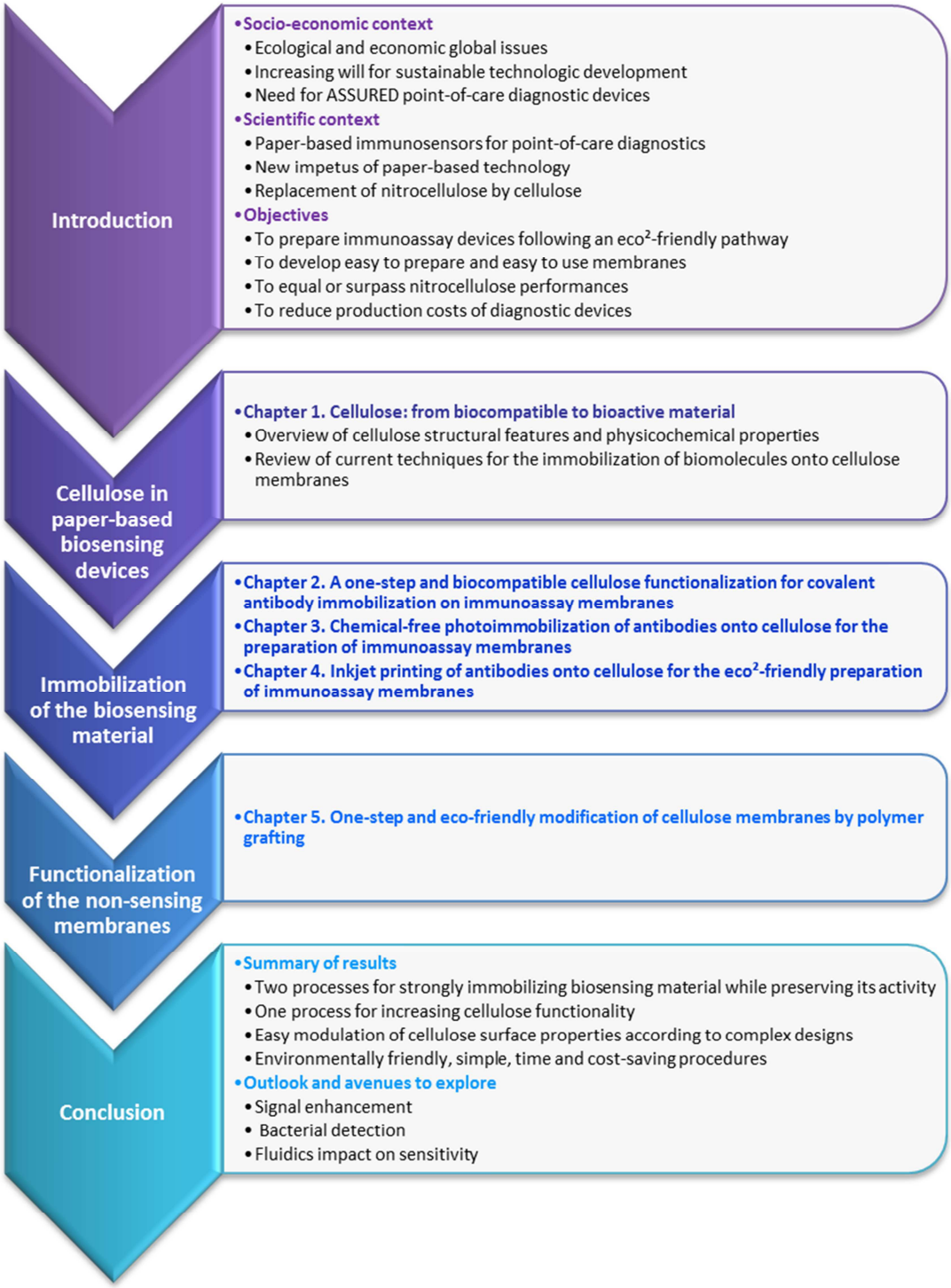

Figure 1: General outline

Chapter 1 Cellulose: from biocompatible to bioactive material

Contents

1. INTRODUCTION 17

2. CELLULOSE: A BIOCOMPATIBLE MATERIAL 18

2.1. FEATURES 18

2.1.1. Structure 18

2.1.1.1. Molecular structure 18

2.1.1.2. Supramolecular structure 19

2.1.1.3. Morphological structure 19

2.1.2. Bioavailability and fiber components 20

2.1.3. Biodegradability 22

2.2. PHYSICOCHEMICAL PROPERTIES 22

2.2.1. Mechanical properties: "the branch bends but does not break" 22

2.2.2. Chemical reactivity: functional cellulose derivatives 23

2.2.2.1. Oxidation 23

2.2.2.2. Amination 24

2.2.2.3. Esterification and etherification 24

2.2.2.4. Radical Copolymerization 24

2.3. FROM PAPYRUS TO NANOMATERIAL 25

2.3.1. Paper 26

2.3.2. Bioactive paper 26

3. BIOMOLECULE-BEARING CELLULOSE: A BIOACTIVE MATERIAL 27

3.1. PHYSICAL METHODS 27

3.1.1. Direct adsorption 28

3.1.2. Adsorption of carrier particles: bioactive inks 28

3.1.3. Confinement 29

3.2. BIOLOGICAL METHODS: BIOAFFINITY ATTACHMENT 29

3.2.1. Cellulose-binding domain (CBD) / Cellulose 29

3.2.2. Protein / Ligand 30

3.2.3. Protein A, G or L / Antibody 30

3.2.4. Metal ion / Chelator 30

3.3. CHEMICAL METHODS 31

3.3.1. Crosslinking 31

3.3.2. Direct covalent bonding 31

3.3.3. Bonding to a polymeric primer 33

4. SUMMARY AND OUTLOOK 33

REFERENCES 35

Credou, J.; Berthelot, T.

Cellulose: from biocompatible to bioactive material.

J. Mater. Chem. B 2014. DOI: 10.1039/C4TB00431K.

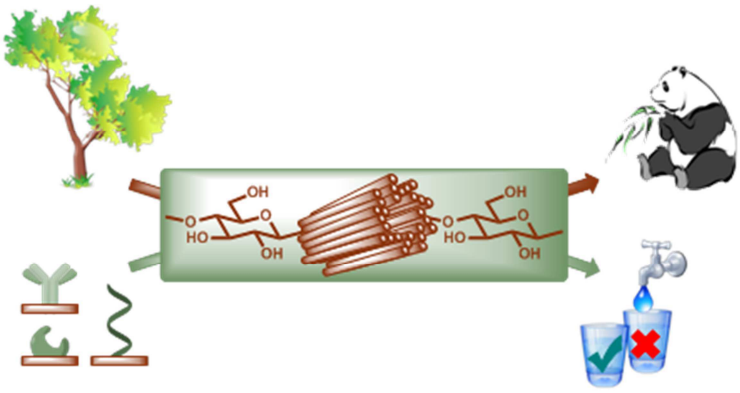

The immobilization of biomolecules onto cellulose paper turns this environmentally friendly material into a platform for diagnostic devices.

Journal of
Materials Chemistry B

FEATURE ARTICLE

View Article Online
View Journal

Cellulose: from biocompatible to bioactive material

Julie Credou and Thomas Berthelot*

Cite this: DOI: 10.1039/c4tb00431k

Since the *papyri*, cellulose has played a significant role in human culture, especially as paper. Nowadays, this ancient product has found new scientific applications in the expanding sector of paper-based technology. Among paper-based devices, paper-based biosensors raise a special interest. The high selectivity of biomolecules for target analytes makes these sensors efficient. Moreover, simple paper-based detection devices do not require hardware or specific technical skill. They are inexpensive, rapid, user-friendly and therefore highly promising for providing resource-limited settings with point-of-care diagnostics. The immobilization of biomolecules onto cellulose is a key step in the development of these sensing devices. Following an overview of cellulose structural features and physicochemical properties, this article reviews current techniques for the immobilization of biomolecules on paper membranes. These procedures are categorized into physical, biological and chemical approaches. There is no universal method for biomolecule immobilization. Thus, for a given paper-based biochip, each strategy can be considered.

Received 18th March 2014
Accepted 8th May 2014

DOI: 10.1039/c4tb00431k

www.rsc.org/MaterialsB

1. Introduction

Cellulose is the most abundant organic chemical on earth. This natural polymer was first mentioned by the French chemist Anselme Payen in 1838.[1] He suggested that the cell walls of almost all plants are constructed of the same substance. He described that a resistant fibrous solid remains behind after treatment of various plant tissues with ammonia and acids, and after subsequent extraction with water, alcohol and ether. By elemental analysis, he deduced its molecular formula to be $C_6H_{10}O_5$. The term "cellulose" was first used one year later in a report of the French Academy of Sciences on Payen's work.[2,3]

The current economic and ecological situations have led to an increasing ecological awareness and a growing will for sustainable technologic and economic development. Thus, scientists are urged to search for environmentally friendly materials and renewable resources. As the main component of

CEA Saclay, IRAMIS, NIMBE, LICSEN (Laboratory of Innovation in Surface Chemistry and Nanosciences), F-91191 Gif sur Yvette, France. E-mail: julie.credou@cea.fr; thomas.berthelot@cea.fr; Fax: +33 169084044; Tel: +33 169086588

Julie Credou entered the Ecole normale supérieure de Cachan (ENS Cachan) in 2007. She received her MSc degree in Chemistry from ENS Cachan and Paris-Sud University in 2011. She is currently a PhD student in the Laboratory of Innovation in Surface Chemistry and Nanosciences (LICSEN) at the French Alternative Energies and Atomic Energy Commission (CEA) (Saclay, France). Under the supervision of Dr Thomas Berthelot and Dr Hervé Volland, her work focuses on the development of paper-based immunosensors for point-of-care diagnostic applications.

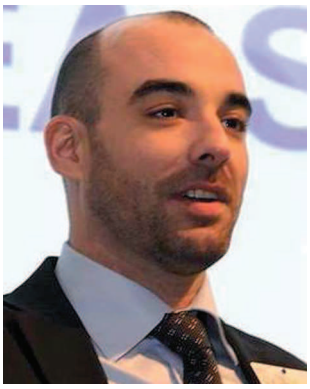

Dr Thomas Berthelot obtained his PhD in Organic Chemistry in 2005 in the Bordeaux I University after interdisciplinary studies at the frontier of Biology and Chemistry. In 2006, he joined the French Alternative Energies and Atomic Energy Commission (CEA) for a post-doctoral fellowship to develop biomimetic polymer membranes for fuel cells. In 2007, he was appointed permanent CEA researcher and he participated in the creation of a surface chemistry start-up (Pegastech SA, France). He currently works at the Laboratory of Innovation in Surface and Nanosciences (LICSEN). His research focuses in NanoMedicine. He is the (co)author of more of than 30 peer review articles in international journals and 24 patents.

plant skeleton, cellulose is an almost inexhaustible raw material.[4,2] It is therefore a key source of sustainable materials.[5] Moreover, thanks to its biocompatibility and biodegradability, cellulose is gaining more and more importance and appears as a grade one material.[6] Apart from its large bioavailability and good biodegradability, cellulose has lots of appealing features. It is rigid, highly crystalline, insoluble in common organic solvents, and therefore an ideal structural engineering material.[6] With special regard to cellulose paper, its wicking properties enable components to travel by capillarity with no need for any external power source. In addition, its biocompatibility and porosity allow biological compounds to be stored in the paper device.[7] Besides, cellulose sheets are inexpensive, available in a broad range of thicknesses and well-defined pore sizes, easy to store and handle, and finally safely disposable.[8]

Because of all these features, a new technological sector has developed and has kept growing within the last ten years: paper-based technology.[9] Paper has attracted scientists' interest since the 19th century. The first urine test strips were developed by the French chemist Jules Maumené in 1850[10] and marketed by the English physiologist George Oliver in 1883.[11,12] A century later, in 1943, Martin and Synge invented paper chromatography[13,14] in order to analyze the amino-acid content of proteins. Contemporaneously, in 1949 Müller and Clegg carried out a study on the preferential elution of a mixture of pigments in a restricted channel designed on paper,[15] hence laying the technical basis of paper-based microfluidics. Few years later, in 1957, the first paper-based bioassay used an enzyme immobilized onto paper in order to detect glucose in urine.[16] In 1982, paper-based immunoassays such as dipstick tests or lateral flow immunoassays (LFIAs) were further developed and marketed.[17–20] They were then extensively employed for point-of-care (POC) diagnostics and pathogen detection,[21,22] with diabetes and pregnancy tests being the most famous.[23,24] Recently, further impetus was given to paper-based microfluidics by Whitesides' research group with the development of three-dimensional microfluidic paper analytical devices (μPADs).[25] This opened the way to many other multiplex paper-based analytical devices.[26–33] Meanwhile, the Sentinel Bioactive Paper Network was formed in Canada in 2005,[34] thereby setting the paper-based bioassay as a whole new section of biosensing research. Thus, cellulose is not anymore the "fibrous solid that remains behind", it is a material platform used to create novel devices for diagnostics, microfluidics, and electronics.

According to the World Health Organization (WHO), diagnostic devices for developing countries should be ASSURED: **A**ffordable, **S**ensitive, **S**pecific, **U**ser-friendly, **R**apid and robust, **E**quipment free and **D**eliverable to end-users.[21,35,36] The aforementioned appealing characteristics of cellulose therefore give paper-based devices a great potential to comply with these requirements and to improve point-of-care (POC) testing. Besides, it would be only logical for this natural biopolymer which is available anywhere to be readily available for use everywhere it is needed.

Among paper-based devices, bioactive papers raise a special interest because they can be useful in many fields including clinical diagnosis[28,35,37,38] and environmental monitoring.[29,39–41] They are the main materials for developing paper-based point-of-care (POC) diagnostic devices and therefore will be the main subject of this paper. Thus, this review focuses on the way to develop a bioactive material from the biocompatible cellulose material. We will therefore concentrate on cellulose as a support for biomolecule immobilization. After describing the related cellulose features such as fiber physicochemical properties, we will then present the existing strategies for biomolecule immobilization onto pure cellulose.

2. Cellulose: a biocompatible material

According to IUPAC Recommendations 2012, biocompatibility is defined as the ability to be in contact with a living system without producing an adverse effect.[42] As a ubiquitous natural biopolymer, cellulose is by definition a biocompatible material.

2.1. Features

2.1.1. Structure. As a polymer, cellulose is a macromolecule and therefore needs to be defined on three structural levels: molecular, supramolecular and morphological levels. On the molecular level, cellulose is described as a single macromolecule. Its chemical constitution, its reactive sites and its potential intramolecular interactions are considered. On the supramolecular level, cellulose is described as a pack of several macromolecules interacting and ordering each other. Importance is attached to aggregation phenomena, crystalline organization and fibrils formation. On the morphological level, structural entities formed by cellulose are described. Layouts made of different supramolecular arrangements are studied.

2.1.1.1. Molecular structure. Cellulose possesses the simplest structure among polysaccharides since it is composed of a unique monomer: glucose under its β-D-glucopyranose form (Fig. 1). Cellulose is a polydisperse, linear, syndiotactic polymer. Glucose molecules are covalently linked through acetal functions between the equatorial hydroxyl groups of C4 and the C1 carbon atoms. This succession of glycosidically linked anhydroglucose units (AGUs) results in a long chain β-1,4-glucan.[2,3,6]

The chain length, also called the degree of polymerization (DP), is expressed as the number of AGUs constituting the chain. The average DP value not only depends on the origin of the raw material, but also on the potential extraction treatments. For example, cellulose from wood pulp has average DP values around 300 and 1700. In the case of cotton and other

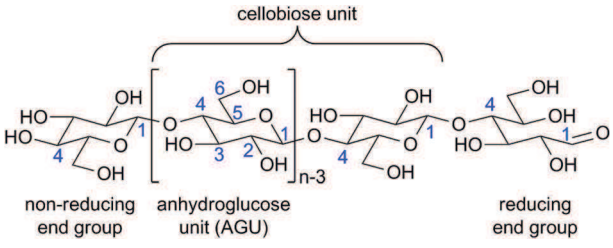

Fig. 1 Cellulose molecular structure (n = DP, degree of polymerization).

plant fibers, DP values range from 800 to 10 000. Similar values are reported in bacterial cellulose.[2]

Each AGU ring adopts the $^4C_1$ chair conformation (Fig. 2). Since the ring substituents and the glycosidic bonds are all in the ring plane (equatorial), this conformation ensures the less van der Waals and steric repulsion between them. It is the most stable conformation and thus the thermodynamically preferred conformation. To comply with this conformation and to accommodate the preferred bond angles of the acetal bridges, adjacent AGUs have their mean planes at an angle of 180° to each other. Hence, two adjacent AGUs define the disaccharide cellobiose (Fig. 1).[2,6]

Furthermore, both ends of the cellulose chain are different (Fig. 1). At one end, the glucose unit is still a closed ring and displays an original C4–OH group. This is the non-reducing end. At the other end, both pyranose ring structures (cyclic hemiacetal) displaying an original C1–OH group and an aldehyde structure are in equilibrium (Fig. 3), thereby conferring reducing properties. This is the reducing end.

As a result of the glucose structure, cellulose contains a large amount of free hydroxyl groups located at the C2, C3, and C6 atoms. These hydroxyl groups, together with the oxygen atoms of both the pyranose ring and the glycosidic bond, form an extensive hydrogen bond network. This network is composed of both intra- and intermolecular hydrogen bonds. While the intramolecular hydrogen bonds are partly responsible for the linear integrity and rigidity of the polymer chain, intermolecular hydrogen bonds result in crystalline structures and other supramolecular arrangements. The main intramolecular hydrogen bond is the O3H–O5′ bond; it is shared by most allomorphs. O2H–O6′ hydrogen bonds also occur in some allomorphs. Both are shown in Fig. 4[6,43]

2.1.1.2. Supramolecular structure. Pure cellulose exists in several allomorphic forms. Native cellulose I crystallized simultaneously in two forms in which chains are packed in parallel: I_α and I_β. On the other hand, chains in regenerated or mercerized cellulose II are arranged antiparallel. Treatment of cellulose I and II with liquid ammonia leads to cellulose III_1 and III_2, respectively, and each allomorph may be converted back to the starting cellulose material. Heat treatment of cellulose III_1 and III_2 leads to cellulose IV_1 and IV_2, respectively, which can also be converted back to the original cellulose.[44]

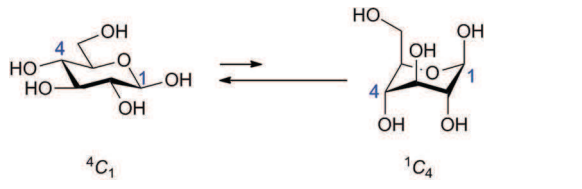

Fig. 2 β-D-glucopyranose conformations.

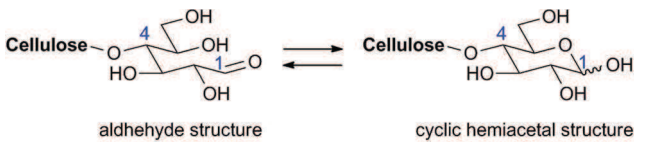

Fig. 3 Reducing end equilibrium.

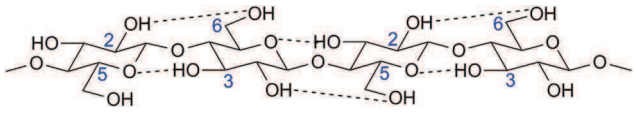

Fig. 4 Intramolecular hydrogen bonding in cellulose.

With respect to cellulose I, the I_α/I_β *ratio* depends on the origin of the cellulose. The I_β form prevails in woody plants and cotton whereas the I_α form dominates in primitive organisms such as *bacteria* or *algae*.[3,45] Cellulose I_α has a triclinic unit cell including one chain whereas I_β has a monoclinic unit cell including two parallel chains. The I_β form is thermodynamically more stable than the I_α form.

Cellulose II is the most stable among cellulose crystal structures. This allomorph can be produced from cellulose I by mercerization (treatment with aqueous sodium hydroxide) or by dissolution and following precipitation (regeneration of a crystalline form of cellulose). This transformation is considered to be irreversible.[43] Cellulose II has a monoclinic unit cell which includes two antiparallel chains.[2]

As stated above, intermolecular hydrogen bonds are greatly responsible for the supramolecular structure of cellulose. They make the chains group together in a highly ordered structure. Cellulose I and II differ by their inter- and intramolecular hydrogen bonds, resulting in different packings: parallel and antiparallel, respectively (Fig. 5). The main intramolecular O3H–O5′ hydrogen bond is shared by both polymorphs. The intramolecular O2H–O6′ hydrogen bond only occurs in cellulose I (both I_α and I_β). Cellulose I has O6H–O3″ intermolecular hydrogen bonds whereas cellulose II has O6H–O2″ intermolecular hydrogen bonds.[2,3]

The chains are usually longer than the crystalline regions. As a consequence, one chain can run from one crystalline region to another, passing through amorphous areas, and thereby holding the ordered regions together.[46,47] The intermolecular hydrogen bonds in the crystalline regions are strong, hence ensuring the resultant fiber is strong as well and insoluble in most solvents. They also prevent cellulose from melting. In the amorphous regions, the intermolecular hydrogen bonds are fewer and looser, enabling the chains to form hydrogen bonds with other molecules such as water. This imparts macromolecular cellulose its hygroscopic and hydrophilic features. Thus, cellulose swells but does not dissolve in water.[46]

Cellulose fibers have amorphous and crystalline regions. Their *ratio*, or crystallinity rate, depends on the origin of cellulose. Cotton, flax, ramie and sisal have high degrees of crystallinity which range from 65% to 70% whereas crystallinity of regenerated cellulose only ranges from 35% to 40%.[6]

2.1.1.3. Morphological structure. Gathering different supramolecular arrangements of cellulose (crystalline and amorphous areas) results in fibrillar elements of nanometer-scale diameters and micrometer-scale lengths.[43,48] These are called fibrils or microfibrils. Assembling these microfibrils together

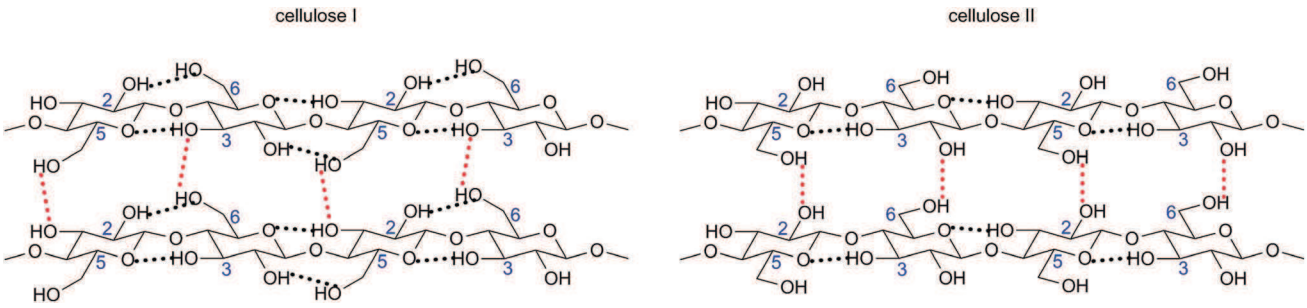

Fig. 5 Supramolecular distinction between cellulose I and cellulose II lies in inter- and intramolecular hydrogen bonds.

results in macrofibrils of micrometer-scale diameters and millimeter-scale lengths. Micro- and macrofibrils represent the building block of the cellulose fiber cell wall.

Plant fibers consist of different cell-wall layers (primary and secondary walls, middle *lamellae*) surrounding the central lumen. The lumen takes part in the water uptake behavior of plant fibers. The primary cell wall must be capable of growth and therefore be flexible. The secondary cell wall has to be rigid in order to avoid buckling.[49] The secondary cell wall accounts for approximately 80% of the entire cell wall thickness. It therefore determines the mechanical properties of the fiber.[46,50] The secondary cell wall is made up of three layers. The thickest is the middle layer which consists of a series of helically wound cellular microfibrils. The angle between the fiber axis and the microfibrils is called the microfibrillar angle. Its average value varies from one fiber to another. Features of each cell-wall layer are provided by the particular fibrillar layout and the amount of other components such as lignin (see next Section 2.1.2).[6,43]

Thus, cellulose forms the basic material of all plant fibers. Fig. 6 presents how cellulose molecules and resultant fibrils take part in the cell walls of plant fibers.

2.1.2. Bioavailability and fiber components. Cellulose is the most abundant form of worldwide biomass.[51] It is the main material of plant cell walls, and therefore the most important skeletal component in plants. Apart from plants which are the dominant cellulose suppliers, cellulose is also produced by *algae*, *bacteria* and *fungi*. Thus, about 1.5×10^{12} tons are biosynthesized annually, thereby leading cellulose to be considered an almost inexhaustible polymeric raw material.[2]

The conventional sources of cellulose are wood pulp and cotton linters.[6] The seed hairs of the cotton plant provide cellulose in almost the pure form. In contrast, the cell wall of woody plants provides a composite material mainly made of cellulose, hemicelluloses and lignin. It may also contain pectin, extractives such as waxes, or even proteins.[2,4,6]

Hemicelluloses are water soluble polysaccharides of low degree of polymerization (100–200). While cellulose is a linear homopolymer of glucose, hemicelluloses are branched heteropolymers made of many different sugars such as glucose, mannose, galactose, xylose and arabinose (see the most abundant sugar monomers in Fig. 7). Sugar *ratio* changes from plant to plant.[3,6]

As for lignin, this is a non-linear polymer made of phenylpropanoid units. Its whole structure has not been fully resolved yet (see monomers and a representative fragment structure in Fig. 8) and its monomer *ratio* changes from plant to plant as well. While cellulose is the main building block of wood, lignin is the cement which binds the wood cells together. It is covalently linked to hemicellulose and thus crosslinks polysaccharides, thereby giving rigidity to the plant.[6,52] In addition, lignin plays a key role in controlling the water content within the cell wall and conducting water in plant stems. Whereas polysaccharides of plant cell walls are highly hydrophilic and thus permeable to water, lignin contains both hydrophilic and

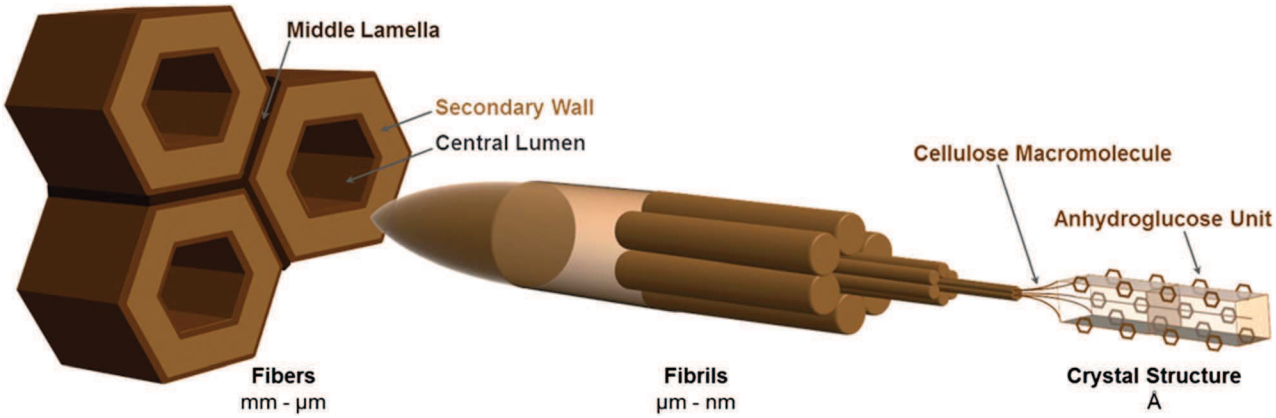

Fig. 6 Contribution of cellulose to the cell wall of plant fiber.

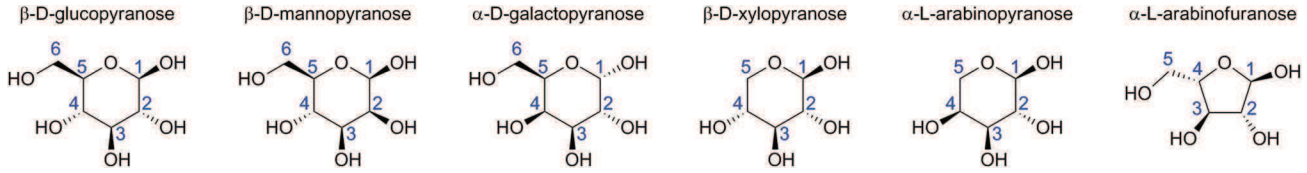

Fig. 7 The most abundant monomers of wood hemicelluloses.

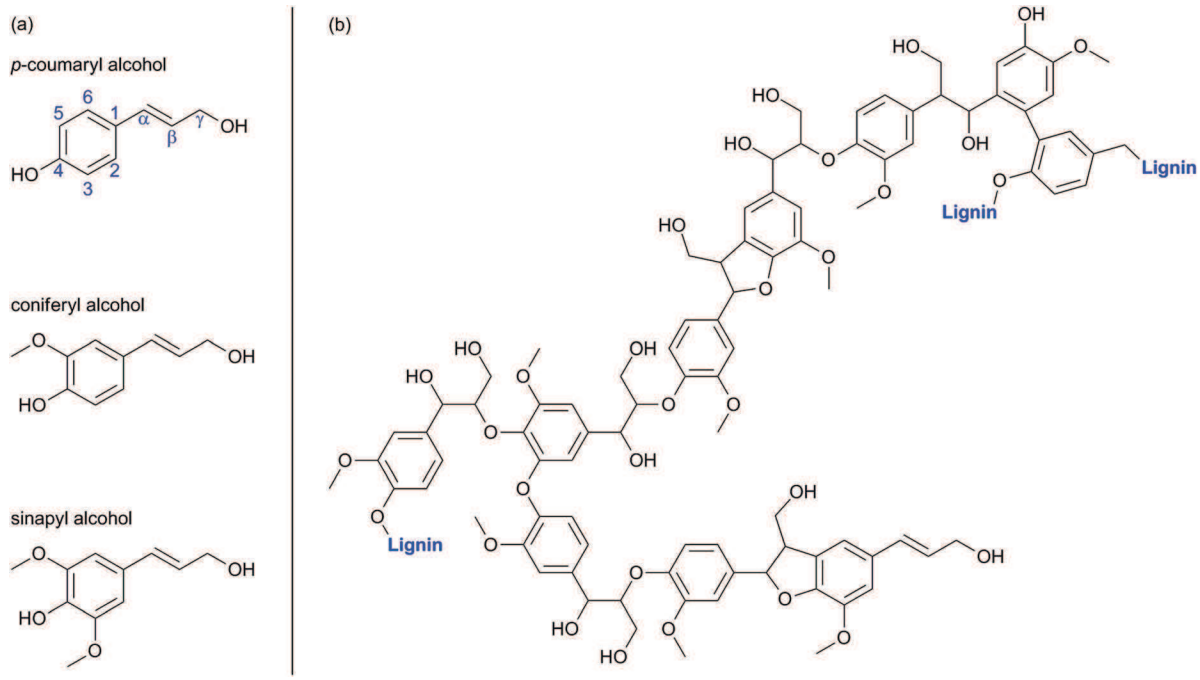

Fig. 8 (a) The three monomers of lignin. (b) A representative fragment of the lignin structure.

hydrophobic groups which make it much less hydrophilic. Since lignin is crosslinked between polysaccharides, it stands in the way and prevents water absorption into the cell walls, thereby enabling water driving. Finally, because of its aromatic nature, lignin is mainly responsible for the color in wood. This feature appears as a drawback regarding papermaking industry. That is why processes such as pulping and bleaching have been developed in order to remove lignin from the wood matrix (see Section 2.3.1).[3]

Pectins are complex heteropolysaccharides mainly composed of (1 → 4)-α-D-galacturonic acid residues. The most abundant pectic polysaccharide is a linear homopolymer of 1,4-linked-α-galacturonic acid called homogalacturonan. The other pectic polysaccharides are made of a backbone of 1,4-linked-α-galacturonic acid residues decorated with side branches consisting of different sugars and linkers.[53] These backbone and sugars are presented in Fig. 9. The amount, structure and composition of pectins vary from plant to plant, but also within a plant depending on the location and the age. Pectins are soluble in alkaline water. They provide flexibility to plants. They also play a role in plant growth, development, morphogenesis, defense, cell–cell adhesion, wall structure, signaling, cell expansion, wall porosity, binding of ions, growth factors and enzymes, pollen tube growth, seed hydration, leaf abscission, and fruit development.[6,53]

The protein content of wood cells is usually low (less than 1%), but can be higher in some grasses. The encountered proteins are structural proteins such as hydroxyproline-rich glycoproteins, glycine-rich proteins and proline-rich proteins.[4]

The extractives are all substances resulting from wood extraction processes that are not an integral part of the cellular structure. They are made soluble by extraction processes and can be removed by dissolution in solvents that do not dissolve cellulose such as water, ether, alcohol or benzene. The extractive content of the wood material is about 2 to 5%.[3] Extractives can be chemicals such as fats, fatty acids, fatty alcohols, phenols, terpenes, steroids, resin acids, rosin, waxes, *etc.* These chemicals may be encountered as monomers, dimers or polymers.[4] Waxy layers contribute to render the fiber impermeable to water.

All these alien substances associated with the cellulose matrix are important and should be kept in mind when further dealing with cellulose chemical modifications. Indeed, they occur naturally in cellulose-containing materials and their *ratio* depends on the source of the cellulose (see distribution of these additives within some typical cellulose-containing materials in

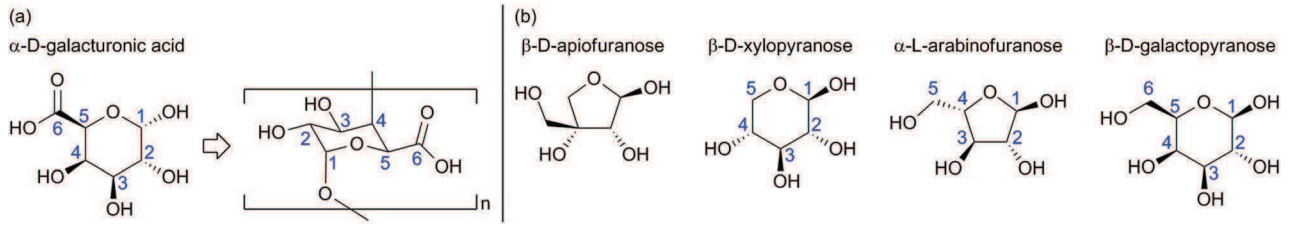

Fig. 9 (a) Galacturonic backbone of pectins. (b) The most abundant sugars of pectins.

Table 1).[43] Thus, depending on the source of the cellulose material and the effectiveness of the purification process, these compounds may occur in the final cellulose product and eventually interfere with cellulose chemical modification.

2.1.3. Biodegradability. The increasing ecological awareness and the growing will for sustainable technologic and economic development have stimulated the search for environmentally friendly materials. In particular, the waste disposal problem has to be addressed quickly. These trends have tempted a large part of scientists to search for materials that can be easily biodegraded or bioassimilated.[6] To these scientists, cellulose therefore appears as a grade one material.

First of all, it is important to notice that cellulose is digestible by all grass-, leave- and wood-eating species, such as cows, pandas, beetle *larvae* and termites. This ability results from a lignocellulose-degrading symbiotic ecosystem located in their digestive tract. This ecosystem consists of *bacteria* or *protozoa* depending on the species which produce enzymes dedicated to break down cellulose.[54–57] The main glycolytic enzymes involved in the biological conversion of cellulose to glucose are endoglucanases, cellobiohydrolases and β-glucosidases. While endoglucanases randomly hydrolyze 1,4-β bonds along the cellulose chains, cellobiohydrolases split off cellobiosyl units from non-reducing end groups and β-glucosidases cleave glucosyl units from non-reducing end groups.[54] There are also other enzymes which are dedicated to hydrolyze the other compounds from plant cell walls such as hemicellulase and xylan 1,4-β-xylosidase.[55,57]

Some *fungi* are also able to break down cellulose. Actually, *fungi* are among the most degradative organisms inducing biodeterioration of paper-based items.[58] Many fungal species (over 200) are involved in paper biodeterioration. The effectiveness and the rate of the deterioration process are affected by environmental conditions (*e.g.* temperature, humidity, light).[59,60] Their main strength is that a single cell is enough to induce proliferation over most solid surfaces. Moreover, they can be "sleeping" for years as spores and then be reactivated under a certain set of conditions.[61]

Because of its sustainability, biocompatibility and biodegradability, cellulose is a material of growing interest to the current economic and ecological climate.

Table 1 Chemical composition of some typical cellulose-containing materials

	Composition (%)			
Source	Cellulose	Hemicellulose	Lignin	Extract
Cotton	95	2	1	0.4
Flax (retted)	71	21	2	6
Jute	71	14	13	2
Hemp	70	22	6	2
Corn cobs	45	35	15	5
Hardwood	43–47	25–35	16–24	2–8
Softwood	40–44	25–29	25–31	1–5
Bagasse	40	30	20	10
Coir	32–43	10–20	43–49	4

2.2. Physicochemical properties

2.2.1. Mechanical properties: "the branch bends but does not break". As stated above, plant cell walls are responsible for the proper growth and structural integrity of plants. As their main component, cellulose plays a key role in the shape and mechanical strength of living plants.[49,62]

Yet, the term strength may not make much sense by itself. In the informal language strength is synonymous with solidity, firmness or rigidity. But actually, the mechanical definition of the strength of a material mainly takes two properties into consideration: (i) the stiffness of the material, which is measured by its Young's modulus and (ii) the tensile strength (or ultimate tensile strength) of the material, which is the maximum stress that a material can withstand while being stretched before breaking. Considering that "the branch bends but does not break" means that plant fibers have low Young's modulus but high tensile strength. The main asset of cellulose fiber is therefore its resilience.

The tensile strength and Young's modulus of commercially important fibers are detailed in Table 2.[50,63,64] Cellulose fibers have relatively high strength (tensile strength), medium stiffness (Young's modulus), and low density. Considering their lower density, the natural fibers compare quite well with glass fiber, but are not as strong as carbon fibers or Kevlar.

Mechanical tests of whole plant or solid wood (macroscopic scale) provide information about their elementary mechanical properties which are partly influenced by tissue interactions. Additionally, the tensile testing of single cellulose fiber provides more information about the effects of the cell-wall structure on the mechanical properties of plant fiber.[50] The tensile strength of elementary fibers is about 1500 MPa. Their Young's modulus depends on their diameter. It ranges from 39 GPa to 78 GPa for fibers having diameters from 35 μm to 5 μm, respectively. From bulk natural fibers to cellulose molecules, the elastic modulus

Table 2 Mechanical properties of natural fibers compared to so-called "strong materials"

Fiber	Density (g cm^{-3})	Tensile strength (MPa)	Young's modulus (GPa)	Elongation at break (%)
Cotton	1.5–1.6	287–597	5.5–12.6	7.0–8.0
Wood fibers (spruce latewood)	—	530–675	20.8–60.1	—
Rayon	1.6	500	40	1.25
Flax	1.5	351	28.5	2.5
Hemp	1.48	820	29.6	3.5
Jute	1.5	579	26.2	1.5
Viscose (cord)	—	593	11.0	11.4
Aramid (Kevlar 49)	1.45	2900	130	2.5
Carbon (NM)	1.86	2700	380	0.7
E-glass	2.54	2200	70	3.1
Portland cement concrete	2.2–2.4	2–5	14–41	—

values range as follows: 10 GPa for wood bulk fiber, 40 GPa for cellulose fiber (after pulping process), 70 GPa for microfibril, and 250 GPa for the cellulose chain (from theoretical calculations).[46] In other words: "the smaller, the stronger".

2.2.2. Chemical reactivity: functional cellulose derivatives. According to the molecular structure of cellulose (Fig. 1), hydroxyl groups in glucose units are responsible for its chemical activity. Under heterogeneous conditions their reactivity may be affected by their inherent chemical reactivity and by steric hindrance stemming either from the reagent or from the supramolecular structure of cellulose itself.[47] Therefore, the accessibility and reactivity of the hydroxyl groups depend on their degree of involvement in the supramolecular structure. In other words, it depends on their involvement in the hydrogen bond network. Intramolecular hydrogen bonding between adjacent AGUs particularly affects the reactivity of the C3 hydroxyl group, which hydrogen binds strongly to the ring oxygen on adjacent AGUs (O3H–O5′ hydrogen bond) whatever the allomorph and is therefore not available to react.[6] In contrast, C2 and C6 hydroxyl groups have multiple and variable options to hydrogen bind, what may result in a lower statistical involvement in the hydrogen bond network, and thus a higher reactivity.[3] Among the three hydroxyl groups in each glucose residue, the one at 6-position (primary alcohol) is described as the most reactive site, far more than hydroxyl groups at 2- and 3-positions (secondary alcohols). However, the relative reactivity of the hydroxyl groups can be generally expressed in the following order: OH–C6 $\gg$ OH–C2 > OH–C3.[47]

The accessibility to these reactive hydroxyl groups also depends on the crystalline structure of the fiber. Chemical reagents cannot penetrate the crystalline regions but only the amorphous area (see Section 2.1.1.2).[47] Activation treatments can enhance the accessibility and the reactivity of cellulose for subsequent reactions. These treatments implement methods such as (i) widening surface *cannulae*, internal pores and interfibrillar interstices, (ii) disrupting fibrillar aggregation, in order to make available additional areas, (iii) troubling the crystalline order, and (iv) modifying the crystal form and therefore changing the hydrogen bonding scheme and the relative availability of the reactive hydroxyls. Among all activation treatments, swelling is the most frequently used procedure and aqueous sodium hydroxide solution is the most common swelling agent. Swelling agents usually penetrate the ordered regions, and split some hydrogen intermolecular bonds. After alkali treatment (such as mercerization), the structure of native cellulose fibers stays fibrillar but the degree of disorder increases, and so does the accessibility.[47]

When cellulose chemically reacts through its hydroxyl groups, the average number of hydroxyl groups per glucose unit that have been substituted defines the degree of substitution (DS) of the cellulose derivatives. Thus, its value ranges from 0 to 3. Because of the relative reactivity and accessibility of the hydroxyl groups, this value is often lower than two, though. Besides, it is not desirable to have all of these hydroxyl groups react in order to keep the structure cohesion and integrity.[65] Considering that the DS value is often between 0 and 1.5,[66] it is laborious to determine if we are only grafting small molecules onto cellulose.[65]

The ways used to modify the chemical composition of synthetic polymers cannot be applied to natural cellulose because regarding cellulose these features are determined by biosynthesis. Chemical modifications have to be conducted on the whole cellulose polymer. Though, introducing functional groups in the final polymer is a way around the problem. These functional groups may impart new properties to the cellulose without destroying its many appealing intrinsic properties.[47]

Many approaches to cellulose functionalization already exist,[67] and many others are under development.[8,68,69] This review focuses on cellulose as a support for biomolecule immobilization and its use for diagnostic devices. Therefore, not all the chemical modifications of cellulose will be presented here. Instead we will concentrate on the chemical modifications which play a role in biomolecule immobilization (see Section 3).

2.2.2.1. Oxidation. Carbonyl and carboxyl groups are very useful for biomolecule immobilization since they can react with primary amines from biomolecules to form imine and amide bonds, respectively (see Section 3.3.2). Carbonyl groups are already present at the reducing end of cellulose chains. Additional carbonyl and carboxyl groups may stem from extraction and purification processes.[2] Yet, those are not sufficient for functionalization and biomolecule immobilization purposes. Therefore, more carbonyl or carboxyl groups would be obtained by oxidation of the hydroxyl groups from the cellulose. Depending on the experimental conditions, the oxidation may be accompanied by the opening of the pyranose ring (Fig. 10).[70]

The most used method of forming carbonyl groups onto the cellulose skeleton is periodate oxidation. Secondary alcohol groups of the glucose units (OH–C2 and OH–C3) are oxidized into the corresponding aldehydes by means of sodium periodate ($NaIO_4$).[40,71,72] This method results in the opening of the pyranose ring by cleavage of the C2–C3 bond (Fig. 10b). Hence, the cellulose structure is locally affected. Depending on the oxidation rate, this may disrupt the linearity of the chain and the supramolecular arrangement to a certain extent.

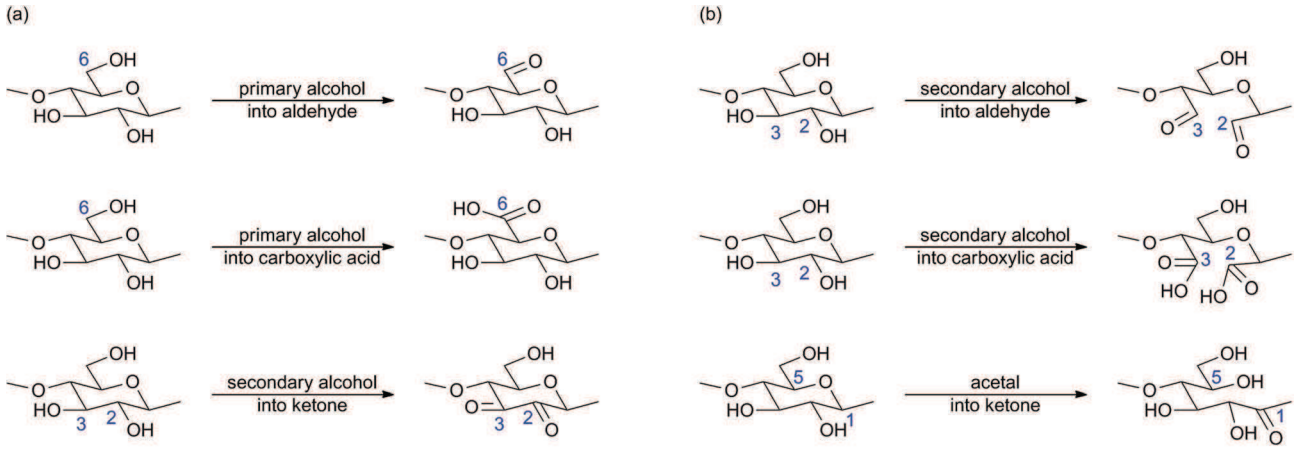

Fig. 10 Main oxidation reactions of cellulose (a) without ring opening and (b) with ring opening.

The usual method of forming carboxyl groups onto the cellulose chain is TEMPO-mediated oxidation. Primary alcohol groups from cellulose (OH–C6) are oxidized into the corresponding carboxylic acids by means of sodium bromide (NaBr), sodium hypochlorite (NaClO) and (2,2,6,6-tetramethyl-piperidin-1-yl)oxyl free radical (TEMPO).[73–75] In this manner, the pyranose ring is not affected by the process and cellulose keeps its structural integrity (Fig. 10a).

2.2.2.2. Amination. Amination of cellulose was used to covalently bind nitrilotriacetic acid (NTA) onto a cellulose film.[76] After loading these films with nickel cations (Ni^{2+}), it is therefore possible to immobilize His-tagged proteins by bioaffinity attachment and develop biosensors or purification systems (see Section 3.2.4).

The amination process implements a complex procedure since usually both cellulose and amino compound added need to be activated before they can react with each other. However, the synthesis of the NTA-modified cellulose was achieved in two main steps: (i) the activation of the primary hydroxyl group from cellulose (OH–C6), and (ii) the S_N2 nucleophilic substitution of this activated hydroxyl by an activated NH_2-terminal NTA derivative (amination process). Fig. 11 illustrates the amination process resulting in nitrilotriacetic acid (NTA)-modified aminocellulose.

First, hydroxyl groups were activated by tosylation. Cellulose was dissolved in a solution of lithium chloride in *N*,*N*-dimethylacetamide (DMA/LiCl) which is the most important solvent system for cellulose in organic synthesis.[2] Tosyl chloride (Ts-Cl) was added, together with triethylamine (Et_3N). The average DS value for the tosylation step was 1.45.[76] On the other hand, the NH_2-terminal NTA derivative was activated by persilylation with trimethylsilyl chloride (TMS-Cl) in toluene in the presence of triethylamine. This activated NTA derivative finally reacted with the cellulose tosylate in a DMSO/toluene mixture (S_N2). This amination procedure resulted in NTA-cellulose. The average DS value for the amination reaction was 0.45.[76]

2.2.2.3. Esterification and etherification. Cellulose esters and cellulose ethers are the most important technical derivatives of cellulose.[2] They find their applications in many industrial sectors including coatings, pharmaceuticals, foodstuffs and cosmetics (Table 3).[47,69,77]

With regard to biomolecule immobilization, cellulose nitrate (also named nitrocellulose) is the most important cellulose derivative. Biomolecules strongly adsorb to nitrocellulose through a combination of electrostatic, hydrogen, and hydrophobic forces.[20] It is therefore the reference material for performing lateral flow immunoassay (LFIA)[18–20,78] (see Section 2.3.2). Cellulose nitrate is formed by esterification of hydroxyl groups from cellulose (primary or secondary) with nitric acid (HNO_3) in the presence of sulfuric acid (H_2SO_4), phosphoric acid (H_3PO_4) or acetic acid (CH_3COOH) (see Fig. 12).[47,67]

Carboxymethyl cellulose (CMC) is another important cellulose derivative used in biomolecule immobilization. It is often coated and strongly (some might say irreversibly[79]) adsorbed onto cellulose (see Section 3.3.3). Thus, it provides carboxyl groups without oxidizing cellulose, thereby avoiding disruption of the hydrogen bond network and breach of the structural integrity. CMC is produced by etherification of hydroxyl groups from cellulose (primary or secondary) with monochloroacetic acid in the presence of sodium hydroxide (NaOH). Cellulose is first activated with sodium hydroxide in order to enhance the reactivity of the hydroxyl groups as electron donors.[43] Then the activated hydroxyl groups will substitute the chloride groups from monochloroacetic acid to yield CMC (see Fig. 13).[80,81]

2.2.2.4. Radical Copolymerization. Cellulose copolymers can be used for enhancing the rate of functional moieties on the cellulose surface. Therefore, they provide lots of anchoring points for biomolecule immobilization.[82,83]

Copolymer grafting onto cellulose is usually performed by free radical polymerization of vinylic compounds. For initiating a graft side chain, a radical site has to be formed on the cellulose backbone. This radical can stem from the homolytic bond cleavage within the glucose unit caused by high-energy irradiation for example, from the decomposition of a functional group such as peroxide, or from a radical transfer reaction initiated by a radical formed outside the cellulose backbone during a redox reaction. The grafting is usually conducted on a solid cellulose substrate with the monomer being in solution.[47,67]

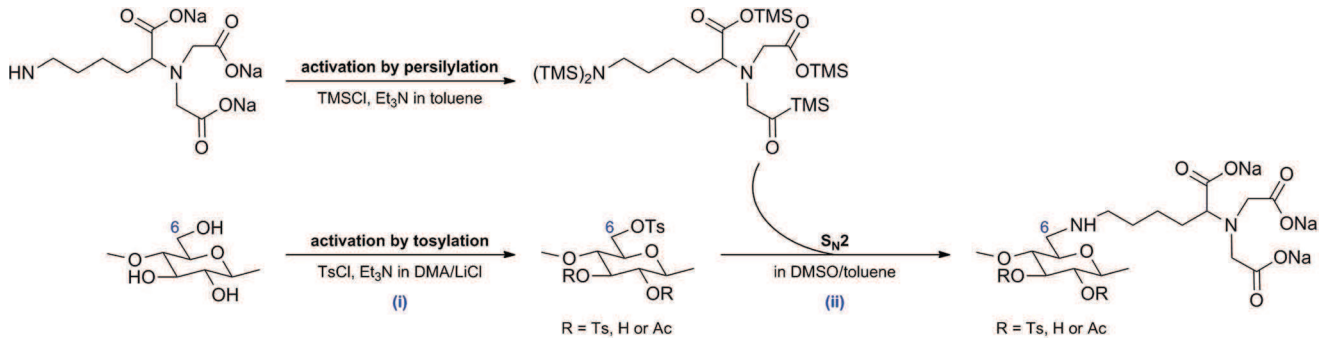

Fig. 11 Synthesis of nitrilotriacetic acid (NTA)-modified amino-cellulose.

Table 3 Important cellulose esters and ethers commercially produced

Cellulose derivative	Worldwide production (tons per year)	Functional moiety	Application
Cellulose xanthate	3 200 000	–C(S)SNa	Textiles
Cellulose acetate	900 000	$-C(O)CH_3$	Coatings and membranes
Cellulose nitrate	200 000	$-NO_2$	Membranes and explosives
Carboxymethyl cellulose (CMC)	300 000	$-CH_2COONa$	Coatings, paints, adhesives and pharmaceuticals
Methyl cellulose	150 000	$-CH_3$	Films, textiles, food and tobacco industry
Hydroxyethyl cellulose	50 000	$-CH_2CH_2OH$	Paints, coatings, films and cosmetics
Ethyl cellulose	4000	$-CH_2CH_3$	Pharmaceutical industry

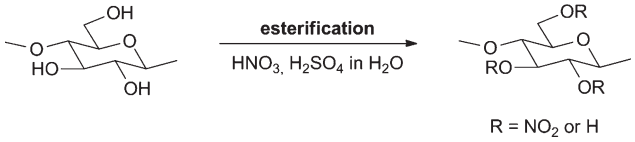

Fig. 12 Esterification of cellulose into nitrocellulose.

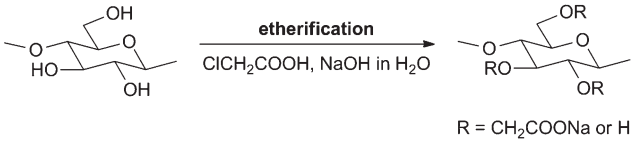

Fig. 13 Etherification of cellulose into carboxymethyl cellulose.

There are many approaches to covalent attachment of polymers to surfaces. They can be classified into the following three categories: (i) the "grafting-to" method, where a pre-formed polymer is coupled with the functional groups that are located on the cellulose backbone, (ii) the "grafting-from" method, where copolymer chains grow from initiating sites on the cellulose backbone, and (iii) the "grafting-through" method, where the cellulose bares a polymerizable group, and hence acts as a macromonomer with which a smaller monomer copolymerizes. Among these three methodologies, the "grafting-from" approach is the most commonly used procedure.[47,65]

With regard to the polymer grafted for the biomolecule immobilization purpose previously mentioned,[82,83] the methodology adopted is the "grafting from" technique. An initiator molecule is employed to start a radical transfer reaction and initiate the copolymerization. The initiator can be either in solution with the monomer[83] or previously grafted to cellulose.[82]

2.3. From papyrus to nanomaterial

Since the Egyptian *papyri*, cellulose has played a significant part in human culture. For thousands of years, wood, cotton and other plant fibers were indispensable materials for clothing and building. For a long time, cellulose has been widely used as a vehicle for the acquisition, storage and dissemination of human knowledge and cultural heritage.[58,84]

The use of this biopolymer as a chemical raw material began 160 years ago with the discovery of the first cellulose derivatives. Subsequently, the global production of cellulose rocketed and the cellulose processing industries such as textile industry received a great impetus by taking advantage of the chemical processes in order to improve their products quality.[2,85]

Nowadays, this ancient material has found new applications and has adopted new forms. For example, cellulose beads (micro- to millimeter scale particles frequently named microspheres, pellets or pearls) are used in many technologic and scientific applications such as chromatography, solid-supported synthesis, protein immobilization or retarded drug release.[72,86] Moreover, since current scientific research heads towards nanomaterials, it is only logical to now encounter nanocellulose (actually fibrils, see Section 2.1.1.3) and cellulose nanocomposites.[5,6,46,87]

But among all these new forms, and through all these years, paper is still by far the dominating cellulose product.[45] It has

even found its place in science with the growing area of paper-based technology.[9]

2.3.1. Paper. Paper was invented during the 2nd century A.D. in China and, independently, during the 7th century A.D. in Mesoamerica. The art craft of making paper spread from the Far East to the Western World in the Middle Ages, and for centuries, cultural resources have been accumulating in archives, libraries and museums worldwide.[84]

Paper is produced from a dilute aqueous suspension of cellulose fibers that is drained through a sieve, pressed and dried, to yield a sheet formed by a network of randomly interwoven fibers. The paper composition varies depending on the process applied, *i.e.* depending on the production period and the technology employed. In Europe during the Middle Ages, paper was made up of pure cellulose fibers from cotton, linen or hemp, usually obtained from rags (long fibers), and animal glue was added as a sizing agent.[84]

In contrast, contemporary paper is manufactured from wood and resultant short fibers containing hemicelluloses and lignin. The process of turning wood into paper is complex and involves many stages.[88] From wood to paper pulp the main steps are: logging, debarking, chipping, screening, pulping, washing, bleaching, and washing. Then, from pulp to paper sheet, there are beating, pressing, drying and rolling.[3] Among these, pulping and bleaching are the most important since they aim at removing lignin, hemicelluloses and other alien substances associated with cellulose within the wood fibers (see Section 2.1.2). Yet these are chemical steps and may affect cellulose integrity. Pulping involves alkaline conditions using hydroxide (HO^-) or sulfanide (HS^-) whereas bleaching employs chlorine, chlorine dioxide, oxygen, ozone or hydrogen peroxide. These treatments may induce a thermal-oxidative stress in polysaccharides, resulting in the formation of various chromophores into the cellulosic pulp.[89] Moreover during this long and complex process, many additives are used to improve paper properties. There are mineral particles (talc, kaolin, calcium carbonate, titanium dioxide, *etc.*) for the whitening purpose, sizing agents such as alkyl ketene dimer (AKD) and alkenyl succinic anhydride (ASA), dry-strength agents, *etc.*[61,88,90,91] Thus, depending on the production process, these compounds may occur in the final cellulose product and eventually affect its physico-chemical properties.

2.3.2. Bioactive paper. It took scientists about seventeen centuries to make paper their own. They started to use it as a material platform for diagnostic devices during the 19th century.[10–12] Although paper-based bioassays such as dipsticks and lateral flow immunoassays (LFIAs) were marketed and extensively employed since the 1950s,[16–20] the term "bioactive paper" appeared only a few years ago, when the Sentinel Bioactive Paper Network was formed in Canada in 2005,[34] and the VTT Technical Research Centre of Finland started its bioactive paper project.[92]

A bioactive paper can be defined as a paper-based product bearing active biomolecules. It is a key component for developing simple, inexpensive, handheld and disposable devices.[93–95] Bioactive papers can be useful in many fields including clinical diagnosis,[28,35,37,38] environmental monitoring[29,39–41] and food quality control.[96–98] The high selectivity of biological entities (such as antibodies or enzymes) for target analytes enables bioactive papers, particularly paper-based biosensors, to be efficient sensors and powerful recognition devices.[41] Moreover, simple paper-based detection devices do not require either any hardware or any specific technical skill. They are inexpensive, rapid and user-friendly and therefore highly promising for providing remote locations and resource-limited settings with point-of-care (POC) diagnostics. Therefore, paper-based biosensors have recently attracted a strong interest.

Dipsticks and lateral flow immunoassays (LFIAs) have already been widely used for point-of-care (POC) diagnostics and pathogen detection,[21,22] with diabetes and pregnancy tests being the most famous.[23,24] Lateral flow immunoassays (LFIAs) ensure specific and sensitive measurements of target analytes by means of the high specificity of the antibody–antigen (Ab–Ag) interaction.[18,100,101] Moreover the simplicity, portability and affordability of these colorimetric detection devices make them ASSURED (Affordable, Sensitive, Specific, User-friendly, Rapid and robust, Equipment-free, and Deliverable to end-users) point-of-care diagnostic devices.[18,19,22,38]

Within the last ten years, the biosensing field has trended towards three-dimensional microfluidic devices and multiplexed assay platforms (Fig. 14).[26–33] An effort has also been made to develop quantitative point-of-care assays.[102] Multiplex assay allows detection of several analytes per sample in a single run by simultaneously carrying out multiple separate assays in discrete regions of the device. To enable more simultaneous detection while avoiding any cross-contamination, the frame material of a multiplex device needs to be patterned with microfluidic channels distributing fixed and equal volumes of a single sample to independent test zones. Regarding paper-based multiplex devices, it means either defining hydrophobic barriers and hydrophilic channels on a piece of cellulose paper or shaping the paper by cutting.[95] Several methods for patterning paper sheets have been developed.[30,95] Among the many processes are photolithography, using SU-8 or SC photoresist,[25,35,99,103] "wax printing" or "wax dipping",[104–106] inkjet printing[107] and laser cutting.[108,109]

Nitrocellulose is the classical material for biomolecule immobilization in LFIAs.[18–20,78] However, this cellulose derivative is relatively expensive, crumbly, flammable[110,111] and cannot withstand most of procedures implemented in the development of new multiplex sensors,[8,30,95] mostly because many of them include a step in which the paper temperature rises above 100 °C.[104,99] This is why the new multiplexed bioassay platforms tend to replace nitrocellulose by pure cellulose which is much more convenient to handle and more safely disposable.[8] Moreover, its bioavailability and biodegradability make cellulose a very attractive material regarding the current economic and ecological climate.

Finally, efficient paper-based bioassays require membranes where biosensing entities such as antibodies are numerous and strongly immobilized.[93] Besides, the immobilization strategy greatly influences biosensor properties.[112,113] The immobilization of biomolecules onto cellulose paper is therefore a key step

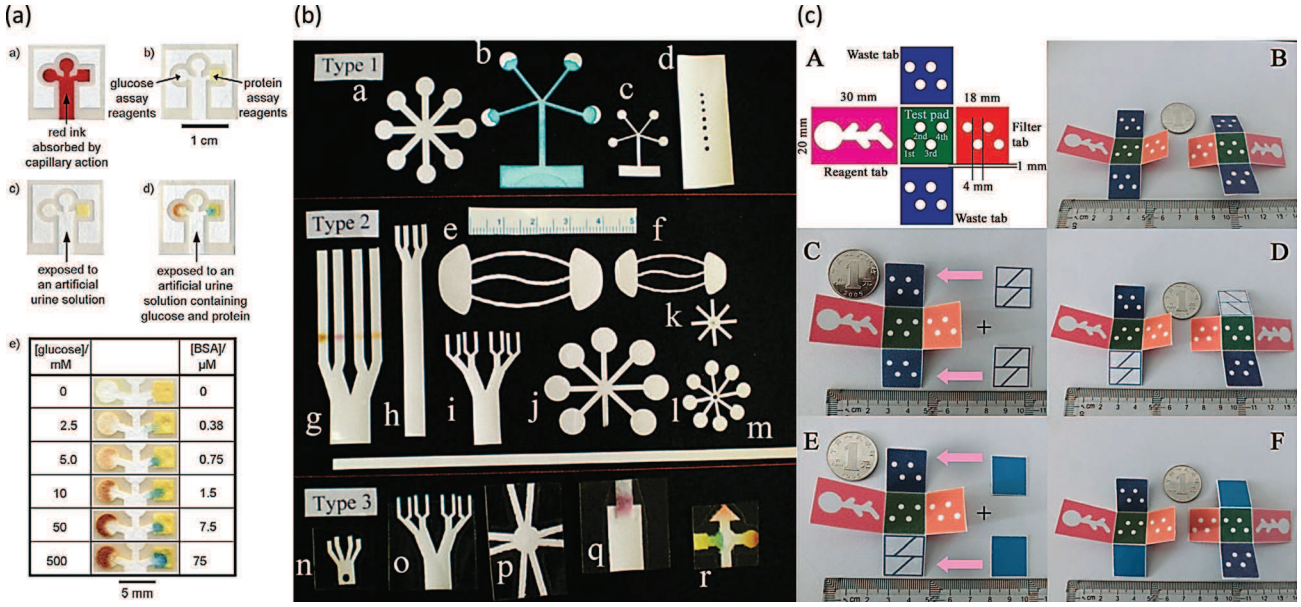

Fig. 14 Few multiplexed assay platforms (a, b and c) and three-dimensional microfluidic device (c) (with (a) reprinted with permission from ref. 99, Copyright © 2007 WILEY-VCH Verlag GmbH & Co. KGaA, Weinheim; (b) reprinted with permission from ref. 26, Copyright 2009 American Chemical Society; (c) reproduced from ref. 33).

in the development of such paper-based sensing devices and bioactive papers in general. Many procedures exist and the following part of this article reviews and categorizes the current techniques for the immobilization of biomolecules onto pure cellulose. A lot of these approaches are not specific to cellulose and can also be conducted on other substrates such as gold or glass. Thus, the methodologies exposed will sometimes be very general. But all the processes presented and all the reactions mentioned thereafter were performed on the pure cellulose substrate.

3. Biomolecule-bearing cellulose: a bioactive material

Immobilization of biomolecules on a solid support has many advantages.[114] It simplifies purification procedures and downstream processing, enables saving and reusing these quite expensive macromolecules and improves their stability.[114–116] Thus, it is often a prerequirement for their utilization in commercial scale processes.[116,86] A few established large-scale applications for immobilized biocatalysts are shown in Table 4.

Immobilization of a molecule can be defined as its attachment to a surface leading to reduction or loss of its mobility.[112] Random orientation and structural deformation of biomolecules during immobilization may reduce their biological activity.[117] Thus, immobilization pathway significantly influences biosensor or biochip properties.[112,113] The main objective should therefore be to control not only the location and density of biomolecules, but also their tertiary structure and their orientation, in order to fully retain or even enhance their biological activity.[94,112] However, there is no universal immobilization method. For a given biochip, the choice of the most appropriate immobilization strategy should take into consideration the physicochemical and chemical properties of both surfaces and biomolecules,[112] the type of transduction used, the nature of the sample intended to be tested and the possibility of multiple use of the sensor.[93,113] Reproducibility, cost and complexity of the immobilization process also need to be considered, especially if industrialization is planned.[113]

With regard to cellulose-based biosensors, immobilization methods which are compatible with automated coating and printing techniques facilitate large-scale and low-cost applications.[93] Cellulose is a rather inexpensive biopolymer, but biomolecules are expensive and must be used efficiently. They should be retained on the extreme surface of the paper substrate in order to be more easily and more quickly accessible to the target, and most importantly in order to concentrate the sensing signal in a visible area (within 10 μm deep).[93,94,118]

There are many approaches to attachment of biomolecules to cellulose. They can be classified into the following three categories: (i) physical methods, where the biomolecule is confined to the support surface because of physical forces (*e.g.* van der Waals, electrostatic or hydrophobic interactions and hydrogen bonding), (ii) biological or biochemical methods, where the biomolecule is bound to the substrate because of biochemical affinity between two components (*e.g.* Ni^{2+}/His-tag, streptavidin/biotin, protein G/human IgG), and (iii) chemical methods, where covalent bonds fix the biomolecule to the support surface.

3.1. Physical methods

Physical methods have the advantage of keeping denaturation of the immobilized biomolecules to a minimum.[119,120] There are conducted in very few steps, with no chemical modifications of

Table 4 Large scale industrial processes using immobilized biomolecules

Enzyme	Process	Production (tons per year)
Glucose isomerase	High fructose corn syrup from corn syrup	10^7
Nitrile hydratase	Acrylamide from acrylonitrile	10^5
Lactase	Lactose hydrolysis, GOS synthesis	10^5
Lipase	Transesterification of food oils	10^5
	Biodiesel from triglycerides	10^4
	Chiral resolution of alcohols and amines	10^3
Penicillin G acylase	Antibiotic modification	10^4
Aspartase	L-Aspartic acid from fumaric acid	10^4
Thermolysin	Aspartame synthesis	10^4

either the surface or the biomolecule. They are therefore simple, fast and economical.

However, the bond between the biomolecule and the cellulose surface is weak and temporary. Biomolecules tend to leak from the support resulting in a gradual loss of biosensor activity. Overloading the support with biomolecules may compensate for leakage, but would increase the cost of the device. In addition, the physical interactions binding biomolecules to the substrate are nonspecific[120,121] and lead to random orientation.[112,113]

Fig. 15 presents the three main physical approaches to immobilization of biomolecules onto cellulose.

3.1.1. Direct adsorption. Adsorption is the simplest immobilization method. The biomolecule and the support are directly bound by reversible noncovalent interactions such as van der Waals, electrostatic or hydrophobic interactions or hydrogen bonding.[113] The strength of the bond therefore varies depending on the interactions at work. Hydrophobic interactions are strong and may cause structural changes in the adsorbed biomolecules and eventually result in the loss of activity.[94,120] Considering that cellulose is hydrophilic and slightly anionic (see structure in Fig. 1), adsorption results from van der Waals forces, hydrogen bonding and ionic interactions depending on the experimental conditions.[47,93] Thus, proteins readily adsorb onto cellulose *via* their cationic patches and tyrosine groups, whereas DNA is repulsed because of its anionic phosphate groups.[93,94] But, whatever conditions picked, interactions at work are not strong enough to ensure permanent immobilization and prevent biomolecules from leaking from cellulose. Moreover, the density of adsorbed biomolecules is often low.[93]

The procedure consists of placing the support in contact with the biomolecules, under suitable conditions of pH and ionic strength for a fixed period of incubation. The support is then thoroughly rinsed to eliminate the non-immobilized species.[121]

This method is hardly used to develop cellulose-based biosensors[32,37,99,122–126] because the amount of molecules adsorbed onto cellulose varies a lot depending on the nature of the biomolecule.[127] Many of them will actually desorb from the fibers (about 40% for antibody molecules).[119,128] It is therefore difficult to perform sensitive and reproducible analysis this way. Hence, this method is mostly used when biomolecules need to be released, as in blood typing.[128–131]

3.1.2. Adsorption of carrier particles: bioactive inks. This method can be considered as a variant to direct adsorption. A component does adsorb onto cellulose because of physical interactions, but it is not the biomolecule itself. It is a carrier particle onto (or into) which the biomolecule is immobilized. Suspensions of such colloidal particles loaded with biomolecules are called bioactive inks. They can be printed, coated or even added during the paper-making process.

This technique has an advantage over classical physisorption: playing with particle size makes it possible to concentrate biomolecules onto exterior surfaces of porous papers.[93] Usually used papers have particle retention ranging from 2.5 to 40 μm.[128,131,132] Thus, antibodies (about 24 nm lateral)[133] or enzymes easily go through the fiber lattice. In

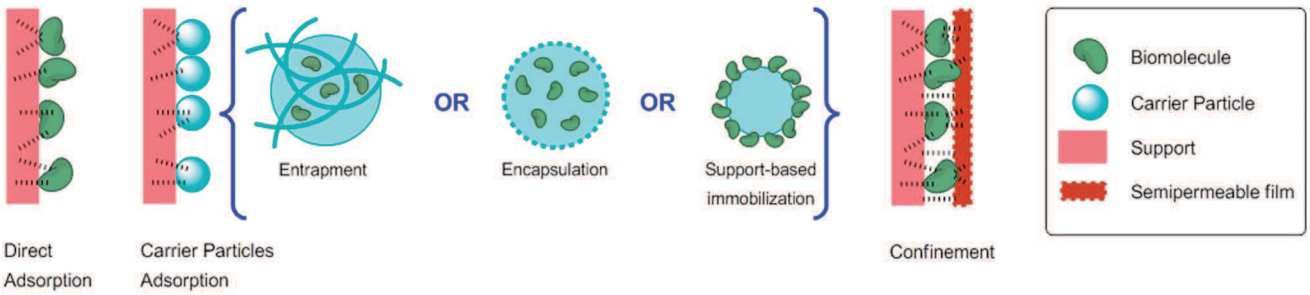

Fig. 15 Physical approaches to immobilization.

contrast, 0.5 micrometer-scale particles[134,135] have size approaching particle retention values and are thereby more easily retained on the surface. Therefore, carrier particles enable immobilizing more biomolecules closer to the surface.[134] In addition, biomolecules immobilized within carrier particles are protected from the external environment and its variations.[136] However, mass transfer limitations and pore-clogging may keep the biomolecules away from their target and eventually result in the loss of efficiency.[93,121,136] On the other hand, immobilization of biomolecules over the carrier particles may also reduce the activity by diluting the bio-signal as carriers can account for up to 99% of the immobilized mass or volume.[136]

Immobilization of biomolecules onto (or into) carrier particles can be performed by any other technique described in this paper: physisorption,[134] covalent coupling[94,137] or bioaffinity attachment.[135] These particles are made of either inorganic compounds such as silica[137] or polymers.[94,134,135] Immobilization of biomolecules within the carrier particles is achieved by entrapment or encapsulation (Fig. 15). Lines are blurred between these two notions. In either case, the biomolecule is still free in solution, but restricted in movement. In the encapsulation process, capsule is responsible for the confinement. In the other process, a lattice structure is accountable for the molecule entrapment.[121,136] Particle is built around the biomolecule which is therefore trapped into the carrier material. Pore size of the capsule (or porosity of the lattice) is defined to ensure that large molecules, such as biomolecules, cannot leak from the particle while small substrates and products can freely go through it and access the biomolecule.[119,121,136]

3.1.3. Confinement. This technique is halfway between direct adsorption and encapsulation. After adsorption onto the support, the biomolecule deposit is covered with a semi-permeable film which will adsorb as well as hold biomolecules in place. Like in the encapsulation process, pore size of the film is defined to allow small analytes to go through while restricting biomolecules motion. Biomolecules are therefore confined between the film and the cellulose surface. The chemical properties of the film can be tuned in order to increase its selectivity regarding crossing species.[97,138] In addition, films made of polyelectrolyte increase cohesion between layers through electrostatic forces.[39,139] These films are either thin layers made of polymers[39,97,139] or actual membranes.[138]

The most famous confinement membrane is the dialysis membrane.[119] Dialysis membranes are made of regenerated cellulose.[140,141] These films only contain cellulose II which is the most stable of cellulose crystal structures.[2,47,142] This structure can be formed from native cellulose (cellulose I) by dissolution, chemical treatment and precipitation (regeneration of the cellulose solid form).[2] There are many processes of producing regenerated cellulose.

As for semipermeable thin films, there can be either just one film or several stacked-up films. The latter arrangement is called the layer by layer technique (LbL). Biomolecules and polyelectrolytes with opposite charges are alternately deposited onto the cellulose. They adsorb and stick together because of electrostatic interactions between alternate layers and eventually result in stabilization of the whole system.[39,113,139]

3.2. Biological methods: bioaffinity attachment

Bioaffinity approaches have the advantage of ensuring controlled orientation of the immobilized biomolecules. Wisely chosen orientation guarantees fully retained biological activity. Incidentally, immobilized biomolecules may appear more active than biomolecules in solution,[115] most likely because of the improvement of their stability and the increase of volume specific biomolecule loading.[116] Besides, although it is non-covalent, bioaffinity attachment is specific and strong, and thus produces robust biosensors. In addition, bioaffinity attachment is reversible and therefore gives the opportunity to develop regenerable and versatile biosensors or even biomolecule purification systems.[112,120]

However, this technique is complex because it usually requires modifications of both biomolecules and substrates. One of the binding partners has to be immobilized onto the support and the other has to be conjugated or expressed in the biomolecule, preferably far away from the active site in order to keep it unspoiled and within reach of its target. Affinity tags are expressed in biomolecules by genetic engineering methods such as site-directed mutagenesis, protein fusion technology and post-transcriptional modification. These methods enable placing tags at well-defined positions on proteins. Unfortunately these methods are very complex, expensive and time-consuming.[112,113,120]

There are two biological approaches to immobilization onto cellulose (Fig. 16). The usual bioaffinity attachment implements modifications of both biomolecules and substrates. Interacting components are protein/ligand, protein/antibody or metal ion/chelator (*e.g.* streptavidin/biotin, protein G/human IgG and Ni^{2+}/His-tag, respectively). The other bioaffinity attachment method is specific to cellulose which can be one of the binding partners. The cellulose substrate is therefore bound to a special protein domain introduced into the biomolecule by genetic engineering: the cellulose-binding domain (CBD).

3.2.1. Cellulose-binding domain (CBD)/cellulose. This is the only method for bioaffinity attachment which does not require modifications of the substrate since it is one of the binding partners. Binding partners are thus cellulose substrates and cellulose binding domains (CBDs) expressed in biomolecules. CBD is a protein domain which can be found in cellulose-degrading enzymes. Its tasks are to make the substrate accessible to the enzyme and to concentrate catalyzing domains on insoluble cellulose substrates. This is why CBD spontaneously

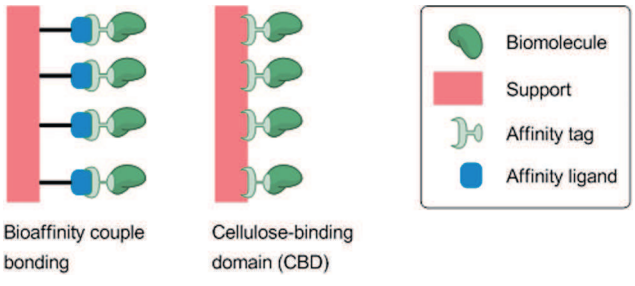

Fig. 16 Biological approaches to immobilization.

adheres to cellulose and can be used as a binding partner. This capacity is partly due to interactions involving several aromatic amino acids from the hydrophobic surface of CBD, as well as hydrogen bonding and van der Waals interactions.[143,144] CBDs are classified into 14 different families based on amino acid sequences, structures and binding specificities.[143] Their size may vary from 3 to 20 kDa and their location within proteins may be N terminal, C-terminal or internal. Some CBDs bind irreversibly to cellulose, whereas others bind reversibly. The latter enable attached proteins to be released from cellulose with denaturing or gentle elution solutions, or even by temperature switches, depending on the CBD's type.[144,145]

Biomolecules that have been fused with CBDs can thus spontaneously bind to cellulose.[93,94] Fusion proteins can therefore be purified by reversible immobilization onto the cellulose column.[146] Immobilized fusion enzymes can be used to produce biocatalysts displaying enhanced performance.[115,147,148] Antibodies directly fused with CBDs,[132,149] or interacting with CBD-fused protein A,[150] can be immobilized onto cellulose and used to achieve immunoassays.

Finally, fusion with proteins such as protein A,[150] protein G, protein L,[151] or streptavidin[152] turns CBDs into bifunctional affinity linkers[94] (see Section 3.2.3).

3.2.2. Protein/ligand. One of the binding partners is first covalently bound to cellulose and then exposed to the other binding partner. Both configurations are equally employed: either a ligand which is bound to cellulose would fix a protein[153,154] or a protein which is bound to cellulose would fix a ligand-fused protein.[73,152,155,156]

There are many protein/ligand couples usable for bioaffinity attachment, among which are avidin/biotin,[73,152,155–158] calmodulin/phenothiazine,[153] and plasminogen activators/*para*-aminobenzamidine.[154] The avidin protein family is composed of multimeric proteins which are able to bind several biotins at once. They can be used as a bifunctional affinity linker, and therefore make possible to attach biotinylated proteins to biotinylated cellulose.[157–159] The (strept)avidin–biotin bond is one of the strongest noncovalent bonds ever known ($K_d \approx 10^{-15}$ M).[113] This bond forms quickly and insensitively to pH, temperature or solvent.[112] Avidin/biotin is the most widely used couple. Therefore, many biotinylated proteins and biotinylation kits are commercially available (Biotin Conjugated Proteins and Enzymes & Biotin Labeling Reagents for Proteins, Thermo Fisher Scientific Inc., Rockford, IL, USA).

3.2.3. Protein A, G or L/antibody. Proteins A, G and L are sometimes called "antibody-binding domains".[151] They specifically interact with the Fc constant region of immunoglobulin G (IgG) molecules which are the usual antibodies for immunoanalysis (Fig. 17).[160] Although noncovalent, the resulting bond is quite strong. For instance, the dissociation constant (K_d) of the protein G–human IgG bond is about 10^{-8} M. While protein A is only able to bind to certain classes of mammalian immunoglobulins, protein G displays broader binding activity.[112,161]

These proteins can be immobilized onto cellulose by any other technique described in this paper: physisorption,[150] covalent coupling[150] or bioaffinity attachment.[151] Then, when they are fixed to cellulose, these proteins ensure specific and ideally-oriented immobilization of antibodies. Indeed, since these proteins fix antibodies by their Fc part, the Fab variable regions point in the opposite direction to the support. Therefore, as they are located on these Fab regions (Fig. 17),[160] the antigen-binding sites remain well accessible for binding with their antigens.[112] The specificity of this coupling is used for the purification purpose,[151,162] while the orientation is useful for developing sensitive immunosensors.[150]

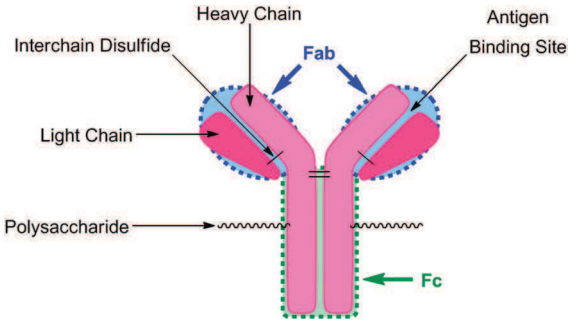

Fig. 17 Detailed structure of an IgG antibody molecule.

3.2.4. Metal ion/chelator. The affinity link between a metal cation and a chelator is a specific and strong noncovalent interaction which forms rapidly. Polyhistidine tag (also called His-tag) is the most popular chelator due to the advantages of small size and charge (in relation to the conjugated protein), low immunogenicity, compatibility with organic solvents, and effective purification. Its size may vary from 2 to 10 histidine residues, but hexahistidine $(His)_6$ (0.84 kDa) is the most widespread form. Its location within protein may be N-terminal or C-terminal. Electron donor groups on the histidine imidazole ring readily form coordination bonds with transition metal ions such as Co^{2+}, Ni^{2+}, Cu^{2+} or Zn^{2+}.[112,144] The strength of the bond varies depending on the cation and stands in the following order: Cu > Ni > Co. Slight modifications may occur depending on the other chelators in the complex.[163] Nevertheless, those divalent cations not only bind to histagged proteins, but also to endogenous proteins that contain histidine clusters. The specificity of the metal–His-tagged protein interaction over metal–endogenous protein interactions stands in the following order: Co > Ni > Cu. Thus, since cobalt exhibits the most specific interaction with histidine tags, it is the preferred cation for purifying His-tagged proteins. On the other hand, copper provides the strongest but least specific interaction. It would therefore be useful for binding previously purified proteins. Nickel is the most widely available metal ion for purifying His-tagged proteins. The reason is that nickel is a good compromise between strength and specificity of the chelating interaction. Incidentally, the specificity can be adjusted depending on working conditions.[144,164–166]

His-tagged proteins can be easily immobilized onto a chelate-modified surface *via* a metal-chelated complex, usually a nickel complex. A matrix ligand such as nitrilotriacetic acid (NTA) or imidodiacetic acid (IDA) is first covalently bound to the surface and then loaded with the metal cation. The chelating interaction between His-tagged biomolecules and the Ni^{2+}–NTA

complex involves the octahedral coordination of the nickel ion (Fig. 18a): two valences are occupied by two imidazole groups from the His-tag and the others by four ligands from the NTA molecule.[112,113] This immobilization is strong ($K_d \approx 10^{-13}$ M)[165] but reversible and the surface can be regenerated under mild conditions using competitive agents or acidic pH. Ligands such as imidazole or any other Lewis base will replace histidine in the complex, while chelating ligands such as ethylenediaminetetraacetic acid (EDTA) will remove the metal cation, both resulting in freeing His-tagged proteins.[113,166] This technique is the most widely used procedure for purifying proteins. Another complex that is sometimes employed to purify His-tagged proteins is cobalt and carboxylmethylaspartate (CMA) (Fig. 18b). Both Ni^{2+}–NTA and Co^{2+}–CMA matrixes have a binding capacity ranging from 5 to 10 mg protein per mL of the matrix resin.[144,165]

Several complexes have been used onto cellulose. There is the usual His-tag–Ni^{2+}–NTA,[76] but also His-tag–Co^{2+}–IDA,[72] or even the titanium–biotin couple.[159] They were used either for the purification purpose,[72] or for developing diagnostic systems.[76]

3.3. Chemical methods

Chemical approaches ensure strong, stable and permanent attachment of biomolecules to cellulose. These methods provide robust biosensors with reproducible results. Moreover, thermal stability of the immobilized biomolecules may increase.[121,167]

On the other hand, these techniques usually require activation or modifications of both substrates and biomolecules. This makes the process more complex and expensive. In addition, these chemical modifications may induce structural changes in biomolecules and a potential partial loss of activity, thereby resulting in the loss of biosensor sensitivity. Furthermore, chemical attachment of biomolecules is not reversible. Immobilized biomolecules cannot be retrieved and used elsewhere later on. But this does not mean that it is not possible to produce regenerable sensors this way. Provided that the sensing biomolecule can be harmlessly free from its analyte (*e.g.* antibody from antigen), the sensor can be used several times.

There are three chemical approaches to immobilization onto cellulose (Fig. 19). These are the most common methods for coupling biomolecules to cellulose. Hence, many activating and crosslinking reagents are commercially available.[168]

3.3.1. Crosslinking. This method has the advantage of immobilizing a large amount of biomolecules onto the support, but is quite expensive. Bi- or multifunctional reagents make biomolecules covalently bind not only to the substrate but also to each other, resulting in a large three-dimensional structure. Since biomolecules are randomly bound to each other, the amount of immobilized biomolecules varies a lot and the attachment process is poorly reproducible. Moreover, distribution and orientation of the immobilized biomolecules are random too, and so are the number and location of anchoring points within biomolecules. All of this may stiffen the biomolecule structure, or even block or distort the active site, what may eventually result in a huge loss of activity.[113,121,169]

Yet, crosslinking is pretty attractive due to its simplicity. This is a one-step procedure which consists of placing the support in contact with the biomolecules together with the crosslinking agent. Glutaraldehyde is a dialdehyde and certainly the most famous bifunctional crosslinker.[28,33,83,105,170,171] It binds primary amines together by forming imine groups on each of its extremities. Imines can be reduced into secondary amines in order to get more stable bonds. Biomolecules, especially proteins, hold lots of primary amines, but cellulose does not. It is therefore necessary to first functionalize cellulose, what is usually done by polymer coating.[28,33,105,170,171] Like cellulose, chitosan is a natural biopolymer made up of glucose units which contains secondary amine moieties. It readily and strongly adsorbs to cellulose because of this structural similarity and its slightly cationic charge in aqueous medium (cellulose is slightly anionic in water).[105,172] It is therefore one of the most coated polymers.

3.3.2. Direct covalent bonding. Covalent bonding is the strongest immobilization method. The biomolecule and the support are directly linked by nonreversible covalent bonds between functional groups from both support and biomolecule surfaces.[121] Functional groups potentially available in proteins for covalent bonding are amine, thiol, carboxyl and hydroxyl groups.[112] The corresponding amino acids, together with the functionalities required on surfaces for attachment are detailed in Table 5. Most of the time, covalent immobilization involves lysine residues (primary amine group) because they are typically present on the surface of the macromolecule, and are usually

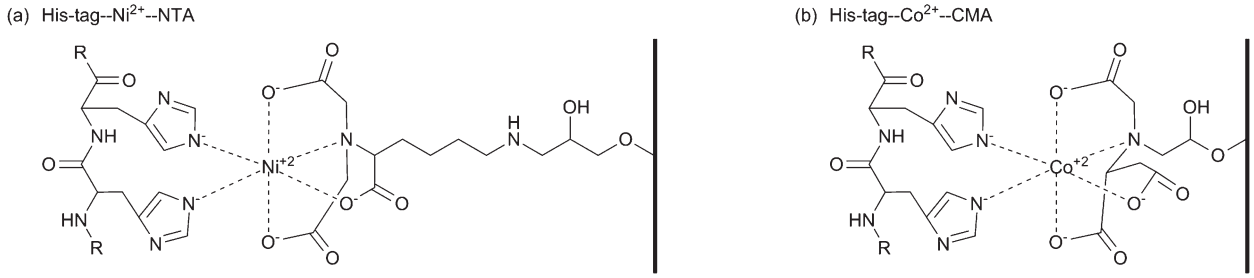

Fig. 18 Models of the interactions between the polyhistidine affinity tag and two immobilized metal affinity chromatography matrices: (a) the nickel–nitrilotriacetic acid matrix (Ni^{2+}–NTA). (b) The cobalt–carboxylmethylaspartate matrix (Co^{2+}–CMA).

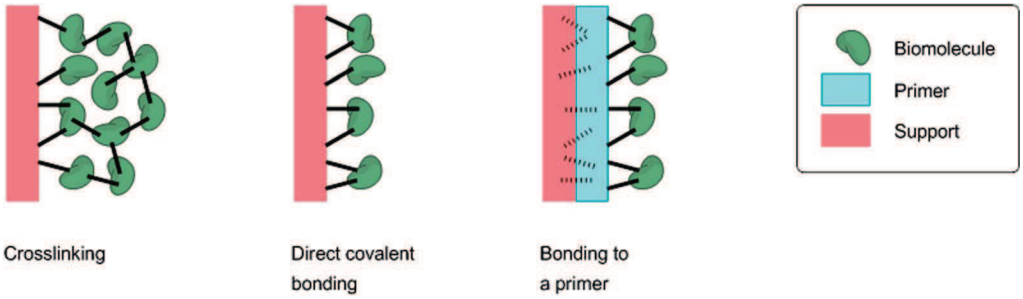

Fig. 19 Chemical approaches to immobilization.

numerous. Yet, if several groups of one biomolecule take part in its attachment (multipoint attachment), its flexibility may be reduced along with its activity.[86,112,173] Likewise, if the active site of the biomolecule contributes to the bonding, its activity may also be affected. According to the molecular structure of cellulose (Fig. 1), hydroxyl groups in glucose units are responsible for its chemical activity. Among the three hydroxyl groups in each glucose residue, the one at 6-position (primary one) is described as the most reactive site, far more than hydroxyl groups at 2- and 3-positions (secondary ones).[47] However, this group cannot directly react with amines, which makes cellulose activation or functionalization necessary in order to covalently bind to proteins.

Covalent bonding usually implements multistep reactions because substrates and/or biomolecules need to be activated before they can react with each other. There are many procedures, but activation methods as well as the nature of the linking bonds are still pretty much the same.[86,121] Generally, biomolecules are linked to cellulose by forming bonds such as amide,[8,73,74,173] imine,[40,83,174] secondary amine[8,68,71,150,173,175–178] and isourea[179] or carbamate[180] (Fig. 20).

Amide bonds are formed by reaction of primary amines from lysine residues with activated esters previously introduced in cellulose, usually *N*-hydroxysuccinimide esters. To form these esters, primary alcohol groups from cellulose are first oxidized into the corresponding carboxylic acids by TEMPO-mediated oxidation[73,74] (see Section 2.2.2.1). Then, those carboxylic acids react with a mixture of 1-ethyl-3-(3-dimethylaminopropyl)-carbodiimide hydrochloride (EDC) and *N*-hydroxysuccinimide (NHS) to form the activated succinimide esters[73,74,173] (Fig. 21).

Imine bonds are produced by condensation of primary amines from biomolecules with carbonyl groups from cellulose. These carbonyl groups may originate from the oxidation of secondary alcohol groups in glucose units, usually by periodate oxidation[40,71,72] (see Section 2.2.2.1) (Fig. 22a). They may also stem from the cellulose functionalization with glutaraldehyde (GA)[83,150,174] (Fig. 22b).

Those imine bonds are sometimes reduced into secondary amines in order to get more stable bonds. Sodium borohydride ($NaBH_4$)[72,150] and sodium cyanoborohydride ($NaBH_3CN$)[71,72] are the usual reducing agents (Fig. 23a). Finally, secondary amines may also result from nitrene insertion[8,68,175] (Fig. 23b) or epoxide ring-opening[72,173] (Fig. 23c).

Many activating and linking reagents are commercially available (Crosslinking Reagents, Thermo Fisher Scientific Inc., Rockford, IL, USA).[168] Whatever bond is chosen, coupling efficiency depends on parameters such as pH, concentration, ionic strength and incubation time. Most importantly, the bonding conditions and parameters need to be optimized for each type of biomolecule.[112]

Table 5 Commonly available functional groups in proteins and surface functionalities required for attachment

Side groups	Amino acids	Surface functionalities
$-NH_2$	Lysine	Carboxylic acid, active ester (NHS), epoxy, aldehyde
–SH	Cysteine	Maleimide, pyridyl disulfide, vinyl sulfone
–COOH	Aspartic acid, glutamic acid	Amine
–OH	Serine, threonine	Epoxy

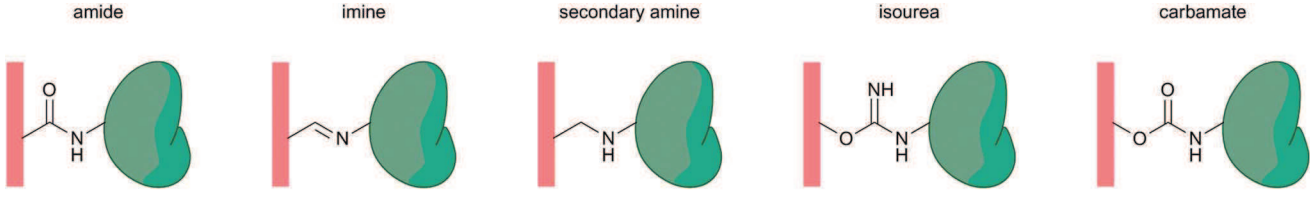

Fig. 20 Nature of the linking bonds between cellulose substrates and biomolecules.

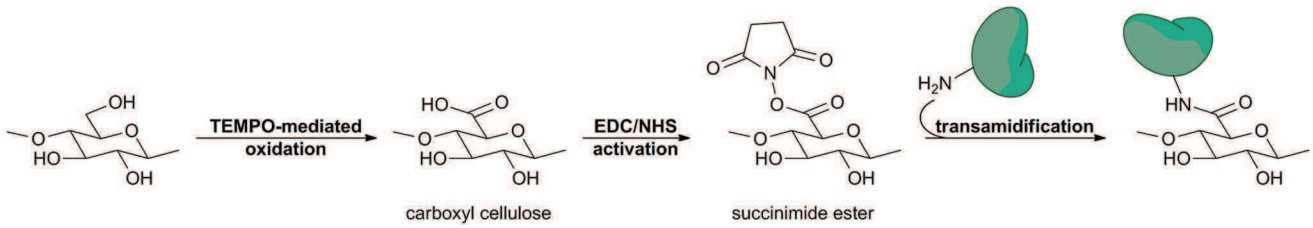

Fig. 21 Amide bond formation.

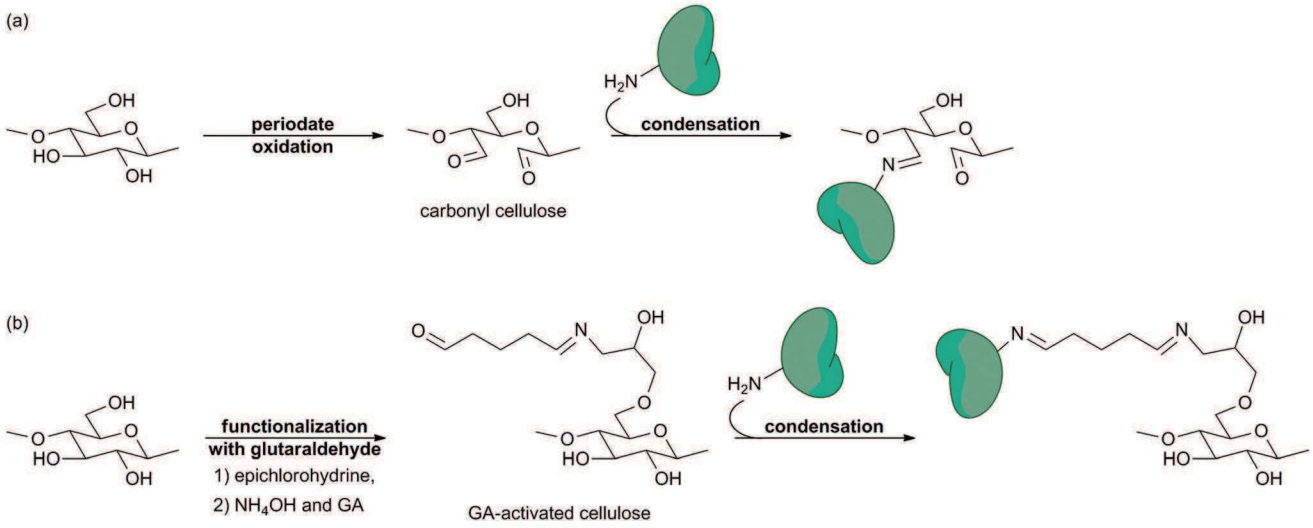

Fig. 22 Imine bond formation (a) through periodate oxidation of cellulose and (b) through functionalization with glutaraldehyde.

3.3.3. Bonding to a polymeric primer. This method can be considered as a variant to direct covalent bonding and may be described as semicovalent. The biomolecule does bind covalently to a substrate, but it is not cellulose itself. It is a polymeric primer previously coated and strongly adsorbed onto cellulose. This polymer provides the functional groups required for covalent bonding and it provides them in large quantities. This technique has the advantages of making the activation of the cellulose substrate simpler and reducing the number of reaction steps. However, since the polymer can desorb from cellulose, this method is less robust than actual covalent bonding.

Many different polymers can be used, but these usually are polysaccharides such as chitosan and carboxymethyl cellulose (CMC) which provide amine and carboxyl groups, respectively (Fig. 24).[28,33,73,79,105,170,171,181] With regard to CMC, some may consider its adsorption onto cellulose as nonreversible.[79] As for chitosan, chemical interactions between the latter and cellulose have been highlighted. According to this study, amine groups from chitosan react with carbonyl groups from cellulose to produce imines.[182] Carbonyl groups can be found at the reducing end group of pristine cellulose or anywhere in the structure of aged cellulose.[61,183]

Finally, another configuration can be employed sometimes. The polymeric primer is first covalently bound to cellulose by radical copolymerization, while the biomolecule is further adsorbed to it.[167,184] Thus, the biomolecule is less likely to get distorted, but the biological material is more likely to leak.

4. Summary and outlook

It has been a long road from papyrus to bioactive paper. Since its invention over five thousand years ago in Egypt, papyrus had long been the dominant writing material. It was then supplanted in Europe by parchment and eventually paper during the Renaissance. Paper's main component, cellulose, was identified during the 19th century by a French chemist and was further used as a chemical raw material, hence giving impetus to textile industry. Paper-based bioassays appeared during the 1950s and were then extensively applied to point-of-care diagnostics. Finally, the term "bioactive paper" came into use in the 2000s.

Recently, paper-based bioassays have trended towards three-dimensional devices and multiplexed assay platforms. Most of the procedures implemented in the production of such sensors are incompatible with the conventional lateral flow immunoassay (LFIA) carrier material, nitrocellulose. In newly developed multiplex biosensors, nitrocellulose thus tends to be replaced by pure cellulose which, besides being more convenient to handle and more safely disposable, is a very attractive material regarding the current ecological climate and growing will for sustainable technologic development.

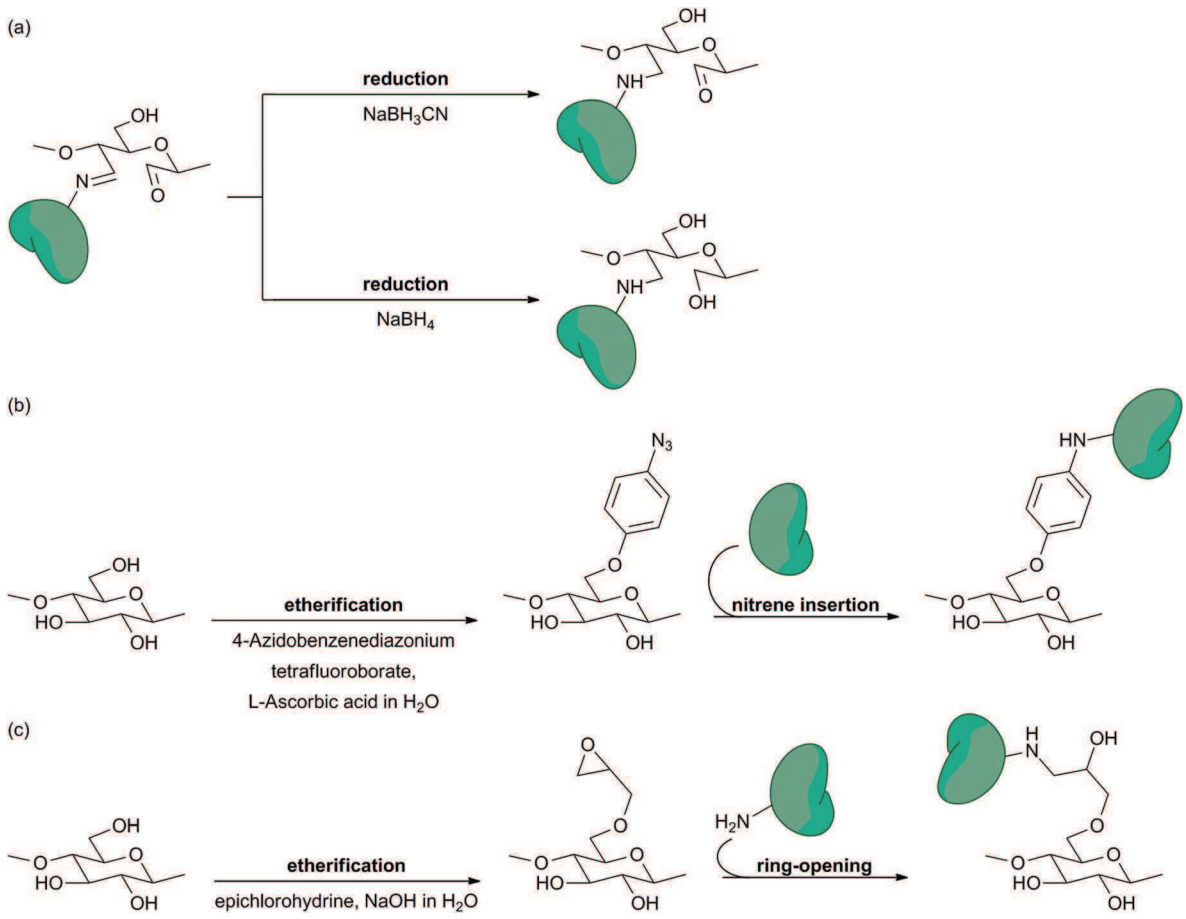

Fig. 23 Several ways to form secondary amine bonds.

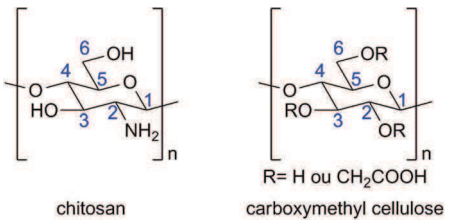

Fig. 24 Structure of chitosan and carboxymethyl cellulose.

Cellulose has indeed lots of appealing properties such as large bioavailability, good biodegradability, biocompatibility and sustainability. This is the most important skeletal component in plants and guarantees their proper growth and structural integrity. Among structural entities of cellulose, microfibrils are stiff but cellulose fibers are resilient, thereby illustrating the duality of the cellulose material. Its behavior towards water is dual too since cellulose swells but does not dissolve in water, hence enabling fluids to wick by capillary action with no need for any external power source. All of its features make cellulose an ideal structural engineering material and a grade one platform for point-of-care diagnostic devices.

The immobilization of biomolecules onto cellulose paper is a key step in the development of paper-based biosensing devices and bioactive papers in general. Many procedures exist and this article has reviewed and categorized the current strategies for the immobilization of biomolecules onto pure cellulose membranes. These methodologies are classified into three major families: (i) physical methods, wherein the biomolecule is retained onto the cellulose support through physical forces such as electrostatic, van der Waals, hydrophobic interactions and hydrogen bonding, (ii) biological or biochemical methods wherein the biomolecule is linked to the cellulose paper through biochemical affinity between two components (*e.g.* Ni^{2+}/His-tag, streptavidin/biotin, protein G/human IgG), and (iii) chemical methods, wherein covalent bonds maintain the biomolecule on the support. Each of these techniques displays specific benefits and drawbacks. The physical approach is the simplest, the fastest and the most cost-saving, but also the weakest way of immobilizing biomolecules onto cellulose. Bioaffinity attachment is certainly the most acute technique since it is site specific and therefore enables controlling orientation of the immobilized biomolecules. Nevertheless, such a method requires complex and expensive genetic engineering procedures. Finally, chemical bonding is the strongest way of immobilizing biomolecules onto cellulose, but potentially the most damaging for these biomolecules. In consequence, there is no universal method for biomolecule immobilization onto

cellulose. For a given paper based biochip, each and every strategy can be considered and new ones will probably arise. The most appropriate methodology should be chosen considering the nature of biomolecule, device and sample, as well as the budget allocated.

In the paper-based biosensor development process, fabrication is not a major difficulty whereas design of these devices remains a challenge since the fluidic path plays a crucial part in the biosensing kinetics and effective sensitivity of the sensor. Another issue is the choice of the transducing system which has to deliver a signal free from the alien substances and additive interferences and to allow for quantitative measurements whenever possible. Finally, preservation is still a tough problem, especially in resource-limited settings. Biomolecules not only have to stay onto the sensor support (leakage prevention), but most importantly they have to stay active, even under harsh conditions such as elevated temperatures. There is therefore a growing need for thermally stable biosensing entities and stabilizing technologies. Once these issues are addressed, new paper-based multiplex bioassays could be widely spread and used for on-site detection in remote areas in the developing world, but also in developed countries in emergency situations, in emergency rooms, at home or in military settings.

References

1 A. Payen, *C. R. Hebd. Seances Acad. Sci.*, 1838, **7**, 1052–1056.
2 D. Klemm, B. Heublein, H.-P. Fink and A. Bohn, *Angew. Chem., Int. Ed. Engl.*, 2005, **44**, 3358–3393.
3 E. J. Kontturi, *Surface chemistry of cellulose: from natural fibres to model surfaces*, Technische Universiteit Eindhoven, 2005, pp. 1–145.
4 J. S. Han and J. S. Rowell, in *Paper and Composites from Agro-based Resources*, ed. R. M. Rowell, R. A. Young, and J. K. Rowell, CRC Press, 1996, pp. 83–134.
5 D. Klemm, F. Kramer, S. Moritz, T. Lindström, M. Ankerfors, D. Gray and A. Dorris, *Angew. Chem., Int. Ed. Engl.*, 2011, **50**, 5438–5466.
6 S. Kalia, B. S. Kaith and I. Kaur, *Cellulose Fibers: Bio- and Nano-polymer Composites*, Springer, Berlin, Heidelberg, 2011.
7 E. J. Maxwell, A. D. Mazzeo and G. M. Whitesides, *MRS Bull.*, 2013, **38**, 309–314.
8 J. Credou, H. Volland, J. Dano and T. Berthelot, *J. Mater. Chem. B*, 2013, **1**, 3277–3286.
9 Materials Research Society, *MRS Bull.*, 2013, **38**, 294–352.
10 J. Maumené, *Philos. Mag. Ser. 3.*, 1850, **36**, 482–482.
11 G. Oliver, *Lancet*, 1883, **121**, 139–140.
12 G. Oliver, *Br. Med. J.*, 1883, **1**, 765.
13 A. H. Gordon, A. J. P. Martin and R. L. M. Synge, in *Proceedings of the Biochemical Society*, Portland Press Ltd., 1943, pp. xiii–xiv.
14 R. Consden, A. H. Gordon and A. J. Martin, *Biochem. J.*, 1944, **38**, 224–232.
15 R. H. Müller and D. L. Clegg, *Anal. Chem.*, 1949, **21**, 1123–1125.
16 A. H. Free, E. C. Adams, M. Lou Kercher, H. M. Free and M. H. Cook, *Clin. Chem.*, 1957, **3**, 163–168.
17 R. Hawkes, E. Niday and J. Gordon, *Anal. Biochem.*, 1982, **119**, 142–147.
18 G. A. Posthuma-Trumpie, J. Korf and A. van Amerongen, *Anal. Bioanal. Chem.*, 2009, **393**, 569–582.
19 B. Ngom, Y. Guo, X. Wang and D. Bi, *Anal. Bioanal. Chem.*, 2010, **397**, 1113–1135.
20 R. C. Wong and H. Y. Tse, *Lateral Flow Immunoassay*, Humana Press, New York, NY, 2009.
21 R. W. Peeling and D. Mabey, *Clin. Microbiol. Infect.*, 2010, **16**, 1062–1069.
22 P. von Lode, *Clin. Biochem.*, 2005, **38**, 591–606.
23 J. Burstein and G. D. Braunstein, *Early Pregnancy: Biology and Medicine*, 1995, **1**, 288–296.
24 T. Chard, *Hum. Reprod.*, 1992, **7**, 701–710.
25 A. W. Martinez, S. T. Phillips and G. M. Whitesides, *Proc. Natl. Acad. Sci. U. S. A.*, 2008, **105**, 19606–19611.
26 E. M. Fenton, M. R. Mascarenas, G. P. López and S. S. Sibbett, *ACS Appl. Mater. Interfaces*, 2009, **1**, 124–129.
27 E. Njumbe Ediage, J. D. Di Mavungu, I. Y. Goryacheva, C. Van Peteghem and S. De Saeger, *Anal. Bioanal. Chem.*, 2012, **403**, 265–278.
28 L. Ge, J. Yan, X. Song, M. Yan, S. Ge and J. Yu, *Biomaterials*, 2012, **33**, 1024–1031.
29 S. M. Z. Hossain, C. Ozimok, C. Sicard, S. D. Aguirre, M. M. Ali, Y. Li and J. D. Brennan, *Anal. Bioanal. Chem.*, 2012, **403**, 1567–1576.
30 X. Li, D. R. Ballerini and W. Shen, *Biomicrofluidics*, 2012, **6**, 011301.
31 P. Lisowski and P. K. Zarzycki, *Chromatographia*, 2013, **76**, 1201–1214.
32 K. Abe, K. Kotera, K. Suzuki and D. Citterio, *Anal. Bioanal. Chem.*, 2010, **398**, 885–893.
33 L. Ge, S. Wang, X. Song, S. Ge and J. Yu, *Lab Chip*, 2012, **12**, 3150–3158.
34 SENTINEL: Bioactive Paper Network, http://www.bioactivepaper.ca/index.php?module=page&id=4000, accessed 31 January, 2014.
35 A. W. Martinez, S. T. Phillips, G. M. Whitesides and E. Carrilho, *Anal. Chem.*, 2010, **82**, 3–10.
36 H. Kettler, K. White and S. Hawkes, *Mapping the landscape of diagnostics for sexually transmitted infections: key findings and recommandations*, World Health Organization, Geneva, Switzerland, 2004.
37 C.-M. Cheng, A. W. Martinez, J. Gong, C. R. Mace, S. T. Phillips, E. Carrilho, K. A. Mirica and G. M. Whitesides, *Angew. Chem., Int. Ed. Engl.*, 2010, **49**, 4771–4774.
38 J. Hu, S. Wang, L. Wang, F. Li, T. J. Lu and F. Xu, *Biosens. Bioelectron.*, 2014, **54**, 585–597.
39 R. S. J. Alkasir, M. Ornatska and S. Andreescu, *Anal. Chem.*, 2012, **84**, 9729–9737.
40 M. Zhang, L. Ge, S. Ge, M. Yan, J. Yu, J. Huang and S. Liu, *Biosens. Bioelectron.*, 2013, **41**, 544–550.
41 C. Sicard and J. D. Brennan, *MRS Bull.*, 2013, **38**, 331–334.
42 M. Vert, Y. Doi, K. Hellwich, M. Hess, P. Hodge, P. Kubisa, M. Rinaudo and F. Schué, *Pure Appl. Chem.*, 2012, **84**, 377–410.

43 P. D. D. Klemm and P. D. T. Schmauder, Hans-Peter Heinze, in *Biopolymers, Vol. 6 Polysaccharides II: Polysaccharides from Eukaryotes*, ed. E. Vandamme, S. De Baets and A. Steinbüchel, Wiley-Blackwell, 2002, pp. 275–287.
44 P. Zugenmaier, *Prog. Polym. Sci.*, 2001, **26**, 1341–1417.
45 N. L. Ahrenstedt, *Surface Modification of Cellulose Materials*, School of Biotechnology Royal Institute of Technology, Stockholm, 2007, pp. 1–50.
46 S. Kalia, A. Dufresne, B. M. Cherian, B. S. Kaith, L. Avérous, J. Njuguna and E. Nassiopoulos, *Int. J. Polym. Sci.*, 2011, **2011**, 1–35.
47 D. Roy, M. Semsarilar, J. T. Guthrie and S. Perrier, *Chem. Soc. Rev.*, 2009, **38**, 2046–2064.
48 T. Zimmermann, E. Pöhler and T. Geiger, *Adv. Eng. Mater.*, 2004, **6**, 754–761.
49 N. Gierlinger and M. Schwanninger, *Spectroscopy*, 2007, **21**, 69–89.
50 S. Wang, S. Lee and Q. Cheng,in *Cellulose: Structure and Properties, Derivatives and Industrial Uses*, ed. A. Lejeune and T. Deprez, 2010, pp. 459–500.
51 R. L. Crawford, *Lignin biodegradation and transformation*, John Wiley & Sons Inc, New York, NY, USA, 1981.
52 M. Chabannes, K. Ruel, A. Yoshinaga, B. Chabbert, A. Jauneau, J. P. Joseleau and A. M. Boudet, *Plant J.*, 2001, **28**, 271–282.
53 D. Mohnen, *Curr. Opin. Plant. Biol.*, 2008, **11**, 266–277.
54 H. König, L. Li and J. Fröhlich, *Appl. Microbiol. Biotechnol.*, 2013, **97**, 7943–7962.
55 R. Koroiva, C. W. O. Souza, D. Toyama, F. Henrique-Silva and a. a. Fonseca-Gessner, *Genet. Mol. Res.*, 2013, **12**, 3421–3434.
56 V. V. Zverlov, W. Höll and W. H. Schwarz, *Int. Biodeterior. Biodegrad.*, 2003, **51**, 175–179.
57 L. Zhu, Q. Wu, J. Dai, S. Zhang and F. Wei, *Proc. Natl. Acad. Sci. U. S. A.*, 2011, **108**, 17714–17719.
58 A. Michaelsen, F. Pinzari, N. Barbabietola and G. Piñar, *Int. Biodeterior. Biodegrad.*, 2013, **84**, 333–341.
59 M. Zotti, a. Ferroni and P. Calvini, *Int. Biodeterior. Biodegrad.*, 2008, **62**, 186–194.
60 F. Pinzari, G. Pasquariello and A. De Mico, *Macromol. Symp.*, 2006, **238**, 57–66.
61 M. C. Area and H. Cheradame, *BioResources*, 2011, **6**, 5307–5337.
62 M. Mutwil, S. Debolt and S. Persson, *Curr. Opin. Plant Biol.*, 2008, **11**, 252–257.
63 Modulus of Elasticity – Young Modulus for some common Materials, http://www.engineeringtoolbox.com/young-modulus-d_417.html.
64 Concrete Properties, http://www.engineeringtoolbox.com/concrete-properties-d_1223.html.
65 E. Malmström and A. Carlmark, *Polym. Chem.*, 2012, **3**, 1702–1713.
66 P.-A. Faugeras, P.-H. Elchinger, F. Brouillette, D. Montplaisir and R. Zerrouki, *Green Chem.*, 2012, **14**, 598–600.
67 D. Klemm, B. Philipp, T. Heinze, U. Heinze and W. Wagenknecht, *Comprehensive Cellulose Chemistry Volume 2 Functionalization of Cellulose*, WILEY-VCH, Weinheim, 1998, vol. 2.
68 S. Kumar and P. Nahar, *Talanta*, 2007, **71**, 1438–1440.
69 T. Heinze and T. Liebert, *Prog. Polym. Sci.*, 2001, **26**, 1689–1762.
70 S. Margutti, S. Vicini, N. Proietti, D. Capitani, G. Conio, E. Pedemonte and A. L. Segre, *Polymer*, 2002, **43**, 6183–6194.
71 S. Wang, L. Ge, X. Song, M. Yan, S. Ge, J. Yu and F. Zeng, *Analyst*, 2012, **137**, 3821–3827.
72 V. Weber, I. Linsberger, M. Ettenauer, F. Loth, M. Ho and D. Falkenhagen, *Biomacromolecules*, 2005, **6**, 1864–1870.
73 H. Orelma, L.-S. Johansson, I. Filpponen, O. J. Rojas and J. Laine, *Biomacromolecules*, 2012, **13**, 2802–2810.
74 H. Orelma, I. Filpponen, L.-S. Johansson, M. Osterberg, O. J. Rojas and J. Laine, *Biointerphases*, 2012, **7**, 61.
75 K. Benhamou, A. Dufresne, A. Magnin, G. Mortha and H. Kaddami, *Carbohydr. Polym.*, 2014, **99**, 74–83.
76 S. Diekmann, G. Siegmund, A. Roecker and D. O. Klemm, *Cellulose*, 2003, **10**, 53–63.
77 M. Granström, *Cellulose Derivatives: Synthesis, Properties and Applications*, Helsinki University Printing House, 2009, pp. 1–120.
78 G. E. Fridley, C. A. Holstein, S. B. Oza and P. Yager, *MRS Bull.*, 2013, **38**, 326–330.
79 H. Orelma, T. Teerinen, L.-S. Johansson, S. Holappa and J. Laine, *Biomacromolecules*, 2012, **13**, 1051–1058.
80 C. Barba, D. Montané, M. Rinaudo and X. Farriol, *Cellulose*, 2002, **9**, 319–326.
81 M. M. Ibrahim, A. Koschella, G. Kadry and T. Heinze, *Carbohydr. Polym.*, 2013, **95**, 414–420.
82 Y. Zhang, R. G. Carbonell and O. J. Rojas, *Biomacromolecules*, 2013, **14**, 4161–4168.
83 M. Monier and A. M. a. El-Sokkary, *Int. J. Biol. Macromol.*, 2012, **51**, 18–24.
84 C. Corsaro, D. Mallamace, J. Lojewska, F. Mallamace, L. Pietronero and M. Missori, *Sci. Rep.*, 2013, **3**, 2896.
85 D. Klemm, B. Philipp, T. Heinze, U. Heinze and W. Wagenknecht, *Comprehensive Cellulose Chemistry Volume 1 Fundamentals and Analytical Methods*, Wiley-VCH, Weinheim, 1998.
86 M. Gericke, J. Trygg and P. Fardim, *Chem. Rev.*, 2013, **113**, 4812–4836.
87 R. J. Moon, A. Martini, J. Nairn, J. Simonsen and J. Youngblood, *Chem. Soc. Rev.*, 2011, **40**, 3941–3994.
88 M. A. Hubbe, R. A. Venditti and O. J. Rojas, *BioResources*, 2007, **2**, 739–788.
89 H. Wondraczek, A. Kotiaho, P. Fardim and T. Heinze, *Carbohydr. Polym.*, 2011, **83**, 1048–1061.
90 P. J. Bracher, M. Gupta and G. M. Whitesides, *Soft Matter*, 2010, 4303–4309.
91 H. Virtanen, H. Orelma, T. Erho and M. Smolander, *Process Biochem.*, 2012, **47**, 1496–1502.
92 S. Aikio, S. Grönqvist, L. Hakola, E. Hurme, S. Jussila, O.-V. Kaukoniemi, H. Kopola, M. Känsäkoski, M. Leinonen, S. Lippo, R. Mahlberg, S. Peltonen, P. Qvintus-Leino, T. Rajamäki, A.-C. Ritschkoff, M. Smolander, J. Vartiainen, L. Viikari and M. Vilkman, *Bioactive paper and fibre products: Patent and literary survey*, 2006.

93 F. Kong and Y. F. Hu, *Anal. Bioanal. Chem.*, 2012, **403**, 7–13.
94 R. Pelton, *Trends Anal. Chem.*, 2009, **28**, 925–942.
95 D. D. Liana, B. Raguse, J. J. Gooding and E. Chow, *Sensors*, 2012, **12**, 11505–11526.
96 H. Anany, W. Chen, R. Pelton and M. W. Griffiths, *Appl. Environ. Microbiol.*, 2011, **77**, 6379–6387.
97 S. M. Z. Hossain, R. E. Luckham, M. J. McFadden and J. D. Brennan, *Anal. Chem.*, 2009, **81**, 9055–9064.
98 M. Vaher and M. Kaljurand, *Anal. Bioanal. Chem.*, 2012, **404**, 627–633.
99 A. W. Martinez, S. T. Phillips, M. J. Butte and G. M. Whitesides, *Angew. Chem., Int. Ed. Engl.*, 2007, **46**, 1318–1320.
100 T. R. J. Holford, F. Davis and S. P. J. Higson, *Biosens. Bioelectron.*, 2011, **34**, 12–24.
101 A. H. Peruski and L. F. Peruski, *Clin. Vaccine Immunol.*, 2003, **10**, 506–513.
102 S. T. Phillips and G. G. Lewis, *MRS Bull.*, 2013, **38**, 315–319.
103 E. Carrilho, S. T. Phillips, S. J. Vella, A. W. Martinez and G. M. Whitesides, *Anal. Chem.*, 2009, **81**, 5990–5998.
104 E. Carrilho, A. W. Martinez and G. M. Whitesides, *Anal. Chem.*, 2009, **81**, 7091–7095.
105 S. Wang, L. Ge, X. Song, J. Yu, S. Ge, J. Huang and F. Zeng, *Biosens. Bioelectron.*, 2012, **31**, 212–218.
106 T. Songjaroen, W. Dungchai, O. Chailapakul and W. Laiwattanapaisal, *Talanta*, 2011, **85**, 2587–2593.
107 A. Määttänen, U. Vanamo, P. Ihalainen, P. Pulkkinen, H. Tenhu, J. Bobacka and J. Peltonen, *Sens. Actuators, B*, 2012, **177**, 153–162.
108 A. V. Govindarajan, S. Ramachandran, G. D. Vigil, P. Yager and K. F. Böhringer, *Lab Chip*, 2012, **12**, 174–181.
109 L. Lafleur, D. Stevens, K. McKenzie, S. Ramachandran, P. Spicar-Mihalic, M. Singhal, A. Arjyal, J. Osborn, P. Kauffman, P. Yager and B. Lutz, *Lab Chip*, 2012, **12**, 1119–1127.
110 Millistak+ HC Filter Devices (with RW01); MSDS No. M114480, Millipore Corporation, Billerica, MA, 2008.
111 Nitrocellulose Membrane Filters; MSDS No. 00000100SDS, Millipore Corporation, Billerica, MA, 2011.
112 F. Rusmini, Z. Zhong and J. Feijen, *Biomacromolecules*, 2007, **8**, 1775–1789.
113 A. Sassolas, L. J. Blum and B. D. Leca-Bouvier, *Biotechnol. Adv.*, 2012, **30**, 489–511.
114 R. DiCosimo, J. McAuliffe, A. J. Poulose and G. Bohlmann, *Chem. Soc. Rev.*, 2013, **42**, 6437–6474.
115 A. Fishman, I. Levy, U. Cogan and O. Shoseyov, *J. Mol. Catal. B: Enzym.*, 2002, **18**, 121–131.
116 A. Liese and L. Hilterhaus, *Chem. Soc. Rev.*, 2013, **42**, 6236–6249.
117 F. Secundo, *Chem. Soc. Rev.*, 2013, **42**, 6250–6261.
118 Millipore, *Rapid Lateral Flow Test Strips Considerations for Product Development*, Millipore Corporation, Billerica, MA, 2008.
119 M. M. F. Choi, *Microchim. Acta*, 2004, **148**, 107–132.
120 S. N. Di Risio, *Fundamental investigation of inkjet deposition and physical immobilization of horseradish peroxidase on cellulosic substrates*, University of Toronto, 2009, pp. 1–200.
121 M. M. M. Elnashar, in *Biotechnology of Biopolymers*, ed. M. M. M. Elnashar, InTech, Rijeka, Croatia, 2011, pp. 3–33.
122 X. Y. Liu, C. M. Cheng, A. W. Martinez, K. A. Mirica, X. J. Li, S. T. Phillips, M. Mascareñas and G. M. Whitesides, in *MEMS 2011*, IEEE, Cancun, MEXICO, 2011, pp. 75–78.
123 S.-N. Tan, L. Ge, H. Y. Tan, W. K. Loke, G. Jinrong and W. Wang, *Anal. Chem.*, 2012, **84**, 10071–10076.
124 J. Yu, L. Ge, J. Huang, S. Wang and S. Ge, *Lab Chip*, 2011, **11**, 1286–1291.
125 J. Yu, S. Wang, L. Ge and S. Ge, *Biosens. Bioelectron.*, 2011, **26**, 3284–3289.
126 G. Zhou, X. Mao and D. Juncker, *Anal. Chem.*, 2012, **84**, 7736–7743.
127 E. Halder, D. K. Chattoraj and K. P. Das, *Biopolymers*, 2005, **77**, 286–295.
128 P. Jarujamrus, J. Tian, X. Li, A. Siripinyanond, J. Shiowatana and W. Shen, *Analyst*, 2012, **137**, 2205–2210.
129 J. Tian, P. Jarujamrus, L. Li, M. Li and W. Shen, *ACS Appl. Mater. Interfaces*, 2012, **4**, 6573–6578.
130 M. Al-Tamimi, W. Shen, R. Zeineddine, H. Tran and G. Garnier, *Anal. Chem.*, 2012, **84**, 1661–1668.
131 J. Su, M. Al-Tamimi and G. Garnier, *Cellulose*, 2012, **19**, 1749–1758.
132 G. Hussack, Y. Luo, L. Veldhuis, J. C. Hall, J. Tanha and R. Mackenzie, *Sensors*, 2009, **9**, 5351–5367.
133 A. Makky, T. Berthelot, C. Feraudet-Tarisse, H. Volland, P. Viel and J. Polesel-Maris, *Sens. Actuators, B*, 2012, **162**, 269–277.
134 P. Peng, L. Summers, A. Rodriguez and G. Garnier, *Colloids Surf., B*, 2011, **88**, 271–278.
135 S. Su, M. M. Ali, C. D. M. Filipe, Y. Li and R. Pelton, *Biomacromolecules*, 2008, **9**, 935–941.
136 D. Brady and J. Jordaan, *Biotechnol. Lett.*, 2009, **31**, 1639–1650.
137 Z. Zhao, J. Tian, Z. Wu, J. Liu, D. Zhao, W. Shen and L. He, *J. Mater. Chem. B*, 2013, **1**, 4719–4722.
138 Y. Xiao and T.-S. Chung, *J. Membr. Sci.*, 2007, **290**, 78–85.
139 P. a. Larsson, S. G. Puttaswamaiah, C. Ly, A. Vanerek, J. C. Hall and F. Drolet, *Colloids Surf., B*, 2013, **101**, 205–209.
140 Thermo Scientific, *Innovative devices for secure sample dialysis*, Thermo Fisher Scientific Inc., Rockford, lL, 2013.
141 Thermo Scientific, Dialysis Methods for Protein Research, http://www.piercenet.com/method/dialysis-methods-protein-research, accessed 27 September, 2013.
142 H. A. Krässig, in *Cellulose, structure, accessibility and reactivity*, Gordon and Breach Publishers, Philadelphia, PA, 1993, vol. 32.
143 I. Levy and O. Shoseyov, *Biotechnol. Adv.*, 2002, **20**, 191–213.
144 K. Terpe, *Appl. Microbiol. Biotechnol.*, 2003, **60**, 523–533.
145 J. Nahálka and P. Gemeiner, *J. Biotechnol.*, 2006, **123**, 478–482.
146 N. Sugimoto, K. Igarashi and M. Samejima, *Protein Expr. Purif.*, 2012, **82**, 290–296.
147 S. Hwang, J. Ahn, S. Lee, T. G. Lee, S. Haam, K. Lee, I.-S. Ahn and J.-K. Jung, *Biotechnol. Lett.*, 2004, **26**, 603–605.
148 H. Park, J. Ahn, J. Lee, H. Lee, C. Kim, J.-K. Jung, H. Lee and E. G. Lee, *Int. J. Mol. Sci.*, 2012, **13**, 358–368.

149 W. Lewis, E. Keshavarz-Moore, J. Windust, D. Bushell and N. Parry, *Biotechnol. Bioeng.*, 2006, **94**, 625–632.
150 Y. Cao, Q. Zhang, C. Wang, Y. Zhu and G. Bai, *J. Chromatogr. A*, 2007, **1149**, 228–235.
151 G. Hussack, B. M. Grohs, K. C. Almquist, M. D. McLean, R. Ghosh and J. C. Hall, *J. Agric. Food Chem.*, 2010, **58**, 3451–3459.
152 K. D. Le, N. R. Gilkes, D. G. Kilburn, R. C. Miller, J. N. Saddler and R. A. J. Warren, *Enzyme Microb. Technol.*, 1994, **16**, 496–500.
153 S. Daunert, L. G. Bachas, V. Schauer-Vukasinovic, K. J. Gregory, G. Schrift and S. Deo, *Colloids Surf., B*, 2007, **58**, 20–27.
154 E. Fasoli, Y. R. Reyes, O. M. Guzman, A. Rosado, V. R. Cruz, A. Borges, E. Martinez and V. Bansal, *J. Chromatogr. B: Anal. Technol. Biomed. Life Sci.*, 2013, **930**, 13–21.
155 R. Y. Tam, M. J. Cooke and M. S. Shoichet, *J. Mater. Chem.*, 2012, **22**, 19402–19411.
156 S. A. Yankofsky, R. Gurevitch, A. Niv, G. Cohen and L. Goldstein, *Anal. Biochem.*, 1981, **118**, 307–314.
157 V. G. Janolino and H. E. Swaisgood, *J. Food Biochem.*, 2007, **26**, 119–129.
158 S. Jung, B. Angerer, F. Löscher, S. Niehren, J. Winkle and S. Seeger, *Chembiochem*, 2006, **7**, 900–903.
159 J. Huang, I. Ichinose and T. Kunitake, *Angew. Chem., Int. Ed. Engl.*, 2006, **45**, 2883–2886.
160 G. T. Hermanson, *Bioconjugate techniques*, Academic Press, London, 2008.
161 J. Turková, *J. Chromatogr. B*, 1999, **722**, 11–31.
162 T. Barroso, M. Temtem, A. Hussain, A. Aguiar-Ricardo and A. C. a. Roque, *J. Membr. Sci.*, 2010, **348**, 224–230.
163 V. Gaberc-Porekar and V. Menart, *J. Biochem. Biophys. Methods*, 2001, **49**, 335–360.
164 Thermo Scientific, His-tagged Proteins, http://www.piercenet.com/browse.cfm?fldID=1470D72F-469A-424B-90F7-2EDBCFBD33FC, accessed 27 September, 2013.
165 J. A. Bornhorst and J. J. Falke, *Methods Enzymol.*, 2010, **326**, 245–254.
166 C. Ley, D. Holtmann, K.-M. Mangold and J. Schrader, *Colloids Surf., B*, 2011, **88**, 539–551.
167 J. Wang, B. Yiu, J. Obermeyer, C. D. M. Filipe, J. D. Brennan and R. Pelton, *Biomacromolecules*, 2012, **13**, 559–564.
168 P. Jonkheijm, D. Weinrich, H. Schröder, C. M. Niemeyer and H. Waldmann, *Angew. Chem., Int. Ed. Engl.*, 2008, **47**, 9618–9647.
169 R. a. Sheldon and S. van Pelt, *Chem. Soc. Rev.*, 2013, **42**, 6223–6235.
170 M. Ornatska, E. Sharpe, D. Andreescu and S. Andreescu, *Anal. Chem.*, 2011, **83**, 4273–4280.
171 W. Liu, C. L. Cassano, X. Xu and Z. H. Fan, *Anal. Chem.*, 2013, **85**, 10270–10276.
172 H. Orelma, I. Filpponen, L.-S. Johansson, J. Laine and O. J. Rojas, *Biomacromolecules*, 2011, **12**, 4311–4318.
173 S. Arola, T. Tammelin, H. Setälä, A. Tullila and M. B. Linder, *Biomacromolecules*, 2012, **13**, 594–603.
174 R. Villalonga, A. Fujii, H. Shinohara, S. Tachibana and Y. Asano, *Sens. Actuators, B*, 2008, **129**, 195–199.
175 U. Bora, P. Sharma, K. Kannan and P. Nahar, *J. Biotechnol.*, 2006, **126**, 220–229.
176 U. Bora, K. Kannan and P. Nahar, *J. Membr. Sci.*, 2005, **250**, 215–222.
177 M. Erdtmann, R. Keller and H. Baumann, *Biomaterials*, 1994, **15**, 1043–1048.
178 A. Yu, J. Shang, F. Cheng, B. A. Paik, J. M. Kaplan, R. B. Andrade and D. M. Ratner, *Langmuir*, 2012, **28**, 11265–11273.
179 V. Kuzmenko, S. Sämfors, D. Hägg and P. Gatenholm, *Mater. Sci. Eng., C*, 2013, **33**, 4599–4607.
180 Y. Wang, S. Wang, S. Ge, S. Wang, M. Yan, D. Zang and J. Yu, *Anal. Methods*, 2013, **5**, 1328–1336.
181 A. C. Araújo, Y. Song, J. Lundeberg, P. L. Ståhl and H. Brumer, *Anal. Chem.*, 2012, **84**, 3311–3317.
182 J. Martínez Urreaga and M. U. de la Orden, *Eur. Polym. J.*, 2006, **42**, 2606–2616.
183 J. Malešič, J. Kolar, M. Strlič, D. Kočar, D. Fromageot, J. Lemaire and O. Haillant, *Polym. Degrad. Stab.*, 2005, **89**, 64–69.
184 A. Aied, Y. Zheng, A. Pandit and W. Wang, *ACS Appl. Mater. Interfaces*, 2012, **4**, 826–831.

Chapter 2 A one-step and biocompatible cellulose functionalization for covalent antibody immobilization on immunoassay membranes

As previously pointed out, direct adsorption of antibodies onto cellulose is too weak to allow the permanent immobilization required in the development of effective immunoassay [49,53,57]. Thus, antibody immobilization onto this substrate is preferentially performed by crosslinking or direct covalent bonding (see Chapter 1), which involve chemical modifications of antibodies and / or substrate [33,49,58]. Coupling intermediates are usually employed [22,33,59–65]. Many are commercially available (Crosslinking Reagents, Thermo Fisher Scientific Inc., Rockford, IL, USA) [66].

Through crosslinking reactions, biomolecules covalently bind to the substrate but also to each other, randomly. Hence, the amount of immobilized antibodies varies a lot. In addition, many of the so immobilized antibodies cannot be reached by their target antigen and are therefore wasted. Consequently, crosslinking method was ruled out in order to optimize the immobilization process in an economically friendly way.

With respect to covalent bonding, the functionalization of cellulose substrate is the most economical and antibody-friendly way to proceed. Following this pathway, cellulose first needs to be functionalized with moieties which are usually involved in bioconjugate techniques [67]. These moieties will then enable to graft antibodies by common bioconjugation procedures which are known as non-damaging for antibody activity. Because it seems the most effective and eco²-friendly method, this strategy has been applied to the process developed and presented thereafter.

Contents

1 INTRODUCTION 43

2 EXPERIMENTAL 44

2.1 REAGENTS AND MATERIALS 44
2.2 SPECTROSCOPIES 44
2.3 CELLULOSE MODIFICATION 45
2.4 GRAFTING OF ANTIBODIES 45
2.4.1 Paper activation: EDC/NHS activation of carboxyl groups 45
2.4.2 Paper activation: SATA derivatization of primary amine groups 45
2.4.3 Antibody activation: Preparation of maleimido-antibodies 45
2.5 IMMUNOASSAYS 45
2.5.1 Preparation of colloidal-gold-labeled antibodies 45
2.5.2 Detection of the grafted antibodies (incubation assay) 46
2.5.3 Detection of antigen by sandwich immunoassay (incubation assay) 46
2.5.4 Immunochromatographic strips (LFIA) 46

3 RESULTS AND DISCUSSION 46

3.1 ONE-STEP CELLULOSE SHEET FUNCTIONALIZATION UNDER SOFT CONDITIONS 46
3.2 COVALENT BINDING OF ANTIBODIES TO CELLULOSE PAPER SHEETS 48
3.3 CONSERVATION OF THE BIOLOGICAL ACTIVITY 49
3.4 USE IN LATERAL FLOW IMMUNOASSAY 50

4 CONCLUSIONS 51

REFERENCES 51

SUPPLEMENTARY MATERIAL 53

Credou, J.; Volland, H.; Dano, J.; Berthelot, T.

A one-step and biocompatible cellulose functionalization for covalent antibody immobilization on immunoassay membranes.

J. Mater. Chem. B 2013, 1, 3277–3286.

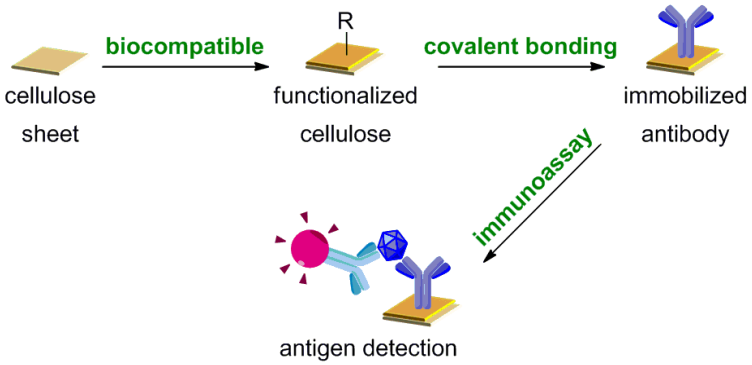

Easy-to-use biomolecule immobilization membranes were produced by a one-step functionalization of cellulose sheets under soft conditions.

Journal of Materials Chemistry B

RSC Publishing

PAPER

View Article Online
View Journal | View Issue

Cite this: J. Mater. Chem. B, 2013, 1, 3277

A one-step and biocompatible cellulose functionalization for covalent antibody immobilization on immunoassay membranes†

Julie Credou,[ab] Hervé Volland,[b] Julie Dano[b] and Thomas Berthelot*[a]

Among bioactive papers, many multiplexed assays implement methods incompatible with the conventional lateral flow immunoassay (LFIA) carrier material, nitrocellulose. Consequently, its replacement by cellulose has to be considered. This technological breakthrough requires a surface chemistry which ensures both the biomolecules covalent grafting to cellulose and the conservation of their biological activity. To comply with these requirements, the process elaborated in this study implements compounds and methods compatible with biological material. While cellulose chemical modification is usually operated under harsh conditions in organic solvents, the diazonium-based functionalization procedure presented here was performed onto cellulose sheets in water and at room temperature. Paper sheets have been successfully modified and bear different chemical functions which enable grafting of biomolecules by common bioconjugate techniques and to perform LFIAs. More generally, the chemical ways developed in this study are suitable for many biomolecules and would be helpful for any sensitive molecule immobilization onto cellulose sheets.

Received 19th March 2013
Accepted 1st May 2013

DOI: 10.1039/c3tb20380h

www.rsc.org/MaterialsB

Introduction

Bioactive papers can be defined as paper-based products bearing active biomolecules. They represent an alternative technology for developing simple, inexpensive, handheld and disposable devices[1–3] and therefore meet the growing interest in improved point-of-care testing (POCT).[1,3–6] Such materials find their applications in many areas including clinical diagnosis,[6–8] food quality control,[9–11] environmental monitoring,[12–14] and in any functional task that may be fulfilled by a biomolecule.[4,15,16] Within the last fifty years, paper-based biosensors have attracted a strong interest, particularly lateral flow assays[17–19] such as pregnancy tests or other urine test strips which are already widely commercially used. Lateral flow immunoassay (LFIA) ensures specific and sensitive measurements of target analytes thanks to the high specificity of the antibody (Ab)–antigen (Ag) interaction.[17] Moreover this is a perfect example of point of care test, designed for a single use outside the laboratory.[19,20] However, LFIAs are still being improved and optimized in order to diversify their application fields. For instance, this type of immunoassay mainly allowed detection of only one agent per sample so far. Therefore, multiplexing appears to be a new challenge.[8,13,21–23]

Indeed, multiplex assay allows detection of several analytes per sample in a single run. In such an assay, multiple independent assays are carried out simultaneously in different test zones of the device. LFIAs with several test lines (mainly two) allowing for multianalyte testing have been developed.[24,25] But more than four test lines can hardly be applied on a single 2 × 0.5 cm strip. To enable more simultaneous detection while avoiding any cross-contamination, multiplex devices need patterned microfluidic channels leading to independent test zones in the frame material. Considering paper-based multiplex devices, it means either defining hydrophobic barriers and hydrophilic channels on a piece of cellulose paper or shaping the paper by cutting.[3] Various methods for patterning paper sheets have been developed.[3,23] Among the numerous processes, there are photolithography, using SU-8 or SC photoresist,[6,26–28] "wax printing" or "wax dipping",[29–31] inkjet printing[32] and laser cutting.[4,5] Many existing methods include a step in which the paper temperature increases: SU-8 is baked at 95 °C,[26] wax is melted and spread through the paper at 150 °C,[31] liquid ink is slightly hot since it is heated around 350 °C in the printer and laser energy heats the paper. Consequently, nitrocellulose which is the classical material for the detection pad which bears biomolecules in LFIA[19,20,33] cannot be used with these methods. Actually, nitrocellulose membranes cannot withstand such patterning conditions as they begin to decompose at temperatures as low as 55 °C, and may undergo autoignition at 130 °C.[34] Furthermore, they are highly flammable and are not compatible

[a]CEA/DSM/IRAMIS/SPCSI/Laboratoire de Chimie des Surfaces et Interfaces (LCSI), Gif sur Yvette, F-91191, France. E-mail: thomas.berthelot@cea.fr; Fax: +33 169084044; Tel: +33 169086588

[b]CEA/DSV/iBiTec-S/SPI/Laboratoire d'Etudes et de Recherche en Immunoanalyse (LERI), Gif sur Yvette, F-91191, France

† Electronic supplementary information (ESI) available. See DOI: 10.1039/c3tb20380h

with many organic solvents employed in those patterning methods, particularly those used for SU-8.[35]

Cellulose paper enables this material issue to be overcome. This biopolymer has actually lots of appealing properties such as large bioavailability, wicking properties allowing migration by capillarity without needing any external power sources, good biocompatibility and biodegradability. It is also inexpensive, available in a broad range of thicknesses and well-defined pore sizes, easy to store and safely disposable.[2,6,36] However, cellulose does not immobilize proteins by adsorption as well as nitrocellulose. Direct adsorption of antibodies onto cellulose might not give reproducible results since Jarujamrus' findings revealed that about 40% of antibody molecules adsorbed onto cellulose paper can actually desorb from the fibers.[37] Since permanent immobilization of biomolecules on paper surfaces is crucial to developing effective paper-based bioassays,[2] biomolecules should therefore be covalently bound to the paper[1,2] and thus cellulose needs to be functionalized.[1,38,39]

Many studies have reported cellulose modifications for covalent immobilization of biomolecules.[1,2] Ideally, covalent chemical bonding immobilization should be conducted under mild conditions, with few side reactions, in few steps, with a minimum of denaturation of the immobilized biomolecule which needs to keep its original functionality.[1,2] Meanwhile, cellulose modifications are frequently performed on cellulose powder or fiber,[40–43] under harsh conditions, in organic solvent, or with highly toxic reagents or side products.[44,45] Photochemical functionalization is a milder approach but still currently conducted in organic solvent.[46] Other processes use a gel or a polymer, physically adsorbed onto cellulose, but still not covalently bound to it.[29,36,47] Biomolecules are then covalently bound to this primer through more or less heavy operating conditions. To the best of our knowledge, no cellulose modification has been done in sheet form, under soft conditions, *i.e.* in an aqueous environment and at room temperature.

Herein, a simple and low-cost approach for functionalizing cellulose in sheet form under soft biocompatible conditions and the use of the so prepared cellulose membranes as biomolecule immobilization media in immunoassays are presented. The cellulose modifications were performed in a single step, in water and at room temperature. The synthetic pathway consisted in an aryldiazonium-based chemistry.[48–50] Various chemical functions were introduced onto cellulose and enabled covalent immobilization of biomolecules by common bioconjugate techniques.[51] To compare the efficiency of the different chemical compounds used we performed two tests: the first one evaluated the antibodies grafting rate and the second one assessed the remaining biological activity after their grafting. All results were analyzed with respect to nitrocellulose as the positive control and to pristine cellulose paper as the negative control regarding protein immobilization. Furthermore, as Posthuma-Trumpie *et al.* reported, no studies comparing the performance of different strip materials could be found.[19] Hence, the antibody-bearing functionalized papers produced in this study were used as a detection pad in lateral flow immunoassays.

Experimental

Reagents and materials

Arylamines (4-azidoaniline hydrochloride, 4-(2-aminoethyl)-aniline, 4-aminobenzoic acid and 4-aminobenzenethiol), 4-nitrobenzenediazonium tetrafluoroborate, *N*-(3-dimethylaminopropyl)-*N*′-ethylcarbodiimide hydrochloride (EDC), *N*-hydroxysulfosuccinimide sodium salt (sulfo-NHS), *S*-acetylthioglycolic acid *N*-hydroxysuccinimide ester (SATA), 4(*N*-maleimidomethyl)-cyclohexanecarboxylic acid *N*-hydroxysuccinimide ester (SMCC) and all chemicals were purchased from Sigma-Aldrich (St Louis, MO, USA). 4-Nitrobenzenediazonium tetrafluoroborate was used as received. 4-Azidobenzenediazonium tetrafluoroborate, 4-(2-ammonioethyl)benzenediazonium tetrafluoroborate, 4-carboxybenzenediazonium tetrafluoroborate and 4-mercaptobenzenediazonium tetrafluoroborate were previously synthesized from the corresponding amines and sodium nitrite in tetrafluoroboric acid solution (HBF_4 48 wt% in H_2O) as already described.[52] CF1 cellulose paper and AE 98 Fast nitrocellulose membrane were from Whatman (Maidstone, Kent, UK), no. 470 absorbent pad from Schleicher and Schuell BioScience GmbH (Dassel, Germany) and MIBA-020 strips backing card from Diagnostic Consulting Network (Carlsbad, CA, USA). Proteins (ovalbumin (OVA), bovine serum albumin (BSA), porcine skin gelatin) were also from Sigma-Aldrich (St Louis, MO, USA). Monoclonal antibodies (mAbs) were produced and characterized as previously described.[53] Buffer reagents were from Merck (Whitehouse Station, NJ, USA). Water used in all experiments was purified with a Milli-Q system (Millipore, Brussels, Belgium). Sephadex G25 was from GE Healthcare Life Sciences (Piscataway, NJ, USA). 96-Well polystyrene microplates (flat-bottom, crystal-clear) were from Greiner Bio-One (Greiner Bio-One S.A.S. Division Bioscience, Les Ulis, France). UV irradiations were carried at room temperature in a CN-15.LC UV viewing cabinet (Vilber Lourmat, Marne-la-Vallée, France). Papers were cut using a laser plotter LaserPro Spirit (GCC Laser Pro, New Taipei City, Taiwan). Test strips were cut using an automatic programmable cutter Guillotine Cutting CM4000 Batch cutting system (BioDot, Irvine, CA, USA). Colorimetric intensity was measured using a Molecular Imager VersaDoc™ MP 4000 System and Quantity One 1-D Analysis Software (Bio-Rad, Hercules, CA, USA).

Spectroscopies

Infrared (IR) spectra were recorded on a Bruker Vertex 70 spectrometer controlled by OPUS software. ATR mono-reflection Pike-Miracle accessory was implemented. The detector was MCT working at liquid nitrogen temperature. Acquisitions were obtained at 2 cm^{-1} resolution after 256 scans.

X-ray photoelectron spectroscopy (XPS) studies were performed with a KRATOS Axis Ultra DLD spectrometer, using monochromatic Al K_α radiation (1486.6 eV) at 150 W and a 90° electron take-off angle. The area illuminated by the irradiation was about 2 mm in diameter. Survey scans were recorded with 1 eV step and 160 eV analyzer pass energy and the high-resolution regions with 0.05 eV step and 20 eV analyzer pass energy. During the data acquisition, the sample surfaces were neutralized with

slow thermal electrons emitted from a hot W filament and trapped above the sample by the magnetic field of the lens system (hybrid configuration). Referring to Johansson and Campbell's work, XPS analysis was carried out on dry samples, together with an *in situ* reference.[54]

Cellulose modification

Cellulose modification was performed in water, in open air and at room temperature. Diazonium salts were either synthesized previously[52] or *in situ*[55] from the corresponding arylamines (1.0 eq.; 0.30 mmol) and sodium nitrite (1.1 eq.; 0.33 mmol; 22.8 mg) in 1.0 M hydrochloric acid (HCl) solution (6 mL). L-Ascorbic acid (0.1 eq.; 0.03 mmol; 5.3 mg) was added to the so prepared 0.05 M aqueous solution of diazonium salt (1.0 eq.; 0.30 mmol in 6 mL of 1.0 M HCl). This mixture was poured dropwise onto a CF1 paper sheet (6 cm^2) and left to incubate for six hours in a glass Petri dish. The membrane obtained was washed with an aqueous solution the nature of which depended on the functionalizing chemical group borne by the paper (see Table 1 in the ESI†). It was subjected to an ultrasonic treatment in the same solution in order to discard any ungrafted matter. It was finally washed with water and dried for 20 minutes at 40 °C in an air oven. All the as functionalized papers were then analyzed using an infrared spectrometer, XPS, dyeing reagents or colorimetric probes in order to point out the chemical groups brought by the modifications. Table 1 in the ESI† summarizes the different operating conditions applied regarding the different chemical groups introduced onto the paper.

Grafting of antibodies

Murine anti-OVA monoclonal antibodies (0.5 mg mL^{-1} in 0.1 M potassium phosphate buffer, pH 7.4, 40 μL cm^{-2} deposit) were immobilized by adsorption onto nitrocellulose (positive control) and onto pristine CF1 cellulose paper (negative control), while they were covalently grafted onto modified CF1 cellulose paper. Results obtained after covalent antibody grafting were compared to positive and negative controls. Several usual bioconjugate techniques[51] were carried out, depending on the groups borne by the paper (see Table 2 in the ESI† for details). Briefly, antibodies were incubated onto nitrocellulose, pristine cellulose and nitroaryl-bearing cellulose without any previous modification of either papers or antibodies. On another hand, carboxyl-bearing cellulose was subjected to EDC/NHS activation prior to antibody incubation; amine-bearing cellulose was derivatized with SATA and transformed into thiolated cellulose; and maleimido-antibodies were incubated onto the thiolated papers. Those activation methods are detailed below. Regarding arylazide-bearing cellulose, antibodies were dropped off; the sample was dried in order to concentrate them and then irradiated.

All the samples obtained after immobilization were washed with 0.1 M potassium phosphate buffer, pH 7.4. The unreacted binding sites on the paper were blocked using a saturating solution to reduce unspecific protein adsorption during immunoassays. The nature of this solution depended on the assay further performed on the papers. After drying for 20 minutes at 40 °C in an air oven, paper sheets were cut using the laser plotter.

Paper activation: EDC/NHS activation of carboxyl groups

An EDC/sulfo-NHS solution (50/60 mM in 0.1 M potassium phosphate buffer, pH 5) was poured onto a carboxyl-bearing paper sheet (40 μL cm^{-2}). After a thirty minute reaction at room temperature, the paper was washed with 0.1 M potassium phosphate buffer, pH 7.4, and dried over absorbent paper.

Paper activation: SATA derivatization of primary amine groups

A 100 mg mL^{-1} solution of SATA in DMF was diluted 10 times in 0.1 M sodium borate buffer, pH 9. This mixture was poured onto an amine-bearing paper sheet (40 μL cm^{-2}). After a one hour incubation at room temperature, the paper was washed with 0.1 M sodium phosphate buffer, pH 6, containing 5 mM EDTA. The thiol function was further deprotected by incubating the paper in 0.1 M hydroxylamine (0.5 mL cm^{-2}) for 30 minutes. After washing with 0.1 M sodium phosphate buffer, pH 6, containing 5 mM EDTA, the thiolated paper was dried over absorbent paper.

Antibody activation: preparation of maleimido-antibodies

Maleimido-antibodies (or SMCC-antibodies) were prepared according to Khreich's protocol.[56] 9 μL of a 10 mg mL^{-1} solution of SMCC in DMF were added to 2 mg of monoclonal antibodies. After a one hour reaction at 20 °C, the maleimido-mAbs were purified on a Sephadex G25 column that was eluted with 0.1 M sodium phosphate buffer, pH 6, containing 5 mM EDTA.

Immunoassays

Grafting rate and biological activity of the immobilized antibodies were evaluated by colloidal-gold-based immunoassays.[19] Since a visible dye was used, the signal intensity was first qualitatively estimated by eye and then by colorimetric measurement. All the reagents were diluted in the analysis buffer (0.1 M potassium phosphate buffer, pH 7.4, containing 0.1% BSA, 0.15 M NaCl, and 0.5% (v/v) Tween 20) for 30 minutes at room temperature in order to reduce nonspecific binding. Incubation assays were performed on circular paper discs (3 mm in diameter; 7 mm^2) whereas LFIAs were conducted on rectangular pads (3 × 5 mm in size; 15 mm^2).

Preparation of colloidal-gold-labeled antibodies

Colloidal-gold-labeled antibodies (tracers)[19] were prepared following a procedure previously described.[56] 4 mL of gold chloride and 1 mL of 1% sodium citrate solution were added to 40 mL of boiling water with constant agitation. Once the mixture had turned purple, this colloidal gold solution was allowed to cool to 20 °C and stored at 4 °C in the dark. 1 mL of this colloidal gold solution, 25 μg of mAb and 100 μL of 20 mM borax buffer, pH 9.3, were mixed and incubated for one hour on a rotary shaker at 20 °C. This led to the ionic adsorption of the antibodies on the surface of the colloidal gold particles. Afterwards, 100 μL of 20 mM borax buffer, pH 9.3, containing 1%

BSA, was added and the mixture was centrifuged at 15 000*g* for 50 minutes at 4 °C. After discarding the supernatant, the pellet was suspended in 250 μL of 2 mM borax buffer, pH 9.3, containing 1% BSA and stored at 4 °C in the dark.

Detection of the grafted antibodies (incubation assay)

In order to reduce nonspecific binding sites, papers were blocked using an albumin saturating solution (0.1 M potassium phosphate buffer, pH 7.4, containing 0.5% BSA and 0.15 M NaCl) for 30 minutes at room temperature. Saturation using a gelatin solution (0.1 M potassium phosphate buffer, pH 7.4, containing 0.5% porcine gelatin and 0.15 M NaCl) overnight at 4 °C was compared to the albumin one.

A goat anti-mouse mAb tracer was first diluted 10 times in the analysis buffer. The assay was performed by incubating an antibody-bearing paper disc into 200 μL of the diluted tracer for two hours on a rotary shaker at 20 °C. The paper disc was further washed with the analysis buffer and dried over absorbent paper. Colorimetric measurement using the molecular imager was performed immediately after the paper had been impregnated with the analysis buffer.

Modified CF1 cellulose papers with no antibody immobilized but BSA (following the same procedure) assessed the unspecific signal due to unspecific adsorption of the tracer onto the saturating matrix during immunoassays.

Detection of antigen by sandwich immunoassay (incubation assay)

In order to reduce nonspecific binding sites, papers were blocked using a gelatin saturating solution overnight at 4 °C.

A solution of OVA and murine anti-OVA mAb tracer (1 μg mL^{-1} and 10-time dilution, respectively) in the analysis buffer was prepared and pre-incubated for 10 minutes. The assay was performed by incubating an antibody-grafted paper disc into 200 μL of this solution for two hours on a rotary shaker at 20 °C. The paper disc was further washed with the analysis buffer and dried over absorbent paper. Colorimetric measurement using the molecular imager was performed immediately after the paper had been impregnated with the analysis buffer.

Sandwich immunoassay without antigen (OVA) assessed the unspecific signal due to unspecific adsorption of the tracer onto the antibody–gelatin matrix during immunoassays. Modified CF1 cellulose papers with no antibody immobilized but gelatin (following the same procedure) assessed the unspecific signal due to unspecific adsorption of the tracer or tracer–antigen complex onto the gelatin matrix during immunoassays.

Immunochromatographic strips (LFIA)

A test strip is composed of a sample pad, a detection pad, and an absorbent pad, all stuck to a backing card. An antibody-bearing paper pad (gelatin saturated) constituted the detection zone whereas the two surrounding sample wicks were made of gelatin saturated papers (Fig. 1). These pads and the absorbent pad were put together onto the backing card previously cut into strips of 5 mm width.

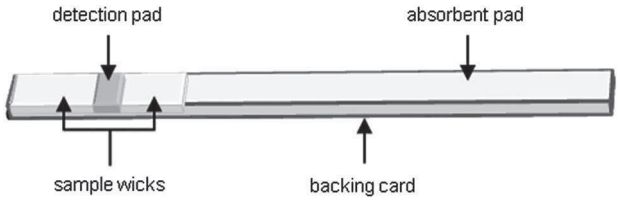

Fig. 1 Schematic design of an immunochromatographic strip.

A solution of OVA and murine anti-OVA mAb tracer (1 μg mL^{-1} and 10-time dilution, respectively) in the analysis buffer was prepared and pre-incubated for 10 minutes. The assay was performed at room temperature by inserting a strip into a well of a 96-well microtiter plate containing 100 μL of this solution. The mixture was absorbed by the pad and the capillary migration process lasted for about 15 minutes. The strip was further dried overnight at room temperature. Colorimetric measurement using the molecular imager was performed immediately after the paper had been impregnated with the analysis buffer.

As for previous sandwich immunoassay, assay without antigen (OVA) and gelatin-grafted modified CF1 cellulose papers assessed the unspecific signal due to unspecific adsorption of the tracer and/or tracer–antigen complex. The usual LFIA control zone of the detection pad was made on a separate strip dipped in the assay solution.

Results and discussion

One-step cellulose sheet functionalization under soft conditions

Whatman CF1 paper was chosen as it is broadly used in immunochromatographic tests. It is known as a high quality paper, made of quite pure and clean cellulose (Fig. 2), and the thickness and wicking properties of which are rather uniform. Therefore, it is sold as dipstick or sample wick but not as medium for preparing a lateral flow immunoassay detection zone as it is used in this study (Diagnostic Components, Whatman, Maidstone, Kent, UK). Moreover, since we used it for the detection pad of colorimetric immunochromatographic strip assays, there is a need to concentrate the signal close to the surface as much as possible. As it is one of the thinnest cellulose sample wicks available (176 μm at 53 kPa), CF1 is a good candidate to comply with this requirement.

These cellulose paper sheets have been modified under soft conditions, in a single step. The synthetic pathway to modify cellulose sheets (Fig. 3) consisted in an aryldiazonium-based

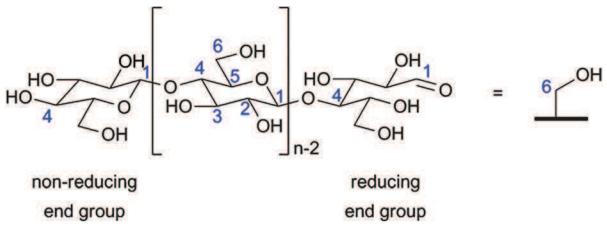

Fig. 2 Cellulose formula and schematic representation.

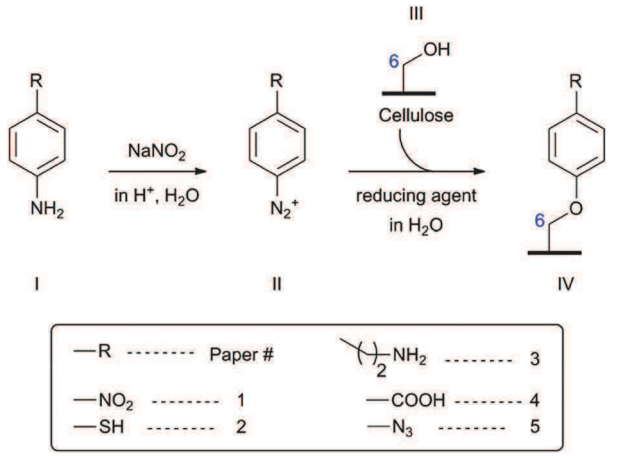

Fig. 3 Preparation of an aryl-R-bearing cellulose membrane and identification of the functionalized papers obtained. Aryldiazonium (II), previously or *in situ* synthesized from the corresponding arylamine (I), is reduced and reacts with cellulose (III) in an aqueous medium to give an aryl-R-bearing cellulose membrane (IV).

surface chemistry.[48,50] Since diazonium salts are known to be free radical polymerization initiators,[48] the mechanism proposed here for cellulose functionalization (Fig. 4) involves a free radical reaction. Whatman CF1 paper is made of 100% cotton linter, which supposes almost pure cellulose as suggested by Kalia *et al.*[57] According to its molecular structure (Fig. 2), hydroxyl groups in glucose are responsible for cellulose chemical activity. Among the three hydroxyl groups in each glucose residue, Roy *et al.* described the hydroxyl at 6-position (primary one) as the most reactive site, far more than hydroxyl at 2-, and 3-positions (secondary ones).[58]

To perform a biocompatible process for cellulose modification, reactions took place in acidic water at room temperature with a biological reducing agent (L-ascorbic acid, also known as vitamin C). Indeed, the poor stability of aryldiazonium salts at high pH led to conduct the diazonium grafting in acidic water with pH $\leq$ 2.[48] In order to check the cellulose stability at low pH, cellulose paper sheets were immersed into a 1.0 M HCl solution for different times at room temperature. No color change of paper and no visible paper hydrolysis (IR spectra, not shown) were observed. These results are in agreement with literature data[59] which describe cellulose hydrolysis occurring only at higher acid concentration and at reflux temperature.

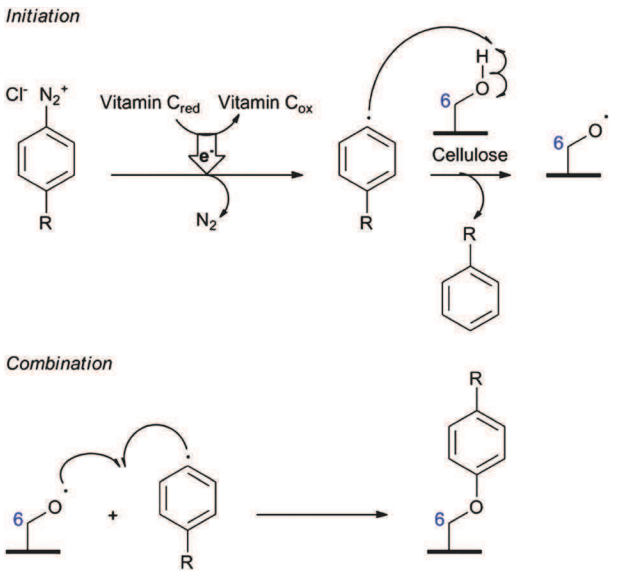

Fig. 4 A proposed mechanism for cellulose functionalization through diazonium-based chemistry.

Cellulose sheets have been successfully modified and bear different chemical groups such as carboxyl, amine or thiol (Fig. 3) which are widely used in bioconjugate techniques.[51] The various functional groups were characterized by different analytical techniques depending on their nature (see Table 3 in the ESI†). ATR-FTIR is the method of choice for analyzing modified surfaces.[60] NO_2 antisymmetric stretching vibration at 1525 $\pm$ 5 cm^{-1} was identified as shown in Fig. 5a. Unfortunately, the intense cellulose spectrum hid most of the characteristic bands pointing out the grafted compounds. Therefore, thiol, amine or carboxyl functions were not clearly identified by ATR-FTIR. To overcome this drawback, XPS was used since it allows the identification of elements within 10 nm deep subsurface layers.[54] The peaks at 164 $\pm$ 0.35 eV and 220 $\pm$ 0.35 eV, attributable to S 2p and S 2s signals, respectively, confirmed that cellulose paper had been modified with arylthiol moieties (Fig. 5b). Cellulose modification by amine functions was confirmed by the peak at 400 $\pm$ 0.35 eV attributable to N 1s (Fig. 5c). Ninhydrin staining (not shown) confirmed this statement. However, since cellulose is a biopolymer made up of glucose units (Fig. 2), CF1 paper is composed of carbon and oxygen and therefore its XPS signal for these two elements is quite strong too (O 1s orbital binding energy at 533 eV, C 1s orbital binding energy at 286 eV noticeable in Fig. 5b).[54] Consequently, it is really difficult to detect a small additional amount of these elements brought by the functionalization, *e.g.* for carboxyl-bearing cellulose. Moreover, because of the ring structure of the cellulose monomer, those carbon and oxygen atoms can barely be distinguished from carbonyl ones. Finally, staining methods, using thin layer chromatography common dyes or colloidal-gold-labeled biomolecules, were also performed. The presence of arylazide moieties onto cellulose was highlighted by the localized UV-grafting (irradiation at 365 nm (1050 $\mu W\ cm^{-2}$) for 15 minutes) of a colloidal-gold-labeled antibody (used as colorimetric probe) dropped off onto the modified paper and partially covered with a mask (Fig. 5d). Thus, almost all the functions were identified except carboxyl groups. Therefore, in this specific case, the cellulose modification was further confirmed through indirect visualization by the following immunoassays. Table 3 in the ESI† summarizes the analysis and the corresponding figures that enabled identification of the chemical functions introduced onto the cellulose surface.

Even though they could appear quite small, all perceptible signals due to functionalization and respective intensities measured either by ATR-FTIR or XPS are consistent with literature data dealing with surface functionalization.[36,61,62] Furthermore, these are consistent with the low values usually

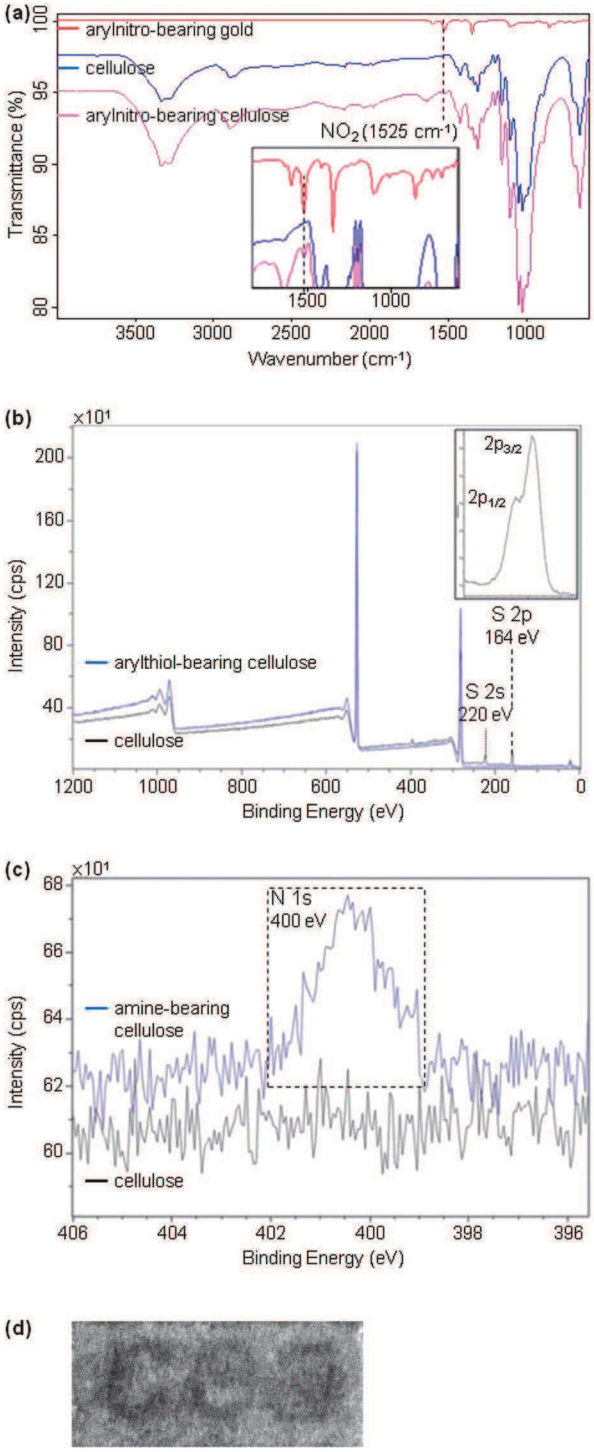

Fig. 5 Analysis of the modified cellulose papers. (a) IR spectrum of nitroaryl-bearing cellulose. The peak corresponding to NO_2 antisymmetric stretching vibration is labeled. (b) XPS survey analysis of arylthiol-bearing cellulose. The peaks corresponding to S 2s and S 2p orbitals are labeled, along with $2p_{1/2}$ and $2p_{3/2}$ electron levels. (c) XPS high-resolution analysis of amine-bearing cellulose. The peak corresponding to the N 1s orbital is labeled. (d) Photolithography on arylazide-bearing cellulose. Arylazide-bearing paper was impregnated with a colloidal-gold-labeled antibody (40 μL cm^{-2}), covered with a mask and irradiated at 365 nm for 15 minutes. After washing with the analysis buffer, the picture was taken using a molecular imager.

obtained when measuring the degree of substitution (DS) of functionalized cellulose.[63] DS is the average number of hydroxyl groups of the glucose unit of the cellulose molecule that have been substituted. Yet, the reactivity of the hydroxyl groups can be affected by their involvement into wide hydrogen bond networks, responsible for the cohesive structure of cellulose fibers.[58] Moreover, it is not desirable to have all of these hydroxyl groups react in order to keep the structure intact.[64] In addition, the accessibility to these groups is dependent on the crystalline structure of the fiber since chemical reagents cannot penetrate the crystalline regions.[58] Considering that, the DS value is often between 0 and 1.5,[63] and laborious to determine if we are not grafting polymers onto cellulose.[64]

Covalent binding of antibodies to cellulose paper sheets

The chemical groups introduced onto cellulose enabled grafting of biomolecules by common bioconjugate techniques.[51] Different conjugation methods were applied, from van der Waals interactions to covalent bonds, depending on the groups borne by the paper. The grafting rate of antibodies onto the different papers was assessed by a colloidal-gold-based immunoassay. This colorimetric detection method is based on the purple color stemming from colloidal gold clusters. Colloidal gold is broadly used in lateral flow assays aiming at monitoring drugs, or analyzing food safety.[18,19,65] This is mostly because it gives rapid and easily readable information.[33]

In order to demonstrate the fixation of the murine antibodies onto cellulose sheets, and evaluate the grafting rate, a colloidal-gold-labeled goat anti-mouse mAb was used as a tracer. After incubation, the colorimetric intensity was measured using an imager. These intensities depended on different incubation parameters (time, temperature, rotation speed) and the moisture content of paper at the time of measurement. Consequently, all papers were incubated at the same time under the same conditions and wet following the same procedure prior to measurement to overcome these measurement drawbacks. The immobilization ability or grafting rate of the modified cellulose papers was measured by the difference between the antibody-grafted paper signal and the BSA-grafted corresponding one displaying the unspecific adsorption of biomolecules (in this case, the tracer). This result was compared to nitrocellulose (positive control) which is assimilated to 100% of antibody immobilization capacity. The colorimetric intensity averages with corresponding standard deviations from 4 different experiments are reported in Fig. 6.

The results from BSA-grafted papers indicated no visible background noise, which revealed no nonspecific biomolecule adsorption. This proved the residual functions blocking and the non-specific binding sites saturation to be effective. Nevertheless, the absence of background noise could also be ascribed to the colloidal gold label and its minimal concentration required to be seen.[20,24]

Firstly, nitroaryl-bearing cellulose (paper #1), a nitrocellulose-like paper, was used to adsorb antibodies through a combination of electrostatic, hydrogen, and hydrophobic forces.[33] After incubation with a goat-anti-mouse tracer, the

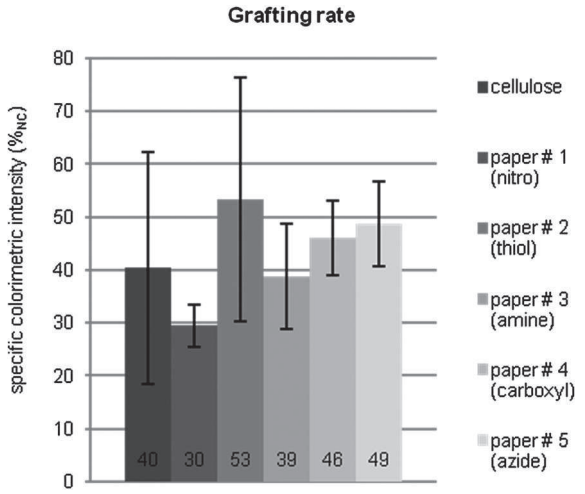

Fig. 6 Mean value and repeatability from 4 different experiments of the measured grafting rates relative to nitrocellulose as a positive control. Paper discs grafted with murine anti-OVA antibodies and saturated with BSA were incubated into a goat anti-mouse tracer antibody for two hours at 20 °C. After washing and impregnating with the analysis buffer, colorimetric measurement was performed using a molecular imager. The grafting rate of the modified cellulose papers was measured by the difference between the antibody-grafted paper signal and the BSA-grafted corresponding one displaying the unspecific adsorption of the tracer onto the saturating matrix.

paper #1 immobilization ability was valued at $30 \pm 4\%_{NC}$ of the nitrocellulose immobilization ability. This result can be explained by (i) a low rate of the nitroaryl group on paper in comparison with the nitro group in nitrocellulose and (ii) the presence of the aryl group which decreases the resulting electron density on the nitro group and the resulting intensities of the local charges present onto the functionalized paper.

On the other hand, the thiolated paper (paper #2) covalently immobilized antibodies by addition of the thiol function onto the maleimide group previously added to the antibody through SMCC derivatization. Paper #2 showed a high immobilization ability of $53 \pm 23\%_{NC}$. However, compared to other functionalized papers, arylthiol-bearing cellulose appears rather yellow and consequently might not be appropriate for some colorimetric assays.

For amine-bearing cellulose (paper #3), SATA and SMCC were preferred to the EDC/NHS method often used.[66,67] Actually, since it activates carboxylic groups in antibodies, this method would result in antibody polymerization through those activated groups and other primary amine functions in antibodies. After amine derivatization with the SATA linker followed by SMCC-antibodies grafting through thiol-maleimide conjugation,[56] the immobilization ability of paper #3 was valued at $39 \pm 10\%_{NC}$.

In another way, carboxyl-bearing cellulose (paper #4) grafted antibodies by forming an amide bond with their primary amine functions. After EDC/NHS activation of the carboxyl group followed by grafting of antibodies, the immobilization ability of paper #4 was valued at $46 \pm 7\%_{NC}$.

With regard to arylazide-bearing cellulose (paper #5), irradiation turned the azide function into a nitrene which is a quick and non-specific reactive function.[45,46] As a result, it might react with any compound on its immediate surrounding: antibodies or solvent molecules. Thus, antibodies had to be concentrated onto the surface so as to increase the grafting rate. This statement was confirmed by noticing the contribution of the drying step which aimed at concentrating antibodies before irradiation (not shown). Its immobilization ability was then valued at $49 \pm 8\%_{NC}$.

The use of a previously or *in situ* synthesized diazonium salt was assessed through papers #3 and 5. The difference was not significant. As cellulose functionalization only takes place with the aryldiazonium function, we assume that this result could be extended to other aryldiazonium salts. However, the *in situ* synthesis might therefore be favored to make the process easier, faster and less solvent-consuming.

With regard to grafting rate results, the different chemical groups borne by papers, and the related bioconjugate techniques, were then compared. Papers bearing thiol, carboxyl and azide (papers #2, 4 and 5, respectively) showed quite similar immobilization abilities which are better than pristine cellulose and nitroaryl-bearing cellulose ones (Fig. 6), displaying the contribution of the covalent antibody immobilization. The repeatability of the result was good, except for thiol-bearing cellulose (paper #2). This lack of consistency could be due to the SMCC derivatization of the antibody that introduces an additional step compared to other bioconjugate techniques and therefore increases the grafting rate variability. The best repeatability was obtained with the arylazide-bearing and carboxyl-bearing papers (papers #5 and 4). In those cases, raw antibodies were used, thus avoiding additional variability, which is consistent with the previous hypothesis concerning thiolated paper. Besides, the method applied to covalently immobilize antibodies onto paper #5 is the fastest and the easiest one to carry out and so should be preferred. Nevertheless, more chemical groups are still being tested in order to increase the grafting rate along with repeatability.

All previous results were collected from BSA saturated papers. This saturation solution was chosen because it is the usual blocking solution in LFIA.[19,56] Results from gelatin saturation are reported and compared to the latter in Fig. 7. The different modified cellulose papers have similar ranking regardless of the saturating solution. Nevertheless, it is obvious that gelatin saturation enhances the specific colorimetric intensity signal and makes the distinction between the different papers clearer. A study carried out by Halder *et al.* on cellulose powder reported that the ranking of proteins in terms of the number of molecules of adsorbed protein per mass of cellulose was gelatin > β-lactoglobulin > lysozyme > BSA when working under fixed physicochemical conditions.[68] This suggests that gelatin surface coverage of cellulose must be better than the BSA one and that gelatin saturation should be preferentially used. This is consistent with our results, and particularly the fact that sandwich immunoassay could not have been done with BSA saturated papers because of too high nonspecific signal.

Conservation of the biological activity

Biological activity of the different antibody-bearing papers was assessed by a colloidal-gold-based sandwich immunoassay. The

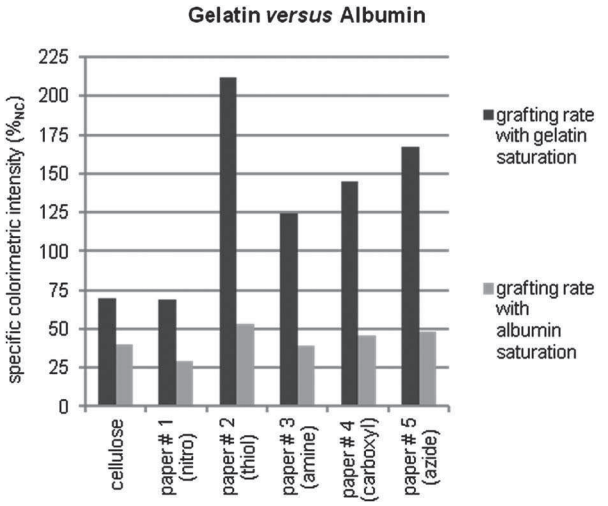

Fig. 7 Grafting rate: a comparison between gelatin and albumin saturations. Paper discs grafted with murine anti-OVA antibodies and saturated with BSA (or gelatin) were incubated into a goat anti-mouse tracer antibody for two hours at 20 °C. After washing and impregnating with the analysis buffer, colorimetric measurement was performed using a molecular imager. The grafting rate of the modified cellulose papers was measured by the difference between the antibody-grafted paper signal and the corresponding BSA-grafted (or gelatin-grafted) paper signal displaying the unspecific adsorption of the tracer onto the saturating matrix.

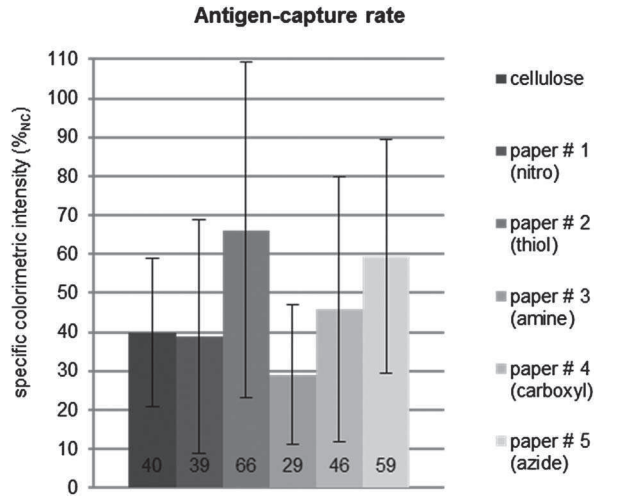

Fig. 8 Mean value and repeatability from 5 different experiments of the measured activity rates relative to nitrocellulose as a positive control. Paper discs grafted with murine anti-OVA capture antibodies and saturated with gelatin were incubated into OVA and murine anti-OVA tracer antibody for two hours at 20 °C. After washing and impregnating with the analysis buffer, colorimetric measurement was performed using a molecular imager. The antigen-capture rate of the modified cellulose papers was measured by the difference between the antibody-grafted paper signal in the presence of OVA and the corresponding one in its absence displaying the unspecific adsorption of tracer onto the matrix.

capture ability of the grafted murine antibodies was assessed using anti-ovalbumin monoclonal antibodies as capture (immobilized on paper) and tracer antibodies (colloidal-gold-labeled). These two antibodies could simultaneously bind ovalbumin (OVA). After incubation in the presence or absence of OVA, the evaluation was made by colorimetric measurements.

The biological activity, or antigen-capture rate, was measured by the difference between the antibody-grafted paper signal in the presence of OVA and the corresponding one in the absence of it. Signals of gelatin-grafted paper that have undergone the same two assays displayed the unspecific adsorption of biomolecules (in this case, the antigen and/or the tracer). The result was compared to nitrocellulose (positive control), which is assimilated to 100% of antigen-capture capacity. The colorimetric intensity averages with the corresponding standard deviations from 5 different experiments are reported in Fig. 8.

Papers bearing thiol, carboxyl and azide (papers #2, 4 and 5, respectively) showed better biological activities than pristine cellulose but are still less efficient than nitrocellulose. Their ranking is still the same as for the grafting rate. Most importantly, these experiments highlight that the grafted antibodies were still able to bind their antigen. Thus, it was validated that biological activity of the covalently bound antibodies had been partially preserved.

Use in lateral flow immunoassay

Colloidal-gold-based sandwich immunoassays previously described were further performed under lateral flow conditions, using antibody-bearing paper as a detection pad. As shown in Fig. 9, signals obtained using this format are similar to ones

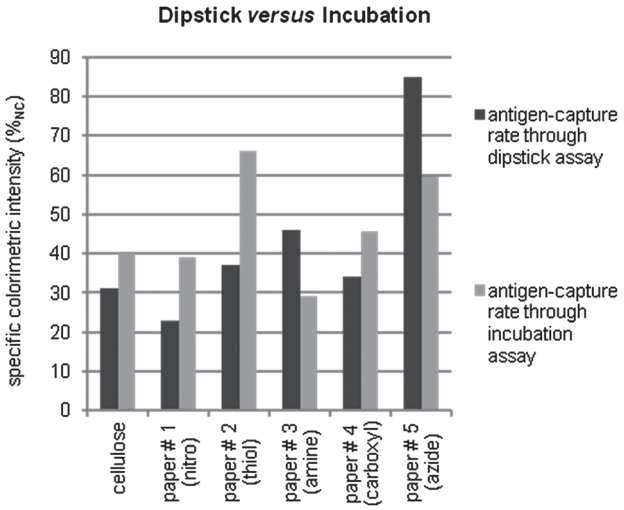

Fig. 9 Immunoassay results: a comparison between dipstick and incubation assays. Paper discs grafted with murine anti-OVA capture antibodies and saturated with gelatin were incubated into OVA and murine anti-OVA tracer antibody for two hours at 20 °C. After washing and impregnating with the analysis buffer, colorimetric measurement was performed using a molecular imager. At the same time, paper pads grafted with murine anti-OVA capture antibodies and saturated with gelatin were integrated into immunochromatographic strips as detection zone. The strips were dipped into OVA and murine anti-OVA tracer antibody solution for absorption. After drying and impregnating with the analysis buffer, colorimetric measurement was performed using a molecular imager. The antigen-capture rate of the modified cellulose papers was measured by the difference between the antibody-grafted paper signal in the presence of OVA and the corresponding one in the absence of it displaying the unspecific adsorption of the tracer onto the antibody–gelatin matrix.

obtained by incubation. Once again, our modified papers appear less efficient than nitrocellulose but more than pristine cellulose. Most importantly, it was proved that our system is usable in lateral flow immunoassay.

Conclusions

A simple, fast, low-cost and biocompatible method for obtaining functionalized paper sheets has been described. This new approach, based on aryldiazonium salt chemistry, is achieved under soft aqueous conditions and through a one-step procedure. Several chemical groups were introduced onto cellulose. The data suggest that this chemical pathway allows functionalization of cellulose with many different chemical functions. As for organic material modification, the main limitation lies in the cellulose analysis. Afterwards, the modified cellulose papers were used to covalently immobilize antibodies and the resulting papers were analyzed and tested under immunoassay conditions. This research was proposed to meet the need for paper-based technology to covalently immobilize biomolecules without damaging their activity. In addition, the investigations of the present study provide a method which might suit many sensitive molecule immobilization onto cellulose sheets. Thus, the expounded method, particularly the functionalized papers obtained this way, provides a powerful tool for biologists willing to use paper-based devices.

Acknowledgements

This work was financially supported by the Commissariat à l'Energie Atomique et aux Energies Alternatives (France). Pascale Jegou is greatly acknowledged for performing the XPS analysis and helping in analyzing XPS data.

References

1 R. Pelton, *Trends Anal. Chem.*, 2009, **28**, 925.
2 F. Kong and Y. F. Hu, *Anal. Bioanal. Chem.*, 2012, **403**, 7.
3 D. D. Liana, B. Raguse, J. J. Gooding and E. Chow, *Sensors*, 2012, **12**, 11505.
4 A. V. Govindarajan, S. Ramachandran, G. D. Vigil, P. Yager and K. F. Böhringer, *Lab Chip*, 2012, **12**, 174.
5 L. Lafleur, D. Stevens, K. McKenzie, S. Ramachandran, P. Spicar-Mihalic, M. Singhal, A. Arjyal, J. Osborn, P. Kauffman, P. Yager and B. Lutz, *Lab Chip*, 2012, **12**, 1119.
6 A. W. Martinez, S. T. Phillips, G. M. Whitesides and E. Carrilho, *Anal. Chem.*, 2010, **82**, 3.
7 C.-M. Cheng, A. W. Martinez, J. Gong, C. R. Mace, S. T. Phillips, E. Carrilho, K. A. Mirica and G. M. Whitesides, *Angew. Chem., Int. Ed.*, 2010, **49**, 4771.
8 L. Ge, J. Yan, X. Song, M. Yan, S. Ge and J. Yu, *Biomaterials*, 2012, **33**, 1024.
9 M. Vaher and M. Kaljurand, *Anal. Bioanal. Chem.*, 2012, **404**, 627.
10 S. M. Z. Hossain, R. E. Luckham, M. J. McFadden and J. D. Brennan, *Anal. Chem.*, 2009, **81**, 9055.
11 H. Anany, W. Chen, R. Pelton and M. W. Griffiths, *Appl. Environ. Microbiol.*, 2011, **77**, 6379.
12 R. S. J. Alkasir, M. Ornatska and S. Andreescu, *Anal. Chem.*, 2012, **84**, 9729.
13 S. M. Z. Hossain, C. Ozimok, C. Sicard, S. D. Aguirre, M. M. Ali, Y. Li and J. D. Brennan, *Anal. Bioanal. Chem.*, 2012, **403**, 1567.
14 M. Zhang, L. Ge, S. Ge, M. Yan, J. Yu, J. Huang and S. Liu, *Biosens. Bioelectron.*, 2013, **41**, 544.
15 R. Derda, S. K. Y. Tang, A. Laromaine, B. Mosadegh, E. Hong, M. Mwangi, A. Mammoto, D. E. Ingber and G. M. Whitesides, *PLoS One*, 2011, **6**, e18940.
16 X. Yang, O. Forouzan, T. P. Brown and S. S. Shevkoplyas, *Lab Chip*, 2012, **12**, 274.
17 T. R. J. Holford, F. Davis and S. P. J. Higson, *Biosens. Bioelectron.*, 2011, **34**, 12.
18 A. H. Peruski and L. F. Peruski, *Clin. Vaccine Immunol.*, 2003, **10**, 506.
19 G. A. Posthuma-Trumpie, J. Korf and A. van Amerongen, *Anal. Bioanal. Chem.*, 2009, **393**, 569.
20 B. Ngom, Y. Guo, X. Wang and D. Bi, *Anal. Bioanal. Chem.*, 2010, **397**, 1113.
21 E. M. Fenton, M. R. Mascarenas, G. P. López and S. S. Sibbett, *ACS Appl. Mater. Interfaces*, 2009, **1**, 124.
22 E. Njumbe Ediage, J. D. Di Mavungu, I. Y. Goryacheva, C. Van Peteghem and S. De Saeger, *Anal. Bioanal. Chem.*, 2012, **403**, 265.
23 X. Li, D. R. Ballerini and W. Shen, *Biomicrofluidics*, 2012, **6**, 011301.
24 C. Zhang, Y. Zhang and S. Wang, *J. Agric. Food Chem.*, 2006, **54**, 2502.
25 A. Y. Kolosova, S. De Saeger, L. Sibanda, R. Verheijen and C. Van Peteghem, *Anal. Bioanal. Chem.*, 2007, **389**, 2103.
26 A. W. Martinez, S. T. Phillips, M. J. Butte and G. M. Whitesides, *Angew. Chem., Int. Ed.*, 2007, **46**, 1318.
27 A. W. Martinez, S. T. Phillips and G. M. Whitesides, *Proc. Natl. Acad. Sci. U. S. A.*, 2008, **105**, 19606.
28 E. Carrilho, S. T. Phillips, S. J. Vella, A. W. Martinez and G. M. Whitesides, *Anal. Chem.*, 2009, **81**, 5990.
29 S. Wang, L. Ge, X. Song, J. Yu, S. Ge, J. Huang and F. Zeng, *Biosens. Bioelectron.*, 2012, **31**, 212.
30 T. Songjaroen, W. Dungchai, O. Chailapakul and W. Laiwattanapaisal, *Talanta*, 2011, **85**, 2587.
31 E. Carrilho, A. W. Martinez and G. M. Whitesides, *Anal. Chem.*, 2009, **81**, 7091.
32 A. Määttänen, U. Vanamo, P. Ihalainen, P. Pulkkinen, H. Tenhu, J. Bobacka and J. Peltonen, *Sens. Actuators, B*, 2012, **177**, 153.
33 *Lateral Flow Immunoassay*, R. C. Wong and H. Y. Tse, Humana Press, New York, NY, 2009.
34 *Millistak+ HC Filter Devices (with RW01)*, MSDS no. M114480, Millipore Corporation, Billerica, MA, 01821 USA, 2008.
35 *Nitrocellulose Membrane Filters*, MSDS no. 00000100SDS, Millipore Corporation, Billerica, MA, 01821 USA, 2011.
36 H. Orelma, T. Teerinen, L.-S. Johansson, S. Holappa and J. Laine, *Biomacromolecules*, 2012, **13**, 1051.

37 P. Jarujamrus, J. Tian, X. Li, A. Siripinyanond, J. Shiowatana and W. Shen, *Analyst*, 2012, **137**, 2205.
38 T. Heinze and T. Liebert, *Prog. Polym. Sci.*, 2001, **26**, 1689.
39 D. Klemm, B. Philipp, T. Heinze, U. Heinze, and W. Wagenknecht, in *Comprehensive Cellulose Chemistry: Functionalization of Cellulose*, Wiley-VCH Verlag GmbH, Weinheim, 1998, vol. 2.
40 M. Baiardo, G. Frisoni, M. Scandola and A. Licciardello, *J. Appl. Polym. Sci.*, 2002, **83**, 38.
41 J. Wang, Y. Z. Wan, H. L. Luo, C. Gao and Y. Huang, *Mater. Sci. Eng., C*, 2012, **32**, 536.
42 H. Orelma, L.-S. Johansson, I. Filpponen, O. J. Rojas and J. Laine, *Biomacromolecules*, 2012, **13**, 2802.
43 M. Monier and A. M. a. El-Sokkary, *Int. J. Biol. Macromol.*, 2012, **51**, 18.
44 A. Aied, Y. Zheng, A. Pandit and W. Wang, *ACS Appl. Mater. Interfaces*, 2012, **4**, 826.
45 U. Bora, P. Sharma, K. Kannan and P. Nahar, *J. Biotechnol.*, 2006, **126**, 220.
46 U. Bora, K. Kannan and P. Nahar, *J. Membr. Sci.*, 2005, **250**, 215.
47 A. C. Araújo, Y. Song, J. Lundeberg, P. L. Ståhl and H. Brumer, *Anal. Chem.*, 2012, **84**, 3311.
48 V. Mévellec, S. Roussel, L. Tessier, J. Chancolon, M. Mayne-L'Hermite, G. Deniau, P. Viel and S. Palacin, *Chem. Mater.*, 2007, **19**, 6323.
49 T. Berthelot, A. Garcia, X. T. Le, J. El Morsli, P. Jégou, S. Palacin and P. Viel, *Appl. Surf. Sci.*, 2011, **257**, 3538.
50 Vincent Mévellec, Sébastien Roussel, Serge Palacin, Thomas Berthelot, Cécile Baudin, Adhitya Trenggono and Guy Deniau, Commissariat à l'Energie Atomique, *Fr. Pat.*, 0655653, 2006; *WO Pat.*, 2008/078052, 2007.
51 G. T. Hermanson, in *Bioconjugate techniques*, Academic Press, London, 2nd edn, 2008.
52 H. Zollinger, in *Diazo Chemistry I: Aromatic and Heteroaromatic Compounds*, Wiley-VCH Verlag GmbH, Weinheim, 1994.
53 N. Khreich, P. Lamourette, P.-Y. Renard, G. Clavé, F. Fenaille, C. Créminon and H. Volland, *Toxicon*, 2009, **53**, 551.
54 L.-S. Johansson and J. M. Campbell, *Surf. Interface Anal.*, 2004, **36**, 1018.
55 J. Lyskawa and D. Bélanger, *Chem. Mater.*, 2006, **18**, 4755.
56 N. Khreich, P. Lamourette, H. Boutal, K. Devilliers, C. Créminon and H. Volland, *Anal. Biochem.*, 2008, **377**, 182.
57 S. Kalia, A. Dufresne, B. M. Cherian, B. S. Kaith, L. Avérous, J. Njuguna and E. Nassiopoulos, *Int. J. Polym. Sci.*, 2011, **2011**, 1.
58 D. Roy, M. Semsarilar, J. T. Guthrie and S. Perrier, *Chem. Soc. Rev.*, 2009, **38**, 2046.
59 Y. Habibi, L. A. Lucia and O. J. Rojas, *Chem. Rev.*, 2010, **110**, 3479.
60 P. O. Andersson, P. Lind, A. Mattsson and L. Österlund, *Surf. Interface Anal.*, 2008, **40**, 623.
61 A. Mesnage, X. Lefèvre, P. Jégou, G. Deniau and S. Palacin, *Langmuir*, 2012, **28**, 11767.
62 A. Garcia, J. Polesel-Maris, P. Viel, S. Palacin and T. Berthelot, *Adv. Funct. Mater.*, 2011, **21**, 2096.
63 P.-A. Faugeras, P.-H. Elchinger, F. Brouillette, D. Montplaisir and R. Zerrouki, *Green Chem.*, 2012, **14**, 598.
64 E. Malmström and A. Carlmark, *Polym. Chem.*, 2012, **3**, 1702.
65 A. Y. Kolosova, L. Sibanda, F. Dumoulin, J. Lewis, E. Duveiller, C. Van Peteghem and S. De Saeger, *Anal. Chim. Acta*, 2008, **616**, 235.
66 X. Yang, L. Hua, H. Gong and S. Ngin, *Anal. Chim. Acta*, 2003, **478**, 67.
67 S. K. Arya, A. K. Prusty, S. P. Singh, P. R. Solanki, M. K. Pandey, M. Datta and B. D. Malhotra, *Anal. Biochem.*, 2007, **363**, 210.
68 E. Halder, D. K. Chattoraj and K. P. Das, *Biopolymers*, 2005, **77**, 286.

Journal of Materials Chemistry B

Supplementary Material

Table 1 Operating conditions for cellulose modification. Diazonium salts section: previously synthesized compounds. Amines section: amine precursors for *in situ* synthesized diazonium salts.

Reagent	Mass for 0.3 mmol (6 mL of 0.05 M solution)	Washing solvent	Chemical function introduced onto paper
Diazonium salts			
4-nitrobenzenediazonium tetrafluoroborate	71.1 mg	Ethanol (96% (v/v) in H_2O)	NO_2
4-mercaptobenzenediazonium tetrafluoroborate	67.2 mg	Ethanol (96% (v/v) in H_2O)	SH
4-carboxybenzenediazonium tetrafluoroborate	70.8 mg	0.1 M sodium hydroxide	COOH
4-(2-ammonioethyl)benzenediazonium tetrafluoroborate	96.8 mg	0.1 M hydrochloric acid	(primary) NH_2
4-azidobenzenediazonium tetrafluoroborate	69.9 mg	Ethanol (96% (v/v) in H_2O)	N_3
Amines			
4-(2-aminoethyl)-aniline	40.9 mg	0.1 M hydrochloric acid	(primary) NH_2
4-azidoaniline hydrochloride	51.2 mg	Ethanol (96% (v/v) in H_2O)	N_3

Table 2 Operating conditions for antibodies grafting.

Paper	Bioconjugate Technique	Antibody grafted
Unmodified paper		
Nitrocellulose (AE98 Fast)	Deposit of the mAb (40 µL cm^{-2}) Overnight incubation at 4°C	anti-OVA mAb
Cellulose (CF1)	Deposit of the mAb (40 µL cm^{-2}) Overnight incubation at 4°C	anti-OVA mAb
Modified cellulose: chemical group borne by paper		
Nitro (NO_2)	Deposit of the mAb (40 µL cm^{-2}) Overnight incubation at 4°C	anti-OVA mAb
Thiol (SH)	Deposit of the maleimido-mAb (40 µL cm^{-2}) Overnight incubation at 4°C	SMCC-anti-OVA mAb
Primary Amine (NH_2)	Thiols introduction Deposit of the maleimido-mAb (40 µL cm^{-2}) Overnight incubation at 4°C	SMCC-anti-OVA mAb
Carboxyl (COOH)	EDC/Sulfo-NHS activation of carboxyl groups Deposit of the mAb (40 µL cm^{-2}) Overnight incubation at 4°C	anti-OVA mAb
Azide (N_3)	Deposit of the mAb (40 µL cm^{-2}) Antibody concentration by drying at 40°C for 30 min in an air oven Irradiation at 365 nm (1050 µW cm^{-2}) for 15 min	anti-OVA mAb

5

Table 3 Characterization of the grafted chemical functions.

Chemical function	Most conclusive analysis	Characteristic signal	Figure
Nitro (NO_2)	IR	NO_2 antisymmetric stretching vibration at 1525 ± 5 cm^{-1} NO_2 symmetric stretching vibration at 1350 ± 5 cm^{-1}	Figure 5 (a)
Thiol (SH)	XPS	S 2p orbital Binding Energy at 164 ± 0.35 eV S 2s orbital Binding Energy at 220 ± 0.35 eV	Figure 5 (b)
Primary Amine (NH_2)	Ninhydrin staining XPS	Brown color specific to primary amines N 1s orbital Binding Energy at 400 ± 0.35 eV	(not shown) Figure 5 (c)
Azide (N_3)	Colloidal-gold-labeled antibody localized grafting	Color from the grafted biomolecule following the mask	Figure 5 (d)
Carboxyl (COOH)	IR & XPS & Dye	Merging into cellulose signal	

Chapter 3 Chemical-free photoimmobilization of antibodies onto cellulose for the preparation of immunoassay membranes

The chemical-free photoimmobilization process presented hereunder was surprisingly discovered during the development of a chemically induced photoimmobilization method for antibody immobilization onto cellulose described in the previous chapter (Chapter 2) [33].

Among the known covalent coupling techniques, photo-immobilization is probably the simplest and the fastest to implement in the preparation of immunoassay devices. The support is generally coated or functionalized with a photoreactive compound and the biomolecule of interest is covalently linked to the support through photoactivation by long-wave UVA light (340 nm - 400 nm) or visible light (400 nm – 800 nm), 365 nm being the usual operating wavelength [67–69]. All the long-wave-UVA-induced photoimmobilization methods described so far have employed photoreactive coupling intermediates, and have further required the functionalization of cellulose [33,60–62,70]. This is why among all the functional groups grafted to cellulose in Chapter 2, there was a photoreactive moiety: arylazide. Long-wave-UVA irradiation turned the azide function into a nitrene which is a quick and non-specific reactive function [60,61]. As a result, it reacted with any compound on its immediate surrounding including antibodies.

In order to check the actual grafting and the photoreactivity of this moiety to cellulose, negative control experiments were performed. Probe antibodies (gold-labeled goat antibodies) were dispensed on both arylazide-cellulose and pristine cellulose. Both impregnated papers were covered with a plastic mask and then irradiated at 365 nm for 15 minutes. Pristine cellulose paper was a negative control. The only immobilization process occurring onto the latter should have been adsorption and nearly no antibodies should have been immobilized. Irradiation should not have patterned the pristine cellulose. However, the “negative control” was clearly “positive”. Pristine cellulose unexpectedly appeared to immobilize probe antibodies when submitted to 365-nm light, just as cellulose functionalized with arylazide photocoupling agents (Figure 2). This experiment was reproduced many times and always led to the same conclusion. A series of tests was therefore conducted in order to evaluate the grafting rate and to prove that the activity of the grafted antibodies was partially preserved. All were conclusive: pristine cellulose immobilizes antibodies when submitted to 365-nm light and these antibodies stay active.

Figure 2: Photo-patterning of probe antibodies on arylazide-cellulose (test) and pristine cellulose (negative control). Photographs were taken with the molecular imager VersaDoc™.

This result was thus patented [71]. At the same time, investigation was continued in order to study the various parameters (photoenergy, wavelength, drying, washing) and to optimize procedures. This study is presented hereunder. As in Chapter 2, all results were analyzed with respect to nitrocellulose since it is the reference material for LFIAs [35–37,50]. But cellulose and nitrocellulose are very different materials. Beyond the obvious chemical difference in molecular structure, the main difference between the commercially available nitrocellulose and cellulose papers lies in their porosity (about 5 µm and 11 µm surface pore size, respectively), the sheet thickness (20 µm and 176 µm thick, respectively), and their resulting surface physical behavior. In order to get free from those physical factors and to only study the immobilization process, all samples were saturated with antibodies by impregnation (40 µL cm^{-2}) prior to photoimmobilization. This whole new process allows antibodies to be strongly immobilized on cellulose without any photocoupling intermediate nor any biomolecule or substrate pretreatment. It advantageously combines the simplicity of physical adsorption and the robustness of chemical covalent bonding.

Contents

1. INTRODUCTION 57

2. EXPERIMENTAL 58

2.1. REAGENTS AND MATERIALS 58
2.2. PHOTOIMMOBILIZATION OF ANTIBODIES 58
2.2.1. General procedure 58
2.2.2. Variable parameters 59
2.3. IMMUNOCHROMATOGRAPHIC ASSAYS (LFIA) 59
2.3.1. Preparation of colloidal-gold-labeled antibodies 59
2.3.2. Preparation of immunochromatographic strips 59
2.3.3. Evaluation of the immobilization rate 60
2.3.4. Evaluation of the activity rate 60
2.4. PHOTOIMMOBILIZATION OF PROBE ANTIBODIES 60

3. RESULTS AND DISCUSSION 60

3.1. OPTIMIZATION OF IMMOBILIZATION PARAMETERS 60
3.1.1. Photoenergy 60
3.1.2. Pre-irradiation drying step 61
3.1.3. Post-irradiation washing step 62
3.1.4. Wavelength 62
3.1.5. Optimal procedure 62
3.2. USE OF VARIOUS PAPER SUBSTRATES 63
3.3. AGEING OF THE MEMBRANES 63
3.4. STRENGTH OF THE IMMOBILIZATION 64
3.5. PROPOSED MECHANISM 64

4. CONCLUSION 64

REFERENCES 65

Credou, J.; Volland H.; Berthelot, T.

Chemical-free photoimmobilization of antibodies onto cellulose for the preparation of immunoassay membranes.

J. Mater. Chem. B 2014. Submitted.

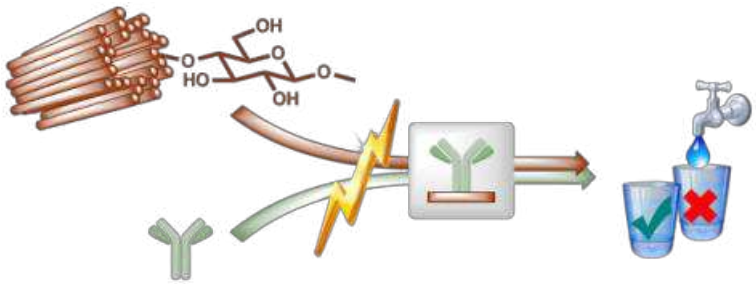

Immunoassay membranes were produced by photoimmobilization of antibodies onto cellulose without any photocoupling intermediate nor any biomolecule or substrate pretreatment.

Journal of Materials Chemistry B

RSCPublishing

ARTICLE

Chemical-free photoimmobilization of antibodies onto cellulose for the preparation of immunoassay membranes

Cite this: DOI: 10.1039/xoxxoooooox

Julie Credou,[a] Hervé Volland[b] and Thomas Berthelot[a]* ,

Received ooth July 2014,
Accepted ooth July 2014

DOI: 10.1039/xoxxoooooox

www.rsc.org/

Paper-based detection devices such as lateral flow immunoassays (LFIAs) are inexpensive, rapid, user-friendly and therefore highly promising for providing resource-limited settings with point-of-care diagnostics. Recently, this biosensing field has trended towards three-dimensional microfluidic devices and multiplexed assay platforms. However, many multiplexed paper-based biosensors implement methods incompatible with the conventional LFIA carrier material: nitrocellulose. It thus tends to be replaced by cellulose. This major material change implies to undertake a covalent immobilization of biomolecules onto cellulose which preserves their biological activity. In this perspective, the immobilization process elaborated in this study is entirely biocompatible. While antibody immobilization onto cellulose usually requires chemical modifications of either the biomolecule and/or the membrane, the light-based procedure presented here was performed without any chemical photolinker. Native biomolecules have been successfully immobilized onto paper sheets which therefore enable to perform LFIAs. More generally, the process expounded herein is fast, simple, cost-saving, environmentally-friendly and would be helpful to immobilize chemical-sensitive biomolecules onto cellulose sheets.

1. Introduction

In various domains such as clinical diagnosis [1–5], drug screening [6–9], food quality control [10–12], and environmental monitoring [13–16], there is a need to easily and rapidly detect biomolecules. Several methods have been developed for manufacturing biosensors, biochips, microarray and other immunoassay devices [17,18,7,19–22]. Within the last thirty years, paper-based biosensors such as lateral flow assays have attracted a strong interest and were extensively developed [23–25]. Among these, blood glucose sensors, pregnancy tests, or urine test strips are the most broadly distributed devices for identifying biomolecules [26,25,27–32].

The preparation of such efficient immunoassay devices requires the robust immobilization of a large number of biomolecules of interest on a support [33]. Because of its ability to immobilize all kind of proteins by a combination of electrostatic, hydrogen, and hydrophobic interactions involving the nitro functions displayed on its surface [28], nitrocellulose constitutes the most commonly used support material for preparing immunochromatographic devices [27,25,28,34]. However, nitrocellulose is an expensive, fragile and inflammable material [35,36], which was shown to be incompatible with newly developed multiplex biosensors such as lab-on-paper devices, microfluidic paper analytical devices (μPADs), or other paper-based analytical devices [21,7,37]. Moreover, some agents such as spores and some bacteria may have difficulty in migrating along nitrocellulose. For these reasons, nitrocellulose is thus progressively replaced by cellulose [37,38].

Cellulose is an affordable biopolymer, which is also biocompatible, biodegradable and easily available [39–42]. It is particularly interesting since it exhibits wicking properties allowing biomolecules in solution to migrate by capillarity without needing any external power sources. It is also available in a broad range of thickness and possesses well-defined pore sizes, is easy to store and safely disposable [37]. Several methods for immobilizing biomolecules onto cellulose are known. They may be classified into three major families: (i) physical methods, wherein the biomolecule is confined to the support through physical forces such as electrostatic, Van der Waals and hydrophobic interactions; (ii) biological or biochemical methods wherein the biomolecule is bound to the support through biochemical affinity between two components (*e.g.* Ni^{2+} / His-tag, streptavidin / biotin, protein G / human IgG); and (iii) chemical methods, wherein covalent bonds link the biomolecule on the support [38]. Nevertheless, each of these methods also displays specific drawbacks. Physical methods implement simple, rapid and cost-saving procedures, and

advantageously limit the necessity for modifying the biomolecule or the support. However, the weak and non-permanent interaction maintaining the biomolecule onto the support also represent a major drawback of these methods, since biomolecules are progressively torn out, thus triggering a loss of activity of the corresponding biosensor. Biological methods allow biomolecules to be immobilized in a specific orientation through strong, specific and reversible interactions with the support. Nevertheless, these methods require complex and expensive engineering procedures wherein the biomolecule and/or the support are modified for introducing a binding conjugate or a binding domain therein. Finally, chemical methods ensure strong, stable and permanent coupling of the biomolecule to its support. The thus-conceived biosensors are robust and provide reproducible results. On the other hand, the chemical treatments performed may modify and alter the structure and/or the activity of the biomolecules. The resulting biosensors may thus lack sensitivity as a consequence of biomolecule alteration.

Among the known covalent coupling techniques, photoimmobilization is probably the simplest and the fastest for preparing bioassay devices. The support is usually coated or functionalized with a photoreactive compound and the biomolecule of interest is covalently linked to the support through photoactivation of the latter. Given that short-wave UV (ultraviolet) light (*i.e.* 100 nm - 340 nm) is known to alter biomolecules [43], photoimmobilization is then generally performed under long-wave UV light (340 nm – 400 nm) or visible light (400 nm - 800 nm) [44–46]. To the best of our knowledge all the photoimmobilization methods described so far have required a photoreactive coupling intermediate [37,47–50] and further functionalization of cellulose through harsh conditions, in organic solvents, or with highly toxic reagents or side products [37]. There is therefore an ongoing need for cost-saving and rapid methods allowing immunoassay devices to be prepared by robust and sustainable binding of biomolecules to cellulose. There is indeed a long-felt need for unmodified antibody immobilization methods displaying a limited number of steps, allowing to save significant amounts of reagents, solvents or adjuvants, and ensuring the preservation of the activity of the biomolecules of interest through the use of mild conditions.

The new process developed and presented herein actually fulfills this need. This is a chemical-free photografting procedure which allows biomolecules to be immobilized onto cellulose without any photocoupling intermediate nor any biomolecule or substrate pretreatment [51]. This is therefore a fast, simple, cost-saving and environmentally-friendly method for native antibody immobilization onto cellulose. The procedure can be summarized as follows: (i) a cellulose sheet was impregnated with an antibody solution; (ii) antibodies were optionally concentrated by drying the impregnated paper; (iii) the system was irradiated for inducing photoimmobilization; and (iv) intensive washing was performed for removing non-immobilized antibodies. After a saturation step aiming at preventing further nonspecific protein adsorption, the so prepared membranes were used as detection zone in lateral flow immunoassays (LFIAs). In these assays, the model antigen selected to validate our procedure was ovalbumin (OVA), and the antibodies directed against its epitopes were murine monoclonal antibodies. Each membrane was subjected to two classes of assay. The first one evaluated the immobilization rate and the second one the biological activity rate. For each membrane, 2 or 3 different samples were tested, depending on the experiment. All results were analyzed with respect to nitrocellulose as the positive control and to pristine unirradiated cellulose paper as the negative control regarding protein immobilization. Various parameters of the photoimmobilization process have thus been optimized, therefore resulting in an optimal procedure which produces membranes challenging nitrocellulose performances.

2. Experimental

2.1. Reagents and materials

Papers used for performing the immunoassay membranes comprise celluloses CF1 and Chr1, as well as AE 98 Fast nitrocellulose from Whatman (Maidstone, Kent, UK) and printing paper Xerox Premier 80 (Ref. 3R91720, Xerox, Norwalk, CT, USA). Immunochromatographic strips were prepared using absorbent pad No. 470 from Schleicher and Schuell BioScience GmBH (Dassel, Germany) and backing card MIBA-020 plastic strips from Diagnostic Consulting Network (Carlsbad, CA, USA). Materials were cut using an automatic programmable cutter Guillotine Cutting CM4000 Batch cutting system from BioDot (Irvine, CA, USA). Proteins (ovalbumin (OVA), Bovine Serum Albumin (BSA) and porcine skin gelatin), as well as chemical products for preparing buffers and colloidal gold solution were obtained from Sigma-Aldrich (St Louis, MO, USA). Water used in all experiments was purified by the Milli-Q system (Millipore, Brussels, Belgium). Monoclonal murine antibodies (murine mAbs) were produced at LERI (CEA, Saclay, France) as previously described [52]. Irradiations were conducted at room temperature in a UV chamber CN-15.LV UV viewing cabinet (Vilber Lourmat, Marne-la-Vallée, France). 96-Well polystyrene microplates (flat-bottom, crystal-clear, from Greiner Bio-One S.A.S. Division Bioscience, Les Ulis, France) were used as container for migrations on immunochromatographic strips. Colorimetric intensity resulting from colloidal gold was quantified with a Molecular Imager VersaDoc^{TM} MP4000, in association with the software Quantity One 1-D Analysis (Bio-Rad, Hercules, CA, USA).

2.2. Photoimmobilization of antibodies

2.2.1. General procedure

Murine monoclonal antibodies directed against OVA epitopes (1 mg mL^{-1} in 0.1 M potassium phosphate buffer, pH 7.4, 40 µL cm^{-2} deposit) were photoimmobilized onto pristine CF1 cellulose paper. They also were adsorbed onto nitrocellulose (positive control) and onto pristine CF1 cellulose paper

(negative control) by regular 1-hour incubation at room temperature. Results obtained after photoimmobilization were compared to positive and negative controls.

Photoimmobilization process can be briefly described as follows: (i) a cellulose sheet was impregnated with an antibody solution; (ii) antibodies were optionally concentrated by drying the impregnated paper; (iii) the system was irradiated for inducing photoimmobilization; and (iv) intensive washing was performed for removing non-immobilized antibodies. For each membrane, an anti-OVA antibody solution was poured onto a 0.25-cm² cellulose sheet (0.5 cm x 0.5 cm in size) at a rate of 40 µL cm^{-2}. Where applicable, drying was performed at 37°C, in a ventilated oven, for 15 minutes. Irradiation was either conducted at 365 nm (1050 µW cm^{-2}) or in visible light (power characteristics not provided). After irradiation, samples were washed with 0.1 M potassium phosphate buffer, pH 7.4, optionally enriched with salts (0.5 M NaCl) and detergent (0.5% (v/v) Tween 20).

Membranes were then saturated with a gelatin solution (0.1 M potassium phosphate buffer, pH 7.4, containing 0.5% (w/v) porcine gelatin and 0.15 M NaCl) for preventing nonspecific protein adsorption on membranes during immunoassays. Saturation was performed by impregnating and incubating the membranes with the gelatin solution overnight at 4°C, and then drying them at 37°C in a ventilated oven for 30 minutes.

2.2.2. Variable parameters

Various parameters of the photoimmobilization process had been optimized in order to determine an optimal procedure. Therefore, the cellulose carrier impregnated with the antibody solution might either be dried or not before the irradiation step. The light used for irradiating the impregnated cellulose carrier might have a wavelength of 365 nm (long-scale UV) or ranging from 400 nm to 800 nm (visible light). With a wavelength of 365 nm, the irradiations were conducted for various periods of time that subjected the impregnated cellulose carriers to different photoenergies ranging from 1 J cm^{-2} to 80 J cm^{-2}. Finally, the washing phosphate buffer could either be pure or enriched with salts and detergent. The efficiency of each parameter was assessed by the immobilization and activity performances of the prepared membranes which were ascertained by immunochromatographic assays.

2.3. Immunochromatographic assays (LFIA)

Immobilization rate and biological activity rate of the immobilized antibodies were evaluated by colloidal-gold-based lateral flow immunoassays (LFIA) [25]. The signal intensity was quantitatively estimated by colorimetric measurement. All results were compared with adsorption on pristine cellulose (negative control) and nitrocellulose (positive control). Considering that adsorption on nitrocellulose is the most frequently used method for immunochromatographic assays, it is herein considered as the reference and has been assimilated to 100% for both the immobilization rate and the activity rate.

All the reagents were diluted in the analysis buffer (0.1 M potassium phosphate buffer, pH 7.4, containing 0.1% (w/v) BSA, 0.15 M NaCl, and 0.5% (v/v) Tween 20), at room temperature, 30 minutes prior to migration in order to reduce nonspecific binding. Each assay was performed at room temperature by inserting a strip into a well of a 96-well microtiter plate containing 100 µL of the test solution. The mixture was successively absorbed by the various pads and the capillary migration process lasted for about 15 minutes. Colorimetric intensity was further measured using the molecular imager. Since this intensity depended on parameters such as temperature and moisture content of paper at the time of measurement, all strips were dried for 30 minutes at 37°C in a ventilated oven and then rehydrated with the analysis buffer just before measurement [37].

2.3.1. Preparation of colloidal-gold-labeled antibodies

Tracer antibodies were labeled with colloidal gold according to a known method previously described [53]. Two types of tracer were prepared: a goat polyclonal antibody anti-mouse tracer to reveal the immobilized murine antibodies, and a murine monoclonal antibody anti-OVA tracer to highlight the capture of OVA by the immobilized antibodies.

Briefly, 4 mL of gold chloride and 1 mL of 1% (w/v) sodium citrate solution were added to 40 mL of boiling water under constant stirring. Once the mixture had turned purple, this colloidal gold solution was allowed to cool to room temperature and stored at 4°C in the dark. 25 µg of antibody and 100 µL of 20 mM borax buffer, pH 9.3, were added to 1 mL of this colloidal gold solution. This mixture was left to incubate for one hour on a rotary shaker at room temperature, therefore enabling the ionic adsorption of the antibodies onto the surface of the colloidal gold particles. Afterwards, 100 µL of 20 mM borax buffer, pH 9.3, containing 1% (w/v) BSA, was added and the mixture was centrifuged at 15 000 g for 50 minutes at 4°C. After discarding the supernatant, the pellet was suspended in 250 µL of 2 mM borax buffer, pH 9.3, containing 1% (w/v) BSA and stored at 4°C in the dark.

2.3.2. Preparation of immunochromatographic strips

An immunochromatographic strip is usually composed of a loading area (or sample pad), a detection area and an absorbent pad, the whole being affixed onto a plastic support. The detection area was therefore formed by an antibody-bearing membrane. Migration was supported by two surrounding sample wicking pads made of the same kind of paper than the detection area, free of antibodies and saturated with gelatin (see Figure 1).

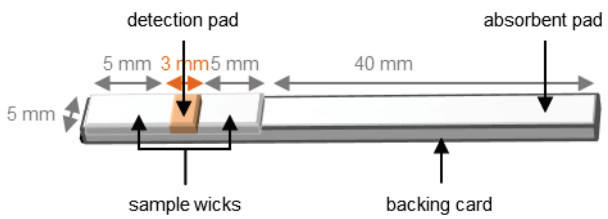

Figure 1: Schematic representation of an immunochromatographic strip.

2.3.3. Evaluation of the immobilization rate

The test solution was composed of a goat anti-mouse tracer diluted 10 times in the analysis buffer. Papers without antibody in the photoimmobilization solution (ungrafted paper) assessed the unspecific signal due to unspecific adsorption of the tracer onto the detection pad. The immobilization rate of the cellulose papers following the various procedures was measured by the difference between the antibody-grafted paper signal and the ungrafted corresponding one.

2.3.4. Evaluation of the activity rate

Two test solutions were prepared and pre-incubated for 10 minutes. The first one was a solution of OVA and murine anti-OVA mAb tracer (1 µg mL^{-1} and 10-fold dilution, respectively) in the analysis buffer. The second one only contained murine anti-OVA mAb tracer diluted 10 times in the analysis buffer. This immunoassay without antigen (OVA) assessed the unspecific signal due to unspecific adsorption of the tracer onto the antibody–gelatin matrix during immunoassays. The biological activity rate of the grafted antibodies was measured by the difference between the antibody-grafted paper signal in the presence of OVA and the corresponding one in the absence of it.

2.4. Photoimmobilization of probe antibodies

Probe antibodies, or colloidal-gold-labeled antibodies (tracers), were photoimmobilized onto pristine CF1 cellulose paper following the general procedure. CF1 cellulose sheet was impregnated with a goat anti-mouse tracer solution (3-time dilution in the analysis buffer, 20 µL cm^{-2} deposit). Drying step was skipped and this system was then irradiated at 365 nm for 1h20 (about 5 J cm^{-2}). Papers were washed overnight with phosphate buffer containing salts and detergent (0.1M potassium phosphate buffer, pH 7.4, containing 0.5 M NaCl and 0.5% (v/v) Tween 20). Colorimetric measurement using the molecular imager was performed immediately after the paper had been slightly dried over absorbent paper.

3. Results and discussion

3.1. Optimization of immobilization parameters

3.1.1. Photoenergy

Because of the available material (CN-15.LV UV viewing cabinet), various photoenergies could only be obtained by various irradiation times. Therefore a drying phenomenon would add to the irradiation one during long term exposures. In order to get free from that additional factor, a pre-irradiation drying step was applied to all samples.

Anti-OVA antibodies were poured onto CF1 cellulose sheets, and further concentrated by drying the impregnated paper (S). The system was then irradiated (I) at 365 nm for various times, corresponding to different energy levels: 16 min (about 1 J cm^{-2}), 2h40 (about 10 J cm^{-2}) and 21h20 (about 80 J cm^{-2}). Papers were then washed 3 times for 5 minutes with phosphate buffer, saturated and eventually dried. These papers were compared to undried and unirradiated impregnated cellulose (negative control) and to nitrocellulose (positive control) which was assimilated to 100% of antibody immobilization capacity (immobilization rate) and antigen-capture capacity (activity rate). The results corresponding to 2 different immobilizations are shown Figure 2 and Figure 3.

Antibodies immobilized onto nitrocellulose or cellulose were revealed by gold-labeled goat anti-mouse tracer antibodies (Figure 2). On gelatin-grafted papers (white panel), no signal was detected (Figure 2a). This absence of unspecific adsorption of tracer molecules proved the gelatin saturation to be effective. On antibody-grafted papers (colored panel), various performances were observed, depending on the photoenergy applied to the system. In the second assay, those immobilized antibodies were exposed to OVA antigen. The capture of the latter by the immobilized antibodies was highlighted by gold-labeled murine anti-OVA tracer antibodies (sandwich immunoassay) (Figure 3). In absence of OVA antigen (white left panel), no signal is detected (Figure 3a). This absence of unspecific adsorption of tracer molecules proved the signal obtained thereafter in presence of OVA to be specific. In presence of OVA antigen (colored right panel), various performances were observed, depending on the photoenergy applied to the system. As can be seen in Figure 2b and Figure 3b, performances of nitrocellulose were reached with an irradiation energy of 10 J cm^{-2}, for both immobilization rate and activity rate.

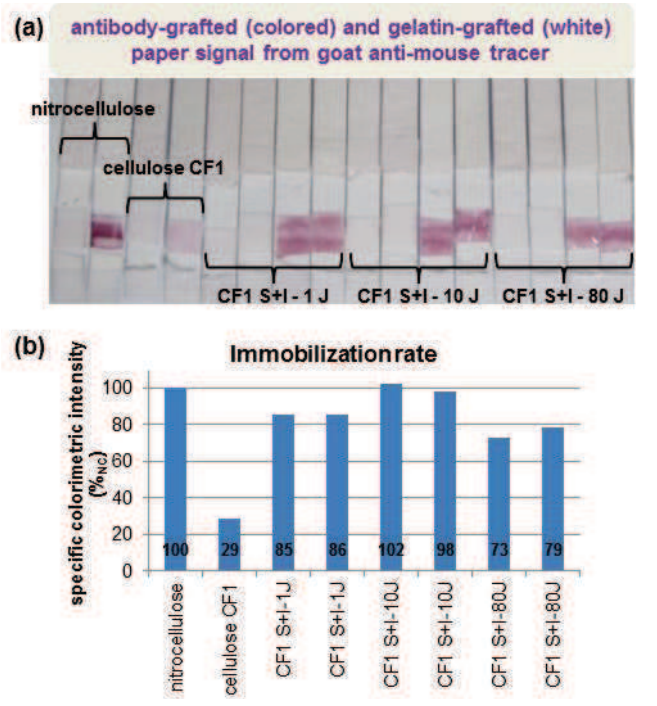

Figure 2: Influence of irradiation energy on antibody immobilization. Antibodies immobilized on nitrocellulose or cellulose, after optional drying (S) of the membrane, and irradiation (I) at 1 J cm^{-2}, 10 J cm^{-2} or 80 J cm^{-2}, are revealed by gold-labeled goat anti-mouse tracer antibodies. On ungrafted papers (white/left panel), no signal is detected. On antibody-grafted papers (colored/right panel), performances of nitrocellulose are reached for an irradiation energy of 10 J cm^{-2}. The results corresponding to 2 different immobilizations are shown for each condition.

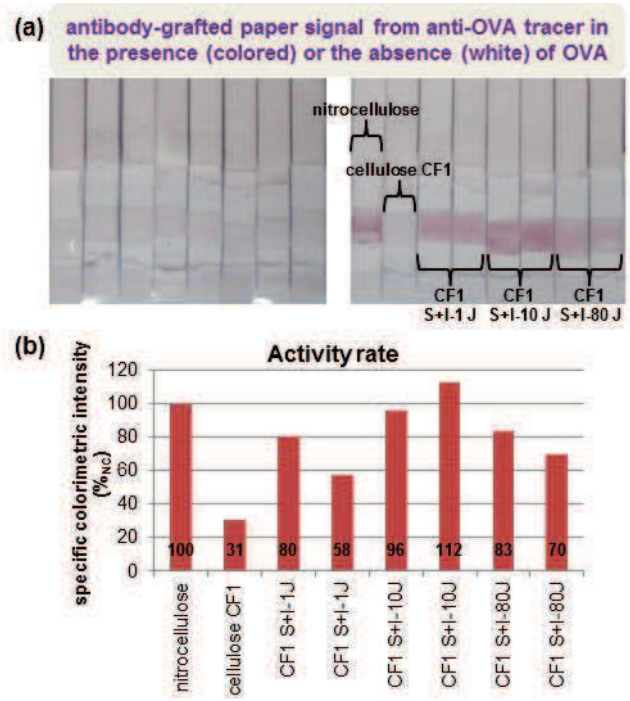

Figure 3: Influence of irradiation energy on biological activity. Antibodies immobilized on nitrocellulose or cellulose, after optional drying (S) of the membrane, and irradiation (I) at 1 J cm^{-2}, 10 J cm^{-2} or 80 J cm^{-2}, are exposed to OVA antigen. The capture of the latter by the immobilized antibodies is highlighted by gold-labeled murine anti-OVA tracer antibodies. In absence of OVA antigen (left panel), no signal is detected. In presence of OVA antigen (right panel), performances of nitrocellulose are reached for an irradiation energy of 10 J cm^{-2}. The results corresponding to 2 different immobilizations are shown for each condition.

3.1.2. Pre-irradiation drying step

Pre-irradiation drying step was performed in order to concentrate antibodies and therefore bring as many of them as close as possible to cellulose surface. Since the drying phenomenon naturally occurs during long term exposure, the influence of this step was assessed upon both short and long irradiation times.

The CF1 cellulose sheets impregnated with anti-OVA antibodies were either dried (S) or left undried (Ø), irradiated (I) at 365 nm, and then washed with 3 successive 5-minute baths in phosphate buffer. Short irradiation time was 16 min (equivalent to 1 J cm^{-2}), while long irradiation time was 2h40 (equivalent to 10 J cm^{-2}). Resulting immobilization and activity rates were assessed and are shown in Figure 4 and Figure 5, respectively. According to these graphs, pre-irradiation drying appears to be required with short irradiation time. Otherwise, antibodies remain in solution, too far away from fibers to be reached by the reactive species and ensure abundant immobilization (see CF1 I samples in Figure 4). In addition, its lower performances compared to the negative control (CF1 samples in Figure 4) suggest this "long-distance" irradiation of undried substrates to be ineffective. The only immobilization process involved in CF1 I sample would therefore be adsorption, just like in negative control sample. Thus the duration of cellulose exposure to antibody solution is the only

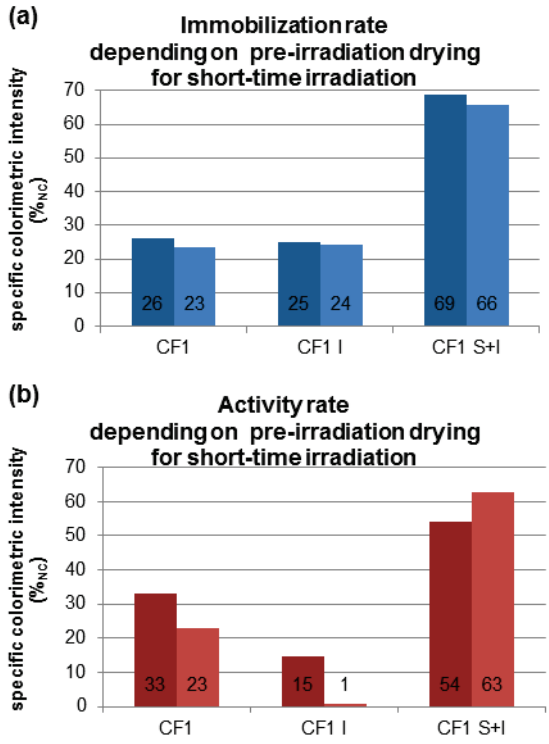

Figure 4: Histograms showing the immobilization (a) and activity (b) rates of antibodies immobilized onto cellulose, after irradiation (I) or drying and irradiation (S+I), for short irradiation time. The results from 2 different immobilizations are presented for each condition.

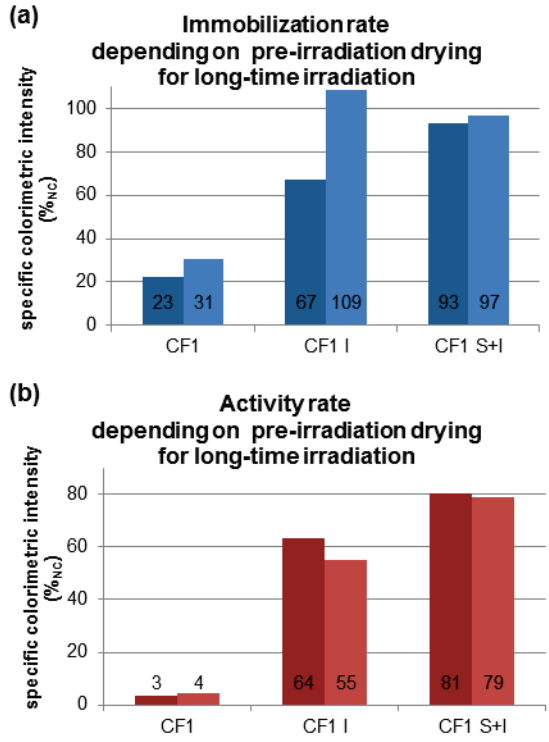

Figure 5: Histograms showing the immobilization (a) and activity (b) rates of antibodies immobilized onto cellulose, after irradiation (I) or drying and irradiation (S+I), for long irradiation time. The results from 2 different immobilizations are presented for each condition.

real difference between these two samples. As a result, a shorter exposure led to lower performances.

On another hand, pre-irradiation drying seems to be beneficial, although not essential, for long irradiation times. As previously noticed, with long irradiation time, drying occurs naturally in the course of irradiation, thereby allowing antibodies to gradually get closer to cellulose surface and to the reactive species.

3.1.3. Post-irradiation washing step

The CF1 cellulose sheets impregnated with anti-OVA antibodies were dried to concentrate the antibodies (S) and then irradiated (I) at 365 nm for 2h40 (about 10 J cm^{-2}). Papers were washed with 3 successive 5-minute baths in either phosphate buffer or phosphate buffer with salts and detergent. The immobilization and activity rates averages with corresponding standard deviations from 3 different experiments are reported in Figure 6. Results confirm that extensive washing with a phosphate buffer with salts and detergent allows maintaining on the surface only molecules that are strongly immobilized. Salts allow the electrostatic interactions between biomolecules and surface to be limited, and the detergent reduces or prevents hydrophobic interactions. Salts and detergent thus do contribute to reduce antibody adsorption. The resulting signal therefore appears to be slightly weaker, but results appear to be more reproducible.

3.1.4. Wavelength

The CF1 cellulose sheets impregnated with anti-OVA antibodies were dried to concentrate the antibodies (S) and then either irradiated at 365 nm for 2h40 (I@365), irradiated under visible light for 2h40 (I@visible) or left unirradiated (Ø). Papers were then extensively washed with phosphate buffer containing salts and detergent. The immobilization and activity rates averages with corresponding standard deviations from 3 different experiments are reported in Figure 7. As can be seen in this figure, irradiation under visible light provides a slightly less efficient immobilization than irradiation at 365 nm which is more energetic. Visible light could therefore be employed with highly UV-sensitive biomolecules. But for most of antibodies 365-nm irradiation is harmless and would be more efficient.

3.1.5. Optimal procedure

According to previous optimization results, the optimal procedure would be: (i) to impregnate cellulose sheet with an antibody solution; (ii) to concentrate antibodies by drying the impregnated paper at 37°C, in a ventilated oven, for 15 minutes; (iii) to irradiate the system at 365 nm for 2h40 (about 10 J cm^{-2}); and (iv) to intensively wash papers with phosphate buffer containing salts and detergent (0.1M potassium phosphate buffer, pH 7.4, containing 0.5 M NaCl and 0.5% (v/v) Tween 20).

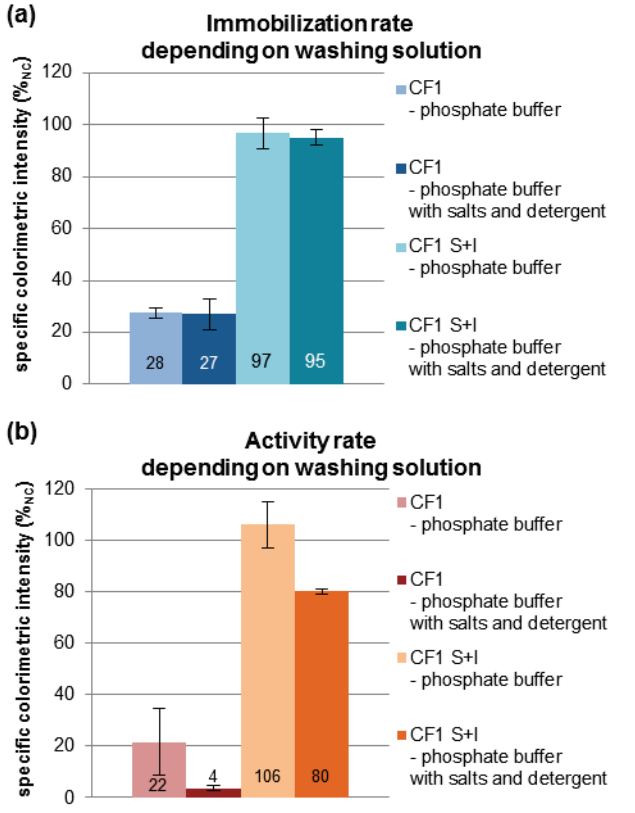

Figure 6: Histograms showing the immobilization (a) and activity (b) rates of antibodies immobilized onto cellulose, after drying, irradiation (S+I) and washing with phosphate buffer or phosphate buffer with salts and detergent. The results from 3 different immobilizations are presented.

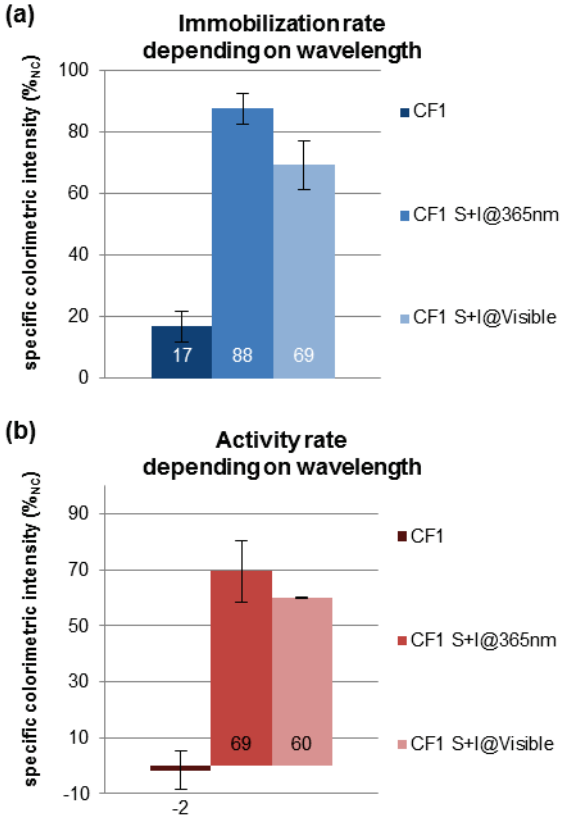

Figure 7: Histograms showing the immobilization (a) and activity (b) rates of antibodies immobilized onto cellulose, after drying (S) and irradiation for 2h40 at either 365 nm (I@365) or under visible light (I@visible). The results from 3 different immobilizations are presented.

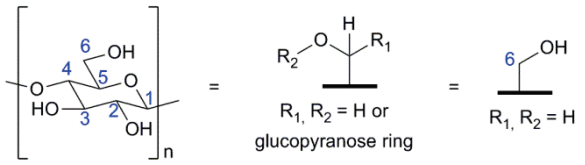

Figure 8: Cellulose formula and schematic representations further used.

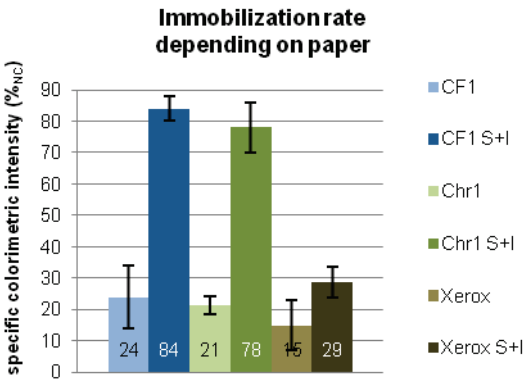

Figure 9: Histogram showing the immobilization rate of antibodies immobilized onto various papers according to the optimal procedure. The results from 3 different immobilizations are presented.

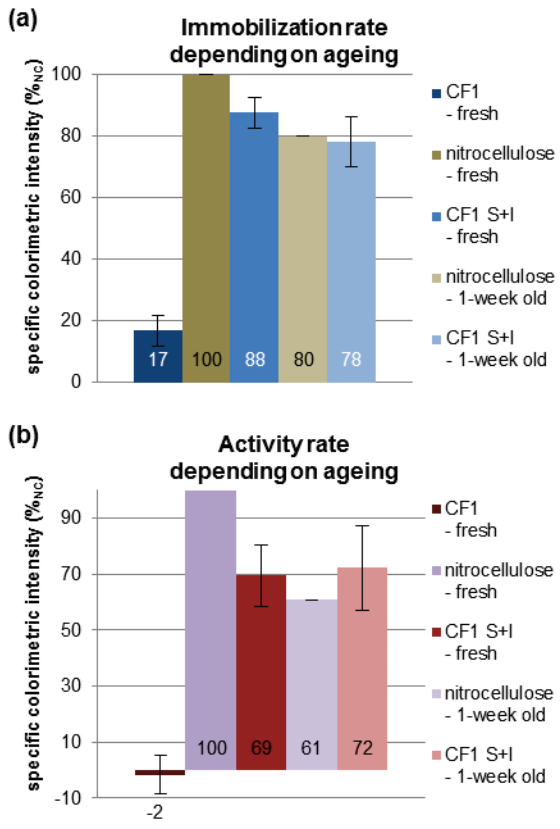

Figure 10: Histograms showing the immobilization (a) and activity (b) rates of antibodies immobilized onto cellulose according to the optimal procedure. Fresh and aged strips were compared. The results from 3 different samples are presented.

3.2. Use of various paper substrates

The versatility of the process was experienced by implementing the optimal procedure to various cellulose paper substrates, namely CF1, Chr1 and Xerox cellulose sheets. CF1 and Chr1 are known as high quality papers, made of quite pure and clean cellulose (Figure 8) and commonly used in laboratories (see "Sample Pads for Immunoassays" section [54] and "Cellulose Chromatography Papers" section [55] from Whatman online catalog, respectively). On another hand, Xerox is a printing paper whose composition is unclear and treatments during papermaking process unknown. The immobilization rate averages with corresponding standard deviations from 3 different experiments are reported in Figure 9. Results indicate that the process elaborated in this study allows the observed signal to be increased, with respect to adsorption alone, independently from the nature of the paper. With regard to Xerox paper, the improvement is remarkably low. Xerox paper is most probably treated for being hydrophobic. This would explain why the antibody solution was hindered to penetrate between the fibers, thereby justifying a lower immobilization rate. The process elaborated here was thus proved to allow a larger quantity of functional antibodies to be strongly immobilized on any type of cellulose carrier or derivative.

3.3. Ageing of the membranes

CF1 cellulose sheets were subjected to the optimal procedure and immunochromatographic strips were assembled. A set of strips was immediately tested. Their immobilization and activity rates averages with corresponding standard deviations from 3 different experiments are reported in Figure 10 ("fresh" panel). The remaining irradiated cellulose strips, as well as positive control strips, were stored in an oven for 7 days at 40°C in order to assess the ageing effects on the prepared membranes. Their immobilization and activity rates averages with corresponding standard deviations from 3 different experiments are reported in Figure 10 ("1-week old" panel). According to these results, ageing of nitrocellulose-based membranes results in a decreased recognition of the grafted antibodies by the goat anti-mouse tracer, as well as in a reduced biological activity. This phenomenon may be explained by the denaturation of the immobilized antibodies. With regard to cellulose-based membranes, signal variability increases with ageing while recognition by goat anti-mouse tracer decreases and may also result from the denaturation of immobilized antibodies. Nevertheless, the observed decrease is less important with cellulose than with nitrocellulose: $\delta(\text{immobilization})_{\text{nitrocellulose}}$ = -20% *vs* $\delta(\text{immobilization})_{\text{cellulose}}$ = -11%. Moreover, the activity rate of cellulose-based membranes remains constant after accelerated ageing, when standard deviations are considered. This may suggest that the binding sites of the antibodies photoimmobilized onto cellulose are not damaged. Another hypothesis would be that the active antibodies are protected from damage because they are "buried" and hidden in the paper substrate whereas they are displayed and vulnerable on the nitrocellulose surface. Cellulose

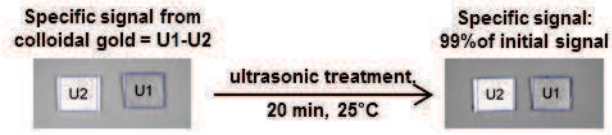

Figure 11: Photoimmobilization of gold-labeled goat anti-mouse tracer antibodies. Photograph was taken with VersaDoc™ Molecular Imager.

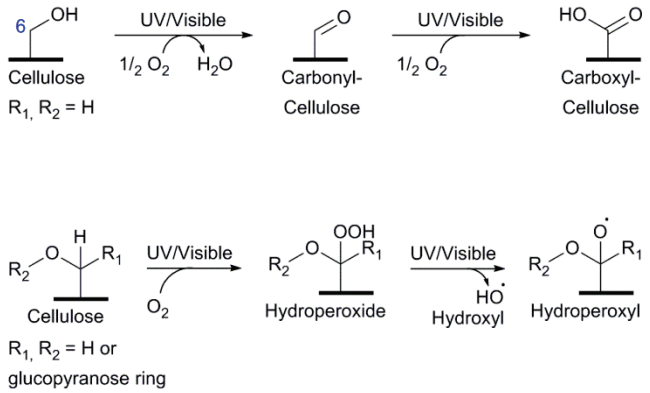

Figure 12: Photooxidation processes occurring in cellulose during photo-ageing according to ref [56].

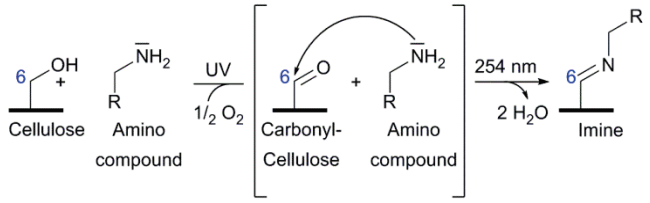

Figure 13: Photooxidation of cellulose treated with amino compounds according to ref [57].

immunoassay membranes prepared according to the process presented here thus appear to be more ageing resistant than nitrocellulose ones, and are therefore more suitable for use after long storage.

3.4. Strength of the immobilization

In order to assess the strength of the photoimmobilization, probe antibodies were immobilized according to the procedure described in section 2.4. After a first colorimetric measurement, the probe-antibody-bearing paper was then immersed in phosphate buffer containing salts and detergent (0.1M potassium phosphate buffer, pH 7.4, containing 0.5 M NaCl and 0.5% (v/v) Tween 20) and subjected to ultrasonic treatment for 20 minutes. Colorimetric intensity was measured again. The colorimetric intensity measured after the ultrasonic treatment amounts to about 99% of the first intensity measured (Figure 11). Considering that the observed signal decrease is comprised within the measuring error deviation, this decrease can therefore be considered as non-significant. In conclusion, the immobilization resulting from the process developed in this study is thus very strong, or even covalent.

3.5. Proposed mechanism

Several studies may raise suggestions about the possible mechanism. Particularly, accelerated photo-ageing experiments demonstrated that cellulose exposure to long-scale UV and visible light ($\lambda \geq 340$ nm) induced extensive oxidative degradation of cellulose, along with formation of hydroxyl radicals and carbonyl groups. Photooxidative reactions resulted in an increase of carbonyl, carboxyl and hydroperoxide content. The species described in that study are depicted in Figure 12 [56]. Furthermore, another study showed that carbonyl groups resulting from cellulose exposure to 254-nm UV light condensed with primary amino groups from species previously poured onto cellulose to form imines (see Figure 13). This phenomenon would be responsible for the yellowing of cellulose papers treated with amino compounds [57], which yellowing also occurs under natural light exposure ($\lambda \geq 280$ nm). To the best of our knowledge, no study has proved this imine formation under 365-nm UV light thus far. However, this is well conceivable given that carbonyl groups are produced during accelerated photo-ageing of cellulose at this same wavelength [56]. In addition these carbonyl groups are easily condensed with primary amines from biomolecules under mild conditions. This is actually a broadly used method for chemically immobilize biomolecules onto cellulose [58].

In light of those readings, two mechanisms could be proposed for the chemical-free photoimmobilization process presented herein: an oxidative mechanism involving carbonyl moieties (Figure 14a) and a radical mechanism (Figure 14b). If the carbonyl mechanism (Figure 14a) actually occurred, nearly no difference should be observed by irradiating the substrate prior to antibody deposit. This verification experiment had been conducted (results not shown) and led to both immobilization rate and activity rate similar to the negative control (pristine unirradiated cellulose paper) values. The carbonyl mechanism was therefore excluded and the radical mechanism (Figure 14b) seemed to be the most likely. Besides, the latter would be consistent with both the need for antibody concentration observed during optimization experiments and the results observed with cellulose pre-irradiation aforementioned. Indeed, radicals have a short lifetime related to a high reactivity and therefore react in short range. Hence, the radicals created by pre-irradiation would have been degraded before the antibody deposit and would lead to results similar to unirradiated papers (above result). In addition, radicals would only react with the closest antibodies which are many more after a concentration step (optimization result). More experiments such as ESR are in progress in order to confirm this hypothesis.

4. Conclusion

A chemical-free photografting procedure for antibody immobilization onto cellulose has been described. This whole new method allows biomolecules to be immobilized onto

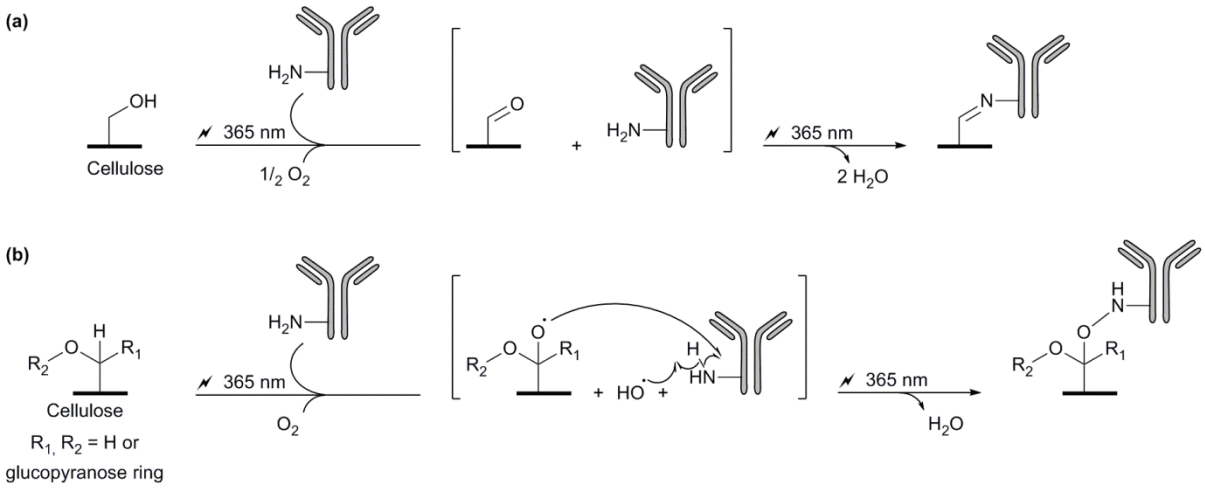

Figure 14: Proposed mechanisms for photoimmobilization of antibodies onto cellulose. The oxidative mechanism (a) is based on references [57,56,58], while the radical mechanism (b) is only based on reference [56].

cellulose without any photocoupling intermediate nor any biomolecule or substrate pretreatment. This process is therefore fast, simple, cost-saving and environmentally-friendly. Various parameters of the photoimmobilization process have been optimized, therefore resulting in an optimal procedure which produces membranes challenging nitrocellulose performances. This research aimed at fulfilling the need for cost-saving and rapid methods allowing robust, abundant and sustainable binding of biomolecules onto cellulose sheets. In addition to the obvious advantages of a chemical-free process, cellulose is an almost inexhaustible raw material with large bioavailability and good biodegradability. More generally, the expounded process provides a powerful tool for immobilizing chemical-sensitive biomolecules onto cellulose sheets.

Acknowledgements

This work was financially supported by the Commissariat à l'Energie Atomique et aux Energies Alternatives (France).

Notes and references

[a] CEA Saclay, IRAMIS, NIMBE, LICSEN (Laboratory of Innovation in Surface Chemistry and Nanosciences), F-91191 Gif sur Yvette, France; E-mails: julie.credou@cea.fr; thomas.berthelot@cea.fr.
[b] CEA Saclay, iBiTec-S, SPI, LERI (Laboratory of Study and Research in Immunoanalysis), F-91191 Gif sur Yvette, France; E-mail: herve.volland@cea.fr.
* Author to whom correspondence should be addressed; E-mail: thomas.berthelot@cea.fr; Tel.: +33 169086588; Fax: +33 169084044.

1. A. W. Martinez, S. T. Phillips, G. M. Whitesides, and E. Carrilho, *Anal. Chem.*, 2010, **82**, 3–10.
2. L. Ge, J. Yan, X. Song, M. Yan, S. Ge, and J. Yu, *Biomaterials*, 2012, **33**, 1024–1031.
3. C.-M. Cheng, A. W. Martinez, J. Gong, C. R. Mace, S. T. Phillips, E. Carrilho, K. A. Mirica, and G. M. Whitesides, *Angew. Chem. Int. Ed. Engl.*, 2010, **49**, 4771–4774.
4. J. Hu, S. Wang, L. Wang, F. Li, T. J. Lu, and F. Xu, *Biosens. Bioelectron.*, 2014, **54**, 585–597.
5. S. Wiriyachaiporn, P. H. Howarth, K. D. Bruce, and L. A. Dailey, *Diagn. Microbiol. Infect. Dis.*, 2013, **75**, 28–36.
6. J. M. Gonzalez, M. W. Foley, N. M. Bieber, P. A. Bourdelle, and R. S. Niedbala, *Anal. Bioanal. Chem.*, 2011, **400**, 3655–3664.
7. D. D. Liana, B. Raguse, J. J. Gooding, and E. Chow, *Sensors*, 2012, **12**, 11505–11526.
8. A. K. Yetisen, M. S. Akram, and C. R. Lowe, *Lab Chip*, 2013, **13**, 2210–2251.
9. G. Zhou, X. Mao, and D. Juncker, *Anal. Chem.*, 2012, **84**, 7736–7743.
10. H. Anany, W. Chen, R. Pelton, and M. W. Griffiths, *Appl. Environ. Microbiol.*, 2011, **77**, 6379–6387.
11. S. M. Zakir Hossain, R. E. Luckham, M. J. McFadden, and J. D. Brennan, *Anal. Chem.*, 2009, **81**, 9055–9064.
12. M. Vaher and M. Kaljurand, *Anal. Bioanal. Chem.*, 2012, **404**, 627–633.
13. R. S. J. Alkasir, M. Ornatska, and S. Andreescu, *Anal. Chem.*, 2012, **84**, 9729–9737.
14. S. M. Zakir Hossain, C. Ozimok, C. Sicard, S. D. Aguirre, M. M. Ali, Y. Li, and J. D. Brennan, *Anal. Bioanal. Chem.*, 2012, **403**, 1567–1576.
15. M. Zhang, L. Ge, S. Ge, M. Yan, J. Yu, J. Huang, and S. Liu, *Biosens. Bioelectron.*, 2013, **41**, 544–550.
16. C. Sicard and J. D. Brennan, *MRS Bull.*, 2013, **38**, 331–334.
17. J. Kirsch, C. Siltanen, Q. Zhou, A. Revzin, and A. Simonian, *Chem. Soc. Rev.*, 2013, **42**, 8733–8768.
18. S. B. Murugaiyan, R. Ramasamy, N. Gopal, and V. Kuzhandaivelu, *Adv. Biomed. Res.*, 2014, **3**, 67.
19. L. Berrade, A. E. Garcia, and J. a Camarero, *Pharm. Res.*, 2011, **28**, 1480–1499.
20. A. Foudeh, T. Fatanat-Didar, T. Veres, and M. Tabrizian, *Lab Chip*, 2012, **12**, 3249–3266.
21. X. Li, D. R. Ballerini, and W. Shen, *Biomicrofluidics*, 2012, **6**, 011301.

22. P. Jonkheijm, D. Weinrich, H. Schröder, C. M. Niemeyer, and H. Waldmann, *Angew. Chem. Int. Ed. Engl.*, 2008, **47**, 9618–9647.
23. T. R. J. Holford, F. Davis, and S. P. J. Higson, *Biosens. Bioelectron.*, 2011, **34**, 12–24.
24. A. H. Peruski and L. F. Peruski, *Clin. Vaccine Immunol.*, 2003, **10**, 506–513.
25. G. A. Posthuma-Trumpie, J. Korf, and A. van Amerongen, *Anal. Bioanal. Chem.*, 2009, **393**, 569–582.
26. R. Hawkes, E. Niday, and J. Gordon, *Anal. Biochem.*, 1982, **119**, 142–147.
27. B. Ngom, Y. Guo, X. Wang, and D. Bi, *Anal. Bioanal. Chem.*, 2010, **397**, 1113–1135.
28. R. C. Wong and H. Y. Tse, *Lateral Flow Immunoassay*, Humana Press, New York, NY, 2009.
29. R. W. Peeling and D. Mabey, *Clin. Microbiol. Infect.*, 2010, **16**, 1062–1069.
30. P. von Lode, *Clin. Biochem.*, 2005, **38**, 591–606.
31. J. Burstein and G. D. Braunstein, *Early Pregnancy*, 1995, **1**, 288–296.
32. T. Chard, *Hum. Reprod.*, 1992, **7**, 701–710.
33. F. Kong and Y. F. Hu, *Anal. Bioanal. Chem.*, 2012, **403**, 7–13.
34. G. E. Fridley, C. A. Holstein, S. B. Oza, and P. Yager, *MRS Bull.*, 2013, **38**, 326–330.
35. Millipore Corporation, *Millistak+ HC Filter Devices (with RW01); MSDS No. M114480*, Millipore Corporation, Billerica, MA, USA, 2008.
36. Millipore Corporation, *Nitrocellulose Membrane Filters; MSDS No. 00000100SDS*, Millipore Corporation, Billerica, MA, USA, 2011.
37. J. Credou, H. Volland, J. Dano, and T. Berthelot, *J. Mater. Chem. B*, 2013, **1**, 3277–3286.
38. J. Credou and T. Berthelot, *J. Mater. Chem. B*, 2014. DOI: 10.1039/C4TB00431K.
39. J. S. Han and J. S. Rowell, in *Paper and composites from agro-based resources*, eds. R. M. Rowell, R. A. Young, and J. K. Rowell, CRC Press, 1996, pp. 83–134.
40. D. Klemm, B. Heublein, H.-P. Fink, and A. Bohn, *Angew. Chem. Int. Ed. Engl.*, 2005, **44**, 3358–3393.
41. S. Kalia, B. S. Kaith, and I. Kaur, *Cellulose Fibers: Bio- and Nano-Polymer Composites*, Springer Berlin Heidelberg, Berlin, Heidelberg, 2011.
42. D. Klemm, F. Kramer, S. Moritz, T. Lindström, M. Ankerfors, D. Gray, and A. Dorris, *Angew. Chem. Int. Ed. Engl.*, 2011, **50**, 5438–5466.
43. B. A. Kerwin and R. L. Remmele, *J. Pharm. Sci.*, 2007, **96**, 1468–1479.
44. P. Viel, J. Walter, S. Bellon, and T. Berthelot, *Langmuir*, 2013, **29**, 2075–2082.
45. H. Volland, P. Pradelles, F. Taran, L. Buscarlet, and C. Creminon, *J. Pharm. Biomed. Anal.*, 2004, **34**, 737–752.
46. G. T. Hermanson, *Bioconjugate techniques*, Academic Press, London, 2008.
47. P. Tingaut, R. Hauert, and T. Zimmermann, *J. Mater. Chem.*, 2011, **21**, 16066–16076.
48. S. Kumar and P. Nahar, *Talanta*, 2007, **71**, 1438–1440.
49. U. Bora, P. Sharma, K. Kannan, and P. Nahar, *J. Biotechnol.*, 2006, **126**, 220–229.
50. U. Bora, K. Kannan, and P. Nahar, *J. Memb. Sci.*, 2005, **250**, 215–222.
51. J. Credou and T. Berthelot, 2014. EP14157944.
52. N. Khreich, P. Lamourette, P.-Y. Renard, G. Clavé, F. Fenaille, C. Créminon, and H. Volland, *Toxicon*, 2009, **53**, 551–559.
53. N. Khreich, P. Lamourette, H. Boutal, K. Devilliers, C. Créminon, and H. Volland, *Anal. Biochem.*, 2008, **377**, 182–188.
54. Whatman GE Healthcare, *Sample Pads for Immunoassays*. http://www.gelifesciences.com/webapp/wcs/stores/servlet/catalog/fr/GELifeSciences-fr/products/AlternativeProductStructure_23129/ (accessed May 27, 2014).
55. Whatman GE Healthcare, *Cellulose Chromatography Papers*. http://www.gelifesciences.com/webapp/wcs/stores/servlet/catalog/fr/GELifeSciences-fr/products/AlternativeProductStructure_21507/ (accessed May 27, 2014).
56. J. Malešič, J. Kolar, M. Strlič, D. Kočar, D. Fromageot, J. Lemaire, and O. Haillant, *Polym. Degrad. Stab.*, 2005, **89**, 64–69.
57. M. U. de la Orden and J. Martínez Urreaga, *Polym. Degrad. Stab.*, 2006, **91**, 2053–2060.
58. S. Wang, L. Ge, X. Song, M. Yan, S. Ge, J. Yu, and F. Zeng, *Analyst*, 2012, **137**, 3821–3827.

Chapter 4 Inkjet printing of antibodies onto cellulose for the eco²-friendly preparation of immunoassay membranes

Though the aforementioned process (Chapter 3) was ecologically and economically friendly, the procedure implemented to impregnate paper with antibodies resulted in biomolecule wastage. Indeed, a large part of the dispensed antibodies was superfluous. Many grafted antibodies were not even involved in the visible signal since only the coloring from the entities located near the surface (within 10 µm deep) is actually visible [72]. In order to reduce this matter wastage, the biomolecule dispensing was further localized onto selected specific areas of the cellulose substrate by means of inkjet printing. Inkjet printing is a versatile technology allowing low-cost and high throughput deposition of variable kinds of solutions (biomolecules, polymers, solvents, metals) onto different types of substrates (cellulose, polymer, glass, silicon) and according to any desired design [73,74]. It is considered an environmentally friendly process, thereby appearing as a very attractive approach regarding the economic and ecological objectives. Moreover, this localized dispensing of antibodies would allow to pattern and modulate surface sensing properties of cellulose membranes. Therefore, it would permit to obtain multiplexed membranes with several biosensing properties on a single sheet.

In addition, since the photoimmobilization procedure previously described is chemical free, the solution to be printed only contains antibodies and buffer salts. As a result, these antibody-containing aqueous inks would be stable in the cartridge and should be easily printable. Still, ink rheological behavior was analyzed before printing in order to check the printability of these solutions. Native antibodies have thus been successfully printed and immobilized onto cellulose paper sheets which therefore enable to perform LFIAs. Membranes' performances were evaluated in terms of visual detection limit and challenged nitrocellulose performances.

Contents

1. INTRODUCTION 71

2. EXPERIMENTAL 72

2.1. REAGENTS AND REACTION MATERIALS 72
2.2. CHARACTERIZATION MATERIALS 73
2.3. SUBSTRATES PRETREATMENT 73
2.4. IMMOBILIZATION PROCEDURE 73
2.4.1. Printing 73
2.4.2. Immobilization 74
2.5. IMMUNOCHROMATOGRAPHIC ASSAYS (LFIA) 74
2.5.1. Preparation of colloidal-gold-labeled antibodies 74
2.5.2. Preparation of immunochromatographic strips 74
2.5.3. Assessment of the immobilization 74
2.5.4. Assessment of the biological activity and determination of the visual detection limit 74
2.6. PATTERNED PHOTOIMMOBILIZATION OF PROBE ANTIBODIES 75

3. RESULTS AND DISCUSSION 75

3.1. LOCALIZED IMMOBILIZATION OF PROBE ANTIBODIES 75
3.2. FROM CLASSICAL AUTOMATIC DISPENSING TO INKJET PRINTING OF ANTIBODIES 75
3.3. INKJET PRINTING OF ANTIBODIES ONTO VARIOUS SUBSTRATES 76
3.3.1. Inks 77
3.3.1.1. Composition 77
3.3.1.2. Rheology 77
3.3.2. Initial substrates 77
3.3.2.1. Molecular structure 77
3.3.2.2. Surface chemical analysis 78
3.3.2.3. Surface morphological structure 78
3.3.3. Printed substrates 79
3.3.3.1. Surface chemical analysis 79
3.3.3.2. Surface morphological structure 80
3.3.4. Lateral Flow Immunoassays (LFIAs) 80
3.4. INKJET PRINTING OF COMPLEX DESIGNS 81

4. CONCLUSION 82

REFERENCES 82

Credou, J.; Faddoul, R.; Berthelot, T.

Inkjet printing of antibodies onto cellulose for the eco²-friendly preparation of immunoassay membranes.

ACS Applied Materials & Interfaces 2014. Submitted.

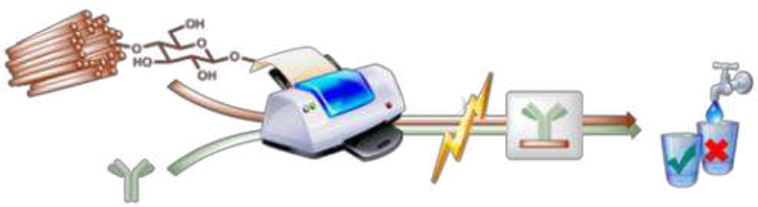

Immunoassay membranes were produced by inkjet printing and chemical-free photoimmobilization of antibodies onto cellulose.

ACS Applied Materials & Interfaces ACSPublishing

ARTICLE

Inkjet printing of antibodies onto cellulose for the eco²-friendly preparation of immunoassay membranes

Cite this: DOI: 10.1039/xoxxooooox

Julie Credou, Rita Faddoul and Thomas Berthelot*,

Received ooth July 2014,
Accepted ooth July 2014

DOI: 10.1039/xoxxooooox

www.acsami.org

The current global issues have stimulated the search for both ecologically and economically friendly (eco²-friendly) materials and processes. As a sustainable and affordable biopolymer, cellulose is an ideal material for developing diagnostic devices. Recently, paper-based bioanalytical devices have trended towards three-dimensional microfluidic platforms allowing multiplex diagnosis. This technological mutation now challenges the production process of those devices. The whole design, as well as the biosensing material immobilization, should be as eco²-friendly as possible. To this end, the biomolecule immobilization process presented here combines a chemical-free photografting procedure with inkjet printing which is a versatile and environmentally friendly dispensing method. While many printing cycles are usually achieved to get efficient immune answers, only one to five printing passes were sufficient in this study. Antibodies have been successfully printed and immobilized onto paper sheets. These membranes were further used to perform lateral flow immunoassays. The visual detection limits observed were identical to those usually displayed by the classical dispensing method, regardless the membrane material. The process developed herein is simple, time and cost-saving as well as environmentally friendly. More generally, it is a powerful tool for robust and abundant immobilization of chemical-sensitive proteins onto various cellulose-based papers and according to complex designs.

1. Introduction

The current ecological and economic global issues have result in an increasing will for sustainable technologic development. Hence, the search for renewable-resources-based procedures and environmentally friendly materials and processes, as well as cost-saving approaches, has been stimulated widely [1].

As the main component of plant skeleton, cellulose is an almost inexhaustible raw material [2,3] and the most abundant form of worldwide biomass (about 1.5 x 10^{12} tons per year) [4]. It is therefore an affordable biopolymer with lots of appealing properties such as large bioavailability, good biodegradability and biocompatibility [2,3,5,6]. Moreover, cellulose is insoluble in most usual organic solvents. It swells but does not dissolve in water, hence enabling aqueous fluids and their contained components to penetrate within the fibers matrix and to wick by capillarity with no need for any external power source. With special regard to cellulose paper, porosity combined to biocompatibility allows biological compounds to be stored in the paper device [7]. Besides, cellulose sheets are available in a broad range of thicknesses and well-defined pore sizes, easy to store and handle, and lastly safely disposable [8–10]. All of its features make cellulose an ideal structural engineering material and a grade one platform for creating novel devices for diagnostics, microfluidics, and electronics [5]. Thus, a new technological sector has risen within the last ten years: paper-based technology [11]. Though paper-based immunoassay such as dipstick tests or lateral flow immunoassays (LFIAs) have been marketed and extensively employed for point-of-care (POC) diagnostics and pathogen detection since the 80s (diabetes and pregnancy tests being the most famous) [12–19], the recent impetus given to paper-based microfluidics by American, Canadian and Finnish research teams [20–22] has resulted in the development of new paper-based bioanalytical devices with complex designs allowing multiplex diagnosis [23–30].

Equipped with this sustainable, low-cost and easy to use material, the next challenge now lies in the production process. Two parts of the process should therefore be considered: the whole device design and shaping on one hand, and the biosensing material dispensing and immobilization on the other hand.

Regarding the device shaping, the frame material of a multiplex device needs to be patterned with microfluidic channels [1]. Thus, several methods for patterning paper sheets have been developed [27,31]. Among the many processes are photolithography, using SU-8 or SC photoresist [9,20,32,33], “wax

printing" or "wax dipping" [34–36], inkjet printing [37] and laser cutting [38,39].

With regard to the biosensing material, the spatially controlled immobilization of biomolecules is a key step in the development of biosensing devices [40]. Photolithographic methods can be used to control protein immobilization onto selected specific areas of the substrate. Yet, this is a long and complex process composed of many steps. First of all, a photoresist is prepared and deposited onto the substrate through a master form. After UV exposure, the non-exposed regions are developed by chemical treatment. Biomolecules are finally immobilized on the non-developed regions [41,42]. In addition to complexity, and resulting high cost, there is a not insignificant risk for biomolecules to come across traces of the toxic reagents and solvents used in the development step. This is why printing techniques such as micro-contact printing or inkjet printing are often preferred to spatially control biomolecule immobilization [29,43–45]. Compared to photolithography, printing techniques allow quick cycles where only one step – printing biomolecule – is required. Moreover, printing is considered a biocompatible environmentally friendly process. It is a versatile technique enabling the deposition of variable kinds of solutions (biomolecules, polymers, solvents, metals) onto different types of substrates (cellulose, polymer, glass, silicon) and according to any design desired [46,47]. It is a fast dispensing process allowing low-cost, high throughput fabrication [47], and therefore a very attractive approach regarding the economic and ecological goals. However, to be able to detect an immune answer, many printing cycles were needed so far. For example, referring to Abe *et al.* works, 60 print cycles of an immune-sensing ink were necessary to detect 10 µg L^{-1} (*i.e.* 10 ng mL^{-1}) of IgG molecule [29] and 24 cycles of protein ink were inkjet printed in order to detect 0.8 µM of human serum albumin (HSA) (*i.e.* 53.6 µg mL^{-1} since M_{HSA} = 67 kDa) [48]. Moreover, printing is only a dispensing technique and is not sufficient by itself to strongly immobilize biomolecules onto cellulose. Recent findings revealed that about 40% of antibody molecules adsorbed onto cellulose paper can actually desorb from the fibers [49]. Direct adsorption of antibodies onto cellulose is therefore too weak to allow the permanent immobilization required in the development of immunoassay [50]. Cellulose activation or functionalization is thus necessary.

In the present study, printing parameters (jetting voltage and printing resolution) were controlled in order to allow low detection limits (1 to 25 ng mL^{-1}) with only 1 and 5 printing passes. Furthermore, this process combines inkjet printing of biomolecules with a chemical-free photografting procedure previously patented [51,52] which ensures easy, rapid and strong immobilization of antibodies onto cellulose-based papers. Hence, the new process developed and presented herein not only is faster and more cost-saving than the known printing processes implemented in the development of paper-based biosensing devices, but also ensures a strong and precisely localized immobilization of antibodies onto paper. To put the process to the test, a simple lateral flow immunoassay (LFIA) device was first produced and studied. The model antigen used in these assays was ovalbumin (OVA) and the antibodies directed against its epitopes were murine monoclonal antibodies (mAbs). Each prepared membrane was subjected to several immunoassays. The first one evaluated the immobilization rate thanks to a gold-labeled goat anti-mouse tracer antibody. The other ones assessed the biological activity and evaluated the visual detection limit thanks to a gold-labeled murine anti-OVA tracer antibody and OVA dilution series ranging from 0 ng mL^{-1} (negative control) to 500 ng mL^{-1} (positive control). Every experiment was conducted in triplicate. Since adsorption on nitrocellulose is the most frequently used method for immunochromatographic assays [13–15,53], all results were analyzed with respect to nitrocellulose as the reference material. Likewise, the inkjet printing process was compared to the classical automatic dispensing method with BioDot-like systems usually implemented in LFIA preparation [54]. Several parameters of the inkjet printing procedure have thus been optimized, as well as paper substrate pretreatment, therefore resulting in visual detection limits (VDLs) that challenge nitrocellulose values.

2. Experimental

2.1. Reagents and reaction materials

Proteins (ovalbumin (OVA), Bovine Serum Albumin (BSA) and porcine skin gelatin), as well as chemical products for preparing buffers, colloidal gold solution, and substrates pretreatment mixtures were obtained from Sigma-Aldrich (St Louis, MO, USA). Water used in all experiments was purified by the Milli-Q system (Millipore, Brussels, Belgium). Monoclonal murine antibodies (murine mAbs) were produced at LERI (CEA, Saclay, France) as previously described [55]. Goat anti-mouse antibodies (IgG + IgM (H+L)) were purchased from Jackson ImmunoResearch (West Grove, PA, USA).

Papers used for preparing the immunoassay membranes were CF1 cellulose and AE 98 Fast nitrocellulose from Whatman (Maidstone, Kent, UK). Immunochromatographic strips were prepared using Standard 14 sample wick from Whatman (Maidstone, Kent, UK), No. 470 absorbent pad from Schleicher and Schuell BioScience GmBH (Dassel, Germany) and MIBA-020 backing card from Diagnostic Consulting Network (Carlsbad, CA, USA).

Antibody solutions were either printed onto substrates using a laboratory piezoelectric drop-on-demand inkjet printer Dimatix Materials Printer DMP-2831 (Fujifilm, Santa Clara, CA, USA) with 10 pL nominal drop volume cartridge, or dispensed at 1 µL cm^{-1} using an automatic dispenser (XYZ3050 configured with 2 BioJet Quanti Dispenser (BioDot, Irvine, CA, USA)). Irradiations were conducted at room temperature in a UV chamber CN-15.LV UV viewing cabinet (Vilber Lourmat, Marne-la-Vallée, France). Strips were cut using an automatic programmable cutter Guillotine Cutting CM4000 Batch cutting system from BioDot (Irvine, CA, USA). 96-Well polystyrene microplates (flat-bottom, crystal-clear, from Greiner Bio-One S.A.S. Division Bioscience, Les Ulis, France) were used as

container for migrations on immunochromatographic strips. Opaque plastic (double-sided tape) maskings used in the photo-patterning experiments have been designed and prepared with a laser plotter LaserPro Spirit (GCC Laser Pro, New Taipei City, Taiwan), and the software CorelDRAW Graphics Suite (Corel Corporation, Ottawa, Canada).

2.2. Characterization materials

Infrared (IR) spectra of the various substrates were recorded on a Vertex 70 FT-IR spectrometer (Bruker, Billerica, MA, USA) controlled by OPUS software (Bruker, Billerica, MA, USA) and fitted with MIRacle™ ATR (Attenuated Total Reflectance) sampling accessory (PIKE Technologies, Madison, WI, USA). The ATR crystal type was single reflection diamond/ZnSe crystal plate. The FT-IR detector was MCT working at liquid nitrogen temperature. Acquisitions were obtained at 2 cm^{-1} resolution after 256 scans.

X-ray photoelectron spectroscopy (XPS) studies of membranes were performed with an Axis Ultra DLD spectrometer (Kratos, Manchester, UK), using monochromatic Al K_α radiation (1486.6 eV) at 150 W and a 90° electron take-off angle. The area illuminated by the irradiation was about 2 mm in diameter. Survey scans were recorded with 1 eV step and 160 eV analyzer pass energy and the high-resolution regions with 0.05 eV step and 40 eV analyzer pass energy. During the data acquisition, the sample surfaces were neutralized with slow thermal electrons emitted from a hot W filament and trapped above the sample by the magnetic field of the lens system (hybrid configuration). Referring to Johansson and Campbell's work, XPS analysis was carried out on dry samples, together with an *in situ* reference [56].

Microstructure and surface morphology of samples were examined by a JSM-5510LV (JEOL, Tokyo, Japan) scanning electron microscope (SEM) after gold coating (K575X Turbo Sputter Coater (Quorum Technologies Ltd, Ashford, Kent, UK), working at 15 mA for 20 seconds). The images were acquired at various magnifications ranging from 100× to 3 000×. The acceleration voltage and working distance were 4 kV and 17 mm, respectively. Images were acquired applying the secondary electron detector.

Surface roughness, Ra, of the unprinted substrates was measured with an AlphaStep® D-120 Stylus Profiler (KLA-Tencor, Milpitas, CA, USA). Measurements were performed along a line of 1 mm long, with a stylus force of 1 mg and at a speed of 0.05 mm s^{-1}.

Printed solutions viscosity was measured before printing with a MCR 102 Rheometer (Anton Paar, Ashland, VA, USA). Cone-plane geometry was used at a shear rate varying from 100 to 10 000 s^{-1} and at a 24°C temperature. Gap distance was equal to 0.1 mm. Geometry diameter and angle were equal to 5 cm and 1°, respectively.

Colorimetric intensity resulting from colloidal gold on immunochromatographic strips was qualitatively estimated directly by eye at first and then indirectly through a picture taken with a Molecular Imager VersaDoc™ MP4000, in association with Quantity One 1-D Analysis software (Bio-Rad, Hercules, CA, USA). Colorimetric intensity resulting from colloidal gold on masked papers was quantified with the same imager and software.

2.3. Substrates pretreatment

AE 98 Fast nitrocellulose and CF1 cellulose were used as received. In addition, several pieces of CF1 cellulose were treated in order to obtain cellulose sheets enriched with glucose (glucose-cellulose) or paraffin (paraffin-cellulose). Glucose-cellulose was prepared by dipping a CF1 cellulose sheet in a 100 mg mL^{-1} aqueous solution of D-(+)-glucose overnight at 4°C, and then drying it at 37°C in a ventilated oven for 1 hour. Similarly, paraffin-cellulose was prepared by dipping a cellulose sheet in a 10 mg mL^{-1} hot aqueous suspension of paraffin for 1 hour, and then drying it at 37°C in a ventilated oven for 1 hour. The temperature of the aqueous solution needed to be above 60°C for paraffin to melt and mix with water.

2.4. Immobilization procedure

2.4.1. Printing

Antibody solutions were printed onto the raw and pretreated substrates using the Dimatix inkjet printer. Nozzle diameter was 21.5 µm and nominal drop volume was 10 pL. Printing tests were performed at 40 V tension with 15 µm drop spacing. While drop spacing is inversely proportionate to resolution, printing voltage is directly related to the ejected volume. The printed pattern (Figure 1) consisted of two straight lines of 600 µm width and was designed according to usual LFIA strips [54]. The bottom line was therefore dedicated to capture the OVA model antigen (test line). The top line aimed to detect anti-OVA tracer antibodies (control line). Thus, the test line consisted of murine anti-OVA monoclonal antibodies (1 mg mL^{-1} in 0.1 M potassium phosphate buffer, pH 7.4) and the control line of goat anti-mouse polyclonal antibodies (0.5 mg mL^{-1} in 0.1 M potassium phosphate buffer, pH 7.4). Printings made of 1 and 5 layers were compared to the usual automatic dispensing method (1µL cm^{-1} with the BioDot system) [54].

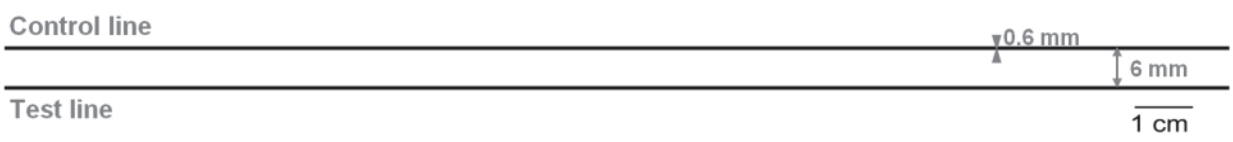

Figure 1. Scheme of the printed pattern.

2.4.2. Immobilization

Two procedures were implemented depending on the nature of the substrate. Thus, antibodies were adsorbed onto nitrocellulose substrate (AE 98 Fast nitrocellulose), while they were photoimmobilized onto cellulose substrates (CF1 cellulose, glucose-cellulose and paraffin-cellulose). Results obtained onto the raw and pretreated cellulose substrates were analyzed with respect to nitrocellulose as the reference material.

According to previous optimization results [51], the photoimmobilization process for antibody immobilization onto cellulose can be described as follows: (i) an antibody solution was dispensed onto a cellulose sheet (see previous section); (ii) antibodies were concentrated by drying of the impregnated paper at 37°C, in a ventilated oven, for 15 minutes; (iii) the system was irradiated at 365 nm (1050 µW cm^{-2}) for 2h40 (about 10 J cm^{-2}) for inducing photoimmobilization; and (iv) papers were intensively rinsed with a washing buffer (0.1M potassium phosphate buffer, pH 7.4, containing 0.5 M NaCl and 0.5% (v/v) Tween 20) for removing non-immobilized antibodies.

Adsorption of antibodies onto nitrocellulose was achieved by regular 1-hour incubation at room temperature and following washing step.

2.5. Immunochromatographic assays (LFIA)

Immobilization rate, biological activity and visual detection limit (VDL) of the antibody-printed membranes were evaluated by colloidal-gold-based lateral flow immunoassays (LFIAs) [13]. The signal intensity was qualitatively estimated directly by eye at first and then indirectly through a picture taken with a Molecular Imager. All results were compared with those obtained with nitrocellulose which is the reference material.

All the reagents were diluted in the analysis buffer (0.1 M potassium phosphate buffer, pH 7.4, containing 0.1% (w/v) BSA, 0.15 M NaCl, and 0.5% (v/v) Tween 20), at room temperature, 30 minutes prior to migration in order to reduce nonspecific binding. Each assay was performed at room temperature by inserting a strip into a well of a 96-well microtiter plate containing 100 µL of the test solution. The mixture was successively absorbed by the various pads and the capillary migration process lasted for about 15 minutes. Colorimetric intensity was immediately estimated by eye and pictures with both regular digital camera and Molecular Imager were taken without delay.

2.5.1. Preparation of colloidal-gold-labeled antibodies

Tracer antibodies were labeled with colloidal gold according to a known method previously described [54]. Two types of tracer were prepared: a goat anti-mouse tracer to reveal the immobilized murine antibodies, and a murine anti-OVA tracer to highlight the capture of OVA by the immobilized antibodies.

Briefly, 4 mL of gold chloride and 1 mL of 1% (w/v) sodium citrate solution were added to 40 mL of boiling water under constant stirring. Once the mixture had turned purple, this colloidal gold solution was allowed to cool down to room temperature and stored at 4°C in the dark. 25 µg of mAb and 100 µL of 20 mM borax buffer, pH 9.3, were added to 1 mL of this colloidal gold solution. This mixture was left to incubate for one hour on a rotary shaker at room temperature, therefore enabling the ionic adsorption of the antibodies onto the surface of the colloidal gold particles. Afterwards, 100 µL of 20 mM borax buffer, pH 9.3, containing 1% (w/v) BSA, was added and the mixture was centrifuged at 15 000 g for 50 minutes at 4°C. After discarding the supernatant, the pellet was suspended in 250 µL of 2 mM borax buffer, pH 9.3, containing 1% (w/v) BSA and stored at 4°C in the dark.

2.5.2. Preparation of immunochromatographic strips

An immunochromatographic strip is usually composed of a sample pad, a detection pad and an absorbent pad, the whole being affixed onto a plastic carrier (or backing card). Thus, an antibody-printed paper pad constituted the detection zone. In order to prevent nonspecific protein adsorption onto the detection membrane during immunoassays, all antibody-printed membranes were saturated with a gelatin solution (0.1 M potassium phosphate buffer, pH 7.4, containing 0.5% (w/v) porcine gelatin and 0.15 M NaCl) overnight at 4°C, and then dried at 37°C in a ventilated oven for 30 minutes. All pads (about 20 cm width) were assembled onto the backing card and then the whole was cut into strips of 5 mm width (see Figure 2).

2.5.3. Assessment of the immobilization

The test solution was composed of a goat anti-mouse tracer diluted 10 times in the analysis buffer. Unprinted parts of detection paper pads assessed the unspecific signal due to unspecific adsorption of the tracer onto the saturating matrix during immunoassays. The immobilization ability of the various paper substrates was therefore assessed by the colorimetric difference between the murine-antibody-printed part of detection pad (test line) and the unprinted corresponding one.

2.5.4. Assessment of the biological activity and determination of the visual detection limit

Ten test solutions were prepared and pre-incubated for 15 minutes. The first one only contained murine anti-OVA mAb

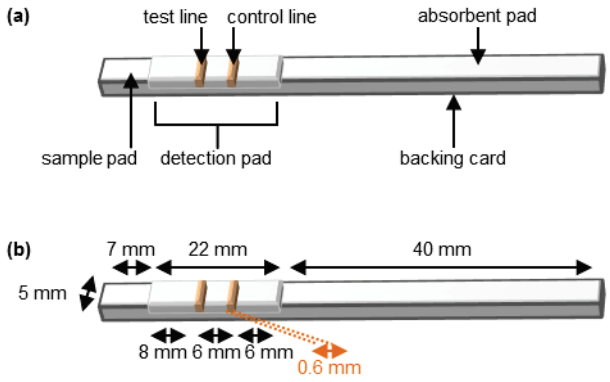

Figure 2. Schematic representation (a) and proportioning (b) of an immunochromatographic strip.

tracer diluted 10 times in the analysis buffer. This immunoassay without OVA antigen (0 ng mL^{-1}) assessed the unspecific signal due to unspecific adsorption of the tracer onto the antibody-gelatin matrix during immunoassays (negative control). The nine others were solutions of murine anti-OVA mAb tracer (10-time dilution) and OVA (dilution series ranging from 1 ng mL^{-1} to 500 ng mL^{-1}) in the analysis buffer.

The biological activity of the various paper substrates was therefore assessed by the colorimetric difference between the antibody-printed paper test-line signal in the presence of OVA and the corresponding one without OVA. Since it captured the excess murine anti-OVA tracer antibodies, the control line prevented false negative results. Its coloring guaranteed that the tracer actually passed through the test line, along with the test solution.

The visual detection limit (VDL) was determined through the OVA dilutions series. It was defined as the minimum OVA concentration resulting in a test-line colored signal significantly more intense than the negative control one.

2.6. Patterned photoimmobilization of probe antibodies

Probe antibodies, or colloidal-gold-labeled antibodies (tracers), were photoimmobilized onto pristine CF1 cellulose paper according to the following procedure. A 2-cm^2 cellulose sheet (2 cm x 1 cm in size) was manually impregnated with a goat anti-mouse tracer solution (3-fold dilution in the analysis buffer, 20 µL cm^{-2} deposit). Drying step was skipped and this system was then irradiated at 365 nm for 1h20 (about 5 J cm^{-2}) through an opaque plastic mask in order to localize the grafting (patterning process). Paper was rinsed overnight with the washing buffer. Colorimetric measurement using the molecular imager was performed immediately after the paper had been slightly dried over absorbent paper. The patterned image was pictured with either digital camera or VersaDoc™ Molecular Imager.

3. Results and discussion

3.1. Localized immobilization of probe antibodies

Photo-patterning consists in transferring an image displayed on a mask towards a substrate through photochemical or photoactivated reactions. This is the fastest and most easily undertaken process ensuring the localization of species onto a flat support according to a well-defined and reproducible pattern. This process was therefore combined to the chemical-free photografting procedure previously patented [51,52] in order to easily and rapidly localize antibodies onto cellulose sheets.

Probe antibodies labeled with colloidal gold were immobilized through a mask in order to directly observe the photo-patterned immobilization of antibodies, and to evaluate the signal/background *ratio* (Figure 3). A selective photoimmobilization of the colloidal-gold-labeled antibody is observed according to the design of the used mask. This confirms the immobilization process to be photo-controlled.

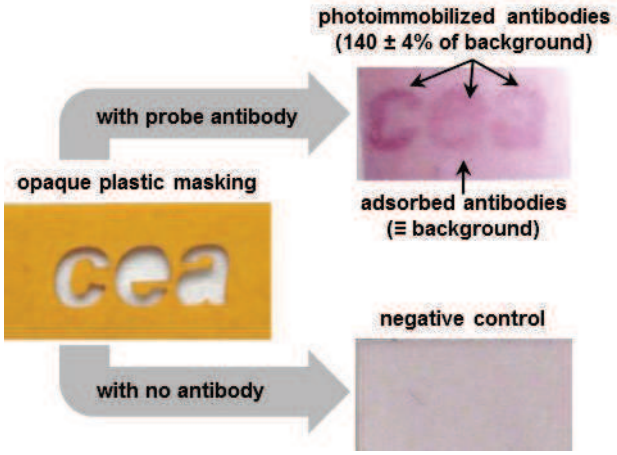

Figure 3. Photo-patterning of gold-labeled goat anti-mouse tracer antibodies. Photographs were taken with a regular digital camera.

The signal/background *ratio* is estimated to be around 140%. Though it is a rather positive result, the high background colorimetric intensity also indicates that lots of antibodies are wasted in this process. That stems from the subtractive nature of the photo-patterning process. Thus, this process was set aside and an additive process such as inkjet printing was further preferred.

3.2. From classical automatic dispensing to inkjet printing of antibodies

Since automatic dispensing with BioDot-like systems [54] is the most frequently used method for antibody dispensing onto immunoassay membranes, the inkjet printing approach was first compared to the latter. That comparison aimed to validate the printing method for its use in the development of immunoassay devices.

Printings made of 1 and 5 layers were therefore compared to the single line deposit from the automatic dispenser (Figure 4). After antibody solutions had been dispensed onto the substrates, the antibodies were either adsorbed onto nitrocellulose or photoimmobilized onto cellulose. First, their immobilization was confirmed by revelation with gold-labeled goat anti-mouse tracer (see control strips in Figure 4). Then, their biological activity was put to the test by exposition to OVA antigen and simultaneously revealed by gold-labeled murine anti-OVA tracer (sandwich immunoassay) (see OVA strips in Figure 4). Each test was performed in triplicate.

The first noticeable result is that the sets of strips obtained with BioDot dispensing method and with 5-layer inkjet printing are visually almost identical. Their coloring is quite strong, while the coloring resulting from 1-layer inkjet printing is obviously weaker. However, this weakness does not seem to lower its performances in terms of visual detection limit (VDL) as further detailed. This same set of strip actually displays slightly thinner and more precise test and control lines than the others, although they are all well-defined, thin and precise. With regard to biological activity, dilutive effect is clearly perceptible. Nevertheless, photographs reveal that the negative control

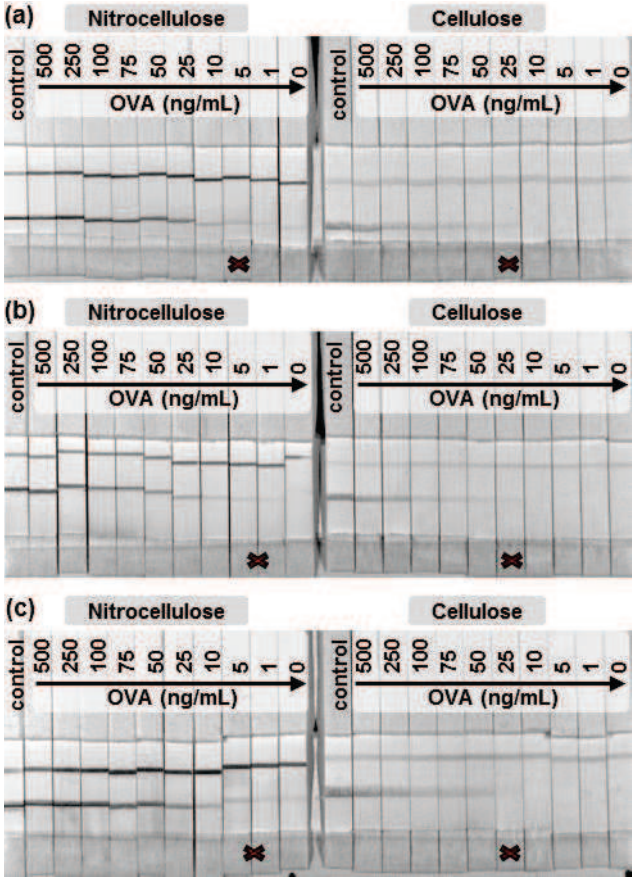

Figure 4. Photographs showing the influence of the dispensing process on biological activity and membrane VDL. The first set of strips (a) results from usual BioDot dispensing method, the second (b) from 1-layer inkjet printing, and the third (c) from 5-layer inkjet printing. Antibodies were adsorbed onto nitrocellulose and photoimmobilized onto cellulose. Their actual immobilization was confirmed thanks to gold-labeled goat anti-mouse tracer (control strips). The capture of OVA antigen by the immobilized antibodies was highlighted by gold-labeled murine anti-OVA tracer (OVA strips). The strips corresponding to the membranes' VDL are labeled with a cross. Photographs were taken with the Molecular Imager. All experiments were reproduced 3 times but only one is shown here.

(OVA at 0 ng mL^{-1}) for nitrocellulose is slightly colored. This raises the issue of false positive results that can be observed with nitrocellulose immunoassay membranes. This issue does not arise with cellulose, most probably because of lower sensitivity. Considering that, the membranes' VDL were appraised as follows: (i) 5 ng mL^{-1} for nitrocellulose and 25 ng mL^{-1} for cellulose with BioDot dispensing method (Figure 4a); (ii) 1 to 5 ng mL^{-1} for nitrocellulose and 25 ng mL^{-1} for cellulose with 1-layer inkjet printing (Figure 4b); and (iii) 1 to 5 ng mL^{-1} for nitrocellulose and 25 ng mL^{-1} for cellulose with 5-layer inkjet printing (Figure 4c).

Each material VDL was therefore identical regardless the dispensing method or the number of layers. Thus, the printing process was indeed proved to be as efficient as the usual automatic dispensing, and therefore totally legitimate regarding its use in the development of immunoassay devices. Moreover, the printing method has the advantage of saving the quite expensive biomolecules dispensed because of the rather low ejected volume. Though an exact ejected volume could not be measured, the maximum dispensed volume was calculated based on the printer features (nominal drop volume, drop spacing and tension). For the selected pattern (a straight line of 600 µm width), the printer was estimated to deliver 0.27 µL cm^{-1} of antibody solution per layer. A maximum of 0.27 µL cm^{-1} of antibody solution was thus dispensed with 1-layer inkjet printing (Figure 4b), a maximum of 1.35 µL cm^{-1} with 5-layer inkjet printing (Figure 4c), and exactly 1 µL cm^{-1} with BioDot dispensing method (Figure 4a). Since a 1-layer printing is efficient enough to determine the VDL, the consumed amount of antibodies is therefore nearly a quarter of the amount consumed with a classical automatic dispenser. Another advantage of printing over classical automatic dispensing is the freedom in design of the printed pattern (see further section 3.4) while the usual automatic dispenser only allows drawing straight lines of rather undefined width.

Regarding the evaluation of the immobilization procedure, photoimmobilization onto cellulose led to VDL results in the same order of magnitude as the values obtained with adsorption onto nitrocellulose. However, cellulose performances appeared slightly lower than nitrocellulose's ($VDL_{cellulose}$=5 $VDL_{nitrocellulose}$). Beyond procedure, this phenomenon might stem from the many differences both chemical and physical between the two substrates. This is why the experiments presented thereafter were dedicated to characterize these differences while trying to compensate for them by cellulose pretreatment.

3.3. Inkjet printing of antibodies onto various substrates

Beyond the obvious chemical difference in molecular structure, the main physical difference between nitrocellulose and cellulose substrates lies in their porosity (about 5 µm and 11 µm surface pore size, respectively) and sheet thickness (20 µm and 176 µm thick, respectively). Since cellulose sheets with same porosity and thickness than nitrocellulose were not commercially available, cellulose pretreatments which aimed to compensate for that by filling cellulose pores were achieved. Given that the filling substance should be inert regarding antibody immobilization process and further immunoassays, two components were selected: glucose and paraffin. Glucose is the molecular repeating unit in cellulose macromolecule (see Figure 7a and b) [1] and therefore was not expected to disturb the immobilization process or further use of the membrane. In addition, its high water solubility (180 mg mL^{-1}) would permit to easily remove it during post-irradiation washing step. Paraffin, a mixture of linear alkanes (see Figure 7b), is well known for its unreactive nature [57]. Unlike glucose, it is insoluble in water and therefore would stick into the fibers after the washing step and during further immunoassays.

Antibody solutions were printed onto the raw (nitrocellulose and cellulose) and pretreated (glucose-cellulose and paraffin-cellulose) substrates. Though 1 layer would have been enough, 5 layers were actually printed in order to get strong color intensity (see results section 3.2). Antibodies were then

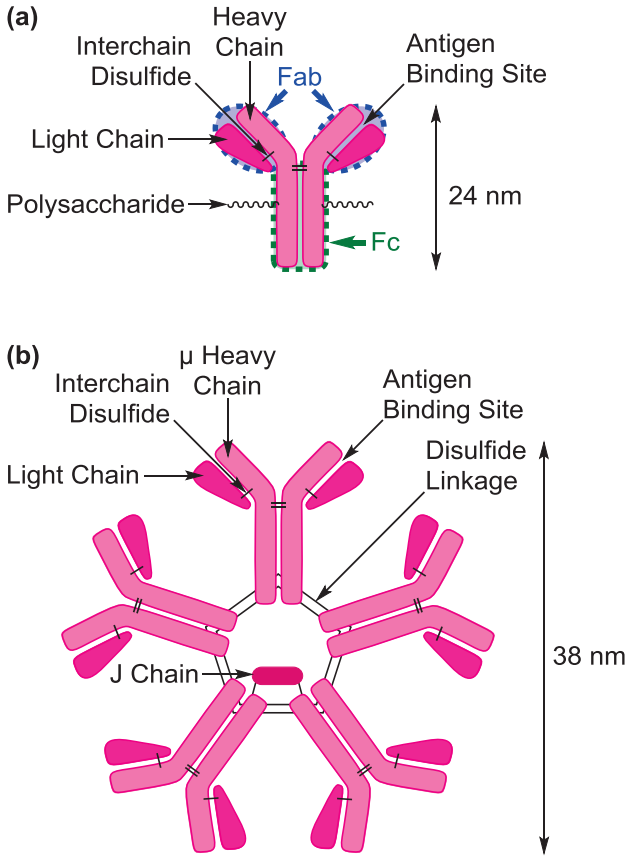

Figure 5. Detailed structure of an IgG antibody molecule (a) and general structure of an IgM antibody molecule (b).

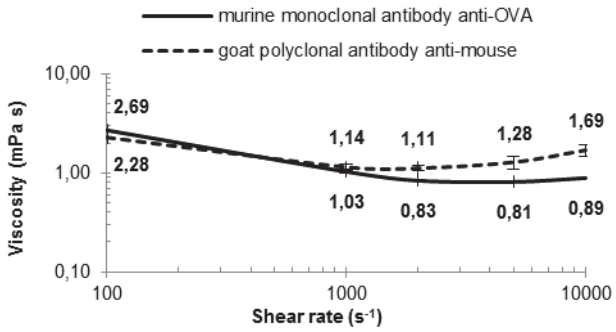

Figure 6. Antibody solutions viscosities at 24°C and shear rate varying from 100 to 10 000 s^{-1}.

$$\dot{\gamma} = \frac{v}{h}$$

Equation 1. $\dot{\gamma}$ is the shear rate (s^{-1}), v is the velocity (m s^{-1}) and h is the gap (m).

adsorbed onto nitrocellulose substrate and photoimmobilized onto cellulose substrates (cellulose, glucose-cellulose and paraffin-cellulose). Surface morphological structure and chemical composition of both raw and pretreated substrates were analyzed prior to printing and afterwards. Printed antibody solutions were characterized as well. Finally, lateral flow immunoassays (LFIAs) ensured the ultimate characterization by evaluating the biological activity and visual detection limit of the various membranes.

3.3.1. Inks

3.3.1.1. Composition

Printed solutions, also called inks, were antibody aqueous solutions. Because of different initial proportions in each antibody stock solution, their final salts content was different. Thus, murine anti-OVA antibody solution (test line ink) actually contained 1 mg mL^{-1} of monoclonal antibody (IgG) and 0.1 M of potassium phosphate in water. Likewise, goat anti-mouse antibody solution (control line ink) contained 0.5 mg mL^{-1} of polyclonal antibody (IgG + IgM), 0.1 M of potassium phosphate and 0.05 M of sodium chloride (NaCl). These variations in salts content, but also in antibody type (IgG and IgM structures are depicted in Figure 5 [58,59]) could greatly influence the surface tension between the antibody ink and the paper substrate, thereby inducing variations in the printing behavior.

3.3.1.2. Rheology

The viscosity of both test line and control line antibody solutions was measured (Figure 6). As reminded in the previous section, test line ink consisted of murine anti-OVA monoclonal antibodies and control line ink of goat anti-mouse polyclonal antibodies. According to Figure 6, control line ink viscosity varies from 2.28 to 1.69 mPa s when shear rate increases from 100 to 10 000 s^{-1}. A slight increase of viscosity is observed at shear rates higher than 2 000 s^{-1}. The control line solution is thus dilatant. Test line ink viscosity varies from 2.69 to 0.89 mPa s for the same shear rate ranges. The test line solution has a shear thinning behavior.

Equation 1 is the expression of the shear rate as a function of gap and printing speed. When shear rate varies from 100 to 10 000 s^{-1}, speed varies from 0.01 to 1 m s^{-1} for a gap of 100 μm (1 x 10^{-4} m). Depending on ink viscosity and printing voltage, jetting speed thus varies from 0.1 to 25 m s^{-1} [60,61]. Hence, high shear rates larger than 10 000 s^{-1} and exceeding the rheometer measuring limits may be estimated.

Ideally, an inkjet printing ink must be Newtonian with a constant viscosity (1 – 10 mPa s) at varying shear rates [62]. Though not Newtonian, biomolecule solutions are inkjet printable because of their low viscosities (< 2 mPa s).

3.3.2. Initial substrates

3.3.2.1. Molecular structure

Cellulose is a natural biopolymer made up of glucose units (Figure 7a). It is the simplest polysaccharide since it is composed of a unique monomer (glucose) which binds to its neighbors by a unique type of linkage (β-1,4 glycosidic bond resulting in acetal function) [1]. According to its molecular structure, hydroxyl groups in glucose units are responsible for cellulose chemical activity [63]. However, this group cannot directly interact with proteins, what makes cellulose activation or functionalization necessary in order to covalently bind to proteins of interest.

Cellulose pretreatments introduced few additive molecules but did not change the native molecular structure of cellulose. Additive substances were adsorbed onto it and partially filled

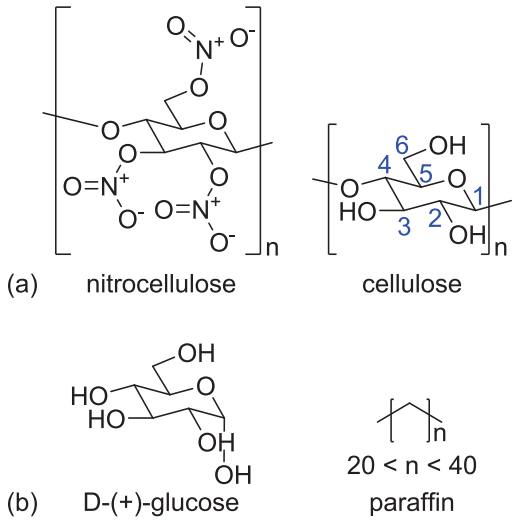

Figure 7. Molecular structures of the paper substrates (a) and filling substances (b).

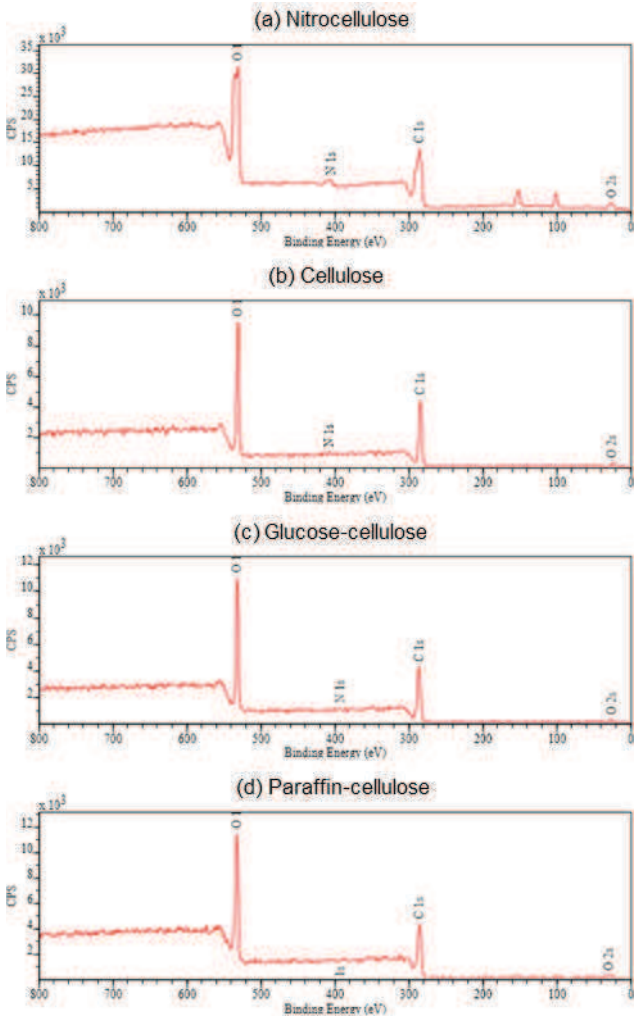

Figure 8. XPS survey analysis of unprinted paper substrates. (a) is spectrum from nitrocellulose sheet, (b) from cellulose, (c) from glucose-cellulose and (d) from paraffin-cellulose. The peaks corresponding to O 1s, C 1s and N 1s orbitals are labeled.

its pores. These additives were glucose and paraffin. While glucose is the molecular repeating unit in cellulose macromolecule, paraffin is a mixture of linear alkanes (see Figure 7b).

Nitrocellulose (also named cellulose nitrate) is the most important cellulose derivative. Biomolecules strongly adsorb to nitrocellulose through a combination of electrostatic, hydrogen, and hydrophobic interactions involving the nitro functions [15]. It is therefore the reference material for performing lateral flow immunoassay (LFIA) [13–15,53]. Cellulose nitrate is formed by esterification of hydroxyl groups from cellulose (primary or secondary) with nitric acid in the presence of sulfuric acid, phosphoric acid or acetic acid (see Figure 7a) [63,64].

These molecular features represent the first, but not most, difference between the nitrocellulose and cellulose-based substrates.

3.3.2.2. Surface chemical analysis

The outer surface layers of paper substrates were analyzed by surface chemical analysis such as XPS and ATR-FTIR, thereby displaying the aforementioned bulk molecular structures.

XPS allows the identification of elements within 10 nm deep subsurface layers [56]. All papers are mainly composed of carbon and oxygen and therefore the XPS signal for these two elements is quite strong on every spectrum shown. Figure 8 displays O 1s orbital Binding Energy at 532 eV ± 0.35 eV, O 2s orbital Binding Energy at 24 eV ± 0.35 eV and C 1s orbital Binding Energy at 284 eV ± 0.35 eV) [56]. Another peak at 405 ± 0.35 eV is noticeable onto nitrocellulose spectrum which is attributable to N 1s orbital.

According to its layout, ATR-FTIR allows the identification of chemical bonds within 2 µm deep subsurface layers [65]. All papers are mainly composed of a cellulosic backbone and therefore the IR signals for its typical bond vibrations are shared by every spectrum shown. Figure 9 displays these common bands attributable to O-H, C-H, C-C, C-O and O-C-O stretching vibrations. Besides, nitrocellulose manifests additional peaks (1638 ± 5 cm^{-1} and 1275 ± 5 cm^{-1}) attributable to N-O stretching vibrations.

3.3.2.3. Surface morphological structure

Beyond the chemical differences in molecular structure, the main difference between nitrocellulose and cellulose substrates lies in their surface physical structure. Thus, topological analysis was conducted in order to quantify the surface morphological structure by measuring its roughness (Ra). SEM imaging allowed visualizing surface morphology and microstructure of the unprinted substrates.

Line profiles of unprinted paper substrates (Figure 10) reveal that nitrocellulose surface is more homogeneous, smoother and has fewer and narrower pores compared to cellulose-based paper surfaces. Since profiles of the three cellulose-based papers were quite similar, only cellulose profile is displayed on Figure 10. Surface roughness (Ra) values (Figure 11) confirm that nitrocellulose is way smoother than cellulose-based papers. Pores size and arrangement pictured by SEM imaging (Figure 12) also corroborate the previous statements. SEM micrographs and roughness profiles predict that with the same ejected

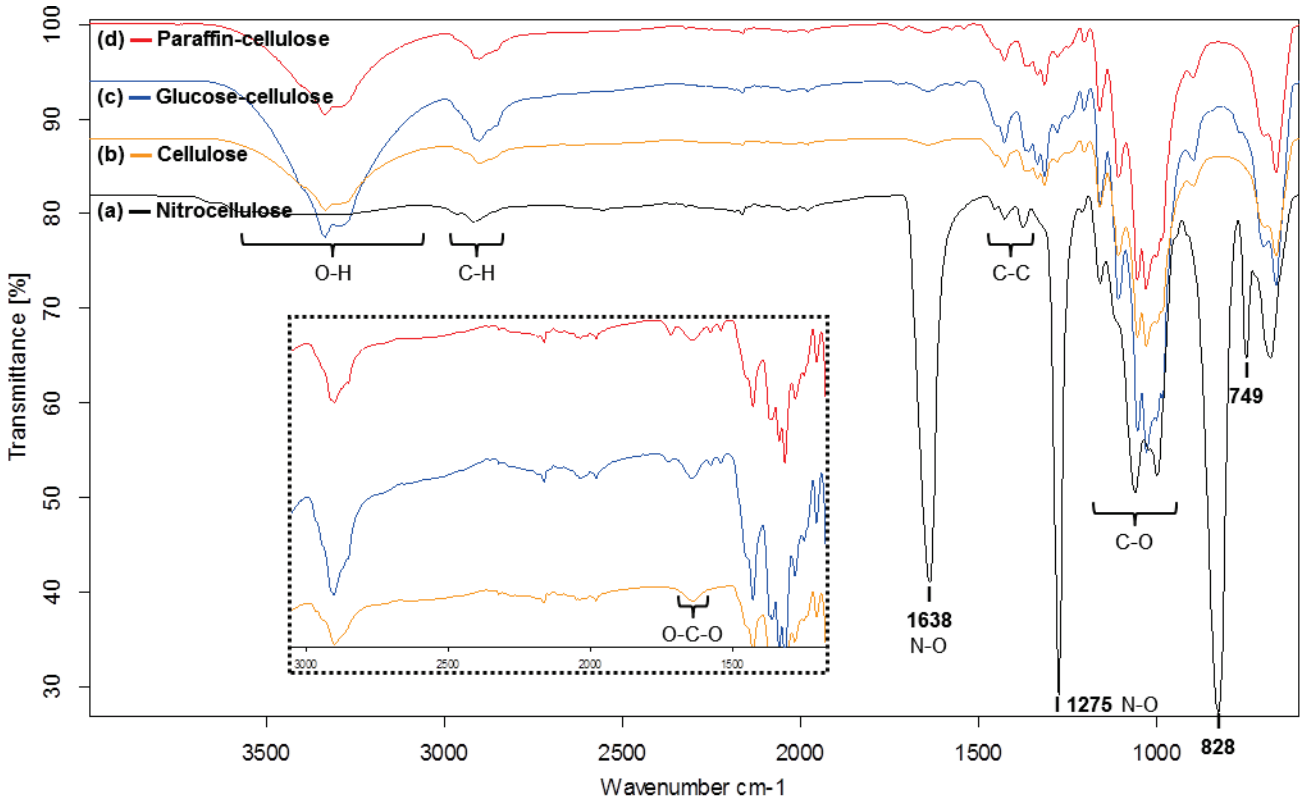

Figure 9. IR spectra of unprinted paper substrates. (a) is spectrum from nitrocellulose sheet, (b) from cellulose, (c) from glucose-cellulose and (d) from paraffin-cellulose. All spectra have several bands in common which correspond to O-H, C-H, C-C, C-O and O-C-O stretching vibrations. The N-O stretching vibrations specific to nitrocellulose are labeled.

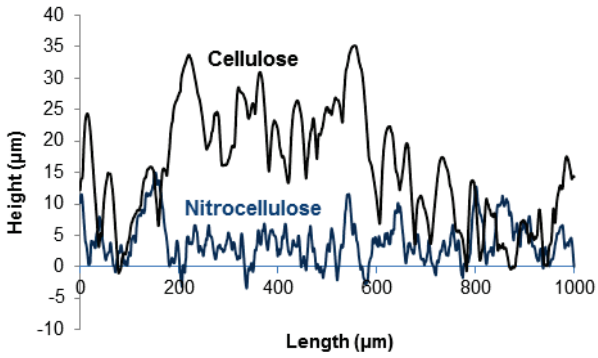

Figure 10. Line profiles of the unprinted paper substrates.

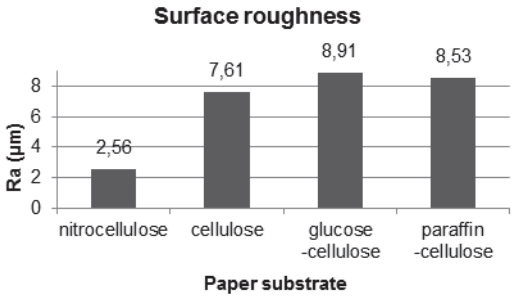

Figure 11. Surface roughness (Ra) of the unprinted paper substrates.

volume of antibodies, thicker and better resolution patterns will be printed on nitrocellulose. Thus, lower visual detection limits are expected to be reached with nitrocellulose membranes. This was supported by Määttänen *et al.* [66] who demonstrated that wetting rate reduces with surface roughness increase. Besides, they explained that ink is quickly and completely absorbed into the depth of porous surfaces, thus leaving less ink deposit onto the substrate surface.

According to SEM imaging (Figure 12), glucose treatment seems to barely affect cellulose surface aspect. On the other hand, when paraffin treatment was performed, fewer pores were observed onto the surface. Regarding surface roughness (Figure 11), an increase was displayed by both glucose and paraffin treatments.

3.3.3. Printed substrates

3.3.3.1. Surface chemical analysis

After antibody had been printed onto the various paper substrates, their outer surface layers were analyzed anew in order to detect any change stemming from the biomolecules. The XPS signal from carbon and oxygen is still quite strong on every spectrum shown (Figure 13). Additional peaks at 397.5 ± 0.35 eV have come out onto all the spectra which are attributable to N 1s orbital from antibody molecules. Since spectra of the three cellulose-based papers were quite similar, only cellulose spectrum is displayed on Figure 13.

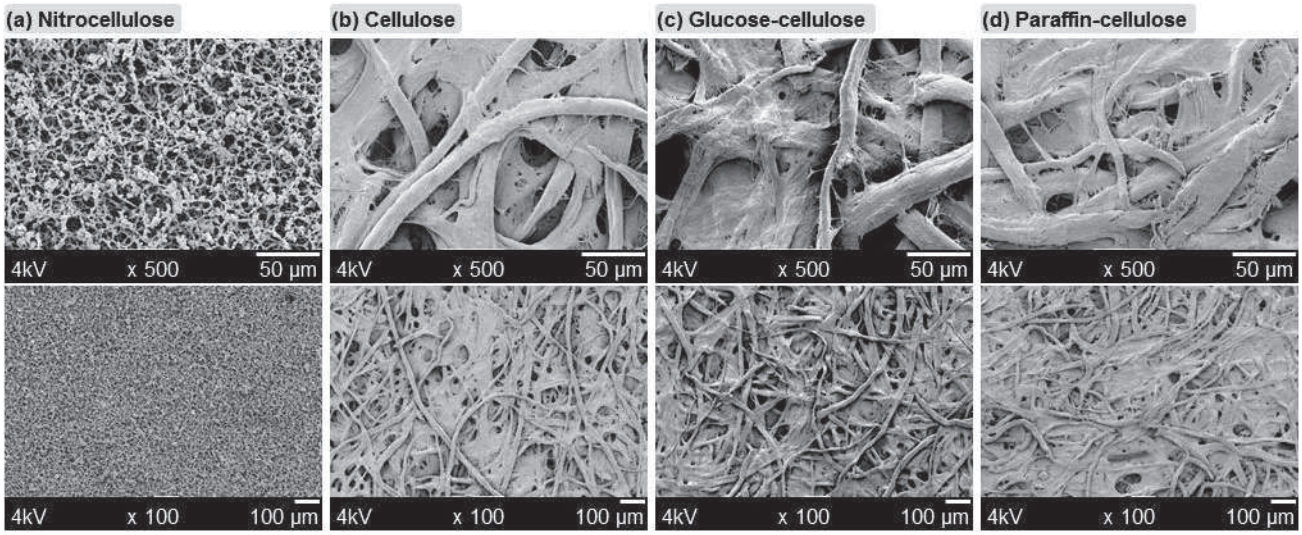

Figure 12. SEM micrographs of unprinted nitrocellulose (a), cellulose (b), glucose-cellulose (c) and paraffin cellulose (d).

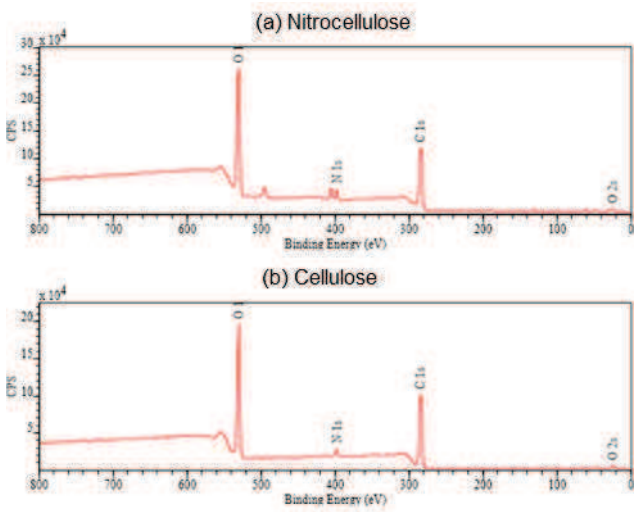

Figure 13. XPS survey analysis of antibody-printed paper substrates. (a) is spectrum from nitrocellulose sheet, (b) from cellulose. The peaks corresponding to O 1s, C 1s and N 1s orbitals are labeled.

With regard to IR analysis, the intense spectra from initial substrates hid most of the characteristic bands pointing out the immobilized antibodies (Figure 14). Therefore, the amide bands specific to proteins are barely perceivable. Only amide II at 1547 ± 5 cm^{-1} could be clearly identified onto nitrocellulose substrates.

3.3.3.2. Surface morphological structure

After antibody had been printed onto the various paper substrates, their surface morphology and microstructure were visualized anew (not shown) by SEM imaging in order to detect any change stemming from the biomolecules. Unfortunately, the microscope resolution was not high enough to enable a direct visualization of antibody deposit. However, a thin new layer seems to have appeared on cellulose-based substrates when comparing to Figure 12.

3.3.4. Lateral Flow Immunoassays (LFIAs)

Antibody solutions were printed onto the raw (nitrocellulose and cellulose) and pretreated (glucose-cellulose and paraffin-cellulose) substrates. 5 layers were printed in order to get strong color intensity. Antibodies were then adsorbed onto nitrocellulose substrate and photoimmobilized onto cellulose substrates (cellulose, glucose-cellulose and paraffin-cellulose). Lateral flow immunoassays (LFIAs) evaluated the biological activity of the printed antibodies and the visual detection limit of the various bioactive membranes, thereby allowing characterization of the various substrates in terms of biosensing performances. First, the immobilization ability of the various membranes was confirmed by revelation with gold-labeled goat anti-mouse tracer (see control strips in Figure 15). Then, their biological activity was assessed by exposition to OVA antigen and revealed by gold-labeled murine anti-OVA tracer (sandwich immunoassay) (see OVA strips in Figure 15). Each test was performed in triplicate.

The first fact to notice is that though antibodies were barely perceivable with the various surface analysis performed (XPS, IR or SEM), they are well visible after either revelation with goat anti-mouse tracer (control strips) or bioactivity assessing immunosandwich (OVA strips). With regard to biological activity, few aforementioned results (see section 3.2) remain. Dilutive effect is still clearly perceptible. There is still a false positive result with nitrocellulose that compels to appraise its VDL at 5 ng mL^{-1} (Figure 15a). The other VDLs are 50 ng mL^{-1} for cellulose (Figure 15b), 10 to 25 ng mL^{-1} for glucose-cellulose (Figure 15c), and 25 to 50 ng mL^{-1} for paraffin cellulose (Figure 15d). While nitrocellulose's VDL is still the same as in section 3.2, cellulose's VDL is now higher. Since all test lines coloring seems weaker than in Figure 4c, this inter-assay variability could originate from tracer variability due to the use of another batch of colloidal gold. On another hand, the intra-assay comparison of the different substrates reveals that both glucose and paraffin enrichment only slightly improved

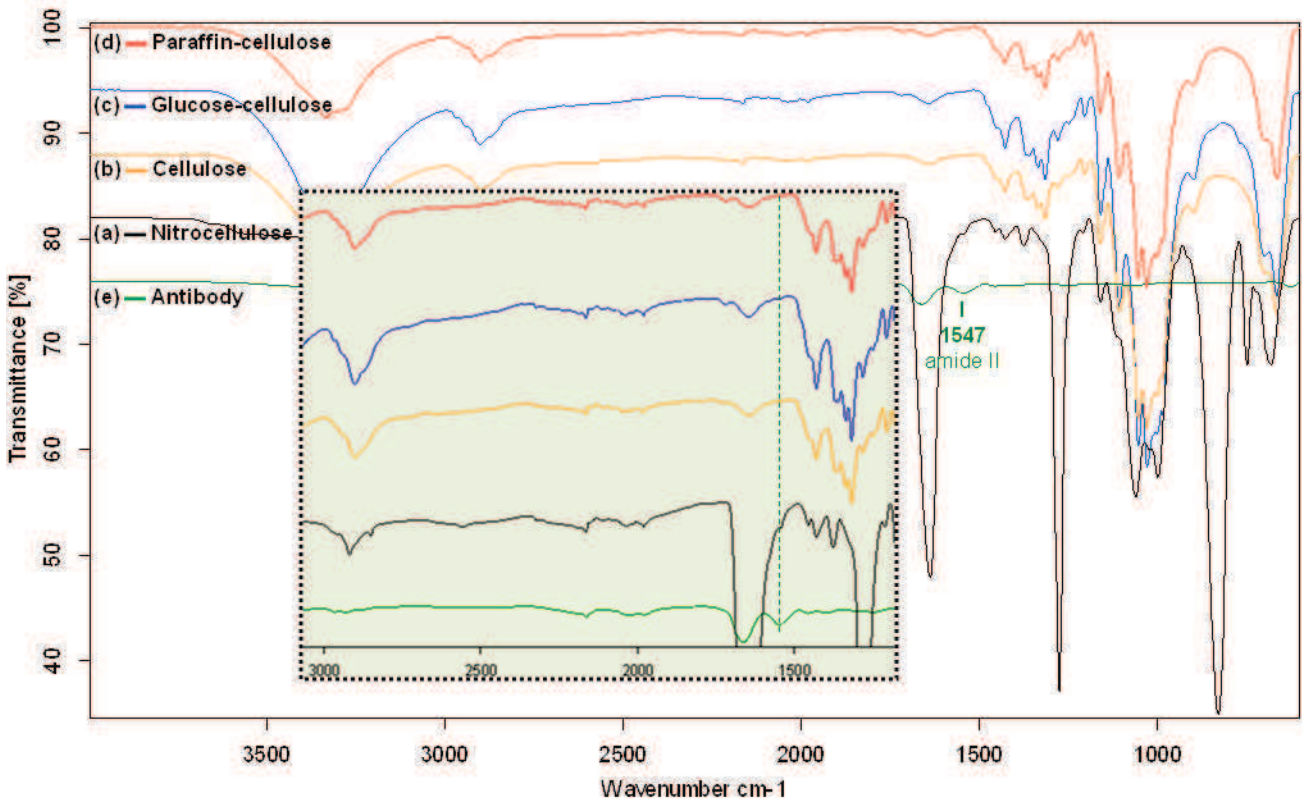

Figure 14. IR spectra of antibody-printed paper substrates. (a) is spectrum from nitrocellulose sheet, (b) from cellulose, (c) from glucose-cellulose and (d) from paraffin-cellulose. All spectra have several bands in common which correspond to O-H, C-H, C-C, C-O and O-C-O stretching vibrations. The N-O stretching vibrations specific to nitrocellulose are labeled.

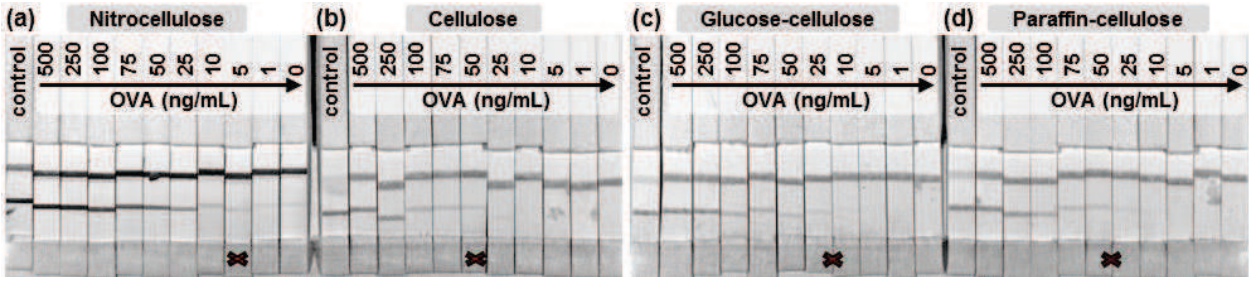

Figure 15. Photographs showing the influence of the substrate and its pretreatment on biological activity and membrane VDL. The first set of strips (a) is made of nitrocellulose, the second (b) of cellulose, the third (c) of glucose-cellulose and the fourth (d) of paraffin-cellulose. Antibodies were adsorbed onto nitrocellulose and photoimmobilized onto cellulose-based substrates. Their actual immobilization was confirmed thanks to gold-labeled goat anti-mouse tracer (control strips). The capture of OVA antigen by the immobilized antibodies was highlighted by gold-labeled murine anti-OVA tracer (OVA strips). The strips corresponding to the membranes' VDL are labeled with a cross. Photographs were taken with the Molecular Imager. All experiments were reproduced 3 times but only one is shown here.

cellulose performances although they are still lower than nitrocellulose's. Besides, glucose-cellulose appeared to be the most sensitive cellulose-based substrate. This could be explained by a slight decrease in surface porosity, as expected; though this decrease was not really significant regarding nitrocellulose porosity. But this most probably stemmed from the preservative and stabilizing effect of glucose on biomolecules [67].

3.4. Inkjet printing of complex designs

As previously mentioned, one advantage of inkjet printing dispensing method is the freedom in design of the printed pattern. This advantage was illustrated here by printing antibodies according to their nature and function, thereby making the user manual not so useful anymore. Since bottom line was dedicated to capture OVA antigen, murine anti-OVA monoclonal antibodies printing drew the abbreviation OVA. Similarly, anti-mouse antibodies were printed on the top line according CTRL abbreviation as the top line aimed to control the smooth progress of the immunoassay. After antibody solutions had been dispensed onto the substrates (1-layer inkjet printing), the antibodies were either adsorbed onto nitrocellulose or photoimmobilized onto cellulose. Their biological activity was put to the test by exposition to OVA

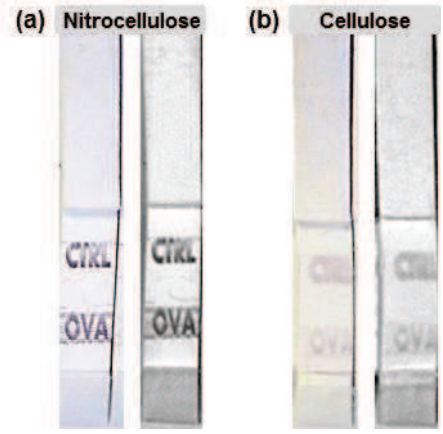

Figure 16. Photographs showing the biological activity of antibodies printed according to a complex design. The first set of strips (a) was produced with nitrocellulose membrane, the second (b) with cellulose. Antibodies were adsorbed onto nitrocellulose and photoimmobilized onto cellulose. The capture of OVA antigen by the immobilized antibodies was highlighted by gold-labeled murine anti-OVA tracer. For each set of strips photographs were taken with both a digital camera (colored left pictures) and the Molecular Imager (grey right pictures).

antigen (500 ng mL^{-1}) and simultaneously revealed by gold-labeled murine anti-OVA tracer (Figure 16). Colors observed, along with their intensities, were consistent with previous results (see section 3.2). Finally, as expected, the drawn patterns allowed direct reading of the test results. This process therefore enables to doubly check the nature of the target antigen (on the box and on the strip), thereby avoiding ambiguousness when box label is partly erased. Firstly, this can permit to save valuable assay devices in remote areas in the developing world. In addition, this double-check can be a huge asset in developed countries in emergency situations, in emergency rooms or in military settings, where the result of the assay impacts on people's lives.

4. Conclusion

A fast, simple, cost-saving and environmentally friendly process for strong and precisely localized immobilization of antibodies onto paper has been described herein. This new approach combines inkjet printing of biomolecules with a chemical-free photografting procedure which together enable to easily, rapidly and permanently immobilize antibodies onto cellulose-based papers according to any pattern desired. The inkjet printing dispensing method has the great advantage of saving the expensive biomolecules. The photografting procedure has the one of being harmless to chemical-sensitive biomolecules. The process was first tested in the development of simple lateral flow immunoassay (LFIA) device and then applied to more complex LFIA devices. Membranes' performances were evaluated in terms of visual detection limit (VDL). Several parameters of the process have been studied (printing parameters, cellulose pretreatment), hence resulting in membranes challenging nitrocellulose performances. Cellulose performances appeared slightly lower than nitrocellulose's though. But this phenomenon probably stemmed from the physical differences, such as surface porosity variation, between nitrocellulose and cellulose substrates.

This research was carried out to meet need for paper-based sensing device development to rapidly, robustly and abundantly immobilize biomolecules onto cellulose sheets according to complex patterns and at low cost. Meanwhile, the first part of the process developed - the inkjet printing dispensing method by itself - also proved itself to be efficient and useful with nitrocellulose reference material. More generally, the expounded process provides a powerful tool for immobilizing chemical-sensitive proteins according to complex patterns and onto various cellulose-based paper sheets.

Acknowledgements

This work was financially supported by the Commissariat à l'Energie Atomique et aux Energies Alternatives (France). Jocelyne Leroy is greatly acknowledged for performing the XPS analysis and helping in analyzing XPS data. Rocio De Miguel Viscasillas and Marine Gay are greatly acknowledged for lending the Sputter Coater and helping in using it.

Notes and references

CEA Saclay, IRAMIS, NIMBE, LICSEN (Laboratory of Innovation in Surface Chemistry and Nanosciences), F-91191 Gif sur Yvette, France; E-mails: julie.credou@cea.fr; rita.faddoul@cea.fr; thomas.berthelot@cea.fr.
* Author to whom correspondence should be addressed; E-mail: thomas.berthelot@cea.fr; Tel.: +33 169086588; Fax: +33 169084044.

(1) Credou, J.; Berthelot, T. *J. Mater. Chem. B* **2014**. DOI: 10.1039/C4TB00431K
(2) Han, J. S.; Rowell, J. S. In *Paper and composites from agro-based resources*; Rowell, R. M.; Young, R. A.; Rowell, J. K., Eds.; CRC Press, 1996; pp. 83–134.
(3) Klemm, D.; Heublein, B.; Fink, H.-P.; Bohn, A. *Angew. Chem. Int. Ed. Engl.* **2005**, *44*, 3358–3393.
(4) Crawford, R. L. *Lignin biodegradation and transformation*; John Wiley & Sons Inc: New York, NY, USA, 1981; pp. 1–154.
(5) Kalia, S.; Kaith, B. S.; Kaur, I. *Cellulose Fibers: Bio- and Nano-Polymer Composites*; Kalia, S.; Kaith, B. S.; Kaur, I., Eds.; Springer Berlin Heidelberg: Berlin, Heidelberg, 2011.
(6) Klemm, D.; Kramer, F.; Moritz, S.; Lindström, T.; Ankerfors, M.; Gray, D.; Dorris, A. *Angew. Chem. Int. Ed. Engl.* **2011**, *50*, 5438–5466.
(7) Maxwell, E. J.; Mazzeo, A. D.; Whitesides, G. M. *MRS Bull.* **2013**, *38*, 309–314.
(8) Pelton, R. *Trends Anal. Chem.* **2009**, *28*, 925–942.
(9) Martinez, A. W.; Phillips, S. T.; Whitesides, G. M.; Carrilho, E. *Anal. Chem.* **2010**, *82*, 3–10.
(10) Credou, J.; Volland, H.; Dano, J.; Berthelot, T. *J. Mater. Chem. B* **2013**, *1*, 3277–3286.
(11) Materials Research Society. *MRS Bull.* **2013**, *38*, 294–352.
(12) Hawkes, R.; Niday, E.; Gordon, J. *Anal. Biochem.* **1982**, *119*, 142–147.
(13) Posthuma-Trumpie, G. A.; Korf, J.; van Amerongen, A. *Anal. Bioanal. Chem.* **2009**, *393*, 569–582.

(14) Ngom, B.; Guo, Y.; Wang, X.; Bi, D. *Anal. Bioanal. Chem.* **2010**, *397*, 1113–1135.
(15) Wong, R. C.; Tse, H. Y. *Lateral Flow Immunoassay*; Wong, R. C.; Tse, H. Y., Eds.; Humana Press: New York, NY, 2009.
(16) Peeling, R. W.; Mabey, D. *Clin. Microbiol. Infect.* **2010**, *16*, 1062–1069.
(17) Von Lode, P. *Clin. Biochem.* **2005**, *38*, 591–606.
(18) Burstein, J.; Braunstein, G. D. *Early Pregnancy* **1995**, *1*, 288–296.
(19) Chard, T. *Hum. Reprod.* **1992**, *7*, 701–710.
(20) Martinez, A. W.; Phillips, S. T.; Whitesides, G. M. *Proc. Natl. Acad. Sci. U. S. A.* **2008**, *105*, 19606–19611.
(21) SENTINEL: Bioactive Paper Network http://www.bioactivepaper.ca/index.php?module=page&id=4000 (accessed Jan 31, 2014).
(22) Aikio, S.; Grönqvist, S.; Hakola, L.; Hurme, E.; Jussila, S.; Kaukoniemi, O.-V.; Kopola, H.; Känsäkoski, M.; Leinonen, M.; Lippo, S.; Mahlberg, R.; Peltonen, S.; Qvintus-Leino, P.; Rajamäki, T.; Ritschkoff, A.-C.; Smolander, M.; Vartiainen, J.; Viikari, L.; Vilkman, M. *Bioactive paper and fibre products: Patent and literary survey*; Oulu, Finland, 2006.
(23) Fenton, E. M.; Mascarenas, M. R.; López, G. P.; Sibbett, S. S. *ACS Appl. Mater. Interfaces* **2009**, *1*, 124–129.
(24) Njumbe Ediage, E.; Di Mavungu, J. D.; Goryacheva, I. Y.; Van Peteghem, C.; De Saeger, S. *Anal. Bioanal. Chem.* **2012**, *403*, 265–278.
(25) Ge, L.; Yan, J.; Song, X.; Yan, M.; Ge, S.; Yu, J. *Biomaterials* **2012**, *33*, 1024–1031.
(26) Zakir Hossain, S. M.; Ozimok, C.; Sicard, C.; Aguirre, S. D.; Ali, M. M.; Li, Y.; Brennan, J. D. *Anal. Bioanal. Chem.* **2012**, *403*, 1567–1576.
(27) Li, X.; Ballerini, D. R.; Shen, W. *Biomicrofluidics* **2012**, *6*, 011301.
(28) Lisowski, P.; Zarzycki, P. K. *Chromatographia* **2013**, *76*, 1201–1214.
(29) Abe, K.; Kotera, K.; Suzuki, K.; Citterio, D. *Anal. Bioanal. Chem.* **2010**, *398*, 885–893.
(30) Ge, L.; Wang, S.; Song, X.; Ge, S.; Yu, J. *Lab Chip* **2012**, *12*, 3150–3158.
(31) Liana, D. D.; Raguse, B.; Gooding, J. J.; Chow, E. *Sensors* **2012**, *12*, 11505–11526.
(32) Carrilho, E.; Phillips, S. T.; Vella, S. J.; Martinez, A. W.; Whitesides, G. M. *Anal. Chem.* **2009**, *81*, 5990–5998.
(33) Martinez, A. W.; Phillips, S. T.; Butte, M. J.; Whitesides, G. M. *Angew. Chem. Int. Ed. Engl.* **2007**, *46*, 1318–1320.
(34) Carrilho, E.; Martinez, A. W.; Whitesides, G. M. *Anal. Chem.* **2009**, *81*, 7091–7095.
(35) Wang, S.; Ge, L.; Song, X.; Yu, J.; Ge, S.; Huang, J.; Zeng, F. *Biosens. Bioelectron.* **2012**, *31*, 212–218.
(36) Songjaroen, T.; Dungchai, W.; Chailapakul, O.; Laiwattanapaisal, W. *Talanta* **2011**, *85*, 2587–2593.
(37) Määttänen, A.; Vanamo, U.; Ihalainen, P.; Pulkkinen, P.; Tenhu, H.; Bobacka, J.; Peltonen, J. *Sensors Actuators B Chem.* **2012**, *177*, 153–162.
(38) Govindarajan, A. V.; Ramachandran, S.; Vigil, G. D.; Yager, P.; Böhringer, K. F. *Lab Chip* **2012**, *12*, 174–181.
(39) Lafleur, L.; Stevens, D.; McKenzie, K.; Ramachandran, S.; Spicar-Mihalic, P.; Singhal, M.; Arjyal, A.; Osborn, J.; Kauffman, P.; Yager, P.; Lutz, B. *Lab Chip* **2012**, *12*, 1119–1127.
(40) Grinenval, E.; Nonglaton, G.; Vinet, F. *Appl. Surf. Sci.* **2014**, *289*, 571–580.
(41) Douvas, A.; Argitis, P.; Misiakos, K.; Dimotikali, D.; Petrou, P. S.; Kakabakos, S. E. *Biosens. Bioelectron.* **2002**, *17*, 269–278.
(42) Petrou, P. S.; Chatzichristidi, M.; Douvas, A. M.; Argitis, P.; Misiakos, K.; Kakabakos, S. E. *Biosens. Bioelectron.* **2007**, *22*, 1994–2002.
(43) Graber, D. J.; Zieziulewicz, T. J.; Lawrence, D. a.; Shain, W.; Turner, J. N. *Langmuir* **2003**, *19*, 5431–5434.
(44) Zakir Hossain, S. M.; Luckham, R. E.; Smith, A. M.; Lebert, J. M.; Davies, L. M.; Pelton, R. H.; Filipe, C. D. M.; Brennan, J. D. *Anal. Chem.* **2009**, *81*, 5474–5483.
(45) Li, X.; Tian, J.; Garnier, G.; Shen, W. *Colloids Surf. B. Biointerfaces* **2010**, *76*, 564–570.
(46) *Printed Organic and Molecular Electronics*; Gamota, D.; Brazis, P.; Kalyanasundaram, K.; Zhang, J., Eds.; Springer US: Boston, MA, 2004.
(47) Birkenshaw, J. *Printed Electronics (Pira on printing)*; Leatherhead, Surrey, UK, 2004; pp. 1–80.
(48) Abe, K.; Suzuki, K.; Citterio, D. *Anal. Chem.* **2008**, *80*, 6928–6934.
(49) Jarujamrus, P.; Tian, J.; Li, X.; Siripinyanond, A.; Shiowatana, J.; Shen, W. *Analyst* **2012**, *137*, 2205–2210.
(50) Kong, F.; Hu, Y. F. *Anal. Bioanal. Chem.* **2012**, *403*, 7–13.
(51) Credou, J.; Berthelot, T. Method for photo-immobilizing biomolecules on a cellulose carrier. EP14157944, March 2014.
(52) Credou, J.; Volland, H.; Berthelot, T. *J. Mater. Chem. B* **2014**.Submitted
(53) Fridley, G. E.; Holstein, C. A.; Oza, S. B.; Yager, P. *MRS Bull.* **2013**, *38*, 326–330.
(54) Khreich, N.; Lamourette, P.; Boutal, H.; Devilliers, K.; Créminon, C.; Volland, H. *Anal. Biochem.* **2008**, *377*, 182–188.
(55) Khreich, N.; Lamourette, P.; Renard, P.-Y.; Clavé, G.; Fenaille, F.; Créminon, C.; Volland, H. *Toxicon* **2009**, *53*, 551–559.
(56) Johansson, L.-S.; Campbell, J. M. *Surf. Interface Anal.* **2004**, *36*, 1018–1022.
(57) Noh, H.; Phillips, S. T. *Anal. Chem.* **2010**, *82*, 4181–4187.
(58) Hermanson, G. T. *Bioconjugate techniques*; Academic Press: London, 2008.
(59) Makky, A.; Berthelot, T.; Feraudet-Tarisse, C.; Volland, H.; Viel, P.; Polesel-Maris, J. *Sensors Actuators B Chem.* **2012**, *162*, 269–277.
(60) Fujifilm. Dimatix Materials Printer DMP-2831 http://www.fujifilmusa.com/products/industrial_inkjet_printheads/deposition-products/dmp-2800/#overview (accessed Jun 4, 2014).
(61) Denneulin, A.; Bras, J.; Carcone, F.; Neuman, C.; Blayo, A. *Carbon N. Y.* **2011**, *49*, 2603–2614.
(62) Blayo, A.; Pineaux, B. In *Proceedings of the 2005 joint conference on Smart objects and ambient intelligence innovative context-aware services: usages and technologies - sOc-EUSAI '05*; ACM Press: New York, NY, USA, 2005; pp. 27–30.
(63) Roy, D.; Semsarilar, M.; Guthrie, J. T.; Perrier, S. *Chem. Soc. Rev.* **2009**, *38*, 2046–2064.

(64) Klemm, D.; Philipp, B.; Heinze, T.; Heinze, U.; Wagenknecht, W. *Comprehensive Cellulose Chemistry Volume 2 Functionalization of Cellulose*; WILEY-VCH: Weinheim, 1998; Vol. 2.
(65) PIKE Technologies. *MIRacle ATR; Product Data Sheet*; Madison, WI, USA, 2014.
(66) Määttänen, A.; Ihalainen, P.; Bollström, R.; Toivakka, M.; Peltonen, J. *Colloids Surfaces A Physicochem. Eng. Asp.* **2010**, *367*, 76–84.
(67) Stevens, D. Y.; Petri, C. R.; Osborn, J. L.; Spicar-Mihalic, P.; McKenzie, K. G.; Yager, P. *Lab Chip* **2008**, *8*, 2038–2045.

Chapter 5 One-step and eco-friendly modification of cellulose membranes by polymer grafting

The non-sensing cellulose parts of paper-based biosensing devices may need to improve or acquire properties such as hydrophobicity, antifouling property or flow rate regulation ability. Hence, cellulose membranes need to be functionalized. In addition, the applied modification procedure should abide by the economic and ecological objectives aforementioned.

By introducing lots of new functional moieties in only one reaction, polymer grafting enables to rapidly alter the physical and chemical properties of cellulose and to increase its functionality without destroying its many appealing intrinsic properties [75]. Polymer grafting to cellulose (also called cellulose graft copolymerization [75]) is usually performed in heterogeneous conditions, *i.e.* on a solid cellulose substrate with the monomer being in solution. Among all existing methodologies, “grafting-from” free radical graft copolymerization of cellulose with acrylic compounds is the most widely employed method for modifying cellulose by polymer grafting [75–83]. Consequently, the work presented thereafter falls within this approach.

Contents

1. INTRODUCTION 89

2. EXPERIMENTAL 90

2.1. REAGENTS AND REACTION MATERIALS 90
2.2. CHARACTERIZATION MATERIALS 90
2.3. CELLULOSE GRAFT COPOLYMERIZATION 90
2.3.1. Dipping procedure 90
2.3.2. Printing procedure 91
2.3.2.1. Ink formulation 91
2.3.2.2. Inkjet printing and graft copolymerization 91

3. RESULTS AND DISCUSSION 91

3.1. ONE-STEP CELLULOSE GRAFT COPOLYMERIZATION 91
3.1.1. Molecular level 91
3.1.2. Surface chemical analysis 92
3.1.3. Surface morphological structure 92
3.2. SPATIALLY CONTROLLED CELLULOSE GRAFT COPOLYMERIZATION 94
3.2.1. Ink behavior 95
3.2.2. Surface chemical analysis 95
3.2.3. Surface morphological structure 95
3.3. INKJET PRINTING OF COMPLEX PATTERNS 95

4. CONCLUSION 97

REFERENCES 97

Credou, J.; Faddoul, R.; Berthelot, T.

One-step and eco-friendly modification of cellulose membranes by polymer grafting.

Biomacromolecules 2014. Submitted.

Cellulose sheets were grafted with several acrylic polymers, first globally through a dipping procedure and then locally by inkjet printing.

Biomacromolecules

ACSPublishing

ARTICLE

One-step and eco-friendly modification of cellulose membranes by polymer grafting

Cite this: DOI: 10.1039/xoxxoooooox

Julie Credou, Rita Faddoul and Thomas Berthelot*,

Received ooth July 2014,
Accepted ooth July 2014

DOI: 10.1039/xoxxoooooox

pubs.acs.org/Biomac

The increasing environmental awareness has stimulated the use of bio-based materials and processes. As an affordable and sustainable biopolymer, cellulose is an ideal engineering material. Beyond paper, cellulose finds applications in many areas such as composites, electronics and drug delivery. To fulfil these new functions, cellulose needs to acquire new properties, what is commonly done by graft polymerization of acrylic compounds. While cellulose modification is usually performed through complex and expensive procedures, the diazonium-based polymer grafting procedure presented here was performed in water, at room temperature, in a short single step. Cellulose sheets have been successfully grafted with several acrylic polymers, first globally through a dipping procedure and then locally by inkjet printing. The process developed herein is simple, eco-friendly and mostly time and cost-saving. More generally, it is a powerful tool for easy, robust and patterned graft copolymerization of cellulose sheets with various acrylic monomers and even bio-based monomers.

1. Introduction

The increasing environmental awareness and the growing will for sustainable technologic development have stimulated the use of biosourced materials and the development of bio-based processes worldwide. Besides, the current economic global issues have incited the search for cost-saving approaches [1,2]. As the main material of plant cell walls, cellulose is the largest form of worldwide biomass (about 1.5 x 10^{12} tons per year) [3]. This biopolymer is therefore the most abundant organic raw material on earth [1]. In addition to its large bioavailability, good biodegradability and biocompatibility, its high functionality and relatively high chain stiffness make cellulose an extremely interesting polymer [4–8]. Moreover, it is insoluble in most usual organic solvents and therefore is considered an ideal structural engineering material [7]. It swells but does not dissolve in water, hence enabling aqueous fluids and their contained components to penetrate within the fibers matrix and to wick by capillarity with no need for any external power source. In addition, cellulose sheets are available in a broad range of thicknesses and well-defined pore sizes, easy to store and handle, and lastly safely disposable [9–11]. Furthermore, the recent impetus given to paper-based microfluidics by American, Canadian and Finnish research teams [12–14] has resulted in the development of new paper-based devices for diagnostics, microfluidics, and electronics [7,15].

Beyond paper and cardboard, cellulose thus finds applications in many diverse areas such as composite materials, textiles, drug delivery systems and personal care products [2]. In order to increase its functionality and the scope of its use, modifications of cellulose biofibers are required. By introducing lots of new functional moieties in one reaction, graft polymerization enables to rapidly alter the physical and chemical properties of cellulose and increase its functionality without destroying its many appealing intrinsic properties [2]. Many properties can be improved or added to cellulose by polymer grafting including hydrophobicity, oil repellency, antimicrobial activity, heat resistance and electrical properties, dimension stability, resistance to abrasion and wear, wrinkle recovery. These additional features allow cellulose to be used for advanced material applications [4].

Cellulose graft copolymerization is usually performed by free radical polymerization of vinylic compounds in heterogeneous conditions, *i.e.* on a solid cellulose substrate with the monomer being in solution. Grafted side chains are initiated by radical formation on the cellulose backbone. This radical may originate from the homolytic bond cleavage within the glucose unit caused by high-energy irradiation for example, from the decomposition of a functional group such as peroxide, or from a radical transfer reaction initiated by a radical formed outside the cellulose backbone during a redox reaction [2,16]. There are three kinds of approaches to covalent attachment of polymers to surfaces: (i) the ‘‘grafting-to’’ method, where a polymer is coupled with the functional moieties from cellulose backbone, (ii) the ‘‘grafting-from’’ method, where copolymer chains grow from initiating sites on the cellulose backbone, and (iii) the ‘‘grafting-through” method, where the cellulose bares a polymerizable group, and hence acts as a macromonomer with

which a smaller monomer copolymerizes. Among these three methodologies, the ''grafting-from'' approach is the most commonly used procedure [2,4]. Consequently, the work presented here focuses on the widely employed "grafting-from" free radical graft copolymerization of cellulose with acrylic compounds.

Many studies have reported cellulose graft copolymerization with acrylic compounds [17–23]. Cellulose modifications have usually been performed under harsh conditions, in organic solvent or with highly toxic compounds so far [17–19,21]. Besides graft polymerization most often implements long-lasting, complex and / or expensive procedures such as ATRP (Atom Transfer Radical Polymerization) [17], RAFT (Reversible Addition-Fragmentation chain Transfer polymerization) [20] and gamma irradiation initiation step [18,20,21]. To the best of our knowledge, no cellulose modification has been done in a rather short one-step reaction and under soft conditions, *i.e.* in water and at room temperature.

Herein, a simple, fast, low-cost and eco-friendly way for graft copolymerization of cellulose sheets under soft and biocompatible conditions is presented. The cellulose modifications were performed in a single step, in water and at room temperature, in one hour or less. The cellulose modification pathway consisted in an aryldiazonium-based polymerization of acrylic monomers (GraftFast™) [24–26]. Two different dispensing methods were employed to impregnated cellulose sheets with copolymerization reaction mixture. Firstly, dipping was performed. Though ecologically friendly, the process produced lots of matter wastage and was therefore not economically friendly. Thus, inkjet printing was further implemented to reduce this wastage by localizing the polymerization mixture onto specific areas of the substrate. Moreover, this versatile dispensing method is considered as a competitive method for patterning flexible or rigid substrates. It is a fast, cost-effective, additive, biocompatible and environmentally friendly method for depositing thin or thick films (0.8 - 20.0 µm) according to complex patterns [27]. Cellulose paper sheets have been successfully copolymerized (or printed and copolymerized) without damaging their intrinsic properties or even their visual aspect. Several acrylic monomers were compared. Furthermore, the inkjet printing process previously described [28] was proved to be an efficient method allowing the patterning of cellulose tapes with grafted polymers.

2. Experimental

2.1. Reagents and reaction materials

4-nitrobenzenediazonium tetrafluoroborate, acrylic acid (AA), 2-hydroxyethyl methacrylate (HEMA), methyl methacrylate (MMA), poly(ethylene glycol) dimethacrylate (PEGDMA), L-ascorbic acid (Vitamin C), tris(bipyridine)ruthenium(II) chloride ($[Ru(bpy)_3]Cl_2$) and polyacrylic acid (M_w = 130 000 g mol^{-1}) were purchased from Sigma-Aldrich (St Louis, MO, USA) and used as received. Water used in all experiments was purified by the Milli-Q system (Millipore, Brussels, Belgium). CF1 cellulose paper was from Whatman (Maidstone, Kent, UK). In the first set of experiments, substrates were dipped into polymerization solutions. In the second one, the polymerization solution was printed onto substrates using a laboratory piezoelectric drop-on-demand inkjet printer Dimatix Materials Printer DMP-2831 (Fujifilm, Santa Clara, CA, USA) with 10 pL nominal drop volume cartridge. Irradiations were carried at 453 nm at room temperature with a Golden Dragon Plus, deep blue LED (OSRAM Opto Semiconductors, Sunnyvale, CA, USA).

2.2. Characterization materials

Infrared (IR) spectra of the various substrates were recorded on a Vertex 70 FT-IR spectrometer (Bruker, Billerica, MA, USA) controlled by OPUS software (Bruker, Billerica, MA, USA) and fitted with MIRacle™ ATR (Attenuated Total Reflectance) sampling accessory (PIKE Technologies, Madison, WI, USA). The ATR crystal type was single reflection diamond/ZnSe crystal plate. The FT-IR detector was MCT working at liquid nitrogen temperature. Acquisitions were obtained at 2 cm^{-1} resolution after 256 scans.

Microstructure and surface morphology of samples were examined by a JSM-5510LV (JEOL, Tokyo, Japan) scanning electron microscope (SEM) after gold coating (K575X Turbo Sputter Coater (Quorum Technologies Ltd, Ashford, Kent, UK), working at 15 mA for 20 seconds). The images were acquired at various magnifications ranging from 100× to 3 000×. The acceleration voltage and working distance were 4 kV and 17 mm, respectively. Images were acquired applying the secondary electron detector.

Surface roughness, Ra, of pristine and copolymerized cellulose substrates was measured with an AlphaStep® D-120 Stylus Profiler (KLA-Tencor, Milpitas, CA, USA). Measurements were performed along a line of 1 mm long, with a stylus force of 1 mg and at a speed of 0.05 mm s^{-1}. The same profiler was used to measure printed polyacrylic acid films thickness and roughness.

Ink viscosity was measured with a MCR 102 Rheometer (Anton Paar, Ashland, VA, USA). Cone-plane geometry was used at a shear rate varying from 100 to 5 000 s^{-1} and at a 24°C temperature. Gap distance was equal to 101 µm. Geometry diameter and angle were equal to 5 cm and 1°, respectively.

2.3. Cellulose graft copolymerization

2.3.1. Dipping procedure

Cellulose modification was performed in water, at open air and room temperature. The 2-mL aqueous reaction mixture contained 0.10 mmol of diazonium salt (23.69 mg; 1.0 eq.), 2 mmol of monomer (20 eq.) and 0.01 mmol of L-ascorbic acid (1.76 mg; 0.1 eq.). Components were first separately dissolved in water and then mixed under stirring in the following order: (i) monomer, (ii) diazonium salt, and (iii) L-ascorbic acid. A CF1 paper sheet (4 cm^2) was dipped into this freshly prepared mixture and left to incubate for one hour in a plastic box. The membrane obtained was rinsed and submitted to ultrasonic

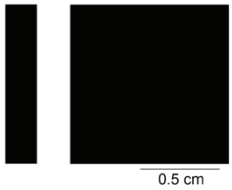

Figure 1. Scheme of the printed pattern.

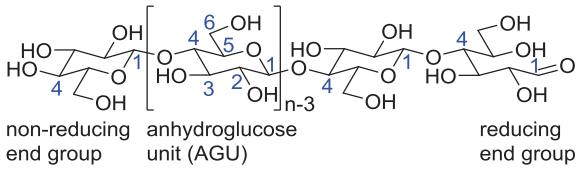

Figure 2. Cellulose molecular structure.

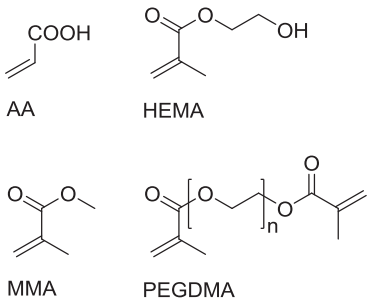

Figure 3. Molecular formulae of the monomers

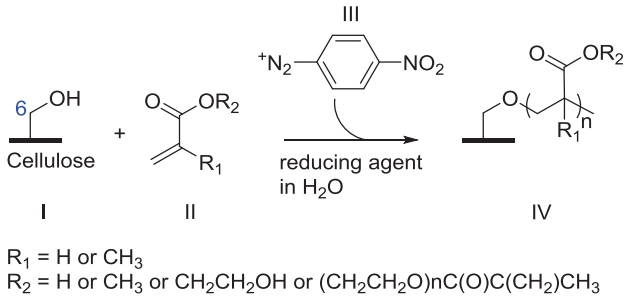

Figure 4. Cellulose graft copolymerization with acrylic monomers. Aryldiazonium (III) is reduced and reacts with cellulose (I) in an aqueous medium to initiate the grafting and polymerization of the monomer (II) and give a polymer-grafted cellulose membrane (IV).

treatment in order to discard any ungrafted matter. A first wash was made with water, a second with ethanol. It was finally dried for 15 minutes at 60°C in an air oven. Several acrylic polymers were thus grafted to cellulose paper. The corresponding monomers were acrylic acid (AA), 2-hydroxyethyl methacrylate (HEMA), methyl methacrylate (MMA) and poly(ethylene glycol) dimethacrylate (PEGDMA). All the so functionalized papers were then analyzed using infrared spectroscopy in order to point out the carbonyl moieties brought by the polymerization. Their microstructure was pictured by SEM imaging. Their surface roughness was measured with a profiler.

2.3.2. Printing procedure

2.3.2.1. Ink formulation

Ink formulation was inspired from our previous work for flexible electronic interconnects [28]. First of all, an aqueous mixture of acrylic acid (AA) monomer and polyacrylic acid (PAA) (13 wt. % of the 14.6 M commercial stock solution and 2.5 wt. % of a 1 wt. ‰ aqueous stock solution, respectively) was prepared. Afterwards, 0.8 wt. % of solid 4-nitrobenzenediazonium tetrafluoroborate (NBD) was added to the previous solution. Finally, tris(bipyridine)ruthenium(II) chloride ($[Ru(bpy)_3]Cl_2$) (1.3 wt. % of a 0.02 M aqueous stock solution) was added to the ink. Hence, the final ink composition was: 2 M of AA, traces of PAA, 0.03 M of NBD and to 2.5 x 10^{-4} M of $[Ru(bpy)_3]Cl_2$.

2.3.2.2. Inkjet printing and graft copolymerization

Acrylic acid aqueous solutions were printed onto cellulose substrates using the Dimatix inkjet printer. Nozzle diameter was 21.5 µm and nominal drop volume was 10 pL. Printing tests were performed at 30 V voltage with 15 µm drop spacing. The printed pattern (Figure 1) consisted of two solid forms of 1 cm x 1 cm and 1 cm x 0.2 cm dimensions. The pattern resolution was equal de 1693 dpi (dot per inch). Printings made of 1, 3 and 6 layers were compared. The patterned surfaces were irradiated at 453 nm (0.75 W cm^{-2}) during 15 minutes (about 675 J cm^{-2}) for inducing polymerization. After irradiation, printed substrates were dipped in distilled water during 5 hours to remove the physisorbed matter. They were finally dried for 60 minutes at 45°C in an air oven.

3. Results and discussion

3.1. One-step cellulose graft copolymerization

3.1.1. Molecular level

Whatman CF1 paper was selected because it is a high quality paper, made of quite pure and clean cellulose (Figure 2), whose thickness and wicking properties are rather uniform (11 µm surface pore size and 176 µm thick). Cellulose is a natural biopolymer made up of glucose units (Figure 2). It is the simplest polysaccharide since it is composed of a unique monomer (glucose) which binds to its neighbors by a unique type of linkage (β-1,4 glycosidic bond resulting in acetal function) [1]. Hydroxyl groups in glucose units are responsible for cellulose chemical activity [2]. Among the three hydroxyl groups in each glucose residue, the hydroxyl at 6-position (primary one) is the most reactive site [1,2].

Cellulose paper sheets have been copolymerized in soft conditions, in a single step and after only one hour incubation. Several acrylic polymers were grafted. The molecular structures of the corresponding monomers are shown in Figure 3. The graft polymerization pathway consisted in an aryldiazonium-based surface chemistry (Figure 4) [24,26]. Diazonium salts are known to be free radical polymerization initiators [24]. Acrylic

graft copolymerization to the pre-existing polymeric cellulose backbone was therefore achieved by free radical graft

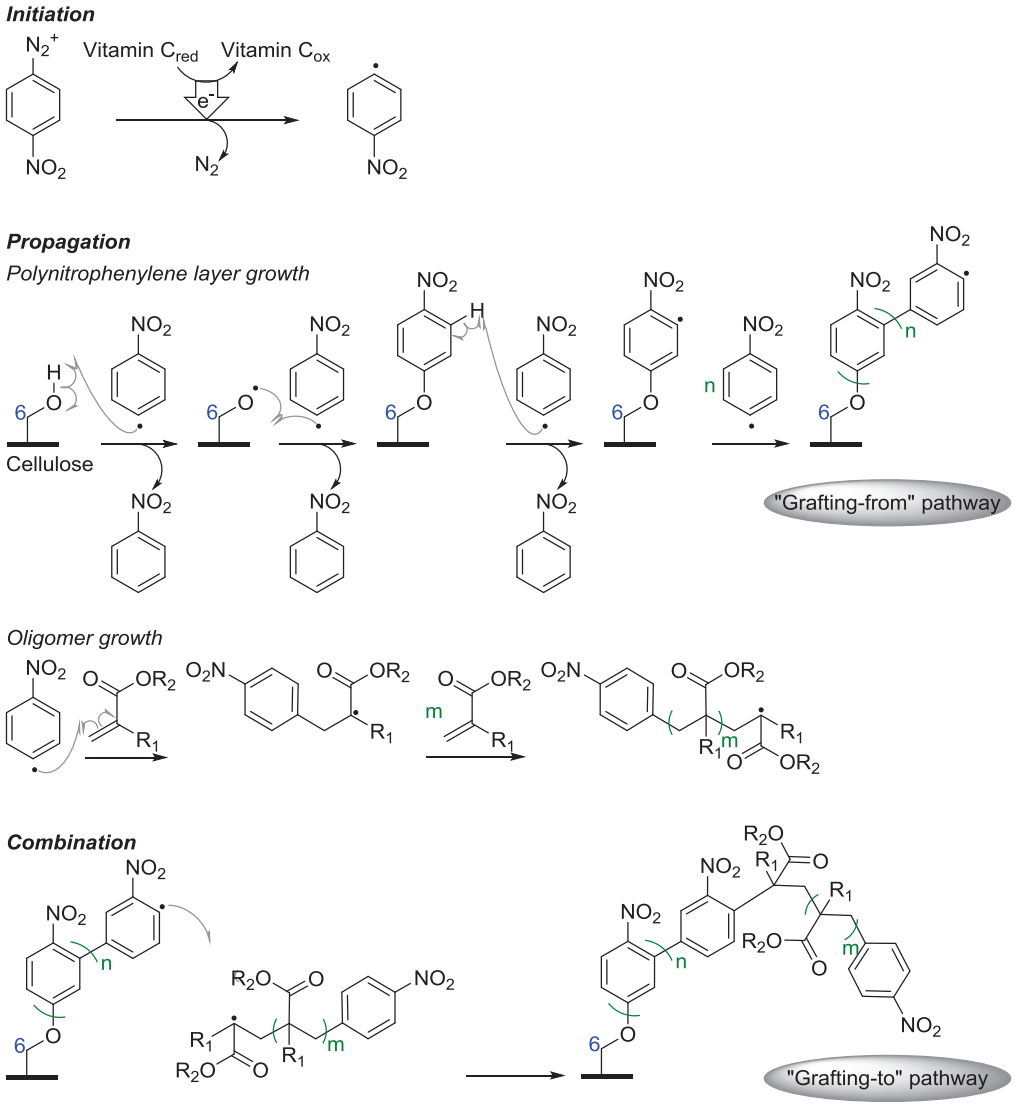

Figure 5. A proposed mechanism of free radical grafting of acrylic polymers onto cellulose.

copolymerization. According to the previously published work by Garcia *et al.* [28], both "grafting-from" and "grafting-to" polymerization pathway are actually involved in the polymer grafting process (Figure 5) [2,29]. Reaction took place in water at room temperature with a biological reducing agent (L-ascorbic acid, also known as vitamin C), thereby resulting in a biocompatible process. Cellulose sheets have been successfully grafted with the different polymers and characterized by several analytical techniques in order to assess the resulting surface chemical composition and morphological structure.

3.1.2. Surface chemical analysis

The outer surface layers of paper substrates were chemically analyzed by ATR-FTIR, thereby displaying the aforementioned bulk molecular structures. According to its layout, ATR-FTIR allows the identification of chemical bonds within 2 µm deep subsurface layers [30]. All papers are mainly composed of a cellulosic backbone and therefore the IR signals for its typical bond vibrations are shared by every spectrum shown. Figure 6 displays these common bands attributable to O-H, C-H, C-C, C-O and O-C-O stretching vibrations. As expected, polymer-grafted cellulose papers manifest additional peaks (1725 ± 5 cm^{-1}) attributable to C=O stretching vibrations from ester moieties of the grafted polymer. Their intensity depends on the monomer used and resulting grafted polymer. They stand in the following order: AA < HEMA < MMA < PEGDMA. On one hand, PEGDMA is predominant because it is a diacrylic monomer. On another hand, since cellulose is a porous material these intensities cannot be directly related to amount and thickness of grafted polymer. More investigations should be conducted in order to analyze surface morphological structure.

3.1.3. Surface morphological structure

Beyond the chemical differences in molecular structure, the various grafted polymers introduced physical and morphological differences between the cellulose substrates.

Thus, in order to quantify the variation in surface morphological structure, topological analysis was conducted by

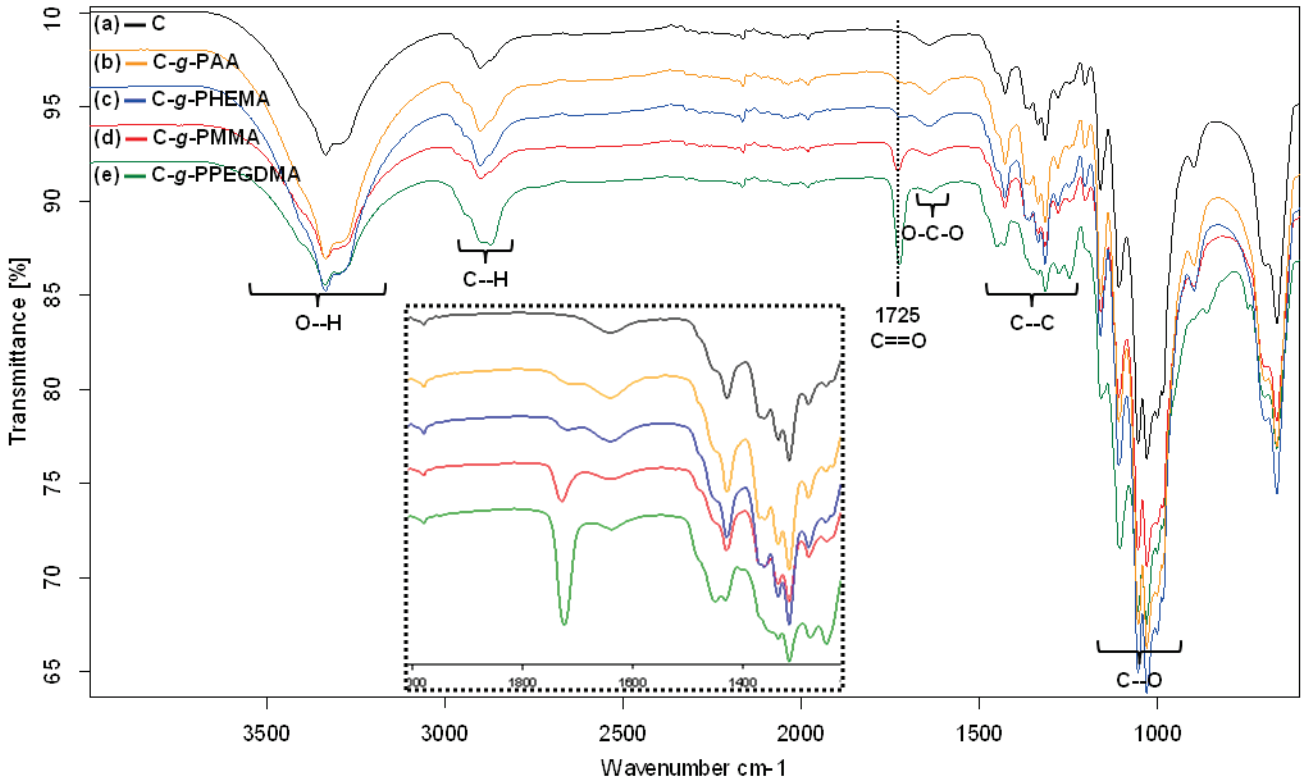

Figure 6. IR spectra of paper substrates after a 1-hour dipping. (a) is spectrum from pristine cellulose sheet, (b) from cellulose copolymerized with acrylic acid (AA) monomer, (c) with 2-hydroxyethyl methacrylate (HEMA), (d) with methyl methacrylate (MMA) and (e) with poly(ethylene glycol) dimethacrylate (PEGDMA). All spectra have several bands in common which correspond to O-H, C-H, C-C, C-O and O-C-O stretching vibrations. The C=O stretching vibrations specific to grafted polymers are labeled.

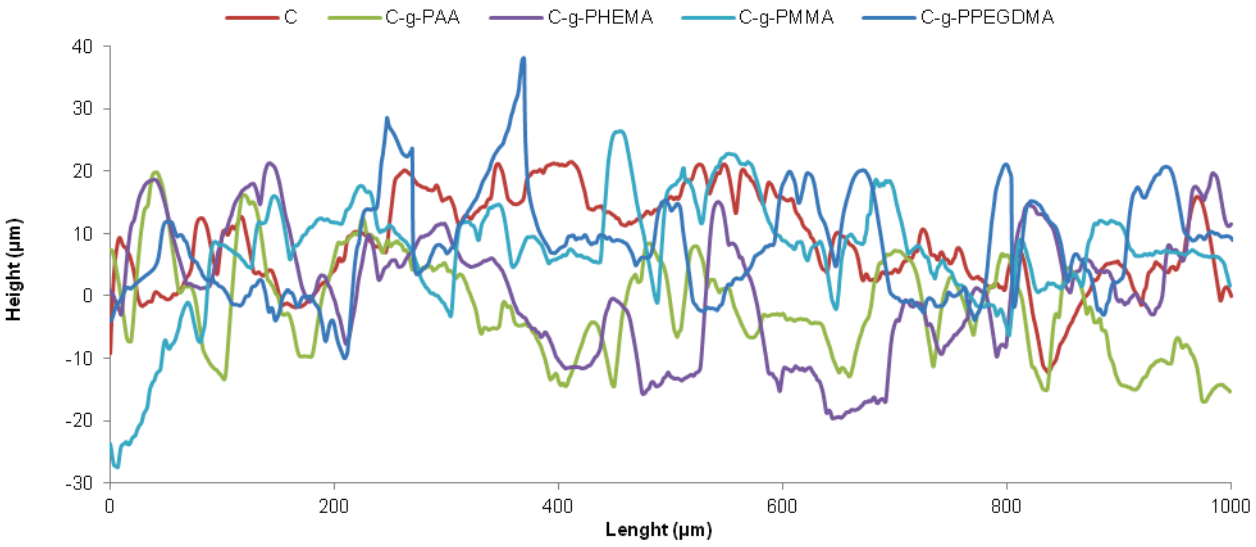

Figure 7. Line profiles of pristine cellulose (C) and polymer-grafted cellulose substrates (C-*g*-polymer).

measuring substrates' roughness (Ra). Morphology and microstructure of the various polymer-grafted cellulose substrates was visualized by SEM imaging. Visual global evaluation was also performed.

Line profiles of pristine cellulose substrate and polymer-grafted cellulose substrates were quite similar (see Figure 7). Substrates were rather heterogeneous, rough, and displays numerous and wide pores. Surface roughness (Ra) values confirmed this high

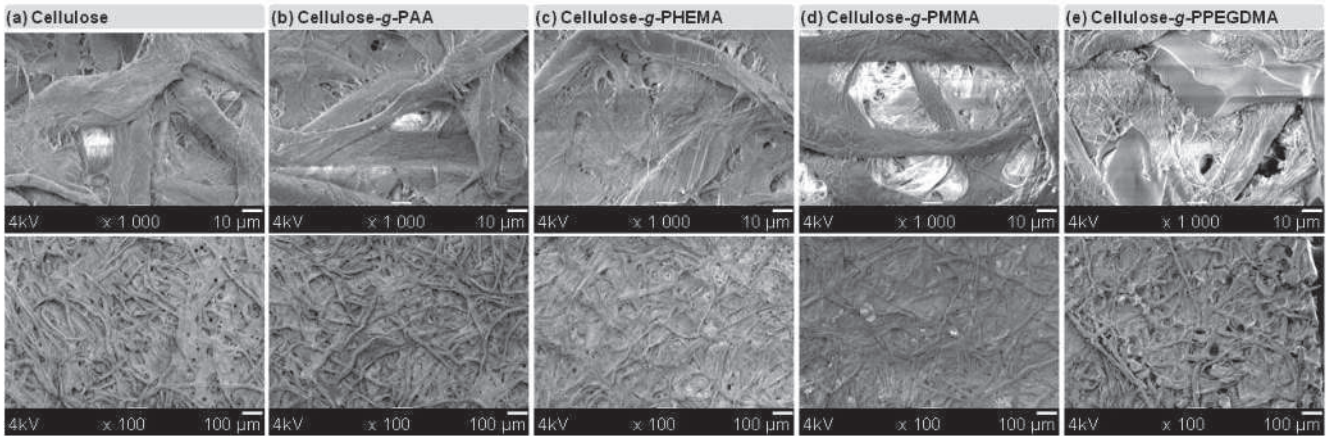

Figure 8. SEM micrographs of (a) pristine cellulose sheet, (b) cellulose copolymerized with acrylic acid (AA), (c) with 2-hydroxyethyl methacrylate (HEMA), (d) with methyl methacrylate (MMA) and (e) with poly(ethylene glycol) dimethacrylate (PEGDMA).

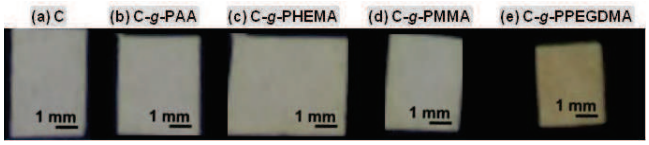

Figure 9. Photographs of (a) pristine cellulose sheet, (b) cellulose copolymerized with acrylic acid (AA), (c) with 2-hydroxyethyl methacrylate (HEMA), (d) with methyl methacrylate (MMA) and (e) with poly(ethylene glycol) dimethacrylate (PEGDMA).

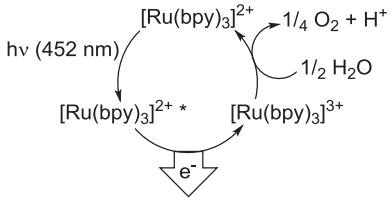

Figure 10. Photoactivated reducing behavior of $[Ru(bpy)_3]^{2+}$.

roughness and were also quite similar. Hence, the average value was 6.45 ± 0.25 µm.

Pores sizes and arrangement pictured by SEM imaging (Figure 8) were consistent with the previous statements. Pristine cellulose substrate and polymer-grafted cellulose substrates looked quite similar. They displayed numerous and wide surface pores. However, differences could be noticed between the various polymer-grafted cellulose substrates. Micrographs revealed that the grafted polymers filled cellulose surface pores, as expected. Progression of the filling extent matched the progression previously observed with IR peak intensities: AA < HEMA < MMA < PEGDMA. Therefore, these intensities could actually be related to an amount of grafted polymer.

Although the microstructures of the several cellulose substrates were different, the various substrates visually appeared quite similar. Except for cellulose-*g*-PPEGDMA which is slightly colored, grafted cellulose substrates were white and displayed no visual difference with pristine cellulose (Figure 9). Cellulose molecular, physical and micro-morphological properties can therefore be modified without impact on the visual aspect of paper.

3.2. Spatially controlled cellulose graft copolymerization

Though the aforementioned process was ecologically friendly, the dipping procedure implemented was not economically friendly. Indeed, a large part of the reaction mixture was not involved in the cellulose graft copolymerization but in the homopolymerization of the added monomer. In order to reduce this matter wastage, the polymerization was further localized onto selected specific areas of the substrate by means of inkjet printing. Printing is a versatile technique allowing the deposition of variable kinds of solutions (biomolecules, polymers, solvents, metals) onto different types of substrates (cellulose, polymer, glass, silicon) and according to any design desired [31,32]. This is fast dispensing process enabling low-cost, high throughput fabrication [32]. Moreover it is regarded as an environmentally friendly process and therefore a very attractive approach regarding the economic and ecological goals.

However, the previous reaction mixture was not printable as was. The polymerization trigger had to stay inactive as long as it was in cartridge otherwise homopolymerization would have taken place before printing. Thus, vitamin C was exchanged for a photoactivated reducing agent: $[Ru(bpy)_3]^{2+}$. $[Ru(bpy)_3]^{2+}$ strongly absorbs at 452 ± 3 nm in aqueous medium [33]. In presence of oxidative quenchers such as aryldiazonium salt, the excited $[Ru(bpy)_3]^{2+}$ * relaxed to $[Ru(bpy)_3]^{3+}$ while transferring an electron to the aryldiazonium, thereby triggering cellulose graft copolymerization. $[Ru(bpy)_3]^{3+}$ is a powerful oxidant (1.29 V *vs.* SCE = Standard Calomel Electrode, in CH_3CN) and would therefore be able to spontaneously oxidize water and return to its original $[Ru(bpy)_3]^{2+}$ form (Figure 10) [34–36].

Reaction was still performed in water at room temperature. Cellulose sheets were successfully printed with a photoactive

ink containing acrylic acid. Cellulose was further copolymerized by irradiating the printed pattern. Resulting substrates were characterized by several analytical techniques

Figure 11. Photographs of printed solid forms on cellulose substrates after irradiation and rising steps: (a) 1-pass printing, (b) 3-pass printing and (c) 6-pass printing.

Table 1. Raw cellulose substrate roughness and printed polyacrylic acid films roughness and thickness.

	Roughness (µm)		Thickness (µm)	
	Before rinsing	After rinsing	Before rinsing	After rinsing
Cellulose	7 ± 1			
1-pass printed cellulose	9 ± 1	7 ± 1	16 ± 3	
3-pass printed cellulose	9 ± 1	8 ± 2	22 ± 4	11 ± 2
6-pass printed cellulose	14 ± 3	9 ± 1	36 ± 9	20 ± 8

in order to assess their surface chemical composition and morphological structure.

3.2.1. Ink behavior

Before printing, ink rheological behavior was analyzed in order to check the printability of the prepared solution. To be inkjet printable, a fluid should be Newtonian with a viscosity in the range of 1 to 10 mPa s [37]. The formulated ink showed a Newtonian behavior with a constant viscosity of 3.2 mPa s at shear rates varying from 100 to 5 000 s^{-1}. Shear stress varied linearly, from 0.3 to 16.2 Pa, as a function of shear rate (100 to 5 000 s^{-1}). The temperature was maintained at 24°C during the whole measurements.

Then, inkjet printing was performed onto cellulose substrates. 1, 3 and 6 printing passes of acrylic acid aqueous ink were printed onto cellulose according to the pattern displayed in Figure 1. Patterned surfaces were further irradiated, rinsed and dried. Photographs of the resulting printed forms are shown Figure 11. When only 1 (Figure 11a) and 3 (Figure 11b) printing passes are deposited, both solid forms are well defined. However, when 6 printing passes are performed (Figure 11c), the larger solid form is not homogeneous. This is probably due to the high ejected ink volume compared to the absorption capability of cellulose fibers [38].

3.2.2. Surface chemical analysis

Figure 12 shows IR spectra of raw cellulose and cellulose printed and copolymerized with acrylic acid. New peaks appeared on cellulose substrates at 1350, 1530 and 1710-1730 cm^{-1} after light induced polymerization of acrylic acid. Peaks around 1530 and 1350 cm^{-1} are attributable to stretching vibrations of nitrophenyl groups from NBD derivatives. Peaks around 1710 – 1730 cm^{-1} are related to the stretching vibrations of carboxylic groups (COOH). Peaks intensity was proportional to the number of passes. After rinsing in distilled water during 5 hours, peaks attributed to NBD could not be identified anymore. Furthermore, even though the carboxylic peaks (1728 cm^{-1}) were still easy to discern, their intensity had decreased. This phenomenon is partially caused by the $COOH/COO^-$ equilibrium resulting from the sustained exposure to distilled water. No copolymer's peak was observed anymore on the spectra corresponding to 1-pass printing. This could be explained by an ejected ink volume too small to allow surface polymerization of acrylic acid.

3.2.3. Surface morphological structure

Printing and graft copolymerization of cellulose with acrylic acid monomer resulted in the formation of a thin film of polyacrylic acid onto cellulose sheet surface. Those films' thicknesses and roughnesses are displayed in Table 1. Roughness values were compared to raw cellulose one. Thus, printing and graft copolymerization made roughness increase from 7 µm to 14 µm (6-pass printing). Grafted films thicknesses varied from 16 µm for 1-pass printing to 36 µm for 6-pass printing. Washing printed substrates with distilled water further allowed removing the physisorbed material, thereby inducing thickness and roughness decrease. Besides, the film resulting from 1-pass printing completely vanished after rinsing. In this case, film thickness could not be measured and the film roughness was equal to raw cellulose one. This might stem from the complete absorption of the small ejected volume of ink by cellulose fibers and pores, hence inhibiting light induced polymerization of acrylic acid onto cellulose surface. Indeed, the grafting efficiency depends, inter alia, on the photoinitiator and the monomer concentrations [39]. Thus, the ejected volume could be a determining factor outlining the thickness of the grafted polymer as well as the polymerization efficiency.

In order to further investigate films morphology, scanning electron microscopy was performed. Surface micrographs of raw cellulose and printed plus copolymerized cellulose are shown in Figure 13. Firstly, raw cellulose and 1-pass printed cellulose looked almost identical. One may suggest that most of the ejected ink had been absorbed by the cellulose surface pores. Then, 3-pass printed and 6-pass printed cellulose appeared quite different from raw cellulose. Fewer pores are observed on the surface which seems more homogeneous, mainly after the 6-pass printing. This results are consistent with Määttänen *et al.* findings [40] which demonstrated that ink is quickly and completely absorbed into the depth of porous surfaces. Thus, in order to enhance ink deposit onto the substrate surface more passes should be performed.

3.3. Inkjet printing of complex patterns

As previously mentioned, one major advantage of inkjet printing dispensing method is the freedom in design of the printed pattern. This advantage was illustrated here by printing a copolymerization mixture according to the nature of the monomer and the resulting polymer grafted to cellulose. Therefore, acrylic acid aqueous ink was printed (6-pass

printing) onto cellulose according to a pattern drawing the abbreviation PAA (Figure 14a). Patterned surface was further irradiated, rinsed and dried. Photograph of the resulting printed

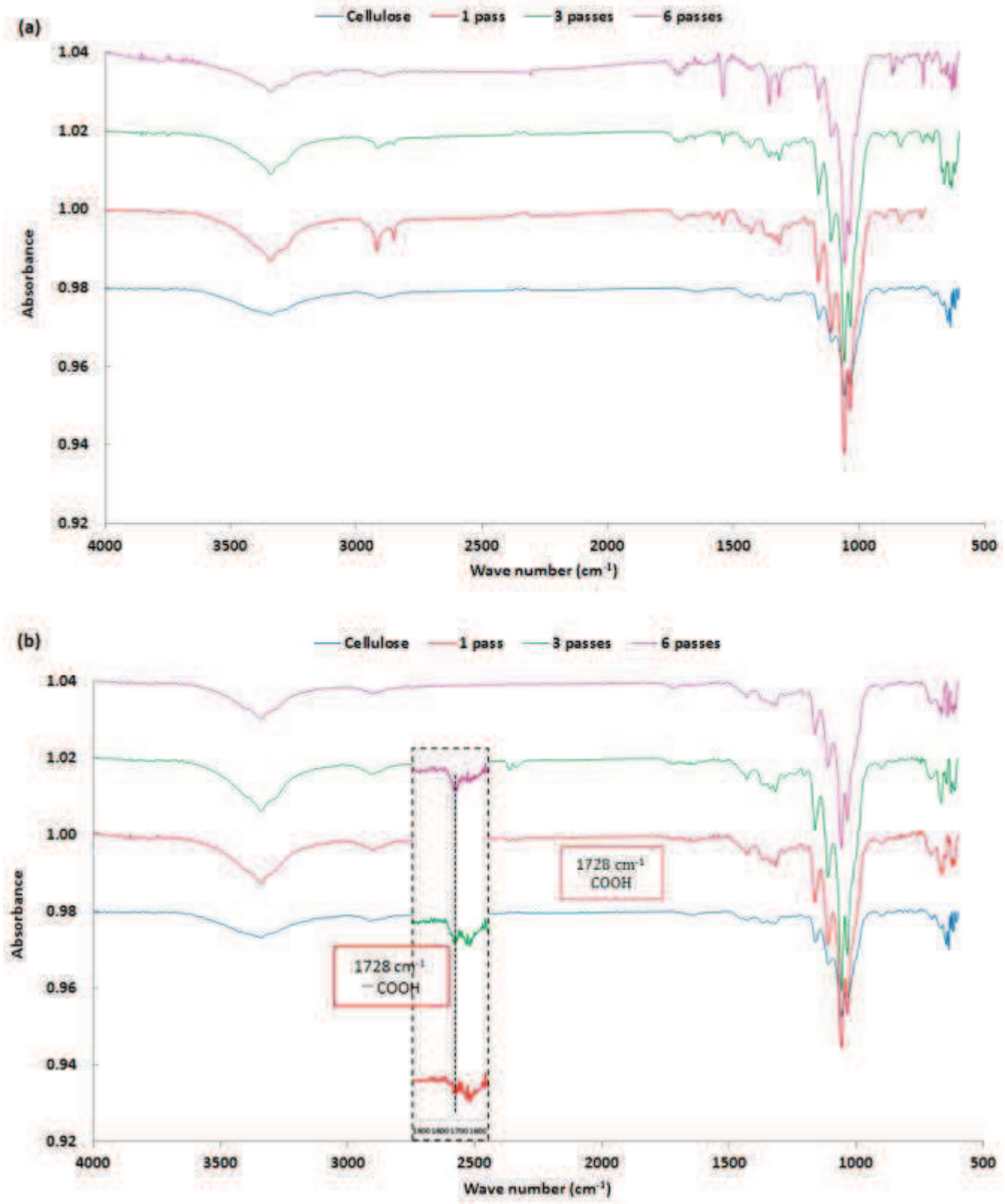

Figure 12. IR spectra of raw cellulose and cellulose printed and copolymerized with acrylic acid monomer. 1-pass printing, 3-pass printing and 6-pass printing were displayed. Spectra from the first set (a) were recorded before rinsing and those from the second (b) after rinsing.

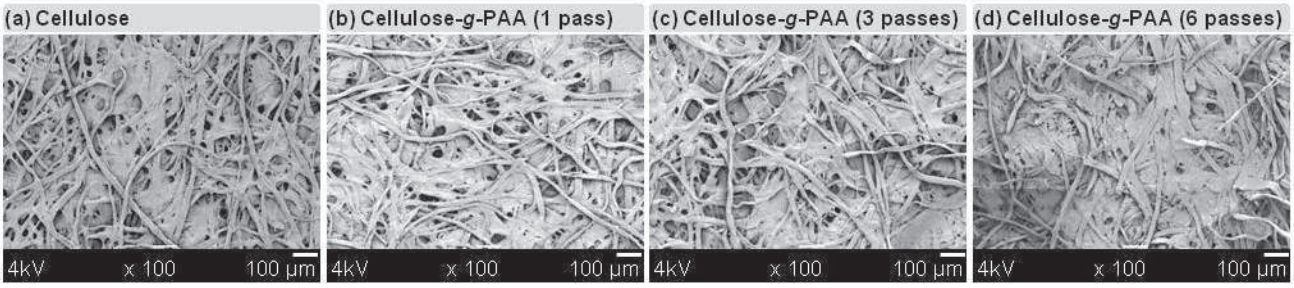

Figure 13. SEM micrographs of raw cellulose (a) and cellulose printed and copolymerized after rising step: 1-pass printing (b), 3-pass printing (c) and 6-pass printing (d) are displayed.

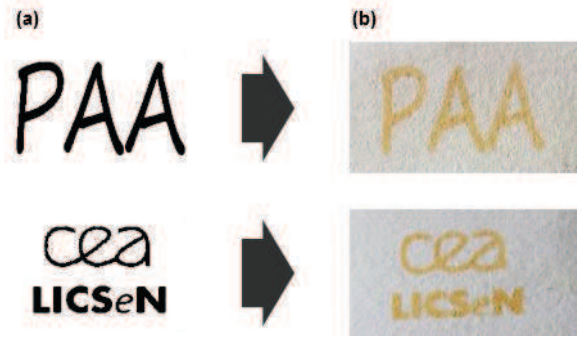

Figure 14. Printed pattern designs (a) and photographs of the solid forms actually printed on cellulose (b).

form is shown in Figure 14b. Visual aspect was consistent with previous results for a 6-pass printing (see section3.2.1). As expected, the drawn pattern allowed direct reading of the grafted polymer. Afterwards, a smaller and thinner pattern was printed in order to assess the resolution of the actually grafted film. Pattern and photograph are shown in Figure 14a and Figure 14b, respectively. They confirmed that this process enables to precisely modulate properties of a cellulose surface according to complex patterns. Spatial control of surface properties is key asset of such a modification process. For instance, precise spatial control of electrical properties is particularly interesting in order to produce paper-based electronic circuit.

4. Conclusion

The work described herein offers a simple, fast, low-cost and eco-friendly way for cellulose surface graft copolymerization. This original approach, based on aryldiazonium salt chemistry, is achieved under soft aqueous conditions and through a one-step reaction. Cellulose sheets have been impregnated with copolymerization reaction mixture by means of two different dispensing methods. Firstly, dipping was performed and enabled to use a biological reducing agent: vitamin C. The process was thus ecologically friendly but not economically friendly. This is why inkjet printing was further implemented. This versatile and economically friendly dispensing method ensured reduction of the matter wastage by localizing the polymerization mixture onto specific areas of the substrate. However, this process modification required to exchange vitamin C for a photoactivated reducing agent: $[Ru(bpy)_3]^{2+}$. Several acrylic polymers were grafted to cellulose. Results suggest that the chemical pathway followed here allows graft copolymerization of cellulose sheet with many different acrylic monomers.

This research was proposed to meet the need of paper-based technology for cost and time-saving methods allowing robust and sustainable graft copolymerization of cellulose sheets. In addition to the simplicity of a one-step reaction, inkjet printing dispensing of the reaction mixture allows to precisely localize the polymerization and to save expensive monomers. Therefore, the expounded process provides a powerful tool for easy and robust graft copolymerization of cellulose sheets with various polymer films and according to complex patterns.

Acknowledgements

This work was financially supported by the Commissariat à l'Energie Atomique et aux Energies Alternatives (France).

Notes and references

CEA Saclay, IRAMIS, NIMBE, LICSEN (Laboratory of Innovation in Surface Chemistry and Nanosciences), F-91191 Gif sur Yvette, France; E-mails: julie.credou@cea.fr; rita.faddoul@cea.fr; thomas.berthelot@cea.fr.
* Author to whom correspondence should be addressed; E-mail: thomas.berthelot@cea.fr; Tel.: +33 169086588; Fax: +33 169084044.

(1) Credou, J.; Berthelot, T. *J. Mater. Chem. B* **2014**. DOI: 10.1039/C4TB00431K.
(2) Roy, D.; Semsarilar, M.; Guthrie, J. T.; Perrier, S. *Chem. Soc. Rev.* **2009**, *38*, 2046–2064.
(3) Crawford, R. L. *Lignin biodegradation and transformation*; John Wiley & Sons Inc: New York, NY, USA, 1981; pp. 1–154.
(4) Malmström, E.; Carlmark, A. *Polym. Chem.* **2012**, *3*, 1702–1713.
(5) Han, J. S.; Rowell, J. S. In *Paper and composites from agro-based resources*; Rowell, R. M.; Young, R. A.; Rowell, J. K., Eds.; CRC Press, 1996; pp. 83–134.
(6) Klemm, D.; Heublein, B.; Fink, H.-P.; Bohn, A. *Angew. Chem. Int. Ed. Engl.* **2005**, *44*, 3358–3393.
(7) Kalia, S.; Kaith, B. S.; Kaur, I. *Cellulose Fibers: Bio- and Nano-Polymer Composites*; Kalia, S.; Kaith, B. S.; Kaur, I., Eds.; Springer Berlin Heidelberg: Berlin, Heidelberg, 2011.

(8) Klemm, D.; Kramer, F.; Moritz, S.; Lindström, T.; Ankerfors, M.; Gray, D.; Dorris, A. *Angew. Chem. Int. Ed. Engl.* **2011**, *50*, 5438–5466.
(9) Pelton, R. *Trends Anal. Chem.* **2009**, *28*, 925–942.
(10) Martinez, A. W.; Phillips, S. T.; Whitesides, G. M.; Carrilho, E. *Anal. Chem.* **2010**, *82*, 3–10.
(11) Credou, J.; Volland, H.; Dano, J.; Berthelot, T. *J. Mater. Chem. B* **2013**, *1*, 3277–3286.
(12) Martinez, A. W.; Phillips, S. T.; Whitesides, G. M. *Proc. Natl. Acad. Sci. U. S. A.* **2008**, *105*, 19606–19611.
(13) SENTINEL: Bioactive Paper Network http://www.bioactivepaper.ca/index.php?module=page&id=4000 (accessed Jan 31, 2014).
(14) Aikio, S.; Grönqvist, S.; Hakola, L.; Hurme, E.; Jussila, S.; Kaukoniemi, O.-V.; Kopola, H.; Känsäkoski, M.; Leinonen, M.; Lippo, S.; Mahlberg, R.; Peltonen, S.; Qvintus-Leino, P.; Rajamäki, T.; Ritschkoff, A.-C.; Smolander, M.; Vartiainen, J.; Viikari, L.; Vilkman, M. *Bioactive paper and fibre products: Patent and literary survey*; Oulu, Finland, 2006.
(15) Materials Research Society. *MRS Bull.* **2013**, *38*, 294–352.
(16) Klemm, D.; Philipp, B.; Heinze, T.; Heinze, U.; Wagenknecht, W. *Comprehensive Cellulose Chemistry Volume 2 Functionalization of Cellulose*; WILEY-VCH: Weinheim, 1998; Vol. 2.
(17) Zhong, J.-F.; Chai, X.-S.; Fu, S.-Y. *Carbohydr. Polym.* **2012**, *87*, 1869–1873.
(18) Takács, E.; Wojnárovits, L.; Koczog Horváth, É.; Fekete, T.; Borsa, J. *Radiat. Phys. Chem.* **2012**, *81*, 1389–1392.
(19) Bongiovanni, R.; Marchi, S.; Zeno, E.; Pollicino, A.; Thomas, R. R. *Colloids Surfaces A Physicochem. Eng. Asp.* **2013**, *418*, 52–59.
(20) Kodama, Y.; Barsbay, M.; Güven, O. *Radiat. Phys. Chem.* **2014**, *94*, 98–104.
(21) Takács, E.; Wojnárovits, L.; Borsa, J.; Rácz, I. *Radiat. Phys. Chem.* **2010**, *79*, 467–470.
(22) Dahou, W.; Ghemati, D.; Oudia, A.; Aliouche, D. *Biochem. Eng. J.* **2010**, *48*, 187–194.
(23) Littunen, K.; Hippi, U.; Johansson, L.-S.; Österberg, M.; Tammelin, T.; Laine, J.; Seppälä, J. *Carbohydr. Polym.* **2011**, *84*, 1039–1047.
(24) Mévellec, V.; Roussel, S.; Tessier, L.; Chancolon, J.; Mayne-L'Hermite, M.; Deniau, G.; Viel, P.; Palacin, S. *Chem. Mater.* **2007**, *19*, 6323–6330.
(25) Berthelot, T.; Garcia, A.; Le, X. T.; El Morsli, J.; Jégou, P.; Palacin, S.; Viel, P. *Appl. Surf. Sci.* **2011**, *257*, 3538–3546.
(26) Mévellec, V.; Roussel, S.; Palacin, S.; Berthelot, T.; Baudin, C.; Trenggono, A.; Deniau, G. Method for preparing an organic film at the surface of a solid substrate in non-electrochemical conditions, solid substrate thus formed and preparation kit. WO 2008/078052, December 19, 2006.
(27) Faddoul, R.; Reverdy-Bruas, N.; Blayo, A. *Mater. Sci. Eng. B* **2012**, *177*, 1053–1066.
(28) Garcia, A.; Hanifi, N.; Jousselme, B.; Jégou, P.; Palacin, S.; Viel, P.; Berthelot, T. *Adv. Funct. Mater.* **2013**, *23*, 3668–3674.
(29) Jenkins, D. W.; Hudson, S. M. *Chem. Rev.* **2001**, *101*, 3245–3274.
(30) PIKE Technologies. *MIRacle ATR; Product Data Sheet*; Madison, WI, USA, 2014.
(31) *Printed Organic and Molecular Electronics*; Gamota, D.; Brazis, P.; Kalyanasundaram, K.; Zhang, J., Eds.; Springer US: Boston, MA, 2004.
(32) Birkenshaw, J. *Printed Electronics (Pira on printing)*; Leatherhead, Surrey, UK, 2004; pp. 1–80.
(33) Zhou, X.; Zhu, D.; Liao, Y.; Liu, W.; Liu, H.; Ma, Z.; Xing, D. *Nat. Protoc.* **2014**, *9*, 1146–1159.
(34) Hara, M.; Waraksa, C. C.; Lean, J. T.; Lewis, B. A.; Mallouk, T. E. *J. Phys. Chem. A* **2000**, *104*, 5275–5280.
(35) Narayanam, J. M. R.; Stephenson, C. R. J. *Chem. Soc. Rev.* **2011**, *40*, 102–113.
(36) Teplý, F. *Collect. Czechoslov. Chem. Commun.* **2011**, *76*, 859–917.
(37) Leach, R.; Pierce, R. *The Printing Ink Manual*; Leach, R.; Pierce, R., Eds.; Springer US: Boston, MA, 1993.
(38) Bergh, M. Absorbent cellulose based fibers Investigation of carboxylation and sulfonation of cellulose, Chalmers University of Technology, Göteborg, Sweden, 2011, pp. 1–57.
(39) Bhattacharya, A.; Misra, B. N. *Prog. Polym. Sci.* **2004**, *29*, 767–814.
(40) Määttänen, A.; Ihalainen, P.; Bollström, R.; Toivakka, M.; Peltonen, J. *Colloids Surfaces A Physicochem. Eng. Asp.* **2010**, *367*, 76–84.

Conclusion

Summary of results

This work was proposed to meet the need for paper-based sensing technology to easily modulate cellulose surface properties according to complex designs. To this end, three processes allowing easy, robust and sustainable modification of cellulose sheets have been developed: two methods for strongly immobilizing biosensing material while preserving its activity, and one for increasing cellulose functionality. In line with the economic and ecological objectives, all procedures developed are environmentally friendly, simple, time and cost-saving.

The first process is a functionalization of cellulose membranes for covalent antibody immobilization. This new approach, based on aryldiazonium salt chemistry, is achieved under soft and biocompatible aqueous conditions and in a single step. Several chemical groups have been introduced onto cellulose. The data suggest that this chemical pathway allows functionalization of cellulose with many different chemical moieties. The modified cellulose papers were further used to covalently immobilize antibodies and the resulting papers were successfully employed as immunoassay membranes.

The second is a chemical-free photoimmobilization process which allows antibodies to be strongly immobilized onto cellulose without any photocoupling intermediate nor any biomolecule or substrate pretreatment. This immobilization technique was further combined to inkjet printing to localize the antibodies according to any desired pattern. With respect to biomolecules, the inkjet printing dispensing method has the great advantage of saving this expensive material, and the photografting procedure has the one of being harmless to them. Native antibodies have been printed and immobilized onto paper sheets. These membranes were successfully employed in immunoassay devices. Their performances were evaluated in terms of visual detection limit and turned out to challenge nitrocellulose performances.

The third is a modification of cellulose membranes by polymer grafting. This original approach, based on aryldiazonium salt chemistry, is achieved in a short single step, under soft and biocompatible conditions. Cellulose sheets have been impregnated with copolymerization reaction mixture by means of two different dispensing methods. First, dipping allowed global modification of paper sheets. Then, inkjet printing enabled to modify specific areas of the substrate. Several acrylic polymers were grafted to cellulose. Results suggest that the followed chemical pathway allows graft copolymerization of cellulose sheet with many different acrylic monomers. Unlike the two first processes which aim to pattern cellulose biosensing properties, this technique was developed in order to increase the functionality of the non-sensing cellulose parts of paper-based devices. Yet, it may be employed for covalent antibody immobilization onto cellulose.

As a consequence, all the strategies developed herein would be helpful to immobilize proteins on selected specific areas of cellulose sheets. More generally, these are powerful tools for easy and rapid modulation of cellulose surface properties according to complex designs, under soft and biocompatible conditions.

Outlook and avenues to explore

In light of this work, new challenges would arise. Nitrocellulose is the reference material for preparing immunochromatographic assays. Thus, the main goal of all the cellulose membranes prepared herein was to equal, or even surpass, nitrocellulose binding ability and VDL performances. However, as pointed out in Chapter 4, cellulose performances appeared slightly lower than nitrocellulose's. This phenomenon most probably stemmed from the physical differences, such as surface porosity variation, between nitrocellulose and cellulose substrates. A true comparison between these two materials would require cellulose sheets with same porosity and thickness than nitrocellulose. Unfortunately, these are not commercially available yet. Therefore, more avenues for signal enhancement should be explored. A first mean would be to replace or enhance colloidal gold label [84,85]. But without taking such drastic measures, other options could be investigated. Efforts may be made regarding the biosensing material immobilization in order to increase the amount of active biomolecules at the extreme surface of the membrane. In this perspective, though Chapter 5 process was developed in order to increase the functionality of the non-sensing cellulose parts of paper-based devices, it may be employed for covalent antibody immobilization onto cellulose. Indeed, an antibody-containing acrylic monomer could be safely used in this biocompatible polymer grafting process, thereby resulting in antibody-grafted cellulose membrane (Figure 3). Besides, such monomer could be easily prepared by amide bond formation between antibody and (meth)acrylic acid *N*-hydroxysuccinimide ester (commercially available). Hence, this strategy should increase

the amount of immobilized antibodies. In addition, this thin polymeric film would reduce the impact of surface porosity on antibody grafting. With more antibodies, closer to the surface, the colorimetric signal should be enhanced. Hopefully, the colorimetric intensity and the detection limit of so prepared immunoassay membranes would reach or surpass nitrocellulose's performances.

On another hand, nitrocellulose tends to be replaced by cellulose partly because agents such as spores and some *bacteria* may have difficulty in migrating along nitrocellulose membranes. Hence, it seems logical to test cellulose membranes prepared according to Chapter 4 process for bacterial detection. Such membranes are expected to show better performances than nitrocellulose. Therefore, several experiments have been conducted in order to explore this possibility. Unfortunately, no conclusion could be drawn because both cellulose and nitrocellulose strips displayed a weak signal on the test line whatever the bacterial concentration. This issue was most probably due to a lack of affinity of the chosen antibodies for their target bacterial antigen. A way to address this issue would be to work with anti-bacterial antibodies which were already proved to be efficient in lateral flow immunoassay. Moreover, efforts to go further into this application of cellulose membranes to bacterial detection should be encouraged. However, once again, signal enhancement appears as a priority for further research.

Lastly, as pointed out in the introduction, preparation of paper-based immunoassay devices requires considering not only the frame material and its modifications, but also the whole device design and the operating procedure. In particular, the fluidic path plays a crucial part in the biosensing kinetics and effective sensitivity of such sensors. In such chromatographic devices, the time during which antigen and antibody are close enough to bind to each other is mainly controlled by the capillary flow rate. The lower the flow rate, the longer this time would be. Therefore, slowing the flow rate increases the chances of forming the antibody-antigen complex, thereby improving sensitivity of the device. Capillary flow rate is controlled by several means including porosity of the membrane, viscosity of the test solution and surfactant *ratio* in this solution [72]. Chapter 5 process enables to modulate surface properties of cellulose membranes. Therefore, it may be employed for modulation of surface porosity. In addition, Preechakasedkit *et al.* proved that the flow rate of the test solution decreased when its viscosity increased, thereby resulting in higher color intensity on the test line [86]. In this study the viscosity of the test solution was regulated by the concentration of saturating components in the analysis buffer. In consequence, buffer viscosity and membranes treatment appear as avenues to explore in order to increase the sensitivity of paper-based immunoassay devices.

In any case, all these new challenges and avenues should be explored while bearing in mind the economic and ecological goals.

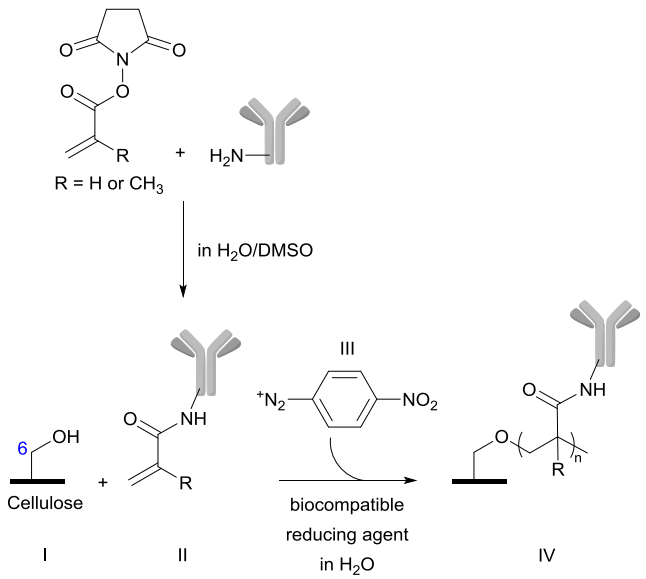

Figure 3: Cellulose graft copolymerization with antibody-containing acrylic monomer. Aryldiazonium (III) is reduced and reacts with cellulose (I) in an aqueous medium to initiate the grafting and polymerization of the antibody-containing acrylic monomer (II) and give an antibody-grafted cellulose membrane (IV).

References

1. Martinez, A. W.; Phillips, S. T.; Whitesides, G. M.; Carrilho, E. Diagnostics for the Developing World: Microfluidic Paper-Based Analytical Devices. *Anal. Chem.* **2010**, *82*, 3–10.

2. Ge, L.; Yan, J.; Song, X.; Yan, M.; Ge, S.; Yu, J. Three-dimensional paper-based electrochemiluminescence immunodevice for multiplexed measurement of biomarkers and point-of-care testing. *Biomaterials* **2012**, *33*, 1024–1031.

3. Cheng, C.-M.; Martinez, A. W.; Gong, J.; Mace, C. R.; Phillips, S. T.; Carrilho, E.; Mirica, K. A.; Whitesides, G. M. Paper-based ELISA. *Angew. Chem. Int. Ed. Engl.* **2010**, *49*, 4771–4774.

4. Hu, J.; Wang, S.; Wang, L.; Li, F.; Lu, T. J.; Xu, F. Advances in Paper-Based Point-of-Care Diagnostics. *Biosens. Bioelectron.* **2014**, *54*, 585–597.

5. Wiriyachaiporn, S.; Howarth, P. H.; Bruce, K. D.; Dailey, L. A. Evaluation of a rapid lateral flow immunoassay for Staphylococcus aureus detection in respiratory samples. *Diagn. Microbiol. Infect. Dis.* **2013**, *75*, 28–36.

6. Gonzalez, J. M.; Foley, M. W.; Bieber, N. M.; Bourdelle, P. A.; Niedbala, R. S. Development of an ultrasensitive immunochromatography test to detect nicotine metabolites in oral fluids. *Anal. Bioanal. Chem.* **2011**, *400*, 3655–3664.

7. Liana, D. D.; Raguse, B.; Gooding, J. J.; Chow, E. Recent advances in paper-based sensors. *Sensors* **2012**, *12*, 11505–11526.

8. Yetisen, A. K.; Akram, M. S.; Lowe, C. R. Paper-based microfluidic point-of-care diagnostic devices. *Lab Chip* **2013**, *13*, 2210–2251.

9. Zhou, G.; Mao, X.; Juncker, D. Immunochromatographic Assay on Thread. *Anal. Chem.* **2012**, *84*, 7736–7743.

10. Anany, H.; Chen, W.; Pelton, R.; Griffiths, M. W. Biocontrol of Listeria monocytogenes and Escherichia coli O157:H7 in meat by using phages immobilized on modified cellulose membranes. *Appl. Environ. Microbiol.* **2011**, *77*, 6379–6387.

11. Zakir Hossain, S. M.; Luckham, R. E.; McFadden, M. J.; Brennan, J. D. Reagentless bidirectional lateral flow bioactive paper sensors for detection of pesticides in beverage and food samples. *Anal. Chem.* **2009**, *81*, 9055–9064.

12. Vaher, M.; Kaljurand, M. The development of paper microzone-based green analytical chemistry methods for determining the quality of wines. *Anal. Bioanal. Chem.* **2012**, *404*, 627–633.

13. Alkasir, R. S. J.; Ornatska, M.; Andreescu, S. Colorimetric paper bioassay for the detection of phenolic compounds. *Anal. Chem.* **2012**, *84*, 9729–9737.

14. Zakir Hossain, S. M.; Ozimok, C.; Sicard, C.; Aguirre, S. D.; Ali, M. M.; Li, Y.; Brennan, J. D. Multiplexed paper test strip for quantitative bacterial detection. *Anal. Bioanal. Chem.* **2012**, *403*, 1567–1576.

15. Zhang, M.; Ge, L.; Ge, S.; Yan, M.; Yu, J.; Huang, J.; Liu, S. Three-dimensional Paper-based Electrochemiluminescence Device for Simultaneous Detection of Pb2+ and Hg2+ based on Potential-Control Technique. *Biosens. Bioelectron.* **2013**, *41*, 544–550.

16. Sicard, C.; Brennan, J. D. Bioactive paper: Biomolecule immobilization methods and applications in environmental monitoring. *MRS Bull.* **2013**, *38*, 331–334.

17. Kirsch, J.; Siltanen, C.; Zhou, Q.; Revzin, A.; Simonian, A. Biosensor technology: recent advances in threat agent detection and medicine. *Chem. Soc. Rev.* **2013**, *42*, 8733–8768.

18. Murugaiyan, S. B.; Ramasamy, R.; Gopal, N.; Kuzhandaivelu, V. Biosensors in clinical chemistry: An overview. *Adv. Biomed. Res.* **2014**, *3*, 67.

19. Berrade, L.; Garcia, A. E.; Camarero, J. a Protein microarrays: novel developments and applications. *Pharm. Res.* **2011**, *28*, 1480–1499.

20. Foudeh, A.; Fatanat-Didar, T.; Veres, T.; Tabrizian, M. Microfluidic Designs and Techniques Using Lab-on-a-Chip Devices for Pathogen Detection for Point-of-Care Diagnostics. *Lab Chip* **2012**, *12*, 3249–3266.

21. Li, X.; Ballerini, D. R.; Shen, W. A perspective on paper-based microfluidics: Current status and future trends. *Biomicrofluidics* **2012**, *6*, 011301.

22. Jonkheijm, P.; Weinrich, D.; Schröder, H.; Niemeyer, C. M.; Waldmann, H. Chemical strategies for generating protein biochips. *Angew. Chem. Int. Ed. Engl.* **2008**, *47*, 9618–9647.

23. Kettler, H.; White, K.; Hawkes, S. *Mapping the landscape of diagnostics for sexually transmitted infections: Key findings and recommandations*; World Health Organization: Geneva, Switzerland, 2004; pp. 1–44.

24. Peeling, R. W.; Mabey, D. Point-of-care tests for diagnosing infections in the developing world. *Clin. Microbiol. Infect.* **2010**, *16*, 1062–1069.

25. Credou, J.; Berthelot, T. Cellulose: from biocompatible to bioactive material. *J. Mater. Chem. B* **2014**. DOI: 10.1039/C4TB00431K.

26. Han, J. S.; Rowell, J. S. Chemical Composition of Fibers. In *Paper and composites from agro-based resources*; Rowell, R. M.; Young, R. A.; Rowell, J. K., Eds.; CRC Press, 1996; pp. 83–134.

27. Klemm, D.; Heublein, B.; Fink, H.-P.; Bohn, A. Cellulose: fascinating biopolymer and sustainable raw material. *Angew. Chem. Int. Ed. Engl.* **2005**, *44*, 3358–3393.

28. Crawford, R. L. *Lignin biodegradation and transformation*; John Wiley & Sons Inc: New York, NY, USA, 1981; pp. 1–154.

29. Kalia, S.; Kaith, B. S.; Kaur, I. *Cellulose Fibers: Bio- and Nano-Polymer Composites*; Kalia, S.; Kaith, B. S.; Kaur, I., Eds.; Springer Berlin Heidelberg: Berlin, Heidelberg, 2011.

30. Klemm, D.; Kramer, F.; Moritz, S.; Lindström, T.; Ankerfors, M.; Gray, D.; Dorris, A. Nanocelluloses: a new family of nature-based materials. *Angew. Chem. Int. Ed. Engl.* **2011**, *50*, 5438–5466.

31. Maxwell, E. J.; Mazzeo, A. D.; Whitesides, G. M. Paper-based electroanalytical devices for accessible diagnostic testing. *MRS Bull.* **2013**, *38*, 309–314.

32. Pelton, R. Bioactive paper provides a low-cost platform for diagnostics. *Trends Anal. Chem.* **2009**, *28*, 925–942.

33. Credou, J.; Volland, H.; Dano, J.; Berthelot, T. A one-step and biocompatible cellulose functionalization for covalent antibody immobilization on immunoassay membranes. *J. Mater. Chem. B* **2013**, *1*, 3277–3286.

34. Hawkes, R.; Niday, E.; Gordon, J. A dot-immunobinding assay for monoclonal and other antibodies. *Anal. Biochem.* **1982**, *119*, 142–147.

35. Posthuma-Trumpie, G. A.; Korf, J.; van Amerongen, A. Lateral flow (immuno)assay: its strengths, weaknesses, opportunities and threats. A literature survey. *Anal. Bioanal. Chem.* **2009**, *393*, 569–582.

36. Ngom, B.; Guo, Y.; Wang, X.; Bi, D. Development and application of lateral flow test strip technology for detection of infectious agents and chemical contaminants: a review. *Anal. Bioanal. Chem.* **2010**, *397*, 1113–1135.

37. Wong, R. C.; Tse, H. Y. *Lateral Flow Immunoassay*; Wong, R. C.; Tse, H. Y., Eds.; Humana Press: New York, NY, 2009.

38. Von Lode, P. Point-of-care immunotesting: approaching the analytical performance of central laboratory methods. *Clin. Biochem.* **2005**, *38*, 591–606.

39. Burstein, J.; Braunstein, G. D. Urine pregnancy tests from antiquity to the present. *Early Pregnancy* **1995**, *1*, 288–296.

40. Chard, T. Pregnancy tests: a review. *Hum. Reprod.* **1992**, *7*, 701–710.

41. Martinez, A. W.; Phillips, S. T.; Whitesides, G. M. Three-dimensional microfluidic devices fabricated in layered paper and tape. *Proc. Natl. Acad. Sci. U. S. A.* **2008**, *105*, 19606–19611.

42. SENTINEL: Bioactive Paper Network http://www.bioactivepaper.ca/index.php?module=page&id=4000 (accessed Jan 31, 2014).

43. Aikio, S.; Grönqvist, S.; Hakola, L.; Hurme, E.; Jussila, S.; Kaukoniemi, O.-V.; Kopola, H.; Känsäkoski, M.; Leinonen, M.; Lippo, S.; Mahlberg, R.; Peltonen, S.; Qvintus-Leino, P.; Rajamäki, T.; Ritschkoff, A.-C.; Smolander, M.; Vartiainen, J.; Viikari, L.; Vilkman, M. *Bioactive paper and fibre products: Patent and literary survey*; Oulu, Finland, 2006.

44. Fenton, E. M.; Mascarenas, M. R.; López, G. P.; Sibbett, S. S. Multiplex lateral-flow test strips fabricated by two-dimensional shaping. *ACS Appl. Mater. Interfaces* **2009**, *1*, 124–129.

45. Njumbe Ediage, E.; Di Mavungu, J. D.; Goryacheva, I. Y.; Van Peteghem, C.; De Saeger, S. Multiplex flow-through immunoassay formats for screening of mycotoxins in a variety of food matrices. *Anal. Bioanal. Chem.* **2012**, *403*, 265–278.

46. Lisowski, P.; Zarzycki, P. K. Microfluidic Paper-Based Analytical Devices (μPADs) and Micro Total Analysis Systems (μTAS): Development, Applications and Future Trends. *Chromatographia* **2013**, *76*, 1201–1214.

47. Abe, K.; Kotera, K.; Suzuki, K.; Citterio, D. Inkjet-printed paperfluidic immuno-chemical sensing device. *Anal. Bioanal. Chem.* **2010**, *398*, 885–893.

48. Ge, L.; Wang, S.; Song, X.; Ge, S.; Yu, J. 3D Origami-based Multifunction-integrated Immunodevice: Low-cost and Multiplexed Sandwich Chemiluminescence Immunoassay on Microfluidic Paper-based Analytical Device. *Lab Chip* **2012**, *12*, 3150–3158.

49. Kong, F.; Hu, Y. F. Biomolecule immobilization techniques for bioactive paper fabrication. *Anal. Bioanal. Chem.* **2012**, *403*, 7–13.

50. Fridley, G. E.; Holstein, C. A.; Oza, S. B.; Yager, P. The evolution of nitrocellulose as a material for bioassays. *MRS Bull.* **2013**, *38*, 326–330.

51. Millipore Corporation *Millistak+ HC Filter Devices (with RW01); MSDS No. M114480*; Millipore Corporation: Billerica, MA, USA, 2008.

52. Millipore Corporation *Nitrocellulose Membrane Filters; MSDS No. 00000100SDS*; Millipore Corporation: Billerica, MA, USA, 2011.

53. Jarujamrus, P.; Tian, J.; Li, X.; Siripinyanond, A.; Shiowatana, J.; Shen, W. Mechanisms of red blood cells agglutination in antibody-treated paper. *Analyst* **2012**, *137*, 2205–2210.

54. Heinze, T.; Liebert, T. Unconventional methods in cellulose functionalization. *Prog. Polym. Sci.* **2001**, *26*, 1689–1762.

55. Klemm, D.; Philipp, B.; Heinze, T.; Heinze, U.; Wagenknecht, W. *Comprehensive Cellulose Chemistry Volume 2 Functionalization of Cellulose*; WILEY-VCH: Weinheim, 1998; Vol. 2.

56. Grinenval, E.; Nonglaton, G.; Vinet, F. Spatially controlled immobilisation of biomolecules: A complete approach in green chemistry. *Appl. Surf. Sci.* **2014**, *289*, 571–580.

57. Choi, M. M. F. Progress in Enzyme-Based Biosensors Using Optical Transducers. *Microchim. Acta* **2004**, *148*, 107–132.

58. Sassolas, A.; Blum, L. J.; Leca-Bouvier, B. D. Immobilization strategies to develop enzymatic biosensors. *Biotechnol. Adv.* **2012**, *30*, 489–511.

59. Arola, S.; Tammelin, T.; Setälä, H.; Tullila, A.; Linder, M. B. Immobilization-stabilization of proteins on nanofibrillated cellulose derivatives and their bioactive film formation. *Biomacromolecules* **2012**, *13*, 594–603.

60. Bora, U.; Kannan, K.; Nahar, P. A simple method for functionalization of cellulose membrane for covalent immobilization of biomolecules. *J. Memb. Sci.* **2005**, *250*, 215–222.

61. Bora, U.; Sharma, P.; Kannan, K.; Nahar, P. Photoreactive cellulose membrane--A novel matrix for covalent immobilization of biomolecules. *J. Biotechnol.* **2006**, *126*, 220–229.

62. Kumar, S.; Nahar, P. Sunlight-induced covalent immobilization of proteins. *Talanta* **2007**, *71*, 1438–1440.

63. Kuzmenko, V.; Sämfors, S.; Hägg, D.; Gatenholm, P. Universal method for protein bioconjugation with nanocellulose scaffolds for increased cell adhesion. *Mater. Sci. Eng. C* **2013**, *33*, 4599–4607.

64. Villalonga, R.; Fujii, A.; Shinohara, H.; Tachibana, S.; Asano, Y. Covalent immobilization of phenylalanine dehydrogenase on cellulose membrane for biosensor construction. *Sensors Actuators B Chem.* **2008**, *129*, 195–199.

65. Yu, A.; Shang, J.; Cheng, F.; Paik, B. A.; Kaplan, J. M.; Andrade, R. B.; Ratner, D. M. Biofunctional Paper via Covalent Modification of Cellulose. *Langmuir* **2012**, *28*, 11265–11273.

66. Thermo Fisher Scientific Inc. Crosslinking Reagents http://www.piercenet.com/cat/crosslinking-reagents (accessed Jun 23, 2014).

67. Hermanson, G. T. *Bioconjugate techniques*; Academic Press: London, 2008.

68. Viel, P.; Walter, J.; Bellon, S.; Berthelot, T. Versatile and nondestructive photochemical process for biomolecule immobilization. *Langmuir* **2013**, *29*, 2075–2082.

69. Volland, H.; Pradelles, P.; Taran, F.; Buscarlet, L.; Creminon, C. Recent developments for SPIE-IA, a new sandwich immunoassay format for very small molecules. *J. Pharm. Biomed. Anal.* **2004**, *34*, 737–752.

70. Tingaut, P.; Hauert, R.; Zimmermann, T. Highly efficient and straightforward functionalization of cellulose films with thiol-ene click chemistry. *J. Mater. Chem.* **2011**, *21*, 16066–16076.

71. Credou, J.; Berthelot, T. Method for photo-immobilizing biomolecules on a cellulose carrier (EP14157944) 2014.

72. Millipore *Rapid Lateral Flow Test Strips: Considerations for Product development*; Millipore Corporation, Ed.; Millipore Corporation: Billerica, MA, 2008.

73. *Printed Organic and Molecular Electronics*; Gamota, D.; Brazis, P.; Kalyanasundaram, K.; Zhang, J., Eds.; Springer US: Boston, MA, 2004.

74. Birkenshaw, J. *Printed Electronics (Pira on printing)*; Leatherhead, Surrey, UK, 2004; pp. 1–80.

75. Roy, D.; Semsarilar, M.; Guthrie, J. T.; Perrier, S. Cellulose modification by polymer grafting: a review. *Chem. Soc. Rev.* **2009**, *38*, 2046–2064.

76. Malmström, E.; Carlmark, A. Controlled grafting of cellulose fibres – an outlook beyond paper and cardboard. *Polym. Chem.* **2012**, *3*, 1702–1713.

77. Zhong, J.-F.; Chai, X.-S.; Fu, S.-Y. Homogeneous grafting poly (methyl methacrylate) on cellulose by atom transfer radical polymerization. *Carbohydr. Polym.* **2012**, *87*, 1869–1873.

78. Takács, E.; Wojnárovits, L.; Koczog Horváth, É.; Fekete, T.; Borsa, J. Improvement of pesticide adsorption capacity of cellulose fibre by high-energy irradiation-initiated grafting of glycidyl methacrylate. *Radiat. Phys. Chem.* **2012**, *81*, 1389–1392.

79. Bongiovanni, R.; Marchi, S.; Zeno, E.; Pollicino, A.; Thomas, R. R. Water resistance improvement of filter paper by a UV-grafting modification with a fluoromonomer. *Colloids Surfaces A Physicochem. Eng. Asp.* **2013**, *418*, 52–59.

80. Kodama, Y.; Barsbay, M.; Güven, O. Radiation-induced and RAFT-mediated grafting of poly(hydroxyethyl methacrylate) (PHEMA) from cellulose surfaces. *Radiat. Phys. Chem.* **2014**, *94*, 98–104.

81. Takács, E.; Wojnárovits, L.; Borsa, J.; Rácz, I. Hydrophilic/hydrophobic character of grafted cellulose. *Radiat. Phys. Chem.* **2010**, *79*, 467–470.

82. Dahou, W.; Ghemati, D.; Oudia, A.; Aliouche, D. Preparation and biological characterization of cellulose graft copolymers. *Biochem. Eng. J.* **2010**, *48*, 187–194.

83. Littunen, K.; Hippi, U.; Johansson, L.-S.; Österberg, M.; Tammelin, T.; Laine, J.; Seppälä, J. Free radical graft copolymerization of nanofibrillated cellulose with acrylic monomers. *Carbohydr. Polym.* **2011**, *84*, 1039–1047.

84. Goryacheva, I. Y.; Lenain, P.; De Saeger, S. Nanosized labels for rapid immunotests. *TrAC Trends Anal. Chem.* **2013**.

85. Agasti, S. S.; Rana, S.; Park, M.-H.; Kim, C. K.; You, C.-C.; Rotello, V. M. Nanoparticles for detection and diagnosis. *Adv. Drug Deliv. Rev.* **2010**, *62*, 316–328.

86. Preechakasedkit, P.; Pinwattana, K.; Dungchai, W.; Siangproh, W.; Chaicumpa, W.; Tongtawe, P.; Chailapakul, O. Development of a one-step immunochromatographic strip test using gold nanoparticles for the rapid detection of Salmonella typhi in human serum. *Biosens. Bioelectron.* **2012**, *31*, 562–6.

Abstract

Since the *papyri*, cellulose has played a significant role in human culture, especially as paper. Nowadays, this ancient product has found new applications in the expanding sector of bioactive paper. Simple paper-based detection devices such as lateral flow immunoassays (LFIAs) are inexpensive, rapid, user-friendly and therefore highly promising for providing resource-limited settings with point-of-care diagnostics. Recently, paper-based biosensing technology has trended towards three-dimensional microfluidic devices and multiplexed assay platforms. Yet, many multiplexed paper-based biosensors implement methods incompatible with the conventional LFIA carrier material: nitrocellulose. It thus tends to be replaced by pure cellulose. This major material change implies to undertake a covalent immobilization of biomolecules on cellulose which preserves their biological activity.

Furthermore, the current global issues have stimulated the search for both ecologically and economically friendly (eco²-friendly) materials and processes. As a sustainable and affordable biopolymer, cellulose is an ideal material for developing diagnostic devices. However, the frame material is not the only aspect to consider. The whole device design and production, as well as the biosensing material immobilization or the non-sensing membranes treatment, should be as eco²-friendly as possible. Hence, the spatially controlled modification of cellulose surface seems crucial in the development of such devices since it enables to save expensive matter and to pattern surface properties. In any case, modification procedures should abide by the economic and ecological objectives aforementioned.

In this perspective, three processes allowing easy, robust and sustainable modification of cellulose sheets were developed. All are environmentally friendly, simple, time and cost-saving, and versatile.

The first procedure is a functionalization of cellulose membranes for covalent antibody immobilization. While cellulose chemical modification is usually operated under harsh conditions in organic solvents, the diazonium-based procedure developed was performed in water, at room temperature, in a single step. Paper sheets have thus been modified and bear different chemical functions which enable to graft biomolecules by common bioconjugate techniques and to perform LFIAs.

The second is a chemical-free photoimmobilization procedure which allowed antibodies to be immobilized on cellulose without any photocoupling intermediate nor any biomolecule or substrate pretreatment. This immobilization technique was further combined to inkjet printing to localize the antibodies according to any pattern desired. Native antibodies have thus been printed and immobilized on paper sheets which therefore enable to perform LFIAs. Membranes' performances were evaluated in terms of visual detection limit and challenged nitrocellulose performances.

The third is a modification of cellulose membranes by polymer grafting. Unlike the two previous processes, this technique was developed in order to increase the functionality of the non-sensing cellulose parts of paper-based devices. Yet, it may be employed as another functionalization method for covalent antibody immobilization on cellulose. While cellulose graft copolymerization is usually performed through complex and expensive procedures, the diazonium-based approach employed was performed in water, at room temperature, in a short single step. Cellulose sheets have thus been grafted with several acrylic polymers, first globally through a dipping procedure and then locally by inkjet printing.

All the strategies developed herein would be helpful to immobilize sensitive proteins on selected specific areas of cellulose sheets. More generally, these are powerful tools for easy and rapid modulation of cellulose surface properties according to complex designs, under soft and biocompatible conditions.

Résumé

Depuis le *papyrus*, la cellulose a tenu un rôle important dans notre culture, en particulier comme papier. Aujourd'hui, ce produit ancien trouve de nouvelles applications dans le secteur des papiers bioactifs. Des dispositifs de détection faits de papier tels que les bandelettes sont peu coûteux, rapides, faciles à utiliser, et donc très prometteurs pour le diagnostic de terrain dans les zones reculées. Récemment, les biocapteurs papier ont évolué vers des dispositifs microfluidiques 3D et des plateformes multiplexées. Or, le développement de ces biocapteurs papier multiplexés fait souvent appel à des méthodes incompatibles avec le matériau classique des bandelettes : la nitrocellulose. Celle-ci tend donc à être remplacée par la cellulose. Ce changement de matériau implique la mise en œuvre d'une immobilisation covalente des biomolécules qui préserve leur activité biologique.

Par ailleurs, les enjeux mondiaux actuels incitent à se tourner vers des matériaux et procédés à la fois respectueux de l'environnement et rentables économiquement. La cellulose est un polymère naturel abondant et donc un matériau idéal pour le développement de dispositifs de diagnostic. Toutefois, le matériau support n'est pas le seul aspect à considérer. L'ensemble de la conception du dispositif, l'immobilisation des agents de capture, le traitement des membranes, tout doit répondre aux défis écologiques et économiques. La modification localisée des surfaces de cellulose semble alors cruciale puisqu'elle permet d'économiser des composés coûteux et de moduler localement les propriétés de surface.

Dans ce contexte, trois procédés de modification facile et durable de feuilles de cellulose ont été développés. Tous sont respectueux de l'environnement, simples, polyvalents et économes aussi bien en temps qu'en argent.

Le premier est une procédure de fonctionnalisation de membranes de cellulose pour l'immobilisation covalente d'anticorps. Tandis que la modification chimique de la cellulose se fait habituellement dans des conditions rudes et dans des solvants organiques, la méthode développée ici a été réalisée dans l'eau, à température ambiante, en une seule étape. Des feuilles de papier ont ainsi été modifiées, portant alors différentes fonctions chimiques permettant de greffer des biomolécules par des techniques de bioconjugaison classiques. Elles ont ensuite été testées comme bandelettes.

Le second est une procédure de photoimmobilisation sans produit chimique qui permet d'immobiliser des anticorps sur la cellulose sans aucun intermédiaire de couplage ni aucun prétraitement des biomolécules ou du substrat. Cette technique a été combinée à l'impression jet d'encre pour localiser les anticorps selon tout motif désiré. Des anticorps natifs ont ainsi été imprimés et immobilisés sur des feuilles de papier qui ont ensuite servi de bandelettes. Leurs performances ont été évaluées en termes de limite de détection et se sont montrées comparables à celles de la nitrocellulose.

Le troisième est une méthode de greffage de polymères sur membranes de cellulose. Contrairement aux précédents, ce procédé vise à augmenter la fonctionnalité des portions non-détectrices des dispositifs papier. Mais il peut aussi être utilisé comme une autre méthode de fonctionnalisation pour l'immobilisation covalente d'anticorps. Alors que le greffage de polymères sur cellulose se fait d'ordinaire par des procédures complexes et coûteuses, l'approche employée ici a été réalisée dans l'eau, à température ambiante, en une seule et courte étape. Des feuilles de cellulose ont ainsi été greffées de divers polyacryliques, d'abord globalement par trempage puis localement par impression.

Toutes ces stratégies peuvent aider à immobiliser de manière localisée des protéines sensibles sur des feuilles de cellulose. Plus généralement, ce sont de puissants outils pour facilement moduler les propriétés des surfaces de celluloses selon des motifs complexes, dans des conditions douces et biocompatibles.